This is to certify that the
dissertation entitled

CATALYTIC PROCESSING OF MONOSACCHARIDES AND SUGAR ALCOHOLS TO VALUE-ADDED PRODUCTS

presented by

Michael William Shafer

has been accepted towards fulfillment
of the requirements for the

Ph.D. degree in Chemical Engineering and Material Science

Dennis J. Miller
Major Professor's Signature

12/21/04
Date

CATALYTIC PROCESSING OF MONOSACCHARIDES AND SUGAR ALCOHOLS TO VALUE-ADDED PRODUCTS

By

Michael William Shafer

A DISSERTATION

Submitted to
Michigan State University
in partial fulfillment of the requirements
for the degree of

DOCTOR OF PHILOSOPHY

Department of Chemical Engineering and Material Science

2004

ABSTRACT

CATALYTIC PROCESSING OF MONOSACCHARIDES AND SUGAR ALCOHOLS TO VALUE-ADDED PRODUCTS

By

Michael William Shafer

The conversion of renewable, bio-based sugars and sugar alcohols to desired C_3 polyols, propylene glycol (PG) and glycerol (GO), is the subject of this dissertation. Catalytic hydrogenolysis of sugar alcohols can give high yields of PG and GO (> 55%); the goal of this work is to achieve even better yields by gaining a more thorough understanding of the underlying mechanism of the reaction.

Through adsorption studies of sorbitol on ruthenium metal and related H-D exchange experiments involving sorbitol hydrogenolysis, we conclude that catalytic hydrogenolysis is the combination of three chemistries: dehydrogenation of the sugar alcohol, alkaline degradation of the unsaturated sugar analog, and hydrogenation of cleaved aldehydic intermediates from the sugar to form polyols. ^{13}C NMR analysis of sorbitol hydrogenolysis in deuterated water showed incorporation of deuterium at C1 of sorbitol, which only can occur with dehydrogenation. Addition of soluble base to sorbitol in the presence of catalyst or to glucose in solution produced significant amounts of lactic acid and other organic acids, indicative of alkaline degradation of sugars via retro-aldol condensation described previously in the literature.

Alkaline degradation of monosaccharides (glucose, fructose, etc.) enables cleavage of sugar feedstock at low temperature with high selectivity toward C_3 products. In addition, intermediates from alkaline degradation can hydrogenate to form propylene

glycol and glycerol. Used simultaneously, the combination of chemistries is a novel approach to convert sugar feedstock to PG and GO. Observation and characterization of alkaline degradation with hydrogenation is the major contribution of this research.

Combining alkaline degradation of sugar and hydrogenation cleaves sugar feedstock and produces PG and GO at temperatures and pressures much lower than those required for hydrogenolysis (40°C, 100 psi vs. 200°C, 1200 psi). The C_3 yield from alkaline degradation with hydrogenation was comparable to that of hydrogenolysis (54% vs. 55%) but at much milder conditions. Analysis of the product distribution also showed potential for further improvement. In some instances, over 80% of the feedstock that underwent alkaline degradation formed desired C_3 products. However, a significant portion of the feedstock hydrogenated to form sugar alcohols, significantly reducing C_3 yield. Specialized catalysts were tested to selectively hydrogenate C_3 intermediates to reduce formation of sorbitol and mannitol and further improve PG and GO yields.

A kinetic model of the alkaline degradation with hydrogenation reaction was developed to mathematically describe the reaction system and provide a prognostic tool for product distributions based on feedstock composition. Concentration versus time data from ten experiments was used to fit a parametric model that accounted for isomerization of sugar feedstock, formation of intermediates from alkaline degradation, hydrogenation of feedstock and intermediates, and adsorption and desorption of products.

Methane production was also explored using carbohydrate feedstock. Glucose, sorbitol, and glycerol readily converted to methane with >90% yield using a 5% Ru/C catalyst at 200°C and 1200 psi H_2. The process may prove economically viable if raw materials are produced on site instead of purchased from an outside source.

To Elizabeth

For your patience

For your laughter

For your spirit

For your love

For you

ACKNOWLEDGMENTS

I would first like to thank Dr. Dennis Miller for his guidance and support as my advisor through my Ph.D. studies. I would also like to thank Drs. James Jackson, Lawrence Drzal, Bruce Dale, and Todd Werpy for serving on my graduate committee. A sincere thank you to group members Frank Jere, Lars Peereboom, Dalila Kovacs, Simona Marincean, Navin Asthana, Atul Dhale, Zhigang Zhang, Dushyant Shekhawat, and Shubham Chopade for discussion and camaraderie. I also want to share my appreciation of Lauren Hendry and Brian Hogle for their assistance with running experiments. Finally, a word of thanks to the support staff in the office of Chemical Engineering and Material Science. Thank you all!

TABLE OF CONTENTS

LIST OF TABLES

LIST OF FIGURES

LIST OF SYMBOLS AND ABBREVIATIONS

English:

a = gas-liquid interfacial area per unit volume of reactor [cm^2 / cm^3]

a = ratio of catalyst surface area to volume of fluid [m^2 / m^3]

A_{area} = Effective area of 1 metal atom [m^2 / atom of metal]

ADS = adsorption

AW_{metal} = Atomic weight of the supported metal [g metal / atom of metal]

$C_{A,L}$ = concentration of liquid phase reactants [mol / L]

$C_{A,S}$ = concentration of liquid phase reactants in the catalyst [mol / L]

$C_{H2,L}$ = concentration of hydrogen in the liquid phase [mol / L]

$C_{H2,S}$ = concentration of hydrogen in the catalyst [mol / L]

$C_{H\cdot S2}$ = concentration of type 2 sites occupied by monatomic hydrogen

C_s = species surface concentration [mol / L]

C_{SO} = Concentration of sorbitol [mol / liter]

C_{V2} = concentration of vacant type 2 sites

CD = condensation products

CZ = Cannizzaro reaction products

% Disp = Metal dispersion – fraction of metal available for adsorbate interaction

d_i = impeller diameter [m]

d_P = Particle diameter [m]

d_T = reactor diameter [m]

D_A = diffusion rate of species A [m / s^2]

D_e = $\varepsilon^2 D_a$ = effective diffusivity [m^2 / s]

DES = desorption

$-E_{act}$ = Activation energy [J / mol]

EG = ethylene glycol

F = fructose

FA = formic acid

g = Gravitational constant [9.8066 m/s^2]

g_c = Gravitational proportionality factor $[1 \frac{kg \cdot m}{s^2 \cdot N}]$

G = glucose

Ga_L = Galileo number of the liquid phase = $\frac{U_L d_P^3 \rho_L^2 g}{\mu_L^2 (1-\varepsilon_B)^3}$ [dimensionless]

GA = glyceraldehyde

GA2 = glycolaldehyde

GLYA = glyceric acid

GLYA2 = glycolic acid

GO = glycerol

H = Henry's Law constant [atm / (mole solute / mole solution)]

H_2, H2 = hydrogen

k = 1st order rate constant [hr^{-1}]

$k_{H\text{-}ADS}$ = rate constant for hydrogen adsorption

$k_{H\text{-}DES}$ = rate constant for hydrogen desorption

k_L = liquid film mass transfer coefficient [m / s]

$k_L a$ = gas-liquid mass transfer [1 / m · s]

k_o = pre-exponential factor [hr^{-1}]

k_s = liquid-solid mass transfer coefficient [m / s]

$k_{S,A}\, a$ = liquid-solid mass transfer of liquid phase reactants [1 / m · s]

$k_{S,H2}\, a$ = liquid-solid mass transfer [1 / m · s]

K = equilibrium constant – k_{ADS} / k_{DES}

K_H = equilibrium constant for hydrogen ($k_{H\text{-}ADS}$ / $k_{H\text{-}DES}$)

L = ratio of catalyst surface area per unit volume fluid [m^2 / m^3]

L = d_p / 6 = characteristic length of the catalyst [m]

LA = lactic acid

M = mannose

M_{SA} = Metal surface area [m^2 / g sample]

MO = mannitol

N = stirring speed [s^{-1}]

N_{min} = minimum stirring speed for catalyst suspension [rotations / sec]

P = pressure

P = partial pressure of solute (H_2) in the gas phase

P_{H2} = hydrogen pressure

PA = pyruvaldehyde

PG = propylene glycol

r = reaction rate [mol / L · s]

$r_{H2\text{-}ADS}$ = rate of hydrogen adsorption

$-r_{SO} = \frac{dC_{SO}}{dt}$ = Rate of sorbitol dehydrogenation [mol / liter / hr]

R = Ideal gas constant [J / mol / K]

R = reaction rate

$-R_G$ = observed reaction rate of the species [kmol / m^3 · s]

Re_L = Reynolds number of the liquid phase = $\frac{U_L \rho_L d_P}{\mu_L (1-\varepsilon_B)}$ [dimensionless]

S_1, S1 = catalytic site – type 1

S_2, S2 = catalytic site – type 2

S_p = External surface area of the catalyst

S_T = surface tension [N / m]

SF_{calc} = Atoms of metal per molecule of adsorbed gas

Sh = Sherwood number [dimensionless]

SO = sorbitol

t = time

T = Temperature [K]

u_G = gas velocity [m / s]

U_L = Superficial liquid velocity [m/s]

V = y-int. of linear best fit for adsorbed volume per gram vs. P [cm^3 gas/g metal]

V_L = volume of the solution [cm^3]

V_p = Volume of the catalyst

w' = catalyst loading [grams catalyst per 100 grams solution]

Weight % = Weight fraction of catalyst that is metal [dimensionless]

x = mole fraction of solute (H_2) in liquid phase

Z = Length of the catalyst bed [m]

Greek:

β = constant determined by impeller geometry

ΔP = Pressure drop through the catalyst [N/m^2]

ε = support porosity [0.6 for the catalyst]

ε_B = Packed-bed void per reactor volume (bed porosity) [dimensionless]

η_{CE} = Wetting efficiency [dimensionless]

$\eta\Phi^2$ = observable modulus

μ_L = Liquid viscosity $[\frac{kg}{m \cdot s}]$

ρ_L = Density of the liquid phase [kg/m^3]

ρ_p = particle density [kg / m^3]

Φ_s = $(6 / d_p) / (S_p / V_p)$ = Sphericity of the catalyst

Chapter 1 - Introduction

1.1 Background

The Miller group at Michigan State University focuses on the evolving technology of renewable resource refining. We seek to produce commodity chemicals from readily available bio-based feedstock. Recent group members studied itaconic acid production[1], lactic acid hydrogenation to propylene glycol[2], stereoretentive amino alcohol synthesis[3], and the processing of sugar alcohols to value-added polyols[4], which provides the thrust of this research.

Previous work focused mainly on hydrogenolysis as the chemistry of choice to produce C_3 polyols, such as glycerol and propylene glycol, from sorbitol and xylitol feedstocks. Using a continuous trickle-bed reactor, Chopade et al.[4] produced these C_3 products with better selectivity and yield than previously reported. The study optimized reactor conditions to achieve these improved results. It did not include, however, insight into the mechanisms of the reaction or reasoning on why yields improved with specific changes to the reaction environment. The research presented delves into the underlying chemistries of hydrogenolysis yielding a deeper understanding of the reaction and alternatives for processing sugars at milder conditions to desired products.

As an introduction to the molecules of interest, Figure 1-1 illustrates desired products of the reactions as well as key intermediates necessary for elevated C_3 yields. *Figure* 1-2 provides illustrations of the monosaccharides and sugar alcohols used as

---

[1] Hogle B. et al., *Ind. Eng. Chem. Res.*, **2001**, *41*, 2069-2073
[2] Zhang, Z. et al., *Appl. Cat. A: Gen.*, **2001**, *219*, 89-98
[3] Jere, F.T., *Org. Lett.*, **2003**, *5*, 527-530
[4] Chopade, S. et al., U.S. Patent 6,291,725, 2001

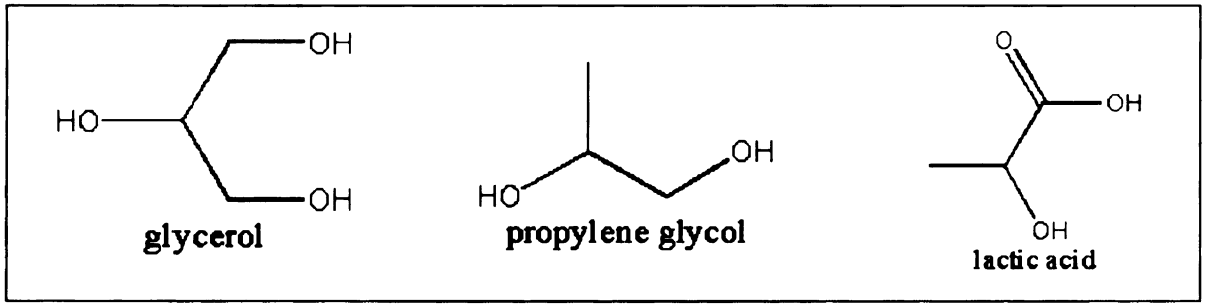

Desired C_3 products

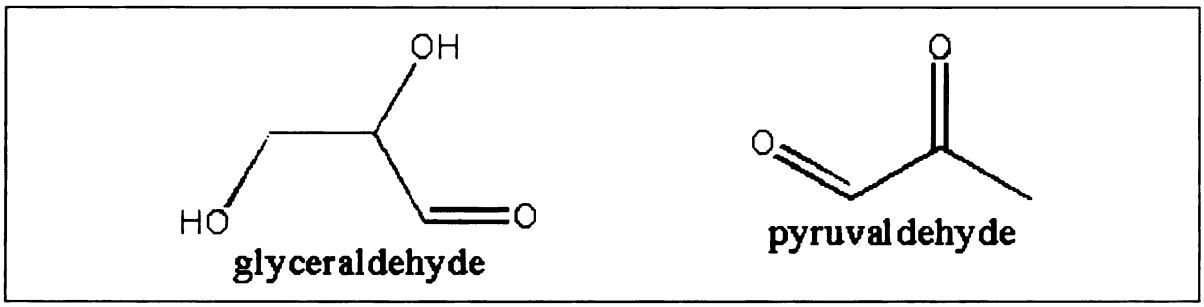

Key C_3 intermediates

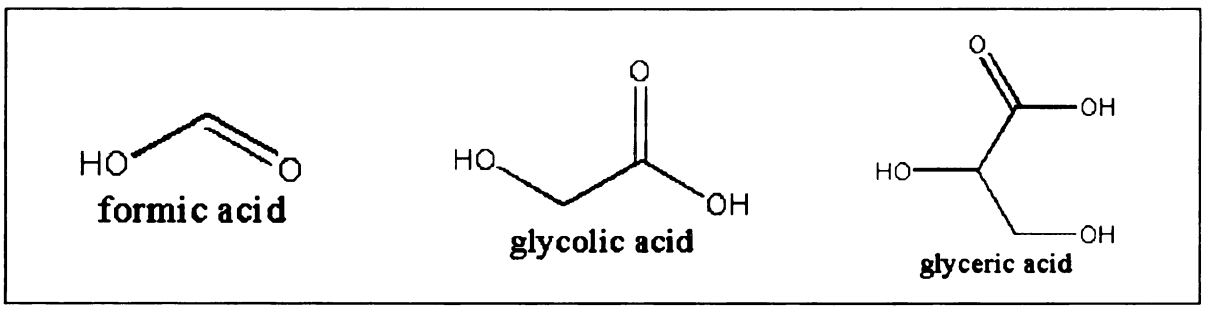

Organic acids formed during reaction

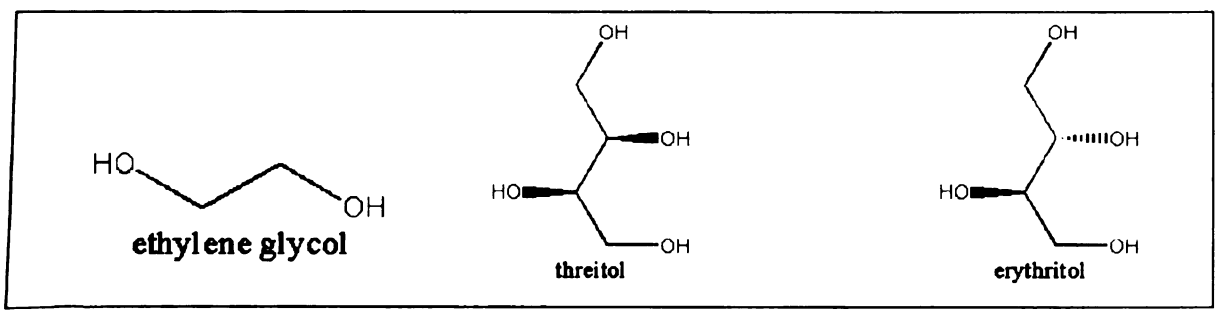

Other polyols formed during reaction

Figure 1-1: Key molecules formed during reaction

feedstock and that form during these reactions. These molecules will be referred to during the course of this dissertation and are provided here as a reference.

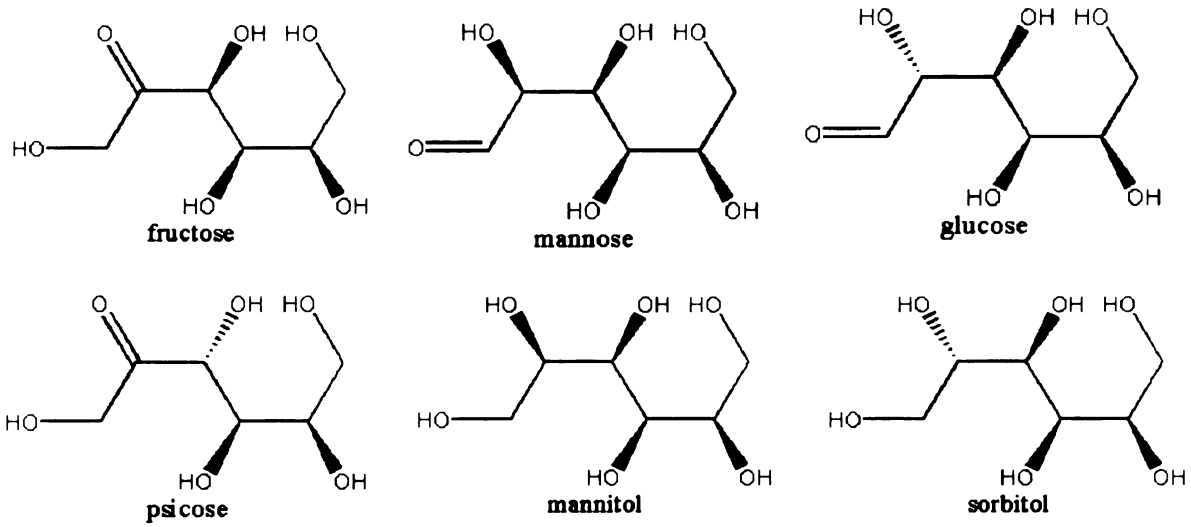

Figure 1-2: Sugars and sugar alcohols of interest as feedstock and reaction intermediates

1.2 Significance

Finding alternatives to petroleum-derived feedstocks for commodity chemical production is the main driver of this research. Petroleum is the carbon source of choice for virtually all organic chemicals[5]. Crude oil supplies, however, appear to be waning in light of increasing global demand. At current usage and production rates, it is estimated that known reserves of petroleum will be depleted in approximately 40 years,[6] although an exact timetable is debatable.[6,7,8] As a result, the U.S. government is supporting initiatives to decrease oil dependence[9], which includes this work.

[5] The American Chemical Society, *Technology Vision 2020: The U.S. Chemical Industry*, July 2001
[6] British Petroleum, *BP Statistical Review of World Energy*, June 2003
[7] British Petroleum, *BP Statistical Review of World Energy*, June 2002
[8] British Petroleum, *BP Statistical Review of World Energy*, June 2001
[9] Biomass Technical Advisory Committee, *Vision for Bioenergy and Biobased Products in the United States*, October 2002

Another interest in this research is the economic potential of converting simple sugars into value-added polyols. Propylene glycol and glycerol sell for $0.65 and $0.75 per pound[10] respectively while sugars are available at $0.06 - $0.12 per pound depending on the degree of refinement[11]. Annual U.S. demand for propylene glycol and glycerol is approximately one billion pounds[12] and 500 million pounds[13] respectively, leaving sizeable markets available. If this technology is successful, it has the advantage of an "environmentally friendly" label as well as a more stable source of carbon.

The specific thrust of this work is to continue development of sugar refining technologies and improve them to produce high yields of C_3 products (i.e. >75% of carbon fed to desired products). The research reported here shows potential improvement on existing technologies as well as an important shift in focus on the reaction environment. Literature regarding hydrogenolysis focuses on C_3 product selectivity and yield instead of the specific mechanistic information necessary to understand the underlying chemistries. This study demonstrates, on the other hand, that hydrogenolysis is actually the combination of three chemistries: dehydrogenation, alkaline degradation, and hydrogenation. With this in mind, we define the effects of these chemistries and produce an improved picture of how the reactants interact.

[10] *Chemical Market Reporter*, **March 15, 2004**, *265*
[11] http://ers.usda.gov/briefing/sugar/Data/data.htm, viewed on August 27, 2004, last update July 13, 2004
[12] *Chemical Market Reporter*, **September 24, 2001**, *260*
[13] *Chemical Market Reporter*, **December 17, 2001**, *260*

1.3 Literature Review

1.3.1 Hydrogenation

Hydrogenation is the addition of gaseous hydrogen to saturate a double bond (e.g. C = O or C = C).[14] Reactions typically require the use of catalyst with a supported metal, such as nickel or platinum, at elevated temperatures (300-350°C) and hydrogen pressures (500-3000 psi) for the addition to occur. Hydrogenation is used extensively in petroleum processing to remove sulfur and nitrogen from oil (hydrotreating), to form lower boiling point compounds from long carbon chain hydrocarbons by cleaving the molecule (hydrocracking), and a number of other reactions.[15] Of particular interest to this work are liquid phase hydrogenations to value-added products from biomass-derived materials.

Bowden and Adkins[16] described ester hydrogenation using a copper chromate catalyst at 250°C and 150-200 atm of H_2 pressure. Although using mainly phenyl esters as reactants, the authors reported hydrogenation (more accurately, hydrogenolysis) of butyl lactate to 1,2-propylene glycol (PG) with 81% yield. Among the substrates studied, 1,2 PG example was unique, compared to the other hydrogenation products, in that it did not maintain optical activity of the feedstock. More recently, Jere et al.[3] found that the loss of chirality was an effect of elevated temperature and not a direct result of reducing the carboxylic acid to an alcohol in their work with alanine, a similarly α-substituted chiral compound.

---

[14] Vollhardt, K. Peter C. and Schore, N.E., *Organic Chemistry*, 2nd Edition, p. 250, W.H. Freeman and Company, New York, 1995

[15] Kroschwitz, J.; Howe-Grant, M., editors, *Kirk-Othmer Encyclopedia of chemical technology*, 4th Edition, **18**, pp. 446-447, Wiley, New York, 1992

[16] Bowden, E.; Adkins, H., *J. Am. Chem. Soc.*, **1934**, *56*, 689-691

Adkins and Pavlic[17] continued work studying ester hydrogenation over Raney nickel in non-aqueous solvent, namely dry ethanol, noting lower temperatures of 25-75°C and similar pressures (150-200 atm) for hydrogenation of amino acid esters. Another paper on ester hydrogenation[18] showed that high loadings of catalyst benefit product yields by lowering the reaction temperature and thus, limiting side product formation. With this work, near quantitative yields of 1,2 PG from ethyl lactate as well as 1,3 diols from malonic acid derivatives were observed.

Carnahan et al.[19] demonstrated the reducing ability of ruthenium (as RuO_2 and Ru/C) at lower temperatures than previous catalysts. Succinic, glycolic, adipic, acetic, and oxalic acid were hydrogenated to their corresponding glycols with yields of 47-80% at temperatures of 140-160°C and H_2 pressures as high as 1000 atm. While these reactions ran at temperatures comparable to those described by Adkins, ruthenium allowed for direct hydrogenation of carboxylic acids instead of their esters. Zhang et al.[2] extended this use of ruthenium to the direct hydrogenation of lactic acid to 1,2 PG, in batch-wise and continuous fashion, with yields in excess of 90% at reduced temperature (130°C) and pressure (70-140 atm).

A number of papers cover the hydrogenation of sugars to sugar alcohols, which is of immediate interest to the research at hand. The Kirk-Othmer handbook[20] describes sorbitol production through batch or continuous hydrogenation of glucose using nickel or Raney nickel as a catalyst. Wisniak et al.[21,22,23] described xylose, glucose, and fructose

---

[17] Adkins, H.; Pavlic, A.A., *J. Am. Chem. Soc.*, **1947**, *69*, 3039-3041
[18] Adkins, H.; Billica, H.R., *J. Am. Chem. Soc.*, **1948**, *70*, 3121-3125
[19] Carnahan, J.E. et al., *J. Am. Chem. Soc.*, **1955**, *77*, 3766-3768
[20] Kroschwitz, J.; Howe-Grant, M., editors, *Kirk-Othmer Encyclopedia of chemical technology*, 4th Edition, **23**, pp. 105-106, Wiley, New York, 1992
[21] Wisniak, J.et al., *Ind. Eng. Chem. Prod. Res. Develop.*, **1974**, *13 (1)*, 75-79
[22] Wisniak, J.; Hershkowitz, M.; Stein, S., *Ind. Eng. Chem. Prod. Res Develop.*, **1974**, *13 (4)*, 232-236

hydrogenation over ruthenium, platinum, Raney nickel, rhodium, and palladium for comparison of activity as well as kinetic studies. Papers by Brahme and Doraiswamy[24], Verma and Gehlaway[25], and van Gorp et al.[26] gave similar accounts of reaction conditions and catalysts utilized. Cerino et al.[27] explored the use of promoters to improve the activity of Raney nickel and combat the common problem of leached metal in the product stream. Guo et al.[28] used a Cr promoter on a Ru-B amorphous catalyst in order to improve activity as well.

Hegedüs et al.[29] attempted selective hydrogenation of fructose to mannitol using a supported copper catalyst and the addition of sodium borate to the reaction. The borate was thought to interact with fructose to form the β-furanose form of the sugar which is more selective toward mannitol. Yields for mannitol were as high as 80% with the drawback of extended reaction times due to inhibition from the borate ions. Heinen et al.[30] pursued selective hydrogenation to mannitol as well by promoting Pt/C and Pd/C catalysts with tin for a mannitol yield of 63%.

Mikkola et al.[31] discussed the effects of solvent properties on xylose hydrogenation. Of particular interest was the balance of organic and aqueous solvent. Water was favorable due to high sugar solubility but organic solutions provided much

---

[23] Wisniak, J.; Simon, R.; *Ind. Eng. Chem. Prod. Res. Dev.*, **1979**, *18 (1)*, 50-57
[24] Brahme, P.H.; Doraiswamy, L.K.; *Ind. Eng. Chem., Process Des. Dev.*, **1976**, *15 (1)*, 130-137
[25] Verma, R.; Gehlawat, J.K.; *J. Chem. Tech. Biotechnol.*, **1989**, *46*, 295-301
[26] van Gorp, K. et al., *Cat. Today*, **1999**, *52*, 349-361
[27] Cerino, P.J.; Fleche, G.; Gallezot, P.; Salome, J.P., *Heterogeneous Catalysis and Fine Chemicals II: proceedings of the 2nd international symposium, Poitiers, October 2-5, 1990*, pp. 231-236, Guisnet M. et al. (editors), Elsevier, Amsterdam; New York, 1991
[28] Guo, H.; Li, H.; Xu, Y.; Wang, M., *Mater. Lett.*, **2002**, *57*, 392-398
[29] Hegedüs, M.; Göbölös, S.; Margitfalvi, J.L., *Heterogenous Catalysis and Fine Chemicals III: proceedings of the 3rd international symposium, Poitiers, April 5-8, 1993*, pp. 187-194, Guisnet, M. et al. (editors), Elsevier, Amsterdam; New York, 1993
[30] Heinen, A.W.; Peters, J.A.; van Bekkum, H., *Carbohyd. Res.*, **2000**, *328*, 449-457
[31] Mikkola, J.-P. et al., *J. Chem. Tech. and Biotech.*, **2001**, *76*, 90-100

higher hydrogen solubility allowing for higher hydrogenation rates. The authors offered an example with an 80:20 water/ethanol blend leading to an approximate 3-fold increase in hydrogenation activity with respect to aqueous media. Further, they noted that solutions above 30% ethanol led to precipitation of sugar at the desired loadings.

A final paper of note from Kusserow et al.[32] describes hydrogenation of glucose using nickel and ruthenium dispersed in molecular sieves. The yield of sorbitol was unimpressive at < 10%, but smaller molecules, such as acrolein, hydrogenate easily. This preference toward smaller, linear molecules may prove useful for hydrogenation of alkaline degradation products (see Section 1.3.3) to glycerol and PG without the competitive formation of sorbitol and mannitol.

1.3.2 Hydrogenolysis

The term hydrogenolysis was coined by Ellis[33] as an extension of other similar reactions, such as hydrolysis, where a bond is broken and then hydrogen is added to the fragments. As an example, Figure 1-3 illustrates sorbitol hydrogenolysis with potential products depending on where the carbon chain is broken. Literature results for hydrogenolysis and alkaline degradation are reported in terms of selectivity and yield. Selectivity is the number of moles of product formed per mole of reactant converted while yield is the number of moles of product per mole of reactant fed to the reaction. All desired products are C_3 compounds (propylene glycol, glycerol, lactic acid). This gives a theoretical maximum for selectivity and yield of 2.0 for C_6 feedstock (glucose, sorbitol, etc.) and 1.0 for C_5 feedstock (xylose, xylitol, etc) based on the carbon available for the reaction.

---

[32] Kusserow, B.; Schimpf, S.; Claus, P., *Adv. Synth. Catal.*, **2003**, *345*, 289-299
[33] Ellis, C., *Hydrogenation of Organic Substances*, 3rd Ed., D. Van Nostrand Company, New York, 1930

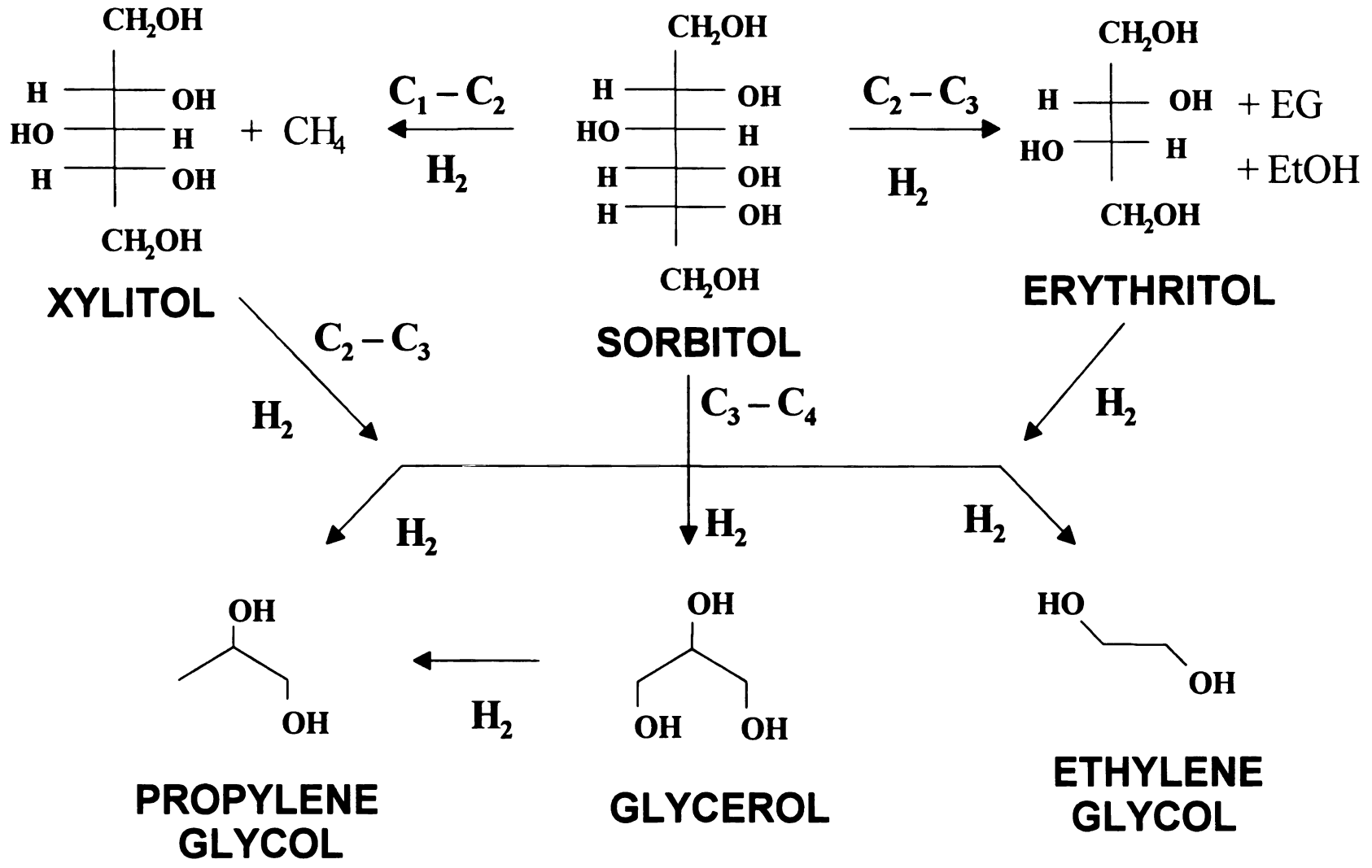

Figure 1-3: Pathways of sorbitol hydrogenolysis

Connor and Adkins[34] conducted hydrogenolysis experiments using a Cu/CrO_x catalyst at 250°C and 2600 psig H_2 on over 70 compounds. These runs included glycerol and mannitol showing 85% and 24% selectivity to PG respectively. Natta et al.[35] with a Cu/CrO_x catalyst used glucose in non-aqueous solvents, namely methanol and ethanol, to form PG with yields as high as 71% at 270°C and 2800 psig H_2. Clark[36] focused on glycerol production using sorbitol as the starting material in aqueous media. The author reported selective carbon chain cleavage at C3-C4 and demonstrated yields of 40%, 17%, and 16% of glycerol, PG, and EG, respectively, using a Ni/Kieselguhr catalyst at 215°C and 2000 psig. Van Ling et al.[37] compared C_3 product distribution of sugar hydrogenolysis and alkaline degradation of sugars (alkaline degradation – see Section 1.3.3). The authors observed similar selectivity to lactic acid, for alkaline degradation, and PG/glycerol, for hydrogenolysis, which confirmed that both reactions use similar pathways to product formation. Sohounloue et al.[38] compared hydrogenolysis of sorbitol at different temperatures and base concentrations (180 – 240°C, pH = 8.5 – 12.5) in aqueous media. The authors reported that elevated $Ca(OH)_2$ loading doubled the reaction rate, higher temperatures under basic conditions (pH = 12.5) increased C_3 selectivity, Ru/SiO_2 showed ten times the activity of Raney nickel, and an activation energy for sorbitol disappearance of 13-16 kcal/mol. Montassier et al.[39] reported 86% selectivity to PG from glycerol using a Raney copper in neutral conditions and a 15/85 split to PG and

---

[34] Connor, R.; Adkins, H., *J. Am. Chem. Soc.*, **1932**, *54*, 4678-4690
[35] Natta, G.; Rigamonti, R.; Beati, E., *Berichte D. Chem. Gesellschaft*, **1943**, *76B*, 641-656
[36] Clark, I., *Ind. Eng. Chem.*, **1958**, *50 (8)*, 1125-1126
[37] van Ling, G.; Vlugter, J., *J. of App. Chem.*, **1969**, *19*, 43-45
[38] Sohounloue, D. et al., *React. Kin. Catal. Lett.*, **1983**, *22 (3-4)*, 391-397
[39] Montassier, C. et al., *Bull. Soc. Chim.*, **1989**, *126 (2)*, 148-155

lactic acid at pH = 14, respectively. Müller et al.[40] demonstrated the use of Ru/C as a hydrogenolysis catalyst. Mannitol feedstock formed glycerol and propylene glycol with 56% yield while fructose yielded 48% to the two products.

Montassier et al.[41] explored the use of a sulfur-modified Ru/C to improve PG selectivity with glycerol hydrogenolysis. Glycerol to PG showed 79% selectivity compared to 91% observed with Raney copper. Xylitol and sorbitol are also mentioned as hydrogenolysis feedstocks. The authors observe C2-C3 cleavage of xylitol with 86% selectivity and 64% selectivity to PG and glycerol with sorbitol.

A number of patents also report conversion of sugar alcohols to C_3 products. Table 1-1 summarizes the product distribution from these runs as well as reaction conditions. Larcher[42] reports a yield of 44 wt% PG from a two step process of glucose hydrogenation and subsequent hydrogenolysis with a Ni/CrO_x catalyst at 275°C and 3000 psig H_2. Rothrock[43] continued this work with similar conditions and added $CaCO_3$ to increase the pH to 10 yielding 28% glycerol and 37% EG/PG. Conradin et al.[44,45,46] used a Ni/kieselguhr catalyst to explore the effect of higher hydrogen pressures and elevated pH. Hydrogenolysis of cane sugar (sucrose) yielded 32% glycerol, 15% EG, and 21% PG. Kasehagen[47] demonstrated 60% selectivity toward glycerol using Ni/Fe/Cu supported on diatomaceous earth in a continuous reactor design. Sirkar[48,49] and Chao et

---

[40] Müller, P.; Rimmelin, P.; Hindermann, J.; Kieffer, R.; Kiennemann, A.; Carré, J., *Heterogeneous Catalysis and Fine Chemicals II*, Guisnet M. et al. (Editors), Elsevier Science Publishers B.V., Amsterdam, 1991
[41] Montassier, C. et al., *J. of Mol. Catal.*, **1991**, *70 (1)*, 99-110
[42] Larchar, A., U.S. Patent 1,963,997, 1934
[43] Rothrock, H., U.S. Patent 2,004,135, 1935
[44] Conradin, F. et al, U.S. Patent 2,852,570, 1958
[45] Conradin, F. et al, U.S. Patent 2,965,679, 1960
[46] Conradin, F. et al, U.S. Patent 3,030,429, 1962
[47] Kasehagen, L., U.S. Patent 3,396,199, 1968
[48] Sirkar, U.S. Patent 4,338,472, 1982

al.[50] used a Ni/SiO_2 catalyst and CaO promoter for glycerol selectivity of 70 wt%. The catalyst however deactivated over time requiring replacement or additional reduction. Arena[51] observed 69% selectivity to glycerol and PG from sorbitol reacted with Ru/SiO_x impregnated with Ti and BaO added as a base promoter. Tanikella[52] produced PG and EG with 40% and 35% selectivity, respectively, using xylitol as a feedstock in a non-aqueous solvent. Dubeck et al.[53,54] modified a Ru/C catalyst with sulfur to increase PG selectivity to 65%. These studies report the highest PG selectivity of the literature reviewed. Andrews and Klaeren[55] introduced the use of a soluble catalyst, $H_2Ru(PPh)_4$, for hydrogenolysis of fructose and demonstrated selectivity to glycerol and EG at 38% and 8% respectively. Gubitosa et al.[56,57,58,59,60] focus on using a trickle-bed reactor and developing catalyst. The authors discuss higher selectivity to C_3 compounds with higher base/sorbitol ratio and demonstrate selectivity to PG – 53%, glycerol – 2%, and lactic acid – 4% and total C_3 selectivity of 59%. Chopade et al.[4] with use of a trickle-bed reactor demonstrate C2-C3 bond cleavage of xylitol with 85% selectivity producing PG and EG with 70% and 68% selectivity respectively. In addition, the authors demonstrated similar C_3 selectivity (58%) as Gubitosa et al.[54] using sorbitol as a feedstock.

---

[49] Sirkar, A., U.S. Patent 4,380,678, 1983
[50] Chao, J.; Hulbers, D., U.S. Patent 4,366,332, 1982
[51] Arena, B., U.S. Patent 4,401,823, 1983
[52] Tanikella, M., U.S. Patent 4,404,411, 1983
[53] Dubeck, M.; Knapp, G., U.S. Patent 4,430,253, 1984
[54] Dubeck, M.; Knapp, G., U.S. Patent 4,476,331, 1984
[55] Andrews, M.; Klaeren, S., U.S. Patent 5,026,927, 1991
[56] Gubitosa, G.; Casale, C., U.S. Patent 5,326,912, 1994
[57] Gubitosa, G.; Casale, C., U.S. Patent 5,354,914, 1994
[58] Gubitosa, G.; Casale, C., U.S. Patent 5,403,805, 1995
[59] Gubitosa, G.; Casale, C., U.S. Patent 5,543,379, 1996
[60] Gubitosa, G.; Casale, C., U.S. Patent 5,600,028, 1997

Table 1-1: Hydrogenolysis Patents

U.S. Patent (Year)	Authors (Assignee)	Catalyst	Base	T (°C)	P (psi)	Significance
1,963,997 (1934)	Larchar (DuPont)	Ni-CrO_x	None	275	3000	First patent for hydrogenolysis of sugars and sugar alcohols
2,004,135 (1935)	Rothrock (DuPont)	Ni-CrO_x	$CaCO_3$ pH = 12	250	3300-4400	Improvement of Larcher with use of base
2,965,679 (1960)	Conradin et al. (Inventa A.G.)	Ni/Kieselguhr	CaO pH = 11	220	1500-11700	High H_2 showed inhibiting effect on reaction
2,868,847 (1959)	Boyers (Engelhard)	Ru/C	None	130	1000	Ru as hydrogenation catalyst
3,396,199 (1968)	Kasehagen (Allied Chemicals)	Ni/Fe/Cu on diatomaceous earth	CaO pH ~ 13	210	2000	Yield of 42 wt% glycerol
4,338,472 (1982)	Sirkar (HRI, Inc.)	Ni/Kieselguhr	$Ca(OH)_2$ pH ~ 13	230	1200-2000	Yield of 70% glycerol, but catalyst deactivated quickly
4,496,780 (1985)	Arena (UOP, Inc.)	Ru / Ti-Al_2O_3	BaO pH ~ 13	180	3200	69% selectivity to glycerol and PG. Ru as catalyst.
4,404,411 (1983)	Tanikella (Du Pont)	Ni / Si-AlO_x	Alkali alkoxide	275	4000	Use of non-aq solvent and heavy base concentrations (20 mol%). Focused on xylitol feedstock.
4,430,253 (1984)	Dubeck (Ethyl Corp.)	Ru/C with $Na_2S{\cdot}9H_2O$	CaO pH ~ 14	250	2400-3300	65% selectivity to PG – highest seen in literature.
5,026,927 (1991)	Andrews et al. (Brookhaven Nat. Labs)	$H_2Ru(PPh_3)_4$	KOH	100	300	Homogenous catalyst. Much milder conditions.
5,210,335 (1993)	Schuster et al. (BASF)	Co/Cu/MnO_x	None	250	4000	Claims 60% yield of PG. Closer to 42% with loss of gases taken into account.
5,403,805 (1995)	Gubitosa et al. (Montecatini Tech.)	Ru/C	NaOH pH = 11	225	2200	Continuous fixed bed reactor. C_3 selectivity at 59%
6,291,725 (2001)	Chopade et al. (MSU)	Ru/C	KOH pH ~ 13	230	1200	85% C2-C3 cleavage selectivity with xylitol. 58% C_3 selectivity with sorbitol.

1.3.3 Alkaline degradation

Lobry de Bruyn and Alberda van Ekenstein[61,62] first noted the isomerization of sugars in their classic papers from the 1890s. They stated that mannose, glucose, and fructose interconvert while in basic media. Nef[63] furthered this notion by also noting the presence of enediol intermediates and numerous products formed from base-catalyzed cleaving. Evans et al.[64] added to the list of sugars involved with isomerization and observe a significant presence of pyruvaldehyde as an intermediate, which converts easily to lactic acid in alkaline media as noted by Denis[65]. Shaffer and Friedemann[66] continued mechanistic work by mapping out Nef's suggestions as well as focusing on lactic acid production. They noted that higher concentrations of base promote lactic acid formation while lower concentrations favor dihydroxyacetone. Two patents also focused on lactic acid production directly from sugars. Braun[67] noted 72-75% yield of lactic acid recovered as a zinc salt from cane sugar (sucrose) while Lock[68] observed 67% yield. Yield to lactic acid is quite good for these methods, but the processes are not amenable to scale-up. Lock suggests dropwise addition of sugar to boiling caustic while Braun uses temperatures in the range of 210-220°C both of which are unfavorable. Table 1-2 summarizes the conditions and yields for the technologies explored.

---

[61] de Bruyn, C. A. L., *Recl. Trav. Chem. Pays-Bas*, **1895**, *14*, 156-165
[62] de Bruyn C. A. L.; van Ekenstein, W. A., *Recl. Trav. Chem. Pays-Bas*, **1895**, *14*, 203-216
[63] Nef, J., *Ann.*, **1907**, *357*, 294-312
[64] Evans, W. L.; Edgar, R. H.; Hoff, G. P., *J. Am. Chem. Soc.*, **1926**, *48*, 2665-2677
[65] Denis, W. *Am. Chem. J.*, **1907**, *38*, 561-594
[66] Shaffer, P. A.; Friedemann, T. E., *J. of Biol. Chem.*, **1930**, *86*, 345-375
[67] Braun, G., U.S. Patent 2,024,565, 1935
[68] Lock, R. H., U.S. Patent 2,382,889, 1945

Table 1-2: Summary of prior art for lactic acid production via alkaline degradation

Sugar Conc.	Base Conc.	Temp (°C)	Conv. (%)	Time	LA Yield (%)	Ref.
0.55 M [1]	5.0 M [a]	37 + 65*	100	18+7 days	50	66
2.0 M [1]	6.0 M [a]	37 + 65*	100	18+7 days	40	66
1.2 M [2]	2.65 M [b]	210-220	100	~2 hours	72-75	67
0.75 M [3]	8.0 M [a]	100	~100	4 hours	67	68
1.8 M [4]	0.45 M [a]	225	61	2 hours	17	69**
1.8 M [4]	0.45 M [a]	225	8	2 hours	3	69**
2.29 M [2]	2.6 M [c]	251-260	100	2.5 hours	47	70
2.29 M [2]	2.6 M [c]	234-238	100	7.5 hours	47	70
2.29 M [2]	2.8 M [c]	234-239	100	7.5 hours	44	70

[1] glucose - [2] cane sugar - [3] sucrose - [4] sorbitol
[a] NaOH - [b] $Ca(OH)_2$ - [c] CaO
* Reaction time was 18 days at 37°C and then 7 days at 65°C
** Reactions used 5% Ru/C to cleave sorbitol under nitrogen

In general, larger base to sugar ratios improved lactic acid yield. Lower temperatures (37°C) slowed the alkaline degradation pathways significantly without the benefit of improved yield to lactic acid. Temperatures of 230-260°C converted the sugars much more readily, but only at the same yields of 40-50%. High base to sugar ratios combined with relatively moderate temperatures (100 – 210°C) led to the highest yields of around 70%.

Work continued with improved mechanisms and calculated rate constants. MacLaurin and Green[71] presented a simple model for isomerization and degradation of glucose, fructose, and mannose to acidic products. They used first order equations with respect to sugar concentration to calculate rate constants. Their results showed that fructose degraded to products an order of magnitude faster than glucose and mannose. de

[69] Tronconi, E. et al., *Chem. Eng. Sci.*, **1992**, *47 (9-11)*, 2451-2456
[70] Montgomery R.; Ranca, R. A., *Ind. Eng. Chem.*, **1953**, *45 (5)*, 1136-1147
[71] MacLaurin, D. J.; Green, J. W., *Can. J. Chem.*, **1969**, *47*, 3947-3955

Wit et al.[72] estimated the kinetics of enediol formation using a UV cuvette and noted intermediate evolution versus time. They also suggested the following mechanism for alkaline degradation:

sugar + OH^- ↔ sugar anion ↔ enediol anion ↔ β-elimination ↔ degradation products

For added completeness, de Bruijn et al. introduced a series of papers[73,74,75,76,77,78] looking at multiple aspects of alkaline degradation. One paper inspected the effect of reaction parameters on the product distribution[71]. They outline the following results:

- C_3 selectivity improved and $>C_6$ acid formation reduced with higher hydroxide concentrations and lower sugar concentrations
- Ca^{2+} promoted lactic acid pathways
- Temperature had no effect on product distribution from 50-90°C

Another paper[73] added psicose as an important sugar intermediate within the degradation mechanism and included kinetic rates of isomerization and cleavage reactions. An additional paper[75] summarized several chemistries occurring in the alkaline environment and describes their contribution to the overall product distribution. The same from Delft University later published a comprehensive review of alkaline degradation[79] summarizing their work as well as providing ample background on the technology.

1.4 Summary

Yields to C_3 products from biomass-derived feedstock are currently at about 60%. The literature shows that hydrogenolysis of sorbitol has the best prospects of becoming commercially viable, based on C_3 yields and possibilities for continuous processes. High

---

[72] de Wit, G.; Kieboom, A. P. G.; van Bekkum, H., *Carbohyd. Res.*, **1979**, *74*, 157-175
[73] de Bruijn, J. M.; Kieboom, A. P. G.; van Bekkum, H., *Recl. Trav. Chim. Pays-Bas*, **1986**, *105*, 176-183
[74] de Bruijn, J. M., et al., *Int. Sugar Journal*, **1987**, *89 (1066)*, 194-210
[75] de Bruijn, J. M.; Kieboom, A. P. G.; van Bekkum, H., *Recl. Trav. Chim. Pays-Bas*, **1987**, *106*, 35-43
[76] de Bruijn, J. M.; Kieboom, A. P. G.; van Bekkum, *J. Carbohyd. Chem.*, **1986**, *5 (4)*, 561-569
[77] de Bruijn, J. M.; Kieboom, A. P. G.; van Bekkum, *Starch*, **1987**, *39 (1)*, 23-28
[78] de Bruijn, J. M.; Touwslager, F.; Kieboom, A. P. G.; van Bekkum, H., *Starch*, **1987**, *39 (2)*, 49-52
[79] de Bruijn, J. M.; Kieboom, A. P. G.; van Bekkum, *Sug. Tech. Rev.*, **1986**, *13*, 21-52

process temperatures, however, contribute to lower C_3 selectivity and yield due to the formation of gases. In addition, high process pressures (1000 psi and higher), while not prohibitive, are less than desirable for scale-up.

For this technology to be successful, the overall yield to propylene glycol, glycerol, and lactic acid needs to be around 75% in order to be competitive with current petroleum-based production methods. Hydrogenolysis and alkaline degradation alone are not sufficient to reach this goal. Understanding the reaction pathways that promote C_3 product formation for each chemistry, however, provides the potential for elevating C_3 yields to the desired levels.

Chapter 2 – Experimental Methods

2.1 Hydrogenolysis

2.1.1 Reactor set-up

Initial experiments with hydrogenolysis used a continuous trickle-bed reactor. The reactor consisted of a 2.5 cm inner diameter stainless steel tube packed with catalyst supported with a stainless steel screen. The column was heated using a PID controller (Omega) connected to heating tape wrapped around the reactor. A thermocouple placed in an axial thermowell provided temperature data to the controller. Liquid was fed to the column using an HPLC pump (Bio-Rad) and gas via mass flow controllers (Porter). To avoid channeling of the liquid feed, a 10 cm long distributor consisting of 2 mm glass beads was added at the top of the column. A back-pressure regulator (Tescom) maintained reaction pressure at the desired set point while mass flow controllers (MFCs) regulated the flow of hydrogen to the system. Rotameters and a buret with soap film measured the volumetric flow rate and allowed calibration of the MFCs. Liquid samples were collected via gas-liquid separation tanks to maintain continuous flow. Post-reactor vents also allowed for sampling of the gas for hydrocarbon production. Figure 2-1 provides a reactor schematic.

2.1.2 Materials for reaction

Sorbitol (99+% Aldrich), potassium hydroxide (85% Aldrich), and ultra-high purity hydrogen (99.999% AGA, BOC) were the main reactants for hydrogenolysis. Feedstock was prepared using HPLC grade water (J.T. Baker). Ultra-high purity helium (99.999% AGA, BOC) was used to purge the reactor and compressed air (21% O_2,

balance N_2 - AGA) was used to passivate the catalyst at the end of the reaction. All components were used without further purification.

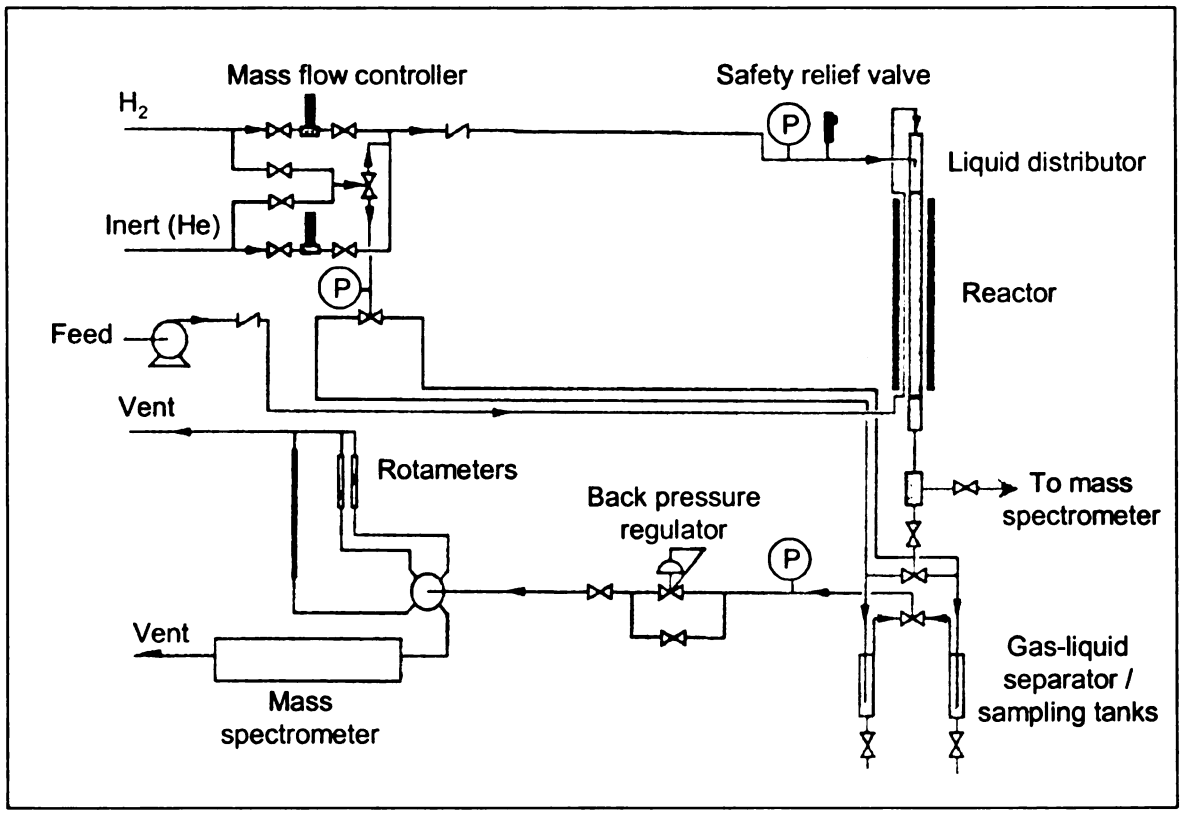

Figure 2-1: Schematic for continuous trickle-bed reactor

2.1.3 Operating procedures

Once the column was packed with the proper catalyst and sealed, the system was pressurized with helium to 1000 psig to detect leaks. When the pressure drop was less than 10 psig over the course of an hour, the reactor was vented and then pressurized again to 300 psig with hydrogen to begin pre-reduction of the catalyst. The column was heated to 150°C and maintained at that temperature for at least two hours. Once complete, the temperature was raised to the desired set point (typically 200-230°C), the column was pressurized with hydrogen (1000-1200 psig), and feedstock (1.5 M sorbitol and 0.18 M

KOH) was then added to the reactor at a rate of 0.3-0.4 mL/min to begin the reaction. Samples were taken periodically to observe the extent of reaction. Once the product distribution remained essentially the same from sample to sample (i.e. steady-state), temperature and/or pressure was adjusted for another set of conditions or the reactor was stopped. Upon completion of the experiment, the catalyst bed was flushed with water and passivated with oxygen.

2.1.4 Analysis

Liquid phase products were analyzed using high performance liquid chromatography (HPLC). Samples were passed through a 0.22 micron filter (Millipore) and then diluted to a 1 wt% basis (i.e. 0.1g of 25 wt% sorbitol solution diluted to 2.5 grams of solution) using 5 mM (0.005 M) sulfuric acid. An internal standard, 2-propanol, was added and the sample was injected into an Aminex HPX-87H column (Bio-Rad) at a temperature of 50°C and a mobile phase of 5 mM sulfuric acid flowing at 0.45 mL/min. Liquid phase products were detected using a refractive index detector (Refractomonitor IV, Thermo-Finnigan) and an ultra-violet detector (UV 3000, Thermo-Finnigan). The ultraviolet wavelength was set at 210 nm to detect unsaturated compounds, namely carboxylic acids. Data were compiled and analyzed using TSP-1000 software (Thermo-Finnigan).

2.2 Adsorption studies

2.2.1 Reactor set-up

Adsorption studies were carried out in a 300 mL batch reactor (Parr Instruments) with internal stirrer and a controller (Wadlow) that maintains temperature within 1°C and

agitation within 5 rpm. The reaction vessel is constructed of 316 stainless steel with an upper temperature limit of 350°C and a maximum allowable working pressure (MAWP) of 3000 psi. To remove samples periodically without disrupting the reaction, a sampling loop was attached. Reactions were agitated with a four-blade marine type impeller and baffles were added to enhance mixing.

2.2.2 Materials for reaction

Ruthenium sponge (-100 mesh, 99.9%, Aldrich) was the metal catalyst used for adsorption studies. Sorbitol (99+%, Aldrich) was the substrate of interest and potassium hydroxide (85+%, Aldrich) was used as well to study effects of pH. Solutions were prepared with HPLC grade water (J.T. Baker). The ruthenium was pre-reduced with UHP hydrogen (99.999%, AGA/BOC) and the reactor was pressurized with UHP helium (99.999%, AGA/BOC) during the adsorption experiment to provide an inert atmosphere. All compounds were used without further purification.

2.2.3 Operating procedures

2.2.3.1 Pre-reduction of catalyst

The ruthenium sponge (typically 10.0 grams) was pre-reduced before each reaction in order to activate the metal surface. Sponge was placed in the reactor, subsequently sealed, and then purged six times with hydrogen gas to remove air from the reaction. Once purged, the reactor was heated to 150°C and pressurized to 200 psig for at least one hour. After this time, the reactor was cooled and then purged with helium to prepare for the reaction.

2.2.3.2 Charging of the feedstock

Feedstock was prepared using sorbitol and HPLC grade water to form 100 grams of solution. Once prepared, helium was bubbled through the liquid to remove dissolved gases. The purged solution was then added to a clean charging vessel and purged again to remove air present in the vessel. The vessel was then connected to the reactor, pressurized, and opened to the reactor to transfer the feedstock solution. Using the charging vessel prevented the addition of oxygen to the reaction, which could deactivate the active catalytic sites on the metal.

2.2.3.3 Sampling

Liquid samples were removed during the reaction via a sample loop. A valve connected to a dip tube within the reactor was opened to place the sample loop in line. A three-way valve was opened to send the liquid sample into the holding area of the loop and closed. A third valve to the atmosphere was opened for sample collection. This process was repeated until 2-5 grams of material was collected. Afterward, the sample loop was blown out with air to remove excess liquid and catalyst by opening the three-way valve to a supply of compressed air.

2.2.4 Analysis

Liquid phase products were analyzed in the same matter as those described in Section 2.1.4. However, samples were not diluted due to low concentrations of organic products.

2.3 Alkaline degradation

2.3.1 Reactor set-up

Two types of alkaline degradation reactions were run: metal-catalyzed and base-catalyzed. The metal-catalyzed runs used ruthenium sponge to initiate carbon-carbon cleavage of saturated polyols, such as sorbitol and xylitol, to products. Base-catalyzed experiments used soluble base, mainly potassium hydroxide, to cleave carbon-carbon bonds in monosaccharides. Both were run in the batch reactor system as described in section 2.2.1.

2.3.2 Materials for reaction

2.3.2.1 Metal-catalyzed degradations

Metal-catalyzed degradation runs used ruthenium sponge (-100 mesh, 99.9%, Aldrich) for reactions. Sorbitol (99+%, Aldrich), xylitol (98%, Aldrich), and glycerol (99+% Aldrich) were used in these reactions. Potassium hydroxide (85+%, Aldrich) was the sole soluble base used in these studies. Solutions were prepared with HPLC grade water (J.T. Baker). Ultra high purity hydrogen (99.999%, AGA/BOC) was used to reduce the ruthenium metal and UHP helium (99.999%, AGA/BOC) served as the reaction gas phase. All compounds were used without further purification.

2.3.2.2 Base-catalyzed degradations

Glucose (99+%, Gibco BRL), fructose (99+%, Aldrich), mannose (99%, Aldrich), and xylose (99%, Aldrich) were the sugar substrates used for reactions with potassium hydroxide (85+%, Aldrich) as the soluble base. Solutions were prepared with HPLC

grade water (J.T. Baker); UHP helium (99.999%, AGA/BOC) served as the reaction gas phase. All compounds were used without further purification.

2.3.3 Operating procedures

2.3.3.1 Pre-reduction of catalyst

The ruthenium sponge used in these reactions was reduced in the same manner as described in Section 2.2.3.1.

2.3.3.2 Charging of the feedstock

Feedstock was prepared by weighing out reactant sugar and potassium hydroxide separately. HPLC grade water was then added to dissolve the sugar and potassium hydroxide separately. The two solutions were then mixed together and water was added to make 100 grams of solution. Once prepared, helium was bubbled through the liquid to remove dissolved gases and charged in the same manner as described in Section 2.2.3.2.

2.3.3.3 Sampling

Liquid samples were removed in the same manner as described in Section 2.2.3.3.

2.3.4 Analysis

Samples removed from the reactor were diluted to a 1 wt% basis of the reactant sugar with HPLC grade water or dilute sulfuric acid to lower the pH of the solution and reduce continued degradation reactions in the sample. Samples were analyzed within 45 minutes of removal from the reactor for true product distributions. Feedstocks with initial sugar concentrations of less than 1 wt% were not diluted. Product distribution was then determined using HPLC as previously described.

Product formation was also confirmed by using gas chromatography-mass spectroscopy (GC-MS). Samples were sent over to the MSU Mass Spectroscopy Facility for analysis. The polyols were dried and trimethylsilated using Bis(trimethylsilyl)trifluoroacetamide (BSTFA) and 1% trimethylchlorosilane (TMCS) as silylating agents with pyridine to remove water. Each product has a distinctive spectrum allowing confirmation of known products and identification of unknown compounds.

2.4 Alkaline degradation with hydrogenation

2.4.1 Reactor set-up

This set of reactions combined the chemistries of alkaline degradation and hydrogenation using a slightly modified version of the batch reactor system described in Section 2.2.1. The sample loop used for these experiments was shortened and had a larger tube diameter as well (1/4" from 1/8"). This allowed for shorter sampling times to minimize the time before analysis of the sample.

2.4.2 Materials for reaction

Several catalysts were used to promote hydrogenation during the reactions. These consisted of 5 wt% Pt/C (Aldrich), 5 wt% Pd/C (Aldrich), and 5 wt% Ru/C (Aldrich). Glucose (99+%, Gibco BRL), fructose (99+%, Aldrich), mannose (99%, Aldrich), and xylose (99%, Aldrich) were the sugar substrates used for reactions with potassium hydroxide (85+%, Aldrich) as the sole soluble base. Solutions were prepared with HPLC grade water (J.T. Baker). Ultra high purity hydrogen (99.999%, AGA/BOC) was used to reduce the catalysts and as a reactant gas. All compounds were used without further purification.

2.4.3 Operating procedures

2.4.3.1 Pre-reduction of catalyst

Of the catalysts used in these experiments, only the 5 wt% Ru/C required pre-reduction. Platinum and palladium return to the zero valence level readily when in the presence of hydrogen, while ruthenium requires high temperature and the presence of hydrogen for reduction. Ruthenium on carbon was placed in the reactor and then sealed. The system was purged six times with hydrogen, pressurized to 200 psig, and then heated to 230°C overnight (12-16 hours). The reactor was then vented and prepared for addition of the reactants.

2.4.3.2 Charging of the feedstock

To address reactivity of the sugar when base is present, the charging procedure was modified. The feedstock was charged in two parts to avoid conversion of the sugar before being added to the reactor. Potassium hydroxide solution was prepared and placed in the charging vessel. Hydrogen was used to pressurize the charging vessel from the bottom to allow hydrogen to bubble through the solution removing other dissolved gases. The vessel was then vented and the process was repeated twice more. Potassium hydroxide was charged to the reactor and heated to 5-7°C above the desired reaction temperature. The sugar feedstock was then fed to the charging vessel, purged in the same manner as potassium hydroxide, and charged to the reactor. The reactor was pressurized with hydrogen and the reaction medium was agitated to commence the run.

2.4.3.3 Sampling

Before each sample, the sample loop was washed with one to three grams of the reactor contents to remove any residual material from previous samples and ensure that fresh material from the reaction was analyzed. After washing, samples were taken in the manner described in Section 2.2.3.3.

2.4.4 Analysis

Samples removed from the reactor were filtered and diluted to a 1 wt% basis of the reactant sugar with 25 mM sulfuric acid to lower the pH of the sample and reduce sample degradation. This was done within ten minutes of drawing the sample. 5000 μL of the diluted material was measured out via pipetter and then 10 μL of 2-propanol added as an internal standard. The prepared sample was then injected to the HPLC column using an auto-injector (LDC/Milton Roy) within 45 minutes of when the sample was first drawn. Dilution and analysis of the samples was done quickly to avoid further degradation of the sample from base-catalyzed reactions. Refractive index and ultra-violet data were stored by computer for analysis using Star Chromatography software (Varian).

2.5 Selective hydrogenation of intermediates

2.5.1 Reactor set-up

These hydrogenations used the batch reactor system as described in Section 2.4.1.

2.5.2 Materials for reaction

2.5.2.1 C_3 versus C_6 selective hydrogenation

Two catalysts, 5 wt% Pt(Ge)/C (Engelhard Italia) and 3 wt% Pt(S)/C (Engelhard Italia), were used for these experiments. Glyceraldehyde dimer (99%, Aldrich) and glucose (99+%, Gibco BRL) were utilized for this study. Solutions were prepared with HPLC grade water (J.T. Baker). Ultra high purity hydrogen (99.999%, AGA/BOC) was used for reactions. All compounds were used without further purification.

2.5.2.2 Product inhibition of glyceraldehyde hydrogenation

The two platinum catalysts were used again for these experiments. Glyceraldehyde dimer (99%, Aldrich) was used as the primary reactant. Saturated products studied for inhibition were ethylene glycol (99%, Spectrum), propylene glycol (99.5%, Jade Scientific), glycerol (99+%, Aldrich), sorbitol (99%, Aldrich), and mannitol (99%, Aldrich). Solutions were prepared with HPLC grade water (J.T. Baker). Ultra high purity hydrogen (99.999%, AGA/BOC) was used for reactions. All compounds were used without further purification.

2.5.2.3 Alkaline degradation with hydrogenation

Materials used were the same as those of the previous alkaline degradation/hydrogenation studies (Section 2.4.2) with the exception of using the Pt(S)/C and Pt(Ge)/C catalysts.

2.5.3 Operating procedures

2.5.3.1 Pre-reduction of catalyst

Prior to reaction, the platinum catalysts were activated by purging the reactor six times with hydrogen. In addition, the catalyst was stirred with water overnight to rewet surfaces that may have dried out during storage to maintain proper activity.

2.5.3.2 Charging of the feedstock

Feedstock was charged in two parts to minimize time for the reactants to reach the desired temperature. The first charge consisted of solution prepared with non-reacting compounds. Table 2-1 below shows the three types of experiments and the order in which materials were charged.

Table 2-1: Order of charging the reactants for experiments

Experiment	1st charge (100 grams)	2nd charge (100 grams)
C_3 selective hydrogenation	Water	Glyceraldehyde plus sugar
Product inhibition	Inhibitor (Sorbitol, PG, etc.)	Glyceraldehyde
Alkaline degradation/ hydrogenation	KOH	Reactant sugar

2.5.3.3 Sampling

Samples were drawn in the same manner as that described in Section 2.4.3.3.

2.5.4 Analysis

2.5.4.1 C_3 versus C_6 selective hydrogenation

Samples were passed through a 0.22 micron filter (Millipore) to remove catalyst from the solution. Samples were not diluted due to relatively low concentrations of

glyceraldehyde or other compounds in the reaction (0.2 - 0.8 wt%). HPLC analysis was carried out as previously described in Section 2.4.4.

2.5.4.2 Product inhibition of glyceraldehyde hydrogenation

Analysis was performed as described in Section 2.5.4.1.

2.5.4.3 Alkaline degradation with hydrogenation

Analysis was performed as described in Section 2.4.4.

2.6 Conversion of carbohydrates to methane via hydrogenolysis

2.6.1 Reactor set-up

The batch reactor system described in Section 2.4.1 was used for these experiments.

2.6.2 Materials for reaction

Catalysts used for this set of reactions were 5 wt% Ru/C (PMC) and 3% Ru/TiO_2 (Degussa). Glucose (99+%, Gibco BRL), sorbitol (99+%, Aldrich), and glycerol (99%, Aldrich) were used for feedstock. Solutions were prepared with HPLC grade water (J.T. Baker). Ultra high purity hydrogen (99.999%, AGA/BOC) was used to reduce the catalysts and as a reactant gas. All compounds were used without further purification.

2.6.3 Operating procedures

2.6.3.1 Pre-reduction of catalyst

Before each experiment, catalyst was loaded into the reactor and sealed. The headspace was then flushed with hydrogen six times to remove air. Both types of

catalysts were pre-reduced overnight at 230°C under 300 psig of hydrogen and then cooled to room temperature. Feedstock was charged to the reactor after this point.

2.6.3.2 Charging of the feedstock

Feedstock was loaded into the charging vessel, purged three times with hydrogen, and then sent to the reactor. The headspace was vented to minimize the amount of hydrogen in the reactor and prevent premature conversion. The reactor was then heated to the desired temperature with mild agitation (~300 rpm). Once at temperature, the reactor was pressurized with hydrogen and agitated at 1000 rpm to begin the reaction.

2.6.3.3 Sampling

Gas samples were removed from the headspace and collected with a 7x7 Tedlar™ gas bag (DuPont) before the liquid sample was taken. The gas bag was filled once with reactor gas, emptied, and filled again to remove residual gas from the previous sample. Liquid samples were drawn in the same manner as those described in Section 2.4.3.3.

2.6.4 Analysis

Gas samples were analyzed using a Varian 3300 gas chromatograph using a Carbosieve SII column (Supleco). Temperatures for the injector and the thermal conductivity detector (TCD) were 250°C and 225°C respectively. The temperature program for the column was 35°C for two minutes followed by a 30°C / min ramp to 225°C. This temperature was held for 15 minutes and then the column was cooled for the next sample. Ultra high purity helium was the carrier gas and data were collected using Star Chromatography software (Varian).

Liquid samples were filtered to remove catalyst from the solution. The sample was then diluted with HPLC water to a 1 wt% basis of the reactant. HPLC analysis, as previously described in Section 2.4.4, was used for product identification.

2.7 Catalyst characterization

Catalysts used in the reactions of interest were characterized using a number of standard methods in order to compare them to other available catalysts and allow for proper replication of experiments. Mercury porosimetry[80] was used to determine pore volume of each catalyst as well as the pore size distribution throughout the particles. Surface area, as determined by the Brunauer-Emmett-Teller (BET) method[81], was also used as a comparative result. Chemisorption of carbon monoxide and hydrogen was used to calculate metal dispersion on the catalysts and served as the final method of characterization used in these studies.

2.7.1 Physisorption

Physisorption measurements, namely the BET method, provide a standard comparison of catalyst surface area between materials. It is also important when manufacturing catalysts to produce consistent supports and dispersion of metal to ensure nearly identical catalytic activity.

2.7.1.1 Equipment

BET surface area measurements were conducted using the Accelerated Surface Area and Porosimetry System or ASAP 2010 (Micromeritics). Software from Micromeritics was used to operate the equipment and analyze the catalyst.

---

[80] Gregg, S.J.; Sing, K.S.W., *Adsorption, Surface Area and Porosity*, 2nd Edition, **1982**, 173-190, New York
[81] Brunauer, S.; Emmett, P.H.; Teller, E., *J. Am. Chem. Soc*, **1938**, *60 (2)*, 309-319

2.7.1.2 Materials

Liquid nitrogen was used to lower the analysis temperature to the required level of 77 K. Ultra-high purity nitrogen (99.999%, AGA/BOC) was used for the nitrogen physisorption experiments. The catalysts from the previous sections were used for analysis.

2.7.1.3 Operating procedure

Samples were first prepared by degassing the material in a pre-weighed glass sample bulb to remove water and other potential contaminants. The sample was then reweighed to determine the actual amount of catalyst present in the sample bulb. Next, the sample was placed in the analysis port and evacuated. The sample bulb was then placed in a Dewar flask of liquid nitrogen and further evacuated until equilibrium was reached. Nitrogen was then dosed in incrementally and the amount of gas physisorbed was recorded. The data were analyzed to determine the surface area of catalyst as described by the BET method.[79]

2.7.2 Chemisorption

Chemisorption serves as another method for characterizing catalysts. Adsorbing gases, such as hydrogen and carbon monoxide, on to activated metal sites provides information about the fraction of active metal that is available for reaction. This measurement, known as dispersion, is another important comparison of catalysts in that the more metal that is available for reaction, the higher the activity. Keeping this parameter consistent is important in catalyst manufacturing and understanding evolution of catalyst behavior from run to run.

2.7.2.1 Equipment

Chemisorption measurements were conducted using the ASAP 2010 and corresponding software (Micromeritics).

2.7.2.2 Materials

Gases used for chemisorption analysis were UHP hydrogen (99.999% AGA/BOC) and carbon monoxide (99.5% BOC). UHP helium (99.999%, AGA/BOC) was used to purge the samples before analysis. The catalysts from the previous sections were used for analysis.

2.7.2.3 Operating procedure

Samples were first prepared by degassing the material in a pre-weighed glass sample tube to remove water and other potential contaminants. The sample was then reweighed to determine the actual amount of catalyst present. Once complete, the sample tube was placed in the analysis port of the ASAP 2010 system. The sample tube was then placed under vacuum and heated to remove adsorbed material on the catalyst. Next, the catalyst was reduced under hydrogen to activate the metal sites. Then, the sample tube was cooled and evacuated again. At this point, analysis commenced with dosing of the analysis gas and subsequent measurement of the adsorbed gas. Dispersion was calculated using the following equation:

$$\%\,\mathrm{Disp} = \frac{100\% \times 100\%}{22414\ \frac{\mathrm{cm}^3}{\mathrm{mole}}} \left(\frac{\mathrm{V} \times \mathrm{SF}_{\mathrm{calc}}}{\frac{\mathrm{Weight}\ \%}{\mathrm{AW}_{\mathrm{metal}}}} \right) \qquad (1)$$

Where:

% Disp = Metal dispersion – fraction of metal available for adsorbate interaction

V = y-int. of linear best fit for adsorbed volume per gram vs. P [cm^3 gas/g metal]

SF_{calc} = Atoms of metal per molecule of adsorbed gas [atom of metal/mole of gas]

Weight % = Weight fraction of catalyst that is metal [dimensionless]

AW_{metal} = Atomic weight of the supported metal [g metal / atom of metal]

Metal surface area was calculated using equation 2-2:

$$M_{SA} = \frac{6.023 \times 10^{23} \ \frac{atoms}{mole}}{22414 \ \frac{cm^3}{mole}} V \times SF_{calc} \times A_{area} \qquad (2)$$

Where:

M_{SA} = Metal surface area [m^2 / g sample]

V = y-int. of linear best fit for adsorbed volume per gram vs. P [cm^3 gas/g metal]

SF_{calc} = Atoms of metal per molecule of adsorbed gas [atom of metal/mole of gas]

A_{area} = Effective area of 1 metal atom [m^2 / atom of metal]

Both calculations were completed by the Micromeritics software and described in the user manual.[82]

[82] *ASAP 2010 Chemi: Accelerated Surface Area and Porosimetry System Operator's Manual*, Micromeritics, **September 1996**, Appendix C

Chapter 3 – Preliminary sorbitol hydrogenolysis studies

The focus of these initial experiments was to become familiar with the hydrogenolysis reaction and develop a mechanistic picture by observing adsorption of sorbitol on ruthenium metal. Previous hydrogenolysis studies at MSU utilized a continuous trickle-bed reactor to conduct the majority of experiments. Subsequently, this apparatus was used to observe the reaction and to mimic similar conditions of this work. In addition, batch reactions of sorbitol hydrogenolysis were used to observe the progression of the reaction over time. Adsorption studies were an extension of this work to determine how sorbitol interacts with the catalytic surface. Of interest was the geometry of adsorption and the amount of adsorption occurring on the catalyst.

3.1 Hydrogenolysis experiments

3.1.1 Overview

Previous work by Chopade et al.[4], involved hydrogenolysis of sorbitol and xylitol to desired C_2 and C_3 products: ethylene glycol (EG), propylene glycol (PG), glycerol (GO), and lactic acid (LA). Initial experiments involved getting familiar with the technology of sugar alcohol conversion. Ideally, one mole of sorbitol fed to the reactor would yield two moles of a C_3 product and this is the basis of comparison for each experiment. Results are reported in terms of ***selectivity***, with units of mole of product per mole of reactant converted, and ***yield***, with units of mole of product per mole of reactant fed. For both selectivity and yield, the maximum value is 2.0 with respect to C_3 products.

Experiments were conducted in both a batch reactor and continuous trickle-bed reactor. Initial sorbitol loadings were 25 wt% (1.5 M) with 1 wt% (0.17 M) potassium hydroxide added as a base promoter. Temperatures varied from 200-210°C with

hydrogen pressures at 1200 psig for trickle bed reactions and 1350 psig for the batch reactor. Reactions were catalyzed with 1.0 grams of 2.5 wt% ruthenium on carbon (PNNL).

Typical product distributions showed selectivity to PG, GO, LA, and EG at 0.57, 0.40, 0.07, and 0.29, respectively, with total C_3 selectivity at 1.04 (52% of quantitative). Conversion varied from 70-95% depending on factors such as temperature and amount of catalyst. These results demonstrate the technology and serve as the base line for the remaining studies.

3.1.2 Mesh size study

Another set of reactions was used to observe the effect of catalyst particles sizes in trickle-bed reactions. Since each individual particle is wetted in the trickle flow regime, changing the size of the solid particle could have an effect on the mass transfer of reactants to the catalytic surface and, thus, affect overall activity. Al-Dahhan and Dudukovic[83] noted the use of fines in trickle bed reactors to increase the wetting of catalyst and maintain consistent packing for reactions as well.

Two sizes of catalyst were used for these runs: coarse particles of 16-30 mesh (937-500 microns) and intermediate particles of 50-100 mesh (300-150 microns). Catalyst was crushed using a mortar and pestle and then sieved using A.S.T.M. standard sieves (W.S. Tyler Inc.). For reactions, the trickle-bed reactor was loaded with 25 grams of pre-reduced ruthenium on carbon catalyst. The catalyst was reduced under 300 psig of hydrogen at 150°C for two hours and then wetted with feedstock solution. Feedstock consisted of 25 wt% sorbitol (1.5 M) and 1.0 wt% potassium hydroxide (0.17 M).

---

[83] Al-Dahhan, M.H.; Dudukovic, M.P., *AIChE Journal*, **1996**, *42 (9)*, 2594-2604

Reactions were carried out at 200°C and 1200 psig H_2 with a liquid flow rate of 0.31 mL/min and hydrogen flow at 50 cm^3/min (STP) to maintain a 5:1 ratio of hydrogen to sorbitol molar flow. The reaction continued until HPLC analysis showed identical or near-identical product distributions of consecutive samples, indicating that steady-state had been achieved.

Product distributions between the three runs were nearly identical after each reaction reached steady-state (i.e. consistent product distribution, conversion, etc. observed in consecutive samples). Table 3-1 shows selectivity for ethylene glycol, propylene glycol, glycerol, lactic acid, and total C_3 products. Conversion and catalyst loading are also provided for comparison.

Table 3-1: Product distribution of trickle-bed experiments

Exp.	Particle Size (mesh #)	Catalyst Loading	PG Sel.	GO Sel.	LA Sel.	C_3 Sel.	Conv.
27	16-30	26.4g	0.57	0.40	0.07	1.04	93%
14	16-30	25.3g	0.51	0.50	0.04	1.04	89%
19	50-100	25.0g	0.52	0.50	0.05	1.07	75%

Selectivity to C_3 products was nearly identical between the three experiments. Propylene glycol shows a slightly higher selectivity in the case of 16-30 mesh catalyst. This, however, is an effect of glycerol formed from sorbitol further converting to propylene glycol. A repetition of the 16-30 mesh experiment showed similar C_3 product distribution as the 50-100 mesh case, confirming the similarities.

One difference between the mesh sizes was the conversion of sorbitol. With 50-100 mesh catalyst sorbitol conversion was significantly lower than that of the 16-30 mesh catalyst. This reduction in conversion may be due to mass transfer effects from the

change in catalyst size. To validate this, complete wetting of the catalyst had to be verified. Al-Dahhan and Dudukovic[84] developed an equation for wetting efficiency in trickle-bed reactors that estimated the fraction of wetted catalyst given reaction conditions. When wetting efficiencies tend toward zero, gas phase reactants diffuse directly into the catalyst, effectively bypassing the liquid phase. This increases the catalytic activity significantly, with respect to fully wetted catalyst, as mass transfer of hydrogen is no longer limited by the solubility of gas in the liquid phase. Figure 3-1 illustrates this difference.

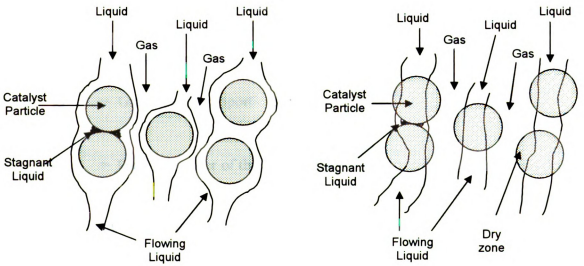

Figure 3-1: Comparison of **(a)** fully wetted and **(b)** partially wetted catalyst

Equation 1 was used for computation of the wetting efficiency:

$$\eta_{CE} = 1.104 \left[\frac{U_L \rho_L d_P}{\mu_L (1-\varepsilon_B)} \right]^{1/3} \left[\frac{1 + \left[\frac{\Delta P/Z}{\rho_L g} \right]}{\frac{d_P^3 \rho_L^2 g \varepsilon_B^3}{\mu_L^2 (1-\varepsilon_B)^3}} \right]^{1/9} \qquad (1)$$

[84] Al-Dahhan, M.H.; Dudukovic, M.P., *Chem. Eng. Sci.*, **1995**, *50 (15)*, 2377-2389

Where:

η_{CE} = Wetting efficiency [dimensionless]

U_L = Superficial liquid velocity [m/s]

ρ_L = Density of the liquid phase [kg/m^3]

d_P = Particle diameter [m]

μ_L = Liquid viscosity $[\frac{kg}{m \cdot s}]$

ε_B = Packed-bed void per reactor volume (bed porosity) [dimensionless]

Re_L = Reynolds number of the liquid phase = $\frac{U_L \rho_L d_P}{\mu_L (1-\varepsilon_B)}$ [dimensionless]

ΔP = Pressure drop through the catalyst [N/m^2]

Z = Length of the catalyst bed [m]

g = Gravitational constant [9.8066 m/s^2]

g_c = Gravitational proportionality factor $[1 \frac{kg \cdot m}{s^2 \cdot N}]$

Ga_L = Galileo number of the liquid phase = $\frac{U_L d_P^3 \rho_L^2 g}{\mu_L^2 (1-\varepsilon_B)^3}$ [dimensionless]

The calculated wetting efficiency was 0.13 and 0.14 for the 16-30 and 50-100 mesh sizes respectively, which showed that the catalyst was not completely wetted. This assumed that the equation was valid outside of the ranges for the liquid phase Reynolds number (Re_L) established by the Duduković paper (0.1 to 10). A pressure drop (ΔP) of 1 and 11 kPa across the catalyst bed (16-30 mesh and 50-100 mesh, respectively) was estimated using the Kozeny-Carman equation[85] (Equation 2), which is applicable for flow through packed beds for Reynolds numbers of less than 1.0.

[85] McCabe, W.L. et al., *Unit Operations of Chemical Engineering*, 5th Edition., p. 153, McGraw Hill Inc., New York, 1993

$$\frac{\Delta P}{Z} = \frac{150\, U_L\, \mu_L}{g_c\, \Phi_s^2\, d_p^2} \frac{(1-\varepsilon_B)^2}{\varepsilon_B^3} \qquad (2)$$

Where:

$\Phi_s = (6 / d_p) / (S_p / V_p)$ = Sphericity of the catalyst

S_p = External surface area of the catalyst

V_p = Volume of the catalyst

A bed porosity (ε_B) of 0.36 was estimated for both mesh sizes using a table from McCabe et al.[86] based on loose packing of spheres. Sphericity of the catalyst was estimated to be 0.7 based on a table with estimates of sphericity for different materials in McCabe et al.[87]

The wetting efficiency is most dependent on the Reynolds number of the liquid phase. For experiments, a liquid volumetric flow rate of 0.32 mL/min was used corresponding to a Reynolds number of approximately 3×10^{-3}. This, expectedly, gave a reduced wetting efficiency. The parameter of interest in this set of studies, the particle diameter (d_P), was used to calculate both the Reynolds number and Galileo number to determine η_{CE}.

With a large pressure drop (i.e. $[\Delta P / Z] / \rho_L g >> 1$), η_{CE} varies with $d_P^{-2/9}$. However, with the low liquid flow rate, the pressure drop was relatively small, which made the effect of a three-fold decrease in particle diameter (750 microns to 250 microns) only a 7% increase of η_{CE} (from 0.13 to 0.14) instead of a potential 28%. Essentially, no further wetting of the catalyst was observed. Thus, the change in particle diameter was

[86] McCabe, W.L. et al., *Unit Operations of Chemical Engineering*, 5th Edition., p. 155, McGraw Hill Inc., New York, 1993
[87] *Ibid.* p. 928

not sufficient to reduce the mass transfer of hydrogen to the catalytic surface and could not account for the drop in conversion.

With mass transfer effects ruled out, the difference in conversion between the two particle sizes must have been due to some other factor, such as reduced residence time due to channeling of the liquid phase or inconsistent reduction of the ruthenium catalyst between reactions. Crushing of the catalyst by mortar and pestle may have closed off pores in the crushed 50-100 mesh catalyst, as well. This, in turn, would seal off active metal from the reaction. Regardless of the drop in conversion, the product distribution was not significantly affected by the change in particle size of the catalyst.

3.1.3 Continuous base addition

This set of experiments used the batch reactor system to observe the effects of adding base over the course of sorbitol hydrogenolysis. Each reaction used potassium hydroxide as a base "promoter" to improve C_3 selectivity, as was consistent with prior work[4]. Over the course of the experiment, pH levels dropped due to formation of organic acids, such as lactic acid. Adding base continuously provided a method for maintaining the pH as a strategy of increasing C_3 selecitivity.

Four experiments were performed comparing the continuous feeding of water and 0.5 wt% potassium hydroxide solution at rates of 0.1 mL/min and temperatures of 200°C and 210°C. All reactions were carried out under 1350 psig H_2 and with catalyst loadings of 1.0 gram (dry basis) of 5 wt% ruthenium on carbon (PMC). Feedstock was 25 wt% sorbitol (1.5 M) and 0.5 wt% KOH (0.08 M). Table 3-2 displays the product distributions from these runs.

Table 3-2: Product distribution of continuous base addition experiments

Exp	Continuous feed	Temp (°C)	PG Sel.	GO Sel.	LA Sel.	C_3 Sel.	Conv.
13	Water	200	0.15	0.28	0.08	0.51	67%
15	0.5% KOH	200	0.21	0.18	0.05	0.44	61%
8	Water	210	0.15	0.26	0.08	0.49	96%
9	0.5% KOH	210	0.18	0.23	0.06	0.47	99%

Results show no improvement in C_3 selectivity with base addition and, in fact, appear to have slightly lower preference toward C_3 materials. The product distribution also shows an apparent preference toward PG for the base addition cases. This is an effect of glycerol dehydrogenating to propylene glycol via a base-catalyzed mechanism. With the maintained pH from base addition, this process was promoted as demonstrated by the increased PG selectivity and decrease in glycerol selectivity.

3.2 Adsorption studies

3.2.1 Overview

In the interest of gaining mechanistic information, a series of adsorption studies was designed to observe interactions between sorbitol and ruthenium metal under an inert atmosphere. A dilute solution of sorbitol was stirred with activated ruthenium metal at constant temperature and sampled as the reaction progressed. A decrease in sorbitol concentration from the bulk liquid phase was assumed to be adsorption. The amount of sorbitol removed from the bulk phase would then be compared to the measured dispersion of the catalyst to compare the number of active sites to the substrate adsorbed. And from this, an estimate of the adsorbed area of sorbitol on the metal surface and relative orientation of the sugar alcohol with ruthenium.

We corroborated evidence of sorbitol dehydrogenation using a deuterium labeling experiment and ^{13}C NMR. Sorbitol was placed in deuterated water (D_2O) and reacted with ruthenium catalyst at 230°C under 1200 psig of deuterium gas. As shown in Figure 3-2, incorporation of deuterium at carbon 1 (C1) was demonstrated by induced splitting in the NMR spectrum. This could only happen with dehydrogenation occurring at C1 followed by hydrogenation of the unsaturated intermediate with deuterium. The result also suggested an end-on adsorption of sorbitol on to ruthenium metal prior to dehydrogenation. This result is contrary to a model presented by Müller et al.[38] which suggests interaction of three hydroxyl groups at the active metal site.

3.2.2 Sorbitol Adsorption Experiments

Ruthenium metal sponge was used for adsorption experiments to provide a sufficient amount of metal surface area without a supporting material. Supports, such as activated carbon can absorb as much as 0.3 grams of substrate per gram. This amount of absorption would make any change in sorbitol concentration due to adsorption on the active metal statistically insignificant. Metal particle diameters were approximately 100-150 microns and the catalyst had an observed BET surface area of 0.5 m^2/gram. For comparison, ten grams of ruthenium sponge has approximately the same metal surface area as one gram of 5 wt% Ru/C catalyst. Solid spheres of the same diameter have an effective surface area of approximately 5×10^{-4} m^2/gram, so the sponge has substantial porosity.

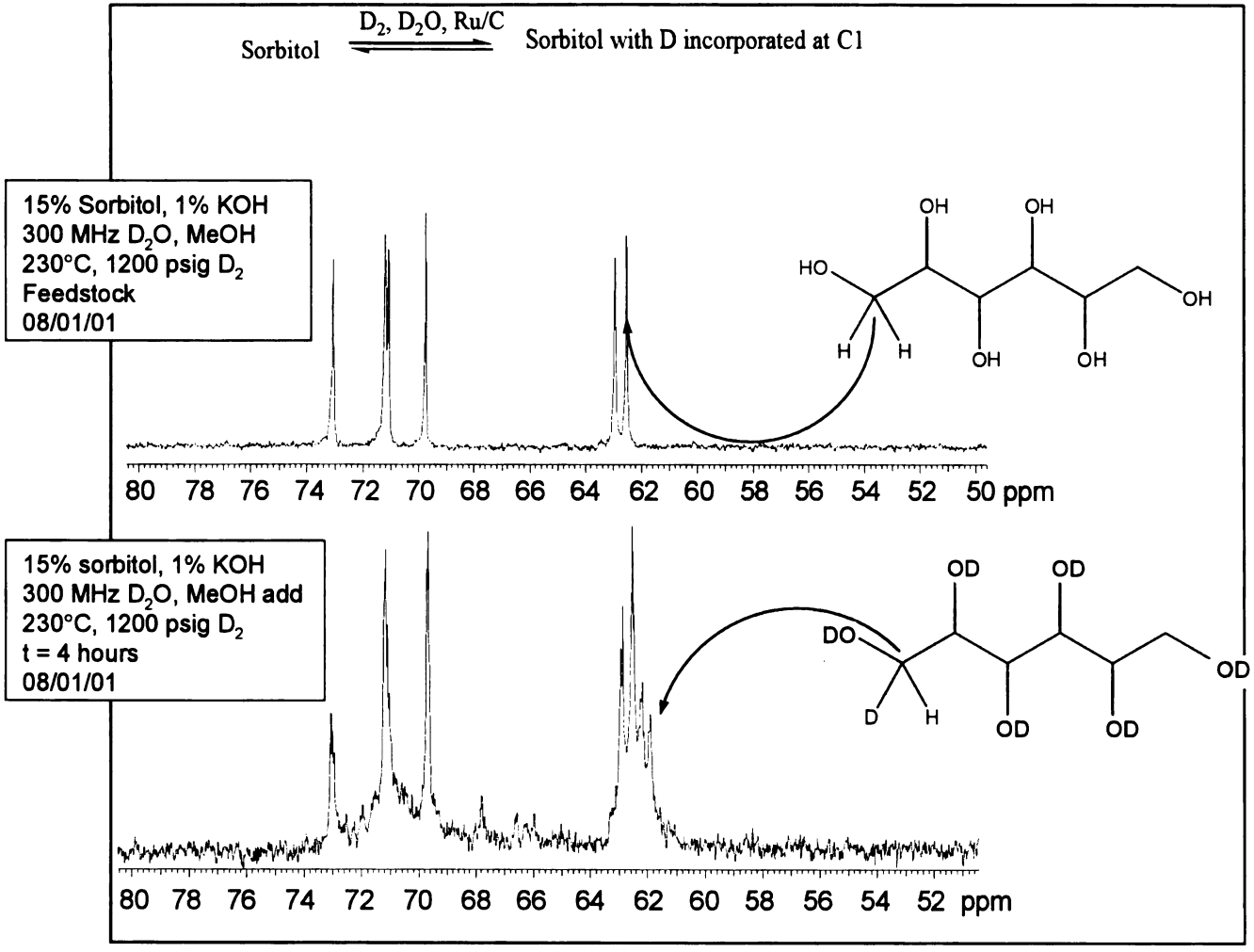

Figure 3-2: ^{13}C NMR study of sorbitol over Ru/C – evidence of dehydrogenation

The catalyst was further characterized using hydrogen and carbon monoxide chemisorption experiments available on the ASAP 2010. Ruthenium metal was reduced at high temperature to remove any strongly bound materials on the surface and then exposed to dosed amounts of hydrogen or carbon monoxide. Based on the amount of gas adsorbed to the metal, the number of active sites was calculated and reported as dispersion. Dispersion is the fraction of metal atoms that adsorb the analysis gas over the total metal atoms available. For the ruthenium sponge, dispersion was found to be 0.06% with a metal surface area of approximately 0.3 m^2 per gram.

With the dispersion known, an estimate of potential sorbitol adsorption was made per gram of sponge. One gram of ruthenium (M.W. 101.06) is roughly 0.01 moles. The amount of this metal active in H_2 chemisorption at 308 K was 0.06% or 6 x 10^{-6} moles. With one molecule of sorbitol adsorbed to each active site, approximately 1 mg of substrate would bind to one gram of sponge.

Another estimate of sorbitol adsorption was based on the BET surface area measurement. From the NMR data, sorbitol adsorption appeared to be end-on. Thus, the adsorbed area of the substrate would be relatively small. An estimate of 30 $Å^2$, or roughly double the adsorbed area of one molecule of nitrogen, was used for each molecule of sorbitol. Thus, covering the 0.5 m^2/gram metal surface area with one monolayer would require 0.5 mg of sorbitol per gram.

Each run consisted of 10.0 grams of ruthenium sponge and 50 mg of sorbitol in 100 mL of water, agitated under helium at 100 psig in a Parr batch reactor. The two estimated values of adsorption per gram of sponge represented a range of 5 to 10 mg of sorbitol. This expected amount of adsorption would lower the concentration of sorbitol

in the liquid phase as measured by HPLC. A larger decrease in concentration would suggest a smaller adsorption area, multi-layer adsorption, a reaction occurring on the metal surface, or a combination of the three. A smaller drop in concentration would indicate no reaction and an effective adsorption area of over 30 $Å^2$. In addition, the activation energy of sorbitol dehydrogenation was determined using a set of five experiments using identical loadings of feedstock (50 mg sorbitol) and catalyst (10.0 grams ruthenium sponge) at different temperatures (100 to 150°C).

3.2.3 Results and Discussion

Experiments showed two surprising results: a larger than expected decrease in sorbitol concentration and the presence of chemical species other than sorbitol in the liquid phase. Apparently, the interaction between ruthenium and sorbitol is not limited to adsorption. A number of liquid-phase products formed that were consistent with polyols and anhydro-products from HPLC analysis. In addition, carbon monoxide and carbon dioxide were produced in the vapor phase, which demonstrated C-C cleavage of sorbitol.

Temperature was also important due to the increased formation of gas as the temperature increased. At 40°C, no discernable amount (<2%) of sorbitol converted or adsorbed to the ruthenium surface. As temperatures increased, liquid phase products, such as mannitol, xylitol, threitol, and glycerol, began to form during the reaction. Carbon balances calculated from HPLC showed a gradual decrease in the amount of carbon in the liquid phase of the reaction, which suggested that material was being adsorbed by the ruthenium metal. Figure 3-3 illustrates the change in sorbitol and total liquid phase product concentrations versus time at 40, 120, and 150°C (Experiments 101, 102, and 100 respectively).

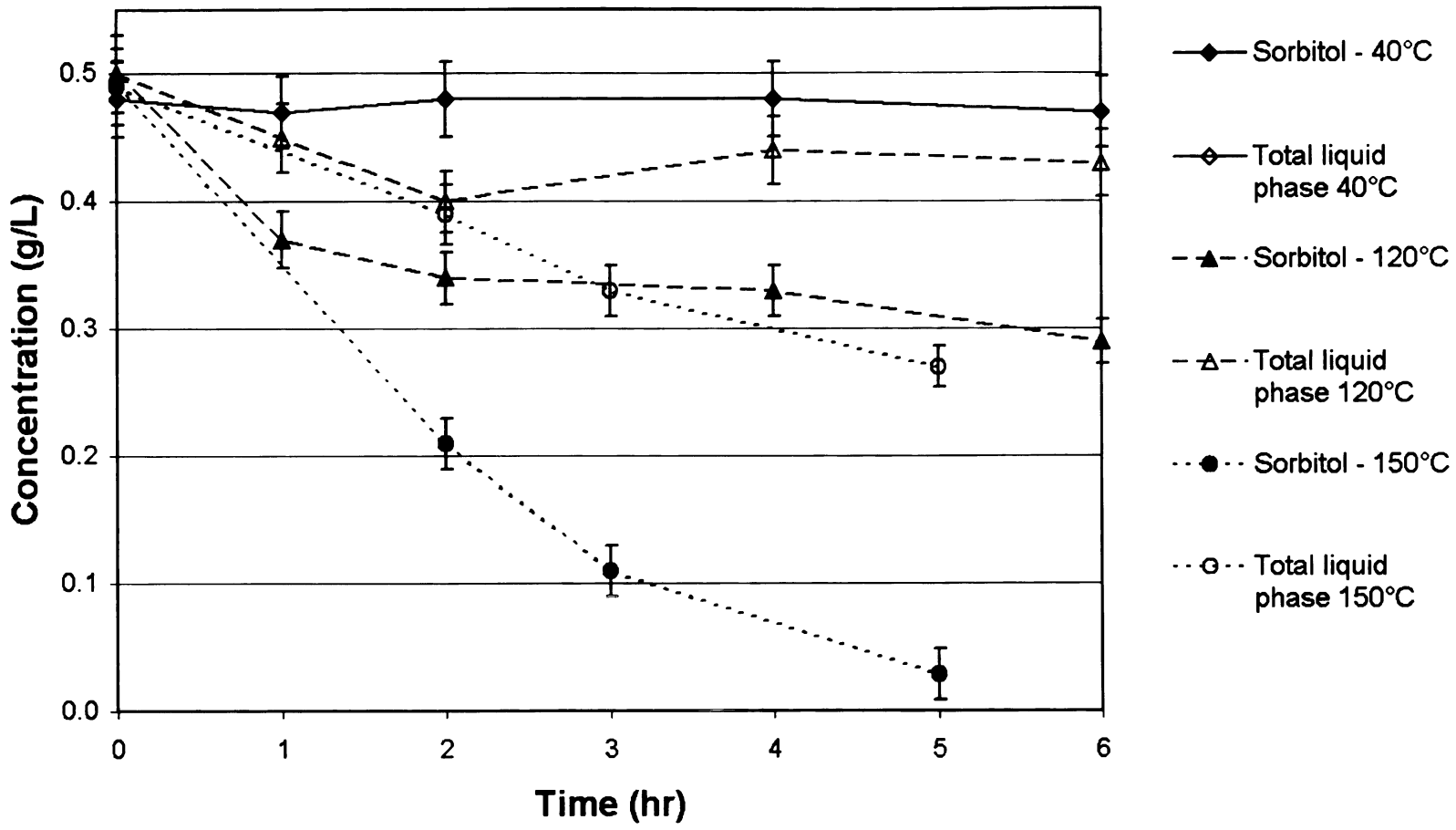

Figure 3-3: Concentration of sorbitol and total liquid phase products vs. Time Sorbitol adsorption experiments

Results from these runs showed an apparent increase in adsorption of organic material to the metal surface. At 120°C, ~7 mg of material, or 0.7 mg/g sponge, was removed from the liquid phase, while at 150°C, 23 mg was removed (2.3 mg/g). The quantity of "adsorbed" material rose with temperature, which did not make sense, and the amount removed from solution at 150°C was well above prior estimates of 0.5 – 1.0 mg/g sponge.

To address these inconsistencies, an extended run was conducted (Experiment 163) at 120°C with the same catalyst loading (10.0 grams of ruthenium sponge) and pressure (100 psig He) of previous adsorption experiments with a similar feedstock of 50 mg of sorbitol in 160 mL of water. No liquid or gas phase samples were taken over the course of the run to avoid the removal of material from the reaction. After 40 hours, the reactor was cooled to room temperature and the gas and liquid samples were taken.

Analysis of the gas phase indicated the presence of carbon dioxide, methane, and ethane in the headspace of the reactor. When the carbon balance included these gases, it closed to nearly 100%, which showed that no detectable amount of material adsorbed to the metal catalyst. HPLC identified a number of products in the liquid phase. The product distribution from this experiment is found in Table 3-3.

Table 3-3: Liquid and gas phase products of sorbitol adsorption at 120°C (Exp. 163)
Conditions: 120°C, 100 psig He, 10.0g Ru sponge, 50 mg sorbitol, 160 mL solution

Products	% of carbon closure*
Sorbitol	52 ± 2
Xylitol	7 ± 1
Mannitol	4 ± 1
Acetic acid	3 ± 1
Threitol	2 ± 1
Glycerol	**
Unknown ***	12 ± 2
Total liquid phase	80 ± 6
Methane	12 ± 2
Carbon dioxide	4 ± 1
Ethane	**
Total gas phase	16 ± 3

* Carbon balance is based on 19.8 mg of carbon from the sorbitol feedstock

** Detected, but not in significant quantity

*** The concentration for unknown compounds was determined by using an average response factor based on known compounds

The energy of activation for sorbitol dehydrogenation was calculated based on our postulated reaction pathway of sorbitol dehydrogenation prior to further reaction. Thus, any change in sorbitol concentration was the result of dehydrogenation. Using a first order rate equation:

$$-r_{SO} = k * C_{SO} \tag{3}$$

$$\frac{dC_{SO}}{dt} = -k \cdot C_{SO} \tag{4}$$

Where:

$-r_{SO} = \frac{dC_{SO}}{dt}$ = Rate of sorbitol dehydrogenation [mol / liter / hr]

k = 1st order rate constant [hr^{-1}]

C_{SO} = Concentration of sorbitol [mol / liter]

From Equation 4, the rate constant k can be estimated by calculating $\frac{dC_{SO}}{dt}$ at the onset of the reaction. Using concentration versus time data, the change of concentration was measured between the first two data points and used to calculate $\frac{dC_{SO}}{dt}$. This result was then divided by the initial sorbitol concentration of 0.5 g/L or 2.74×10^{-3} moles/liter for the value of k. The rate constant was then related to the activation energy of dehydrogenation by Arrhenius' law[88]:

$$k = k_o \exp\left(\frac{-E_{act}}{RT}\right) \qquad (5)$$

Where:

k = 1st order rate constant [hr^{-1}]

k_o = pre-exponential factor [hr^{-1}]

$-E_{act}$ = Activation energy [J / mol]

R = Ideal gas constant [J / mol / K]

T = Temperature [K]

[88] Levenspiel, O., *Chemical Reaction Engineering*, 3rd Edition, p. 27, Wiley, New York, 1999

Transforming the equation:

$$-\ln(k) = \frac{-E_{act}}{RT} + \ln(k_o) \tag{6}$$

Or:

$$-\ln(k) = \frac{-E_{act}}{R}\left[\frac{1}{T}\right] + \ln(k_o) \tag{7}$$

The rate constant k was calculated at temperatures of 100, 110, 120, 135, and 150°C. Plotting -ln(k) versus 1 / T yielded Figure 3-4, which was fitted with a linear trendline. The slope of the trendline represented E_{act} / R, or the activation energy of sorbitol dehydrogenation over the ideal gas constant. From this, an activation energy of 30 kJ / mol was calculated. Table 3-4 displays the calculations from these experiments.

Table 3-4: Calculations for E_{act} of sorbitol dehydrogenation [-ln (k) vs. 1 / T]
Conditions: 0.5 g/L, 10.0g ruthenium sponge, 100 psi helium

Exp.	Temp (K)	1 / T x 10^3 (K^{-1})	$\frac{dC_{SO}}{dt}$ x 10^4 $\left(\frac{moles}{liter \cdot hr}\right)$	Initial C_{SO} x 10^3 $\left(\frac{moles}{liter \cdot hr}\right)$	- ln (k)
109	373	2.68	3.4	2.74	2.07
103	383	2.61	2.6	2.74	2.35
102	393	2.54	7.1	2.74	1.35
111	408	2.45	11.0	2.74	0.92
100	423	2.36	7.7	2.74	1.27

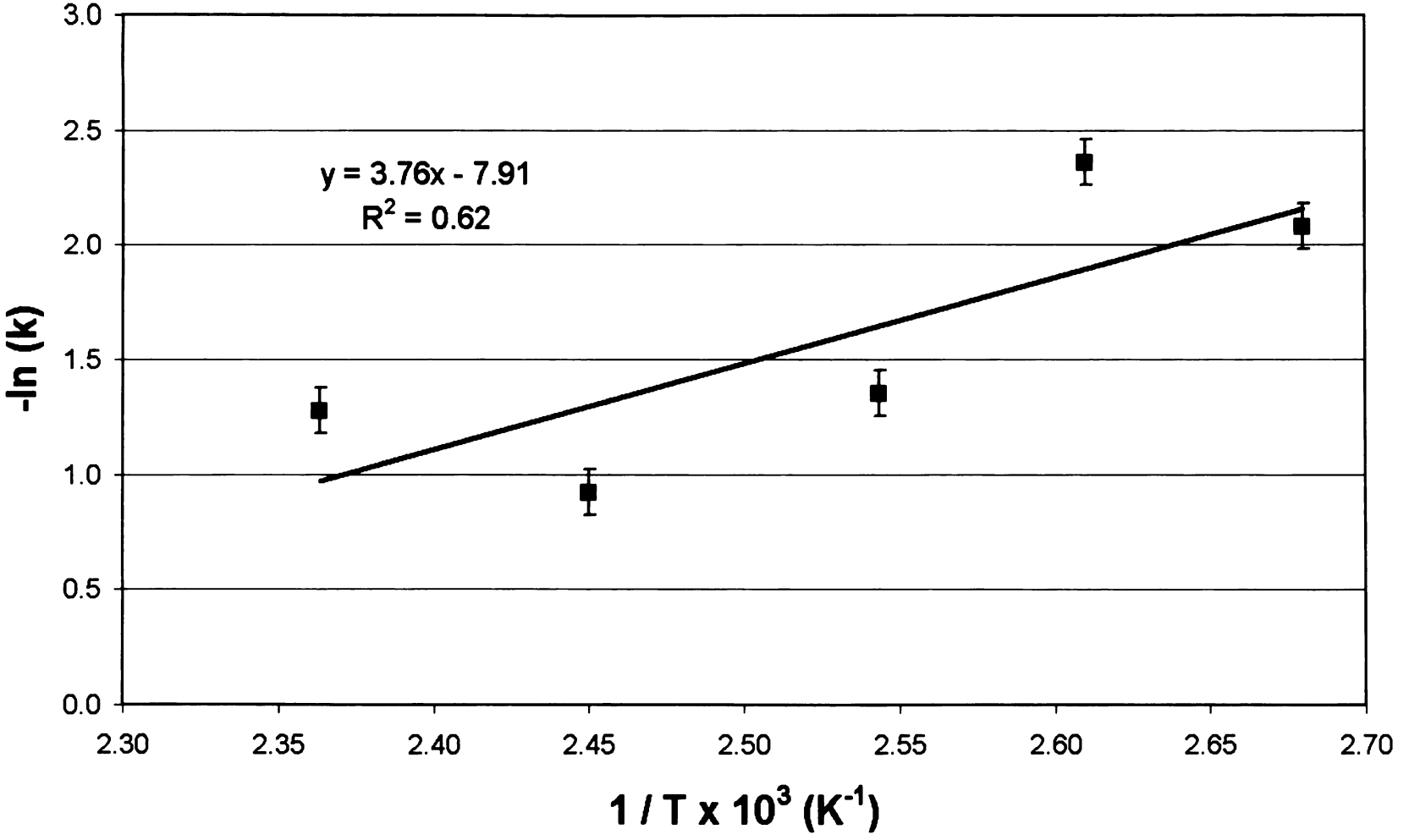

Figure 3-4: Determination of activation energy of sorbitol dehydrogenation

Work by Peereboom[89] focused on an even more dilute system and showed that sorbitol reacted with ruthenium at temperatures as low as 30°C and adsorbed to the catalyst within thirty minutes of contact. After several hours, the amount of sorbitol adsorbed was only 0.1 mg per gram of sponge, which corresponded to an adsorption area of 90 $Å^2$. The amount of sorbitol adsorbed was significantly lower than the initial estimates of 0.5-1.0 mg per gram of sponge. Based on the low temperature of the experiment, this result suggested that sorbitol adsorption has a small activation energy. The small amount of adsorption also suggested 1) a larger than expected adsorption area for sorbitol (3 times larger) with strong adsorption, or 2) sorbitol adsorbs weakly to the metal surface and occupies only a small fraction of the sites. The large adsorbed area would require sorbitol to occupy five to ten active sites on the metal surface in order to prevent additional sorbitol molecules to interact. This would require multiple hydroxyl groups to complex with the catalyst metal. H-D exchange on the carbon chain of sorbitol would then be expected at multiple sites. From Figure 3-2 however, H-D exchange was only observed at C1. Kinetic modeling of glucose hydrogenation to sorbitol also refutes the multiple adsorption site model due to excellent agreement with experimental data when sorbitol adsorption is neglected.[21,22] Thus, weak adsorption of sorbitol is an appropriate conclusion.

3.2.4 Summary

Overall, this set of results illustrates several key steps in the hydrogenolysis process. First, through ^{13}C NMR work and initial HPLC analysis, dehydrogenation was confirmed as the first step of hydrogenolysis. Second, ruthenium and sorbitol react to

[89] Unpublished data from Miller group produced by L. Peereboom

form products regardless of the presence of hydrogen or low temperatures. Ruthenium appeared to lower the activation energy sufficiently to enable dehydrogenation at low temperature. With the addition of high hydrogen pressures, as used in hydrogenolysis, sorbitol is favored over the dehydrogenated intermediate. Higher temperatures are, therefore, necessary to overcome this preference to sorbitol. In addition, the higher temperature allows for sufficient activity in the hydrogenolysis reaction to convert the feedstock within a few hours.

Another important observation is that sorbitol does not remain adsorbed to metal catalyst in appreciable amounts and thus, only weakly adsorbs to active catalyst sites. This is an effect of a larger than expected adsorption area or low energy barriers for adsorption and desorption of the sugar alcohol. The result is consistent with observations of the carbon chain of sorbitol using ^{13}C NMR and with kinetic modeling of glucose hydrogenation to sorbitol reported in the literature.

Sorbitol-metal interaction was studied further by observing the effects of adding base to imitate conditions of hydrogenolysis for a direct comparison. Chapter 4 summarizes these experiments.

Chapter 4 – Metal and base-catalyzed C-C cleavage of sugar alcohol and monosaccharide feedstock

4.1 Metal-catalyzed alkaline degradation

Hydrogenolysis of sorbitol is enhanced by the addition of a base "promoter", typically sodium hydroxide or potassium hydroxide, to produce higher yields of desired C_3 materials: propylene glycol, glycerol, and lactic acid. To study this promoter effect, additional adsorption experiments were conducted with base added to the feedstock. Preliminary results with 0.6 wt% sorbitol (0.033 M) and 1.0 wt% KOH (0.17 M) at 150°C showed production of lactic acid, propylene glycol, glycerol, and ethylene glycol without the addition of hydrogen (Experiment 56).

This result was explored further by using higher concentrations of sorbitol (32 g/L or 0.18 M) to see if this trend in C_3 production continued. In addition, different metal catalysts, temperatures, and initial base concentrations were used to observe the subsequent effect on product distributions. Xylitol and glycerol were also used as feedstock to compare metal-substrate interactions and observe carbon-carbon cleavage tendencies relative to sorbitol. These results are described in detail in the following sections.

4.1.1 Control experiments

Control experiments were used to show that the combination of base and metal was necessary to convert the feedstock. A 0.6 wt% sorbitol solution (0.03 M) with 1.0 wt% KOH (0.16 M) was heated to 150°C for two hours under helium. Less than 1% of the sorbitol reacted, which indicated that base alone was not sufficient to react with sorbitol. Three additional experiments used initial sorbitol concentrations of 0.1, 0.2, and

0.6 wt% (0.0055, 0.011, 0.033 M) with 10.0 grams of ruthenium metal under helium. The rates of reaction for the three runs were 0.032, 0.056, and 0.035 grams of sorbitol per hour, respectively. While the rates were non-zero, each was small enough to demonstrate that metal alone is not sufficient for rapid conversion of the substrate. Thus, the combination of metal catalyst and base in the feedstock is needed for significant conversion of the sorbitol.

4.1.2 Effect of base loading on product distribution

Of the parameters studied, base concentration had the most dramatic effect on the reaction. At high sorbitol concentrations, conversion of the feedstock halted without sufficient potassium hydroxide present. Figures 4-1 and 4-2 illustrate that high pH was necessary for continued reaction. The pH of each sample was measured by an Accumet 950 pH meter (Fisher Scientific). One limitation of the pH meter was higher than expected readings for pH levels > 13. For instance, the feedstock with 1.47 M KOH should have had a pH of 14.2 instead of 14.9 as reported in Figure 4-2. The graph does properly reflect, however, the effect of pH on the conversion of the reaction. Experiments were conducted at 150°C under 100 psig helium with 10.0g ruthenium sponge catalyst.

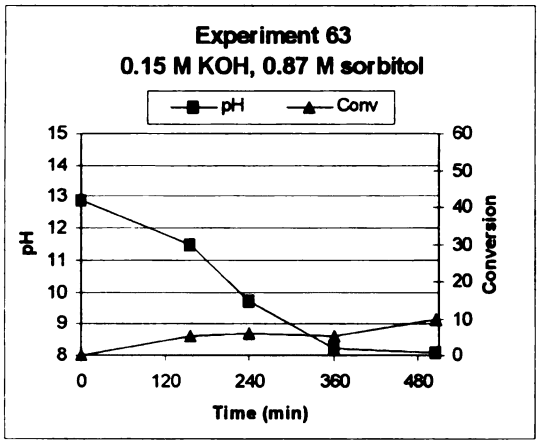

Figure 4-1: pH and conversion vs. time - low base

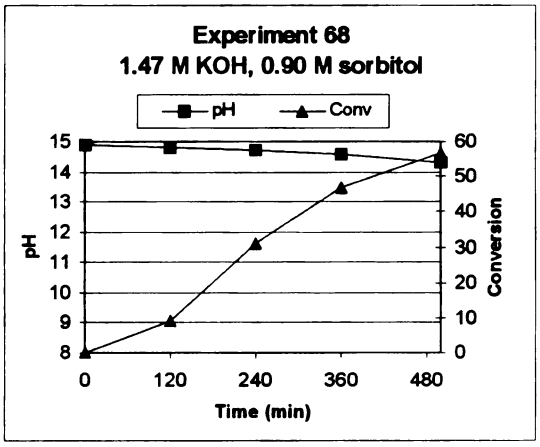

Figure 4-2: pH and conversion vs. time - excess base

In Chapter 3, it was shown that sorbitol adsorbs to the metal surface and dehydrogenates. In these reactions a hexose is thus formed, which is available in the reaction medium to undergo base-catalyzed carbon-carbon cleavage reactions. With sufficient base present, the alkaline degradation pathways continue, presumedly, until the feedstock is exhausted (see Figure 4-2). However, at lower initial base concentrations, organic acids that form neutralize the reaction medium effectively stopping the carbon-carbon cleavage of the transient sugars formed from sorbitol dehydrogenation (Figure 4-1). Quantitatively, 10% of 0.87 M sorbitol converted after 8 hours in Experiment 63. Assuming two moles of organic acid form with each mole sorbitol reacted, ~0.18 M of acids would form and neutralize the 0.15 M KOH in the feedstock. The pH level was still above neutral at the end of the experiment, which is explained by the formation of non-acidic products, such as propylene glycol and glycerol, which do not neutralize KOH. When the transient sugars stopped reacting, sorbitol ceased to react as well. This could be explained in two ways:

1) When sorbitol dehydrogenates to form a hexose, the hexose adsorbs to the catalyst surface. With sufficient base, the sugar desorbs and reacts toward products. When the base is exhausted, the glucose remains on the catalyst surface with higher affinity than the sorbitol, effectively shutting down the dehydrogenation reaction.

2) The dehydrogenation reaction is reversible between sorbitol and the sugar formed. With alkaline degradation, the sugar continues to convert to products, which promotes dehydrogenation. When the degradation stops, sorbitol and the glucose analog reach an equilibrium, which halts any further conversion of sorbitol.

Of the two options, the first is inconsistent with published results. Several papers[19-22] that involve the hydrogenation of sugars to sugar alcohols note that the reaction is between chemisorbed hydrogen and unadsorbed sugar based on kinetic models. This suggested that the sugars produced from dehydrogenation do not compete for the active sites used by sorbitol.

In addition to reduced activity in the reaction, the product distribution at lower initial base concentration shifted toward making propylene glycol instead of lactic acid. This was attributed to reduced rates of organic acid formation at lower pH[73], which allowed hydrogenation of unsaturated intermediates to occur. These intermediates, such as glyceraldehyde and pyruvaldehyde, form via retro-aldol condensation and further react to form other intermediates, recondense, or rearrange to form organic acids. When hydrogen and catalyst are present, they may also hydrogenate, which would account for the production of glycerol and propylene glycol. However, in these reactions, only helium was added to the reactor. Thus, for PG to form, hydrogen must have been

obtained from the sorbitol feedstock or from the residual hydrogen on the pre-reduced catalyst.

Chemisorption experiments show that 0.07 cm^3 (STP) of hydrogen adsorb per gram of ruthenium sponge. This corresponds to 0.7 cm^3 or 10^{-6} moles of hydrogen that would have been available to each reaction. Runs from this set of studies typically produced 10^{-3} moles of propylene glycol and glycerol, which would more than exhaust the supply of hydrogen on the catalyst. Thus, the hydrogen source must be from the sorbitol feedstock.

Overall, the selectivity to C_3 products did not change significantly between experiments, but the distribution of the C_3 products did change at different base concentrations. As discussed earlier, experiments with lower levels of base showed higher selectivity toward propylene glycol while higher initial base concentrations in the feedstock produced more potassium lactate. While the majority of C_3 product was lactic acid, there was a clear shift toward propylene glycol, as seen in Table 4-1. Results are reported in terms of selectivity, which reflects the number of moles of product formed per mole of sorbitol reacted. Propylene glycol (PG) and lactic acid (LA) are reported separately. C_3 selectivity is the combination of the C_3 products propylene glycol, lactic acid, glyceric acid, and glycerol.

Table 4-1: C_3 product distribution – effect of initial base concentration

Exp	Sorb. Conc.	KOH Conc.	PG Sel.	LA Sel.	C_3 Sel.	FA Sel.	Conv.	Carbon Bal.	t (hr)
58	0.03 M	0.15 M	0.16	0.53	0.68*	2.10	96%	97%	2.5
64	0.03 M	0.15 M	0.12	0.67	0.79*	1.73	97%	104%	3.0
62	0.18 M	0.15 M	0.16	0.65	0.81*	1.13	43%	95%	8.0
80	0.18 M	0.83 M	0.05	0.70	0.85	0.95	91%	87%	8.0
67	0.18 M	0.83 M	0.06	0.77	0.83*	1.15	99%	85%	7.0
63	0.87 M	0.16 M	0.25	0.62	0.87*	1.02	11%	101%	8.5
68	0.90 M	1.47 M	0.05	0.81	0.85*	0.76	62%	86%	8.3

* C_3 sel. for these experiments did not include glycerol or glyceric acid due to lack of UV spectroscopy

For experiments 58, 62, 63, 64, 67, and 68, the ultra-violet response at 210 nm was not recorded for the samples. Propylene glycol and lactic acid were observed using the refractive index response. However, glycerol and glyceric acid were not identified because the peaks could not be resolved. Formic acid and glycerol have very similar retention times with the column conditions used for HPLC analysis. Likewise, the responses for sorbitol and glyceric acid overlap, which made quantification difficult. When used in combination with the UV response, the combination of glyceric acid and sorbitol as well as formic acid and glycerol can be resolved. Experiment 80 used both UV and RI responses to resolve all four components. Glycerol and glyceric acid had a selectivity of 0.04 and 0.09 respectively. With the inclusion of glycerol, the apparent concentration of formic acid decreased. Thus, the reported selectivity of formic acid for reactions, with the exception of Experiment 80, is inflated.

Table 4-2 lists other minor products of the reactions. C_2 products of ethylene glycol (EG) and glycolic acid (GlyA2) are included along with formic and acetic acids (FA, AA). Changes in base and sorbitol concentrations did not show a large change

between selectivity among the experiments. There appears to be a slight preference toward ethylene glycol and glycolic acid with lower initial base concentrations with respect to the sorbitol concentration. The effect, however, is not significant enough to report conclusively.

Table 4-2: C_1 and C_2 product distribution – effect of initial base concentration

Exp	Sorb. Conc.	KOH Conc.	EG Sel.	GlyA2 Sel.	AA Sel.	FA Sel.
58	0.03 M	0.15 M	0.04	0.22	—	2.10
64	0.03 M	0.15 M	0.06	0.21	—	1.73
62	0.18 M	0.15 M	0.12	0.17	—	1.13
80	0.18 M	0.83 M	0.05	0.12	0.10	0.95
67	0.18 M	0.83 M	0.03	0.14	—	1.15
63	0.87 M	0.16 M	0.08	0.22	—	1.02
68	0.90 M	1.47 M	0.04	0.13	—	0.76

Another effect of higher initial base concentrations was an increase in gas products. The carbon balance steadily decreased when more potassium hydroxide was added to the feedstock. This reflected the production of carbon dioxide and methane as the reaction progressed. Quantitative results were not determined for these runs, but the gas products CH_4 and CO_2 were consistent with gas samples from the adsorption experiments reported in Chapter 3.

4.1.3. Effect of catalyst metal on product distribution

This group of experiments compared the product distribution of the alkaline degradation reactions that used 10.0 grams of ruthenium sponge, 1.0 grams of ruthenium on carbon, and 1.0 grams of palladium on carbon as catalysts. Both ruthenium catalysts were pre-reduced to activate the metal (see Section 2.3.3.1) while palladium required no

pre-reduction. Feedstock concentrations of sorbitol and potassium hydroxide remained consistent for each run at 0.18 M and 0.85 M respectively. Reaction temperature and pressure were at 150°C and 100 psig of helium.

The three catalysts showed similar selectivity to C_3 products, and more specifically, toward lactic acid as shown in Table 4-3. Palladium had higher selectivity and yield toward C_3 products, but the activity of the catalyst, i.e. the rate of sorbitol conversion, was not as high as the ruthenium catalysts. Both ruthenium catalysts also formed significantly more formic acid compared to palladium. Since gas formed with the palladium catalyst (73% carbon balance) and alkaline degradation pathways are solution based, the lower selectivity to formic acid with palladium was due to conversion of formic acid precursors to gas.

Table 4-3: C_3 product distribution at 6 hours – effect of catalyst metal

Exp	Catalyst	PG Sel.	LA Sel.	GO Sel.	GlyA Sel.	C_3 Sel.	FA Sel.	Conv.	Carbon Bal.
80	Ru sponge	0.05	0.68	0.04	0.09	0.86	0.95	91%	87%
69	Ru/C	0.10	0.68	—	0.06	0.84	0.79	80%	79%
83	Pd/C	0.09	0.72	0.05	0.12	0.98	0.10	71%	79%

The C_2 product distribution (Table 4-4) between experiments showed no notable change between catalyst metal. Ethylene glycol (EG), glycolic acid (GlyA2), and acetic acid (AA) all form in small amounts. Production of ethylene glycol further demonstrates the in situ production of hydrogen during the reaction.

Table 4-4: C_2 product distribution at 6 hours – effect of catalyst metal

Exp	Catalyst	EG Sel.	GlyA2 Sel.	AA Sel.	Conv.	Carbon Bal.
80	Ru sponge	0.05	0.12	0.09	91%	87%
69	Ru/C	0.07	0.05	—	80%	79%
83	Pd/C	0.09	0.02	0.11	72%	79%

4.1.4 Effect of temperature

Three reactions conducted at 150, 170, and 190°C were used to observe the effect of temperature on product distribution. The initial concentration for sorbitol and KOH remained at 0.18 M and 0.85 M, respectively, and the reaction gas was helium at 100 psig. Table 4-5 summarizes the findings from these runs.

Table 4-5: C_3 product distribution – effect of reaction temperature

Exp.	Temp. (°C)	PG Sel.	LA Sel.	C_3 Sel.	FA Sel.	Conv.	Carbon Bal.	t (hr)
80	150	0.05	0.70	0.82	0.95	91%	87%	6.0
76	170	0.04	0.72	0.76	0.96	98%	70%	4.0
77	190	0.04	0.62	0.70	1.09	100%	71%	2.0

Selectivity to lactic acid and C_3 products decreased slightly from 150 to 190°C, while formic acid production remained essentially constant. Gas formation was promoted with higher temperatures as evident from decreasing carbon balances. Further, at 190°C, gas continued to form as the reaction progressed.

C_2 products converted into gas as the reaction temperature increased, as seen in Table 4-6. Ethylene glycol and glycolic acid diminished with higher temperatures while acetic acid production remained constant.

Table 4-6: C_2 product distribution – effect of reaction temperature

Exp	Temp (°C)	EG Sel.	GlyA2 Sel.	AA Sel.	Conv.	Carbon Bal.
80	150	0.05	0.12	0.09	91%	87%
76	170	0.02	0.06	0.09	98%	69%
77	190	0.00	0.04	0.09	99%	69%

4.1.5 Effect of feedstock

In addition to sorbitol, xylitol and glycerol were used as feedstocks to observe similar metal-polyol interactions already studied. Xylitol is of interest from earlier work at MSU.[4] Glycerol is of interest because of its production from bio-diesel synthesis. The similar structure of xylitol, glycerol, and sorbitol (i.e. saturated polyols) allowed comparisons of dehydrogenation and patterns in the carbon-carbon cleavage selectivity. Initial concentrations of xylitol and glycerol were 0.18 M with a base concentration 0.85 M. Reactions were carried out at 150°C under 100 psig of helium.

Xylitol showed the same general type of product distribution as sorbitol degradation. Lactic acid was the primary C_3 product with smaller, but significant amounts of propylene glycol and glycerol observed as well. Formation of PG and glycerol further demonstrated the initial dehydrogenation step and degradation of the subsequent sugar seen with sorbitol. Formic and glycolic acids also formed in significant amounts, which was consistent with alkaline degradation pathways. Table 4-7 summarizes the product distribution after six hours.

Table 4-7: Product distribution from alkaline degradation of xylitol (Experiment 79)

PG Sel.	GO Sel.	LA Sel.	GlyA Sel.	C_3 Sel.	EG Sel.	GlyA2 Sel.	FA Sel.	Conv.	C Bal.	t (hr)
0.05	0.05	0.48	0.08	0.66	0.03	0.18	0.76	62%	92%	6.0

Maximum selectivity with xylitol for C_3 products and formic acid (FA) is 1.0 and 5.0 respectively.

Presumedly, C_3 and C_2 selectivity would be nearly the same with cleavage of C2 and C3 of the xylitol carbon chain. However, glycolic acid (GlyA2) and ethylene glycol (EG) account for only one third of the total C_3 produced. This discrepancy can be explained, however, by the limited number of reactions available for the C_2 aldehydic intermediate glycolaldehyde. After retro-aldol condensation of the C_5 sugar to glyceraldehyde (C_3) and glycolaldehyde (C_2), the C_3 intermediate can undergo β-elimination of hydrogen to pyruvaldehyde and further react to form lactic acid, which happened readily as seen in Table 4-7. However, glycolaldehyde cannot undergo β-elimination of hydrogen because it does not have a β carbon. Thus, the intermediate can only hydrogenate to ethylene glycol, undergo a Cannizzaro reaction to form glycolic acid and ethylene glycol, or recondense with other intermediates to react further. From the low selectivity of glycolic acid and ethylene glycol, glycolaldehyde must recondense with higher selectivity.

Two runs with glycerol compared different proportions of glycerol to potassium hydroxide and the effect on product distribution (see Table 4-8). Both reactions converted glycerol to lactic acid with the highest selectivity. The lower concentration run, however, showed significantly higher selectivity toward lactic acid, propylene glycol, and glyceric acid (0.66 versus 0.39). Further, selectivity to formic acid was much lower at the reduced base concentration (0.60 versus 1.03). The lower carbon balance for

the higher glycerol and potassium hydroxide loadings also showed increased gas production.

Table 4-8: Product distribution from alkaline degradation of glycerol

Exp	GO Conc.	KOH Conc.	PG Sel.	LA Sel.	C_3 Sel.	FA Sel.	Conv.	Carbon Bal.	t (hr)
72	0.065 M	0.15 M	0.10	0.44	0.66	0.60	81%	98%	6.0
78	0.18 M	0.85 M	0.06	0.30	0.38	1.03	62%	82%	6.0

Maximum selectivity with glycerol for C_3 products and formic acid (FA) is 1.0 and 3.0 respectively.

The C_2 product distribution (Table 4-9) also showed carbon-carbon cleaving of glycerol in addition to C_3 products. Ethylene glycol selectivity remained constant while selectivity to glycolic acid dropped from Experiment 72 to 78.

Table 4-9: C_2 product distribution – alkaline degradation of glycerol

Exp	GO Conc.	KOH Conc.	EG Sel.	GlyA2 Sel.	Conv.	Carbon Bal.
72	0.065 M	0.15 M	0.03	0.14	81%	98%
78	0.18 M	0.85 M	0.03	0.04	82%	82%

4.1.6 Summary

For alkaline degradation of sugar alcohols to occur, both base and an activated metal catalyst are necessary to see significant conversion of the feedstock. Dehydrogenation of a primary hydroxyl group over the metal catalyst is the first step of the reaction as seen from product distributions and gas formation. Dehydrogenation and subsequent degradation of the sugar explains the formation of intermediates during the reaction as well as the presence of saturated polyols formed via hydrogenation (e.g. PG, GO, and EG). These could not form without free hydrogen in the system or adsorbed

hydrogen on the catalyst. Chemisorbed hydrogen from the reduction step of the catalyst only accounts for 10^{-6} moles of hydrogen while the hydrogenated products need $\sim 10^{-3}$ moles of H_2 in order to form. Thus, H_2 is produced from the feedstock.

The reaction temperatures and pressures were significantly reduced with respect to hydrogenolysis while maintaining similar selectivity to C_3 products, albeit with lower feedstock concentrations. The addition of base to the reaction allowed for continued conversion without the need for higher temperatures. To bring this reaction further, the sugar alcohol feedstocks were replaced with monosaccharides. Since dehydrogenation is the first step of alkaline degradation of sorbitol, it seemed prudent to start with a sugar instead to remove the dehydrogenation step and directly react to products. Section 4.2 describes the efforts taken in this direction.

4.2 Solution-based alkaline degradation

Base-catalyzed carbon-carbon cleavage of monosaccharides, otherwise known as alkaline degradation, has been well researched with several papers covering mechanisms, product distributions, and the various chemistries associated with the reactions.[61-77] Since the literature is well-developed, only a few experiments were necessary. These runs served to confirm literature results, increase familiarity with the chemistry, and improve analytical techniques to identify and quantify products. The process variables of temperature, feedstock sugar, and initial sugar concentration in the feedstock were varied to observe transient behavior of the reactants and products. No metal catalyst was used for these experiments, as none was needed to cleave the sugars.

4.2.1 Effect of temperature - alkaline degradation

Experiments in which the temperature was varied demonstrated how readily alkaline degradation proceeds. Runs at 70°C and 150°C completed in 30 minutes or less and gave nearly identical product compositions. When the temperature was reduced to 40°C, the reaction slowed sufficiently to observe changes in concentrations of reactants and products over time. Typical runs at 40°C lasted six hours with intermittent sampling every 30 to 60 minutes. Table 4-10 outlines the major products of glucose degradation at 40°C. Glucose and potassium hydroxide concentrations of the feedstock were 0.18 M and 0.85 M respectively.

Table 4-10: Product distribution – alkaline degradation of glucose

Exp	Isom Sel.	LA Sel.	GlyA Sel.	C_3 Sel.	GlyA2 Sel.	AA Sel.	FA Sel.	Conv.	C Bal.	t (hr)
90	0.19	0.90	0.09	0.99	0.07	0.04	0.28	87%	97%	6.0

Consistent with results reported in literature, lactic acid was the primary C_3 product from the degradation reaction with a minor amount of glyceric acid. Unlike the sorbitol degradation reactions, no glycerol or propylene glycol was produced. No metal catalyst was present to hydrogenate intermediates and no hydrogen was evolved from dehydrogenation of sorbitol, which explains this result. Yields of lactic acid reportedly increase with further decreases in the process temperature.[77] However, the reaction times increase a significant amount with little gain in lactic acid selectivity. At 22°C, complete conversion of glucose and fructose feedstock takes over two days, as shown in Figure 4-3, while even lower temperatures require several weeks.[64]

4.2.2 Effect of feedstock sugar – alkaline degradation

Reducing the temperature further to 22°C provided insight on the reactivity of glucose, fructose, and mannose. Plotting the combined concentration of these sugars versus time over the course of the reaction showed that fructose was more reactive than glucose, which was much more reactive than mannose. Figure 4-3 illustrates this point. By using the total concentration of the three sugars, the isomerization reactions were ignored and only the conversion to degradation products accounted for the decrease in sugar concentration.

The result was consistent with MacLaurin[69] and illustrated how fructose cleaves readily to the intermediates necessary for organic acid production. Glucose and mannose did not convert as quickly, which reflected the need for each to isomerize to fructose before products formed.

4.2.3 Effect of initial sugar concentration – alkaline degradation

A final set of experiments involved varying the initial concentration of feedstock sugar while maintaining a constant base loading. From de Bruijn et al.[72], low concentrations of sugar produce higher selectivity to lactic acid relative to higher sugar loadings. Experimental results confirmed this result with glucose and xylose as reported in Table 4-11. The de Bruijn paper conjectured that the increase in C_3 selectivity is due to the lower ionization constant (pK_a) for sugars at lower concentrations (see Table 4-12). The lower pK_a increased ionization of the sugars and enhanced isomerization rates, via an enediol intermediate, relative to higher sugar concentration experiments. This increased the residence time of fructose in the reaction medium. Retro-aldol condensation of fructose then produced lactic acid with higher selectivity. Also, with less sugar, less

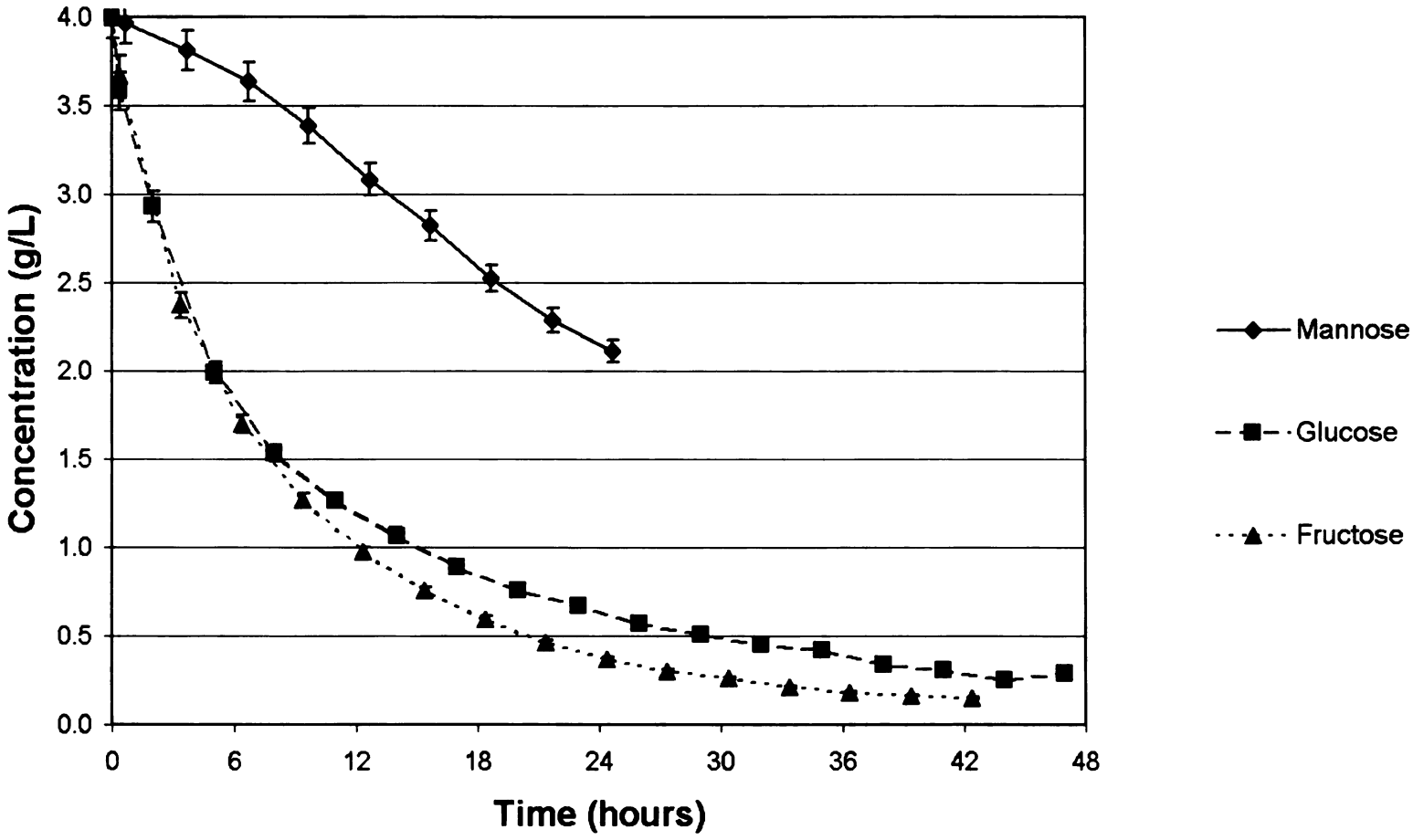

Figure 4-3: Total sugar concentration from mannose, glucose, and fructose feedstock vs. Time
Conditions - 22°C, 0.002 M sugar, 1.0 M NaOH

organic acid was produced to neutralize the base. Since the retro-aldol condensation and rearrangement reactions necessary for lactic acid production are base-catalyzed, the reduced amount of neutralization allowed the reactions to go to completion without competition from other side reactions, again enhancing the selectivity. The reactions were conducted under helium at 150°C and 100 psig of total pressure with 0.85 M potassium hydroxide in the feedstock.

Table 4-11: C_3 yield of high and low concentrations of xylose and glucose

Exp	Reactant	Conc. (M)	LA Sel.	GlyA Sel.	C_3 Sel.	% of theoretical	t (hr)
85	Xylose	0.01	0.90	0.00	0.90	90%	1.0
84	Xylose	0.18	0.57	0.05	0.62	62%	2.0
82	Glucose	0.01	1.31	0.22	1.53	76%	1.0
88	Glucose	0.18	0.76	0.24	1.00	62%	1.5

Table 4-12: pK_a values for glucose and fructose at varying concentrations

Conc. (M)	Glucose	Fructose
0.01	12.7	12.5
0.50	13.8	
1.14	14.0	14.2

4.2.4 Summary

Alkaline degradation provides a method to cleave sugars to C_3 products with high selectivity at relatively low temperatures. Fructose showed the highest rate of conversion of the sugars tested with glucose at a somewhat lower activity and mannose at a much lower level. Reduced concentrations of initial sugar feedstock increased the selectivity to lactic acid, which was consistent with the literature.

The main product of alkaline degradation is lactic acid instead of the more desirable products, propylene glycol and glycerol. In order to shift this product distribution, hydrogenation is necessary. Conceptually, the main intermediates from the degradation pathways, glyceraldehyde and pyruvaldehyde, could be hydrogenated as they form to yield glycerol and propylene glycol, respectively. This act of "capturing" the aldehydic intermediates would shift the C_3 product distribution away from lactic acid and toward the desired polyols without the high temperatures required for hydrogenolysis. Chapter 5 addresses this strategy.

Chapter 5 - Alkaline degradation with hydrogenation

5.1 - Overview

The combination of hydrogenation and alkaline degradation represents the main work of the research presented. Chapters 3 and 4 parsed sorbitol hydrogenolysis into distinct chemical reactions that occur simultaneously: dehydrogenation of sorbitol to a hexose complex, base-catalyzed carbon-carbon cleavage of the sugar into aldehydic intermediates, and subsequent hydrogenation of these intermediates into saturated products. Using those results, experiments were conducted to eliminate the first step of the process by starting with a sugar instead of a sugar alcohol and then optimize the remaining two reactions to produce propylene glycol, glycerol, and lactic acid.

Previous work by de Bruijn et al.[77] outlines pathways for glyceraldehyde and pyruvaldehyde production from the sugar cleavage reactions. Simple hydrogenation of these aldehydes produces glycerol and propylene glycol directly. The strategy of this work was to promote hydrogenation of the intermediates as they formed to increase yields of glycerol and propylene glycol, reduce organic acid production (namely lactic acid), and do all of this at lower temperatures and hydrogen pressures relative to hydrogenolysis. The results are summarized below.

5.2 – Parametric study: alkaline degradation with hydrogenation

A parametric study was used to observe a number of variables over a range of values. Hydrogen pressure, type of catalyst, catalyst loading, concentration of base, sugar loading, and temperature were the process variables adjusted to see corresponding changes in product distribution. Results from each section are presented in tabular form with the following descriptions:

Hyd: Fraction of starting material hydrogenated to a sugar alcohol.

Iso: Fraction of feedstock sugar that isomerized to a different C_6 sugar.

Deg: Fraction of feedstock that formed non-C_6 products via alkaline degradation.

Conv: The fraction of feedstock sugar that hydrogenated, isomerized, or degraded. I.e. Conv. = Hyd. + Iso. + Deg

C_3 sel: Selectivity of the reaction to form the C_3 products glycerol, propylene glycol, lactic acid, and glyceric acid. That is, the number of moles of C_3 products formed with respect to the number of moles of feedstock sugar that reacted. For example, if 0.1 moles of glucose reacted and formed 0.16 moles of C_3 products, C_3 sel. would be equal to 0.16 / 0.1 or 1.6 moles of C_3 product per mole of glucose reacted. The maximum value of C_3 sel. is 2.0, based on C_6 feedstock.

Max C_3: The maximum amount of C_3 product that could form based on the amount of converted feedstock sugar. Max C_3 = 2*Deg, which reflects the potential formation of two moles of C_3 products from one mole of C_6 sugar.

% of Max: C_3 sel. divided by Max C_3. This result relates the amount of C_3 products that were produced to the maximum amount of C_3 products that could have been produced based on the fraction of feedstock sugar that degraded.

C_3 yield: The amount of C_3 products formed with respect to the amount of feedstock charged to the reactor. C_3 yield has units of mole product formed per mole of feedstock fed.

Standard conditions for each reaction were 40°C at 100 psig of hydrogen with an agitation rate of 1000 rpm. Five percent ruthenium on carbon was the standard catalyst loaded at 0.1 grams, dry basis, which was pre-reduced at 230°C overnight at 200 psig of hydrogen. The feedstock for each reaction was 100 grams of total solution consisting of 3.17 wt% (0.18 M) fructose and 5.3% (0.85 M) potassium hydroxide. The high level of potassium hydroxide was necessary to promote the desired base-catalyzed reactions of fructose (e.g. retro-aldol condensation) with improved yields, with respect to lower base

loadings. Since fructose could produce two equivalents of organic acid, super-stoichiometric loadings of base was necessary to maintain high pH levels throughout the reaction. In addition, higher pH levels have been shown to increase the yield of C_3 products.[77]

Variations of hydrogen pressure, initial base concentration, feedstock sugar, and other parameters were observed to determine the effect on product distribution. The studies are summarized below.

5.2.1 – Effect of catalyst

Three traditional hydrogenation catalysts were used to investigate their use in the combined reaction. 5 wt% Ru/C (Aldrich), 5 wt% Pt/C (Aldrich), and 5 wt% Pd/C (Aldrich) were selected for the study. Loading was 0.1 grams (dry basis) for each catalyst, which reacted with 100 grams of solution containing 0.18 M fructose and 0.85 M KOH. Table 5-1 outlines the overall C_3 production for each metal after 6 hours of reaction and compares the extent of alkaline degradation to hydrogenation.

Table 5-1: Overall C_3 production and reaction comparison – Effect of catalyst metal
Conditions - 40°C, 100 psig, 0.18 M fructose, 0.85 M KOH, 0.1g catalyst

Exp	Metal	Conv.	Hyd.	Iso.	Deg.	C_3 sel.	Max C_3	% of max	C_3 yield
146	Ru/C	95%	0.15	0.11	0.69	1.00	1.38	72	0.94
138	Pt/C	96%	0.23	0.10	0.62	0.87	1.24	70	0.84
139	Pd/C	94%	0.16	0.12	0.67	1.02	1.34	76	0.96

The final product distributions were remarkably similar between the three active metals used in the experiments. Platinum showed a higher preference toward sugar hydrogenation than palladium and ruthenium, which reduced the overall C_3 yield for the

metal. Ruthenium and palladium, however, looked essentially identical. Further examination of the C_3 product distribution in Table 5-2 resolved the decision for the choice of metal.

Table 5-2: C_3 product distribution of Ru/C and Pd/C experiments
Conditions - 40°C, 100 psig, 0.18 M fructose, 0.85 M KOH, 0.1g catalyst

Exp	Catalyst	PG Sel.	GO Sel.	LA Sel.	GlyA Sel.	C_3 sel.	C_3 yield
146	Ru/C	0.25	0.19	0.51	0.04	1.00	0.94
139	Pd/C	0.15	0.16	0.67	0.04	1.02	0.96

Table 5-2 shows that the ruthenium catalyst promoted the hydrogenation of intermediates toward propylene glycol and glycerol with higher selectivity than palladium. The polyol products are preferred over organic acids because of higher sale value and because acids form potassium salts under these reaction conditions and must be precipitated out of solution and sufficiently acidified to form the free acid for further processing. This series of separations would add significant cost to the process. Thus, ruthenium on carbon was chosen for the remainder of the parametric study.

5.2.2 – Effect of temperature

Papers regarding hydrogenation[19-24] and alkaline degradation[69, 77] show significant changes in the individual reaction rates and product yields when temperature changes. For simultaneous alkaline degradation and hydrogenation, it was not known if the reactions would have corresponding changes in conversion or if one would dominate the conversion. Table 5-3 shows product distributions from three runs at 30, 40, and 50°C

for comparison. Reaction times were 6 hours, 6 hours, and 3 hours for 30, 40, and 50°C respectively.

Table 5-3: C_3 and C_6 production and reaction comparison – Effect of temperature Conditions - 100 psig, 0.18 M fructose, 0.85 M KOH, 0.1g 5% Ru/C catalyst

Exp	Temp. (°C)	Conv.	Hyd.	Iso.	Deg.	C_3 sel.	Max C_3	% of max	C_3 yield
143	30	78%	0.43	0.14	0.22	0.30	0.44	68	0.23
146	40	95%	0.15	0.11	0.69	1.00	1.38	72	0.94
153	50	99%	0.08	0.02	0.89	1.10	1.78	62	1.09

The rate of alkaline degradation was enhanced as reaction temperatures increased from 30 to 50°C with respect to hydrogenation. The sugar cleavage reactions consisted of 89% of the conversion at 50°C while it was only 22% at 30°C. Raising the temperature provided a means to limit sugar hydrogenation and potentially improve C_3 yields by promoting the degradation reactions. However, the conversion of the fructose to C_3 products was not as efficient at 50°C, as seen by the '% of max' column. Only 62% of the degraded sugar was converted to C_3 products compared to 70% at 30 and 40°C. At 50°C, pathways toward glyceraldehyde were promoted (i.e. degradation), as well as condensation reactions toward undesired products, which caused the '% of max' to drop.

Table 5-4 provides a comparison of C_3 product distributions with different temperatures. Though it increased conversion, the increase in temperature also promoted lactic acid formation over the desired polyols, propylene glycol and glycerol.

Table 5-4: C_3 product distribution – Effect of temperature

Conditions - 100 psig, 0.18 M fructose, 0.85 M KOH, 0.1g 5% Ru/C catalyst

Exp	Temp (°C)	PG Sel.	GO Sel.	LA Sel.	C_3 sel.	C_3 yield
143	30	0.03	0.22	0.05	0.30	0.24
146	40	0.25	0.19	0.51	1.00	0.94
153	50	0.24	0.09	0.70	1.10	1.09

5.2.3 – Effect of hydrogen pressure

Another factor affecting the competition between alkaline degradation and hydrogenation was the amount of hydrogen present over the course of the experiment. Alkaline degradation of the feedstock sugar occurs regardless of hydrogen pressure because it is a solution-based chemistry. However, when higher concentrations of hydrogen are present, hydrogenation becomes more prominent and affects the product distribution. A range of five hydrogen pressures, from 0 to 200 psig, was used to observe the effects on C_3 and C_6 product selectivity at 40°C.

Table 5-5: Selectivity of alkaline degradation with hydrogenation – H_2 pressure effect

Conditions – 40°C, 0.18 M fructose, 0.85 M KOH, 0.1g 5% Ru/C catalyst

Exp	Total P* (psig)	Conv.	Hyd.	Iso.	Deg.	C_3 sel.	Max C_3	% of max	C_3 yield
147	25	93%	0.13	0.13	0.66	0.93	1.32	70	0.87
149	50	93%	0.14	0.08	0.71	0.95	1.42	67	0.88
146	100	95%	0.15	0.11	0.69	0.99	1.38	72	0.94
140	200	96%	0.37	0.07	0.52	0.81	1.04	78	0.78

* Reaction gas was essentially hydrogen since the vapor pressure of water at 40°C is 1.1 psi.

The experiments yielded somewhat surprising results regarding hydrogenation activity. Hydrogen pressures of 25 to 100 psig showed little change in the amount of

sorbitol and mannitol formed. However, raising the pressure to 200 psig more than doubled the selectivity and yield to sugar alcohols. At the lower pressures, hydrogenation appeared to be 0^{th} order with respect to hydrogen, while at 200 psig, the rise in sugar alcohol production coincided with the rise in pressure. Figure 5-1 and Table 5-5 illustrate these results. This effect is partially attributed to uncertainties with concentration measurements (± 3%) but is not readily explained.

Distributions of the cleaved hydrogenation products of ethylene glycol, propylene glycol, and glycerol show a similar effect with the lower pressure experiments versus the 200 psig experiment, as seen in Table 5-6. Concentration versus time data of propylene glycol and glycerol also confirms the sequence of intermediate formation in the alkaline degradation. From de Bruijn et al.[77], two moles of glyceraldehyde form from fructose via the retro-aldol condensation. Glyceraldehyde then undergoes a β-elimination of water to form pyruvaldehyde. Pyruvaldehyde then hydrogenates to propylene glycol or forms lactic acid via a base-catalyzed isomerization. Thus, glycerol, from glyceraldehyde, should form before propylene glycol forms from pyruvaldehyde. This effect is illustrated in Figure 5-2 at 50 psig of hydrogen pressure.

Table 5-6: Selectivity of alkaline degradation with hydrogenation – H_2 pressure effect
Conditions – 40°C, 0.18 M fructose, 0.85 M KOH, 0.1g 5% Ru/C catalyst

Exp	Total P (psig)	EG sel.	PG Sel.	GO Sel.	LA Sel.
147	25	0.03	0.19	0.10	0.56
149	50	0.04	0.21	0.13	0.53
146	100	0.05	0.25	0.19	0.51
140	200	0.05	0.18	0.33	0.30

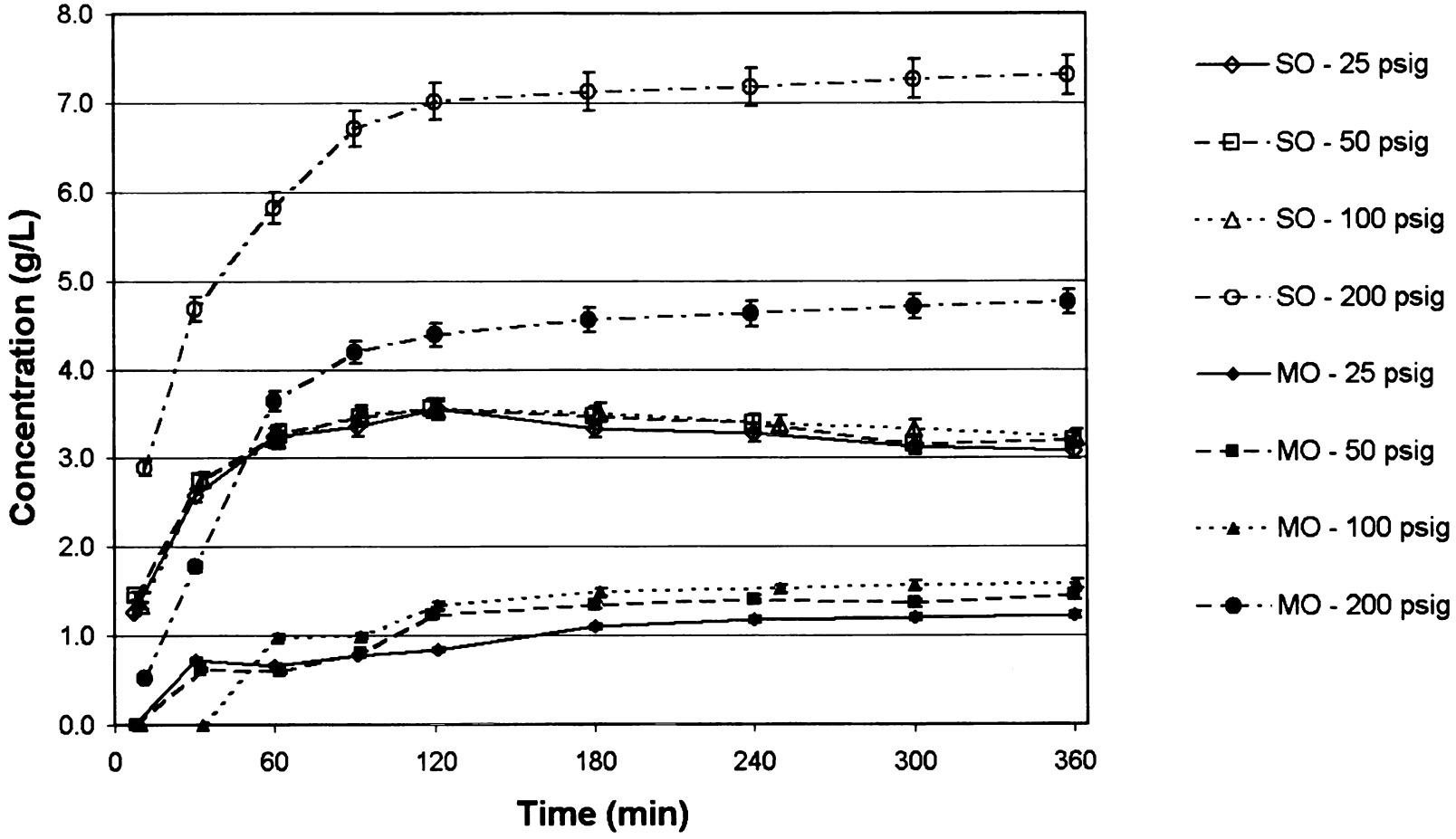

Figure 5-1: Concentration of sorbitol (SO) and mannitol (MO) vs. Time - Hydrogen effect
Conditions – 40°C, 0.18 M fructose, 0.85 M KOH, 0.1g 5% Ru/C catalyst

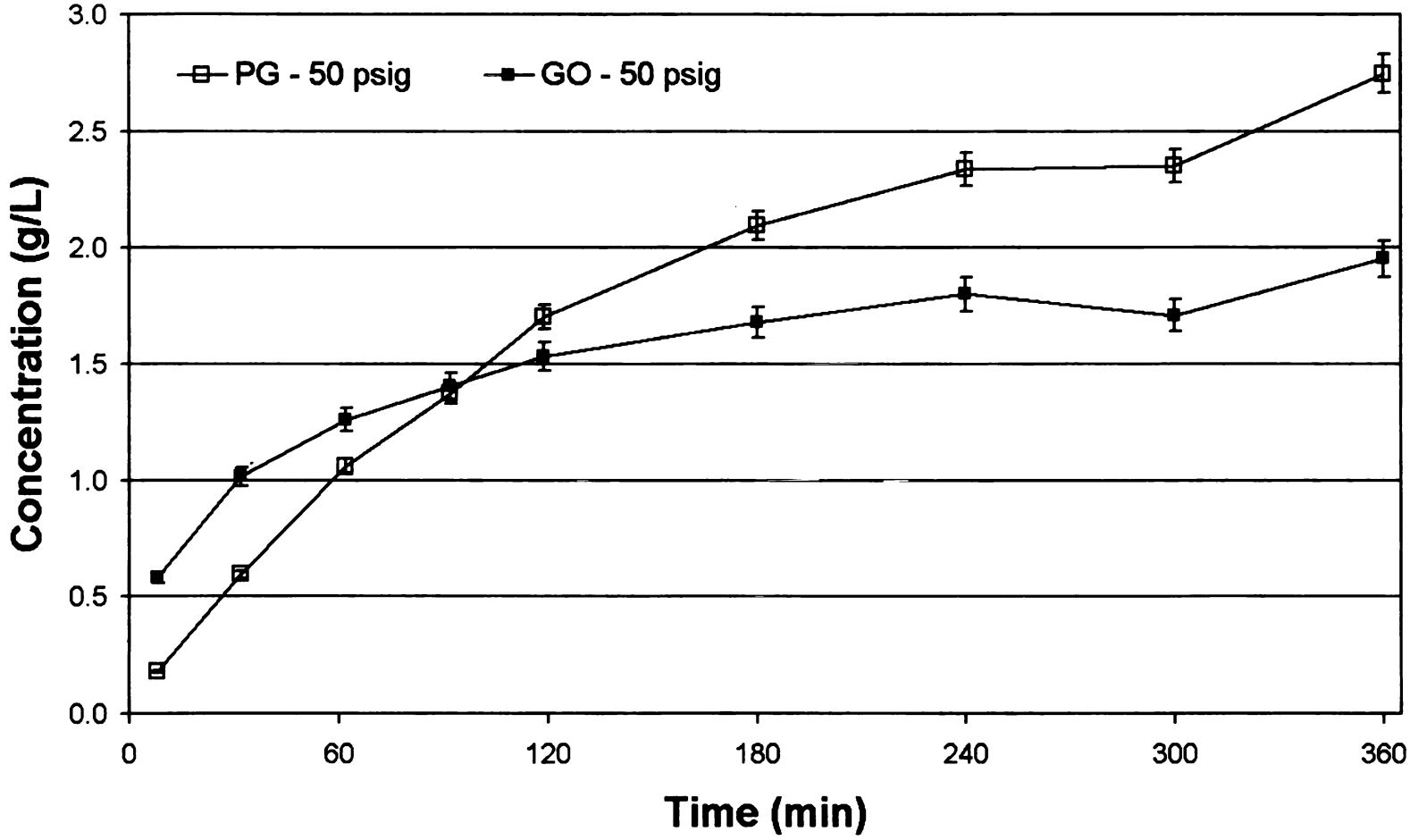

Figure 5-2: Concentration of propylene glycol (PG) and glycerol (GO) vs. Time - Hydrogen effect
Conditions – 40°C, 0.18 M fructose, 0.85 M KOH, 0.1g 5% Ru/C catalyst

Further, from Table 5-6 and Figure 5-2, more PG was produced than glycerol by the end of the reaction. This suggests that as more glyceraldehyde becomes available, the rate of conversion to pyruvaldehyde is faster than the hydrogenation of glyceraldehyde to glycerol. Thus, more pyruvaldehyde becomes available for hydrogenation to PG or rearrangement to lactic acid. But, as hydrogen pressure is increased, this difference in activity decreases. More glycerol is formed, which limits the extent of conversion of the glyceraldehyde-pyruvaldehyde pathway and decreases the amount of pyruvaldehyde available to form PG. This effect is evident from the crossover between PG and GO selectivity in Table 5-6 with increasing pressure and greater selectivity for glycerol relative to PG at a total pressure of 200 psig.

5.2.4 – Effect of catalyst loading

Catalyst loading was another parameter adjusted to observe the hydrogenation–alkaline degradation competition. Additional amounts of catalyst should lead to increased hydrogenation activity as more catalytic sites are present for materials to react. The purpose of this set of runs was to maximize C_3 yield by changing the amount of catalyst at constant temperature (40°C), pressure (100 psig total), initial fructose concentration (0.18 M), and initial KOH concentration (0.85 M). Four experiments, with loadings of 0.0 to 0.20 grams of catalyst, were used. Table 5-7 displays the overall product distributions from this set.

Table 5-7: Comparison of catalyst loading for alkaline degradation with hydrogenation Conditions – 40°C, 0.18 M fructose, 0.85 M KOH, 100 psig H_2, 5% Ru/C catalyst

Exp	Catalyst loading	Conv.	Hyd.	Iso.	Deg.	C_3 sel.	Max C_3	% of max	C_3 yield
90*	0.00g	87%	0.00	0.16	0.71	0.90	1.42	65	0.78
115	0.05g	94%	0.14	0.10	0.70	0.97	1.40	69	0.91
146	0.10g	95%	0.15	0.11	0.69	0.99	1.38	72	0.94
152	0.20g	96%	0.25	0.08	0.63	0.89	1.26	71	0.85

* Feedstock for experiment 90 was 0.18 M glucose instead of fructose

Higher catalyst loading showed higher activity toward hydrogenation, as expected, but the effect was not as dramatic as that of the rise in hydrogen pressure. This suggests that the surface concentration of hydrogen is more important than the number of active sites available for hydrogenation

This set of experiments showed 0^{th} order behavior with respect to catalyst loading, similar to the hydrogen effect, as illustrated in Figure 5-3. At low catalyst loadings (0.05 and 0.10 gram) virtually no change was observed in sorbitol and mannitol production. At the 0.20 gram loading, a significant increase in sugar alcohol production was observed.

Table 5-8 provides the C_3 selectivity data from these runs. Changes in C_3 selectivity were also similar to those observed in the hydrogen effect studies. Preference toward glycerol grew as the amount of catalyst increased. Acid formation was also inhibited with the increase in active metal available indicating that the extent of hydrogenation of C_3 intermediates increases with increased catalyst loading.

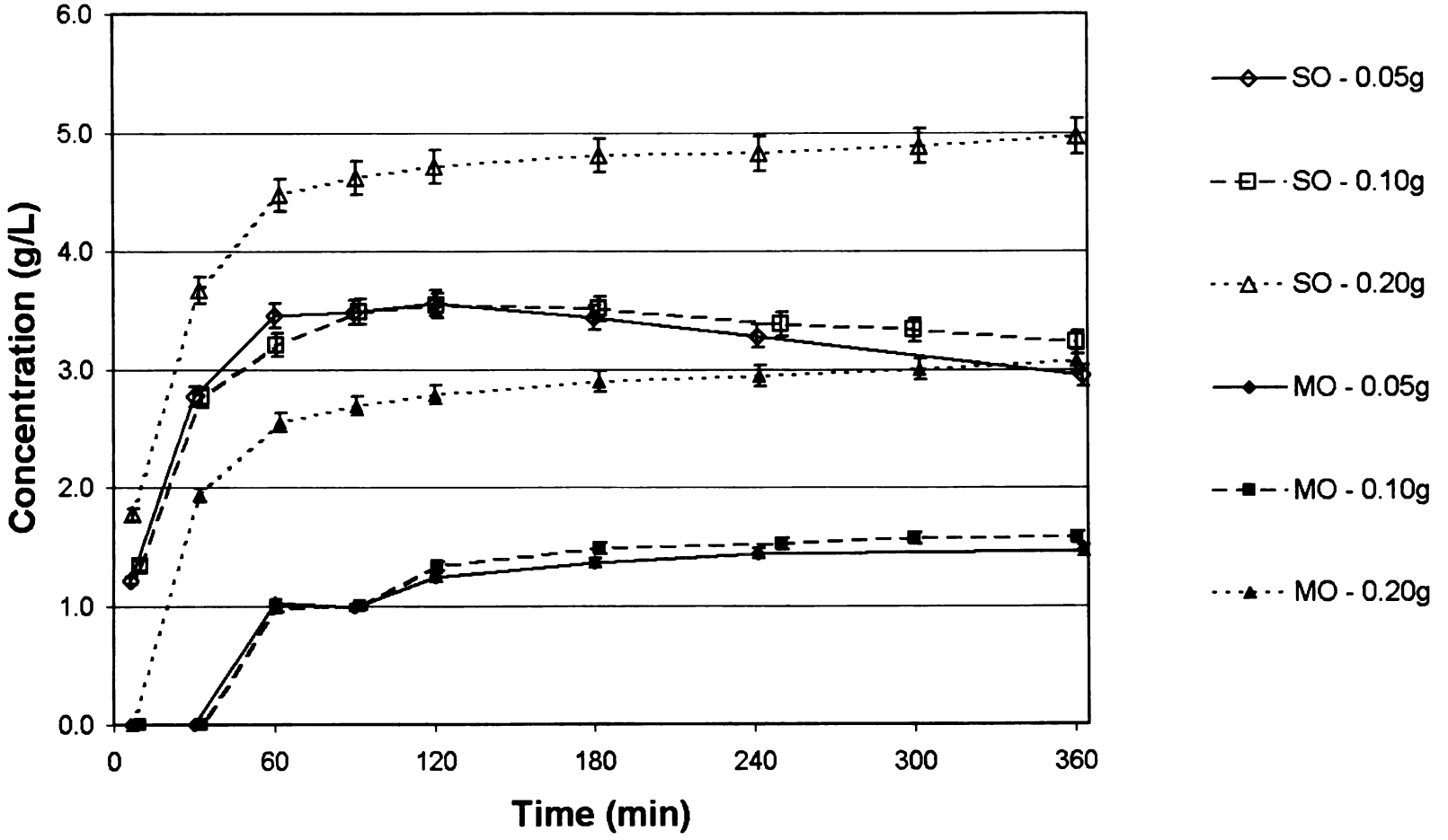

Figure 5-3: Concentration of sorbitol (SO) and mannitol (MO) vs. Time - Effect of catalyst loading
Conditions – 40°C, 0.18 M fructose, 0.85 M KOH, 100 psig H_2, 5% Ru/C catalyst

Table 5-8: Selectivity of EG, PG, GO, and LA – effect of catalyst loading
Conditions – 40°C, 0.18 M fructose, 0.85 M KOH, 100 psig H_2, 5% Ru/C catalyst

Exp	Catalyst loading	EG sel.	PG Sel.	GO Sel.	LA Sel.
90*	0.00g	0.00	0.00	0.00	0.90
115	0.05g	0.04	0.16	0.16	0.65
146	0.10g	0.05	0.25	0.19	0.51
152	0.20g	0.06	0.29	0.33	0.24

* Feedstock for experiment 90 was 0.18 M glucose instead of fructose

5.2.5 – Effect of initial base concentration

One potential problem with the alkaline degradation concept is the need for excessive amounts of base. Potassium hydroxide is relatively inexpensive, but the addition of another raw material cuts into potential profit margins. In addition, downstream neutralization would be necessary to extract acidic products. Corrosion of the metal reactor becomes an issue as well at the high pH levels required.

High pH levels are important, however, in order to maintain selectivity to C_3 products at low temperature and hydrogen pressure. The retro-aldol condensation reaction is base-catalyzed and has the potential for high selectivity to C_3 products (> 75% of theoretical) with monosaccharide feedstock. Thus, the thrust of this set of experiments was to determine how the product distribution changes with different loadings of potassium hydroxide. Table 5-9 outlines the overall C_3 and C_6 selectivity.

Hydrogenation activity rose dramatically as the amount of base in the feedstock decreased. Selectivity to the sugar alcohols climbed from 0.15 to 0.79 mole of sugar alcohol produced per mole of fructose reacted when the base concentration was cut by 80%. The amount of base was not sufficient to favor cleavage of the sugar over

hydrogenation. However, the 0.38 M loading demonstrated that feedstock that does undergo degradation forms C_3 materials with essentially the same preference as the higher loading, as seen in the '% of max' column in Table 5-8. Thus, at lower base loadings, higher C_3 yields may be possible, but with 0.1 grams of catalyst and 100 psig of H_2 present, hydrogenation was too fast to realize them.

Table 5-9: C_3 and C_6 selectivity of reaction with varying base concentration
Conditions – 40°C, 0.18 M fructose, 100 psig H_2, 0.1g 5% Ru/C catalyst

Exp	KOH Conc.	Conv.	Hyd.	Iso.	Deg.	C_3 sel.	Max C_3	% of max	C_3 yield
146	0.85 M	95%	0.15	0.11	0.69	0.99	1.38	72	0.94
116	0.38 M	92%	0.50	0.11	0.30	0.41	0.60	68	0.38
117	0.17 M	97%	0.79	0.05	0.13	0.12	0.26	46	0.12

Table 5-10 lists the C_3 product distribution from the series of experiments at different base loadings. The results show that alkaline degradation slows down significantly with reduced levels of base. This is consistent with observations by de Bruijn et al.[72] and was confirmed by the lack of propylene glycol and lactic acid formed at the 0.17 M loading.

Table 5-10: Selectivity of EG, PG, GO, and LA – effect of initial base concentration
Conditions – 40°C, 0.18 M fructose, 100 psig H_2, 0.1g 5% Ru/C catalyst

Exp	KOH Conc.	EG sel.	PG Sel.	GO Sel.	LA Sel.
146	0.85 M	0.05	0.25	0.19	0.51
116	0.38 M	0.04	0.09	0.27	0.04
117	0.17 M	0.01	0.01	0.10	0.00

5.2.6 – Effect of initial sugar concentration

Results from literature[77] and earlier experiments with alkaline degradation (see Section 4.2) showed that low sugar concentrations led to high C_3 selectivity. Higher C_3 selectivity meant promoted degradation pathways and potential to realize higher C_3 yields when hydrogenation was added. Three levels of sugar concentration were used to see if higher yields would be realized in the presence of hydrogen and catalyst. Table 5-11 displays the overall selectivity from the reaction.

Table 5-11: C_3 and C_6 selectivity of reaction with varying sugar concentration Conditions – 40°C, 0.85 M KOH, 100 psig H_2, 0.1g 5% Ru/C catalyst

Exp	Init. Sugar Conc.	Conv.	Hyd.	Iso.	Deg.	C_3 sel.	Max C_3	% of max	C_3 yield
119	0.06 M	97%	0.57	0.04	0.37	0.50	0.74	68	0.37
144	0.12 M	96%	0.22	0.09	0.64	1.09	1.28	85	1.05
146	0.18 M	95%	0.15	0.11	0.69	0.99	1.38	72	0.94

Decreasing the sugar concentration from 0.18 M to 0.12 M showed an improvement in C_3 selectivity. However, further reduction to the 0.06 M loading reversed the trend with a reduced efficiency to C_3 products. The improvement gained by lowering the sugar content was offset by the increase in hydrogenation activity to the sugar alcohols. With a lower proportion of feedstock to catalytic sites, the hydrogenation reaction was promoted and decreased the potential C_3 yield.

One other interesting observation was the constant amount of sugar alcohol produced between the three concentrations. Hydrogenation selectivity of 0.57, 0.22, and 0.15 for the feedstock concentrations of 0.06 M, 0.12 M, and 0.18 M, respectively, yielded 0.0034, 0.0026, and 0.0024 moles of sorbitol and mannitol combined. This

suggested 0^{th} order hydrogenation kinetics with respect to sugar concentration. Thus, with higher sugar loading, more of the feedstock should undergo degradation pathways to potentially form C_3 products. However, too much sugar led to higher levels of organic acid formed, which lowered the solution pH and reduced C_3 selectivity via retro-aldol condensation.

5.2.7 – Effect of feedstock sugar

The final group of experiments involved the specific sugar used as feedstock for the reaction. Alkaline degradation of fructose, glucose, and mannose showed that fructose had the highest activity of the three. Table 5-12 compares the product distributions from the three sugars.

Table 5-12: C_3 and C_6 selectivity product distribution – effect of feedstock sugar
Conditions – 40°C, 0.18 M sugar, 0.85 M KOH, 100 psig H_2, 0.1g 5% Ru/C catalyst

Exp	Feed sugar	Conv.	Hyd.	Iso.	Deg.	C_3 sel.	Max C_3	% of max	C_3 yield
146	Fructose	95%	0.15	0.11	0.69	0.99	1.38	72	0.94
141	Glucose	90%	0.28	0.10	0.52	0.76	1.04	73	0.68
142	Mannose	75%	0.21	0.18	0.36	0.59	0.72	82	0.44

In the presence of hydrogenation catalyst, fructose showed the highest rate of conversion to products. Fructose also showed the highest activity toward degradation suggesting that it was the main intermediate leading into the sugar cleavage reactions. Mannose demonstrated a surprisingly high proportion of degraded material converting to C_3 products. However, the slower rate of reaction to C_3 products (i.e. 'Deg.') in comparison with fructose made it less appealing. The relatively high selectivity to

mannitol (hydrogenation product) also reduced the C_3 selectivity and yield significantly. Table 5-13 compares the C_3 product distribution from the three feedstock sugars.

Table 5-13: Selectivity of EG, PG, GO, and LA – effect of feedstock sugar
Conditions – 40°C, 0.18 M sugar, 0.85 M KOH, 100 psig H_2, 0.1g 5% Ru/C catalyst

Exp	Feedstock sugar	EG sel.	PG Sel.	GO Sel.	LA Sel.
146	Fructose	0.05	0.25	0.19	0.51
141	Glucose	0.06	0.21	0.30	0.25
142	Mannose	0.05	0.15	0.20	0.24

Both glucose and mannose showed higher selectivity to glycerol than propylene glycol. Fructose, on the other hand, had higher selectivity to propylene glycol than glycerol. In addition, selectivity to lactic acid was significantly higher for fructose. This suggested that glucose and mannose form glyceraldehyde at a slower rate than fructose, presumably by isomerizing to fructose before undergoing the retro-aldol condensation to glyceraldehyde. The regulated reaction had the benefit of producing a higher fraction of C_3 products in polyol form (67% for glucose and 59% for mannose) versus the direct route with fructose (46% of C_3's to PG and GO). But, the extended time to form the necessary intermediates allowed more time for hydrogenation of the sugar feedstock, thus lowering their overall attractiveness as feedstocks.

5.3 – Summary and significance of results

The parametric studies described in this chapter serve to better define the reaction environment of the alkaline degradation – hydrogenation reaction. Through these experiments, the concept of "capturing" active C_3 aldehydic intermediates to form the

desired products of propylene glycol and glycerol was proven and carried out at temperatures and pressures significantly lower than usual hydrogenolysis conditions (40°C and 100 psig H_2 with sugar feedstock versus 230°C and 1200 psig H_2 with sugar alcohol feedstock).

Each of the parameters studied played an important role in developing the product distribution at the end of the reaction. Temperature showed the largest effect. Alkaline degradation pathways were enhanced a significant amount with just a 10°C increase in the process temperature. The loading of potassium hydroxide had a large effect as well. Superstoichiometric amounts of base with respect to the sugar feedstock were necessary to maintain good selectivity to C_3 products and to continue alkaline degradation chemistry. Without sufficiently high pH, the degradation reactions shut down and allowed feedstock hydrogenation to take over.

Hydrogen pressure and catalyst loading were also crucial in determining product distributions. An overload of either diminished C_3 yields significantly by hydrogenating the feedstock sugar to its corresponding sugar alcohol. These two studies also confirmed suggested pathways for degradation chemistry simply by observing the concentration versus time data. Taking the pathways already developed, product distributions were fairly easy to explain, even as the reactions progressed.

The study that involved the different feedstock sugars also highlighted a potential strategy for further C_3 yield improvement. Preference to C_3 products is based mainly on the conversion of fructose into glyceraldehyde. From that intermediate, several different reactions can occur, diminishing selectivity to desired products. However, if glyceraldehyde is hydrogenated immediately, those pathways are eliminated. Glucose

and mannose demonstrated this concept by maintaining high efficiency to C_3 products with a preference toward glycerol and propylene glycol. Hydrogenation of the sugar must be avoided, however, to have desirable C_3 yields.

Experiment 144 (40°C, 100 psig H_2, 0.12 M fructose, 0.85 M KOH, 6 hour reaction time) showed the most promising results from this group of studies. Of the reacted feedstock that followed the alkaline degradation pathways, 85% was converted to the desired C_3 products of propylene glycol, glycerol, lactic acid, and glyceric acid ('% of max). From Table 5-14, 64% of the fructose feedstock underwent alkaline degradation ('Deg'). Potentially, this could produce 1.28 moles of desired C_3 per mole of fructose reacted ('Max C_3'). A selectivity of 1.09 moles of C_3 per mole of fructose reacted was observed ('C_3 sel.'), which led to a '% of max' of 85%. Experiment 152 (50°C, 100 psig H_2, 0.18 M fructose, 0.85 M KOH, 6 hour reaction time) has a higher C_3 yield than Experiment 144, however, the efficiency to C_3 products is much lower (62% vs. 85%). In addition, Experiment 144 has the added potential of recycling to further improve the overall C_3 yield. The hydrogenation products of sorbitol and mannitol can be converted to glycerol and propylene glycol with yields of ~70% of theoretical. This would increase the overall C_3 yield by 0.3 (70% * 0.22 moles sugar alcohol per mole fructose * 2 moles of C_3 per mole of C_6) to 1.35 moles of C_3 per mole of fructose fed. Further, the isomerized sugars can further react to form the same desired C_3 products to raise the final yield to 1.4 moles C_3 per mole of fructose fed, or 70% of theoretical.

Table 5-14: Comparison of Experiments 144 and 153

Exp	Init. Sugar Conc.	Conv.	Hyd.	Iso.	Deg.	C_3 sel.	Max C_3	% of max	C_3 yield
144	0.12 M	96%	0.22	0.09	0.64	1.09	1.28	85	1.05
153	0.18 M	99%	0.08	0.02	0.89	1.10	1.78	62	1.09

The overall C_3 yield of the process was diminished due to the use of a conventional catalyst that indiscriminately hydrogenated both sugar feedstock and degradation intermediates. Thus, sugar feedstock that could have formed the desired C_3 products instead, was converted into mannitol or sorbitol. A catalyst that preferentially hydrogenates glyceraldehyde and pyruvaldehyde instead of feedstock sugar would be of great benefit to this system. Candidate catalysts for this selective hydrogenation are discussed in Chapter 7.

In addition to observing the effects of various parameters on the overall product distribution of the reaction, a kinetic model of the reaction system was developed. Derivation and comparison of the model to experimental results is discussed in Chapter 6.

Chapter 6 – A kinetic model for simultaneous alkaline degradation and hydrogenation

6.1 - Overview

This chapter outlines efforts to describe the alkaline degradation – hydrogenation reaction rates with a mathematical model. Several papers describe pathways, mechanisms, and kinetics for sugar hydrogenation[19-23] and for alkaline degradation[69-76]. The work presented here seeks to combine the two reactions into a general model. The next sections summarize mass transfer calculations of reactant transport through the reaction, describe the derivation of the model, outline assumptions made to simplify the network of reactions, discuss the method used for calculating concentration versus time, and compare the final model and data collected.

6.2 – Mass transfer calculations

Mass transfer rates of the reactants were calculated to ensure that the derived kinetic model was based on surface rates of reaction in the catalyst instead of mass transport of reactants between phases. Several correlations from the literature were used to calculate minimum stirring rates for catalyst suspension and mass transfer coefficients for these experiments and are described below.

6.2.1 – Catalyst suspension

To ensure proper mixing of catalyst within reactor, it was necessary to make sure that the catalyst was completely suspended in the solution as the reaction progressed. This maximized the amount mass transfer area of the catalyst for transport of hydrogen

and unsaturated intermediates to the metal sites. Zwietering[90] proposed a correlation for minimum stirring speed necessary to completely suspend catalyst within a baffled vessel:

$$N_{min} = \frac{\beta \cdot d_p \cdot \mu_L^{0.1} \cdot g^{0.45} \cdot \left(\rho_p - \rho_L\right)^{0.45} \cdot w^{0.13}}{\rho_L^{0.55} \cdot d_i^{0.85}} \qquad (1)$$

Where:

N_{min} = minimum stirring speed for catalyst suspension [rotations / sec]

β = constant determined by impeller geometry

w = catalyst loading [grams catalyst per 100 grams solution]

d_p = particle diameter [m]

μ_L = liquid viscosity [kg / m·s]

g = gravitation constant [9.8066 m / s^2]

ρ_p = particle density [kg / m^3]

ρ_L = liquid density [kg / m^3]

d_i = impeller diameter [m]

Reactions used 0.1 grams of catalyst per 100 mL of solution, which required a minimum stirring speed of approximately 400 rpm. An agitation rate of 1000 rpm was used to ensure complete suspension of the catalyst.

6.2.2 – Three phase mass transfer

For hydrogenation reactions to occur within this system, unsaturated reactants from the liquid phase and hydrogen from the gas phase must undergo the following steps to reach the active metal sites in the catalyst in order to react:

[90] Zwietering, T. H., *Chem. Eng. Sci.*, **1958**, *8*, 244

1. Transport of hydrogen from the gas phase to the gas-liquid interface
2. Transport of hydrogen from the gas-liquid interface to the bulk liquid
3. Transport of hydrogen and unsaturated reactants (e.g. glucose, fructose, glyceraldehyde) from the liquid phase to the catalyst surface through the solid-liquid interface
4. Intraparticle diffusion of hydrogen and reactants through the catalyst pores
5. Adsorption of reactants on the active sites of the catalyst
6. Surface reaction (e.g. glucose + H_2 → sorbitol)
7. Desorption of products

Figure 6-1 illustrates the phases of the reaction and relative concentration of reactants from the gas and liquid phases.

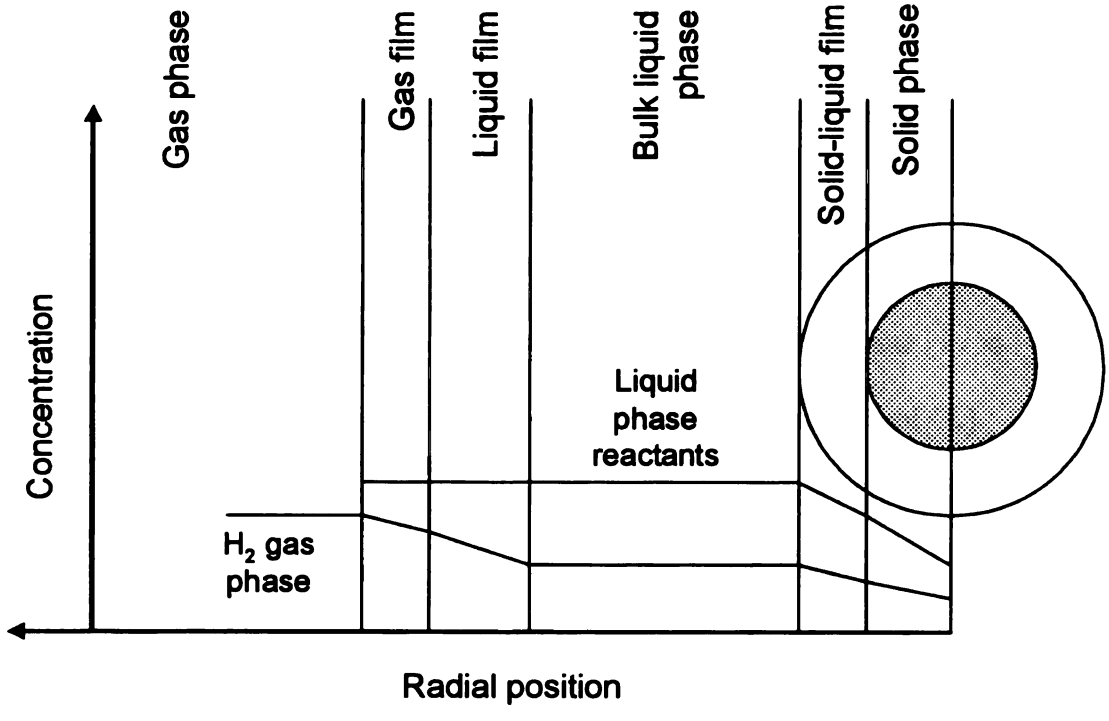

Figure 6-1: Mass transfer in a three phase catalytic reaction

6.2.3 – Reaction rate and mass transfer

Hydrogen and the liquid phase reactants pass through interfaces between phases to react. The rate of transfer of the compounds between phases can affect the overall reaction rate depending on the relative rates of mass transfer for each reactant. For calculations, liquid phase reactants are assumed to have the characteristics of fructose.

Gas-liquid transfer:

$$-R_{G\text{-}H2} \cdot L = k_L a \, (C_{H2,\,G} - C_{H2,\,L}) \qquad (2)$$

Liquid-solid transfer:

$$-R_{G\text{-}H2} \cdot L = k_{S,H2}\, a \, (C_{H2,\,L} - C_{H2,\,S}) \qquad (3)$$

$$-R_{G\text{-}A} \cdot L = k_{S,A}\, a \, (C_{A,\,L} - C_{A,\,S}) \qquad (4)$$

Where:

$-R_G$ = observed reaction rate of the species [kmol / $m^3 \cdot s$]

L = ratio of catalyst surface area per unit volume fluid [m^2 / m^3]

$k_L a$ = gas-liquid mass transfer [1 / $m \cdot s$]

$k_{S,H2}\, a$ = liquid-solid mass transfer [1 / $m \cdot s$]

$k_{S,A}\, a$ = liquid-solid mass transfer of liquid phase reactants [1 / $m \cdot s$]

$C_{H2,\,L}$ = concentration of hydrogen in the liquid phase [mol / L]

$C_{A,\,L}$ = concentration of liquid phase reactants [mol / L]

$C_{H2,\,S}$ = concentration of hydrogen in the catalyst [mol / L]

$C_{A,\,S}$ = concentration of liquid phase reactants in the catalyst [mol / L]

In these equations, the driving force for mass transfer is the difference in concentration between phases, which can be measured directly or calculated (e.g. hydrogen concentration in the liquid phase with Henry's Law). The mass transfer coefficients from the expressions can be determined experimentally or calculated based on correlations in the literature. With values for reactant concentration and mass transfer coefficients, the observed reaction rate may be calculated.

In addition, the maximum amount of mass transfer for each reactant may be determined by setting the driving force equal to the higher of the two concentrations:

$$\text{Maximum G-L mass transfer rate} = k_L a \, (C_{H2,\,G} - C_{H2,\,L}) \quad (5)$$

$$\text{Maximum L-S mass transfer rate} = k_{S,A}\, a \, (C_{A,\,L}) \quad (6)$$

$$k_{S,H2}\, a \, (C_{H2,\,L}) \quad (7)$$

The maximum rate of mass transfer for each reactant is compared to the observed reaction rate. If the observed reaction rate is significantly less than the maximum rate of mass transfer then the reaction is not mass transfer limited.

6.2.4 – Gas-liquid mass transfer coefficient

For these reactions, the gas phase comprised of hydrogen and water vapor. However, with a process temperature of 40°C, the partial pressure of water was only 1.1 psi. This accounted for less than 3% of the gas phase at the lowest reaction pressure of the experiments considered (Experiment 147, 25 psig) and was subsequently assumed to be hydrogen for calculation purposes.

To estimate the mass transfer of hydrogen from the gas phase to the liquid phase, concentrations of hydrogen in both phases and the value for the mass transfer coefficient

were needed. The gas phase concentration was calculated using the ideal gas law and the liquid phase concentration was calculated using Henry's Law[91]:

$$P = Hx \tag{8}$$

Where:

P = partial pressure of solute (H_2) in the gas phase

H = Henry's Law constant [atm / (mole solute / mole solution)]

x = mole fraction of solute (H_2) in liquid phase

Henry's law constant for hydrogen at 40°C is 75,100 atm / (mole H_2 / mole water)[92], which corresponds to a solubility of 1.1×10^{-5} moles / cm^3. For calculation purposes, the solubility of hydrogen was assumed to be the same as that of water.

The gas-liquid mass transfer coefficient (k_La) was calculated using correlations from Yagi and Yoshida[93] and Bern et al.[94] The correlation from Yagi and Yoshida was used to adequately predict CO_2 adsorption for a glycerol-water system at 30°C and is as follows:

$$Sh = \frac{k_L a d_i^2}{D_A} = 0.06\left(\frac{d_i^2 N \rho_L}{\mu_L}\right)^{1.5}\left(\frac{d_i^2 N^2}{g}\right)^{0.19}\left(\frac{\mu_L}{\rho_L D_A}\right)^{0.50}\left(\frac{\mu_L u_g}{S_T}\right)^{0.60}\left(\frac{N d_i}{u_G}\right)^{0.32} \tag{9}$$

Where:

Sh = Sherwood number [dimensionless]

k_La = gas-liquid mass transfer [1 / m · s]

---

[91] Felder, R.M.; Rousseau, R.W., *Elementary Principles of Chemical Processes*, 2nd Ed., p. 248, Wiley, New York, 1986

[92] Perry, R.H.; Green, D.W., *Perry's Chemical Engineers' Handbook*, 7th Ed., p. 2-126, McGraw-Hill, New York, 1997

[93] Yagi, H.; Yoshida, F., *Ind. Eng. Chem. Proc. Des. Dev.*, **1975**, *14*, 488

[94] Bern, L.; Lidefelt, J.O.; Schoon, N.H., *J. Am. Chem. Soc.*, **1976**, *53*, 463

d_i = impeller diameter [m]

D_A = diffusion rate of species A [m / s^2]

N = stirring speed [s^{-1}]

ρ_L = liquid density [kg / m^3]

μ_L = liquid viscosity [kg / m·s]

g = gravitational constant [9.8066 m / s^2]

u_G = gas velocity [m / s]

S_T = surface tension [N / m]

The correlation developed by Bern (Equation 9) was based on a slurry reactor used to hydrogenate oil in a mass transfer controlled regime and sufficiently predicted gas-liquid mass transfer for 30 and 500 liter reaction vessels.

$$k_L a = \frac{0.011 \cdot N^{1.16} \cdot d_i^{1.979} \cdot u_g^{0.32}}{V_L^{0.0521}} \qquad (10)$$

k_L = liquid film mass transfer coefficient [m / s]

a = gas-liquid interfacial area per unit volume of reactor [cm^2 / cm^3]

d_i = impeller diameter [cm]

N = stirring speed [s^{-1}]

u_g = gas velocity [cm / s]

ρ_L = liquid density [g / cm^3]

V_L = volume of the solution [cm^3]

6.2.5 – Liquid-solid mass transfer coefficient

Transfer of hydrogen and the liquid phase reactants from the bulk liquid phase to the catalyst surface is necessary for the reaction to occur. The liquid-solid mass transfer coefficient, k_S, is determined for all reactants using the Boon-Long equation.[95]

$$\frac{k_s d_p}{D_A} = 0.046 \cdot \left(\frac{2\pi^2 d_p d_T N}{\mu_L}\right)^{0.283} \left(\frac{\rho_L^2 g d_p^3}{\mu_L^2}\right)^{0.173} \left(\frac{w' V_L}{d_p^3}\right)^{-0.011} \left(\frac{d_T}{d_p}\right)^{0.019} \left(\frac{\mu_L}{\rho_L D_A}\right)^{0.461} \quad (11)$$

Where:

k_s = liquid-solid mass transfer coefficient [m / s]

d_p = particle diameter [m]

D_A = diffusion rate of species A [m^2 / s]

d_T = reactor diameter [m]

N = stirring speed [s^{-1}]

μ_L = liquid viscosity [kg / m·s]

ρ_L = liquid density [kg / m^3]

g = gravitational constant [9.8066 m / s^2]

w' = catalyst loading [kg / 100 kg solution]

V_L = liquid volume [m^3]

The mass transfer area for the liquid-solid interface is calculated using properties of the catalyst and the conditions of the experiment:

$$a = \frac{6w'\rho_L}{d_p \rho_p} \quad (12)$$

---

[95] Boon-Long, S.; Laguerie, C.; Couderc, J.P., *Chem. Eng. Sci.*, **1978**, *33*, 813

Where:

a = ratio of catalyst surface area to volume of fluid [m^2 / m^3]

w' = catalyst loading [g catalyst / 100g solution]

ρ_L = liquid density [kg / m^3]

d_p = particle diameter [m]

ρ_p = particle density [kg / m^3]

With values for k_s and a, the liquid-solid mass transfer rate may be determined.

6.2.6 – Intraparticle mass transfer

The final step for hydrogenation is the diffusion of the reactants through the pores of the catalyst to the active metal sites. The Weiss-Prater[96] criterion was used to compare the rate of mass transfer within the catalyst and the reaction rate:

$$\eta\Phi^2 = \frac{-r \cdot L^2}{C_s \cdot D_e} \qquad (13)$$

Where:

$\eta\Phi^2$ = observable modulus

r = reaction rate [$mol / L \cdot s$]

L = $d_p / 6$ = characteristic length of the catalyst [m]

C_s = species surface concentration [mol / L]

D_e = $\varepsilon^2 D_a$ = effective diffusivity [m^2 / s]

ε = support porosity [0.6 for the catalyst]

[96] Weiss, P.B.; Prater, C.D., *Adv. Catal.*, **1954**, *6*, 143

The observable modulus is the ratio of the observed reaction rate to the effective diffusion rate in the catalyst particle. If $\eta\Phi^2 < 1$, then the rate of mass transport is greater than the reaction rate and the reaction is not mass transfer limited. Otherwise, the reaction rate is limited by the diffusion of reactant in the catalyst.

6.2.7 – Results from mass transfer calculations

The maximum mass transfer rates for hydrogen and the liquid phase reactants (assumed to be fructose) were calculated for the experiment with the highest rate of hydrogenation (Experiment 140 – 40°C, 200 psig H_2, 0.18 M fructose, 0.1g 5 wt% Ru/C catalyst). Table 6-1 reports these results.

Table 6-1: Mass transfer calculations for Experiment 140

Equation	Description	Rate (solution basis) [kmol / m^3·s]	
$k_La \cdot C_{H2}$	Maximum G-L mass transfer of H_2 (Bern)	6.7×10^{-3}	
$k_La \cdot C_{H2}$	Maximum G-L mass transfer of H_2 (Yagi, Yoshida)	3.6×10^{-3}	
$k_La \cdot C_{H2,S}$	Maximum L-S mass transfer of H_2 (Boon-Long)	7.5×10^{-5}	
$k_La \cdot C_{A,S}$	Maximum L-S mass transfer of fructose (Boon-Long)	1.2×10^{-4}	
$R_{H2,\,MAX}$	Observed maximum reaction rate of hydrogen	6.6×10^{-5}	
$R_{A,\,MAX}$	Observed maximum reaction rate of fructose	6.6×10^{-5}	
$\eta\Phi^2$	Observed modulus for H_2		9.5×10^{-5}
$\eta\Phi^2$	Observed modulus for fructose		5.2×10^{-4}

Mass transfer of hydrogen from the vapor phase to the liquid phase was not rate limiting as the rate of transfer was two orders of magnitude faster than the maximum rate of liquid-solid mass transfer. Further, the mass transfer of hydrogen and fructose was larger than the maximum observed reaction rate. However, this difference was not large enough to definitively state that transport of the reactants was not rate-limiting. As the reaction progressed, however, the rate of hydrogen consumption dropped significantly, which removed potential mass transport limitations. Finally, the observable modulus for both hydrogen and fructose show that the reactants diffuse readily through the catalyst pores (i.e. $\eta\phi^2 << 1$). Thus, the surface reaction was rate limiting and not the mass transport of reactants.

6.3 – The kinetic model

The difficulty of modeling this system lies in the number of different reactions that occur simultaneously. The alkaline degradation and hydrogenation reactions were first examined separately and then combined to form the complete model. Each section summarizes the assumptions made for these reactions.

Nomenclature for rate constants will describe the direction of the reaction. For instance, $k_{M\text{-}F}$ is the rate constant for the isomerization of mannose to fructose. $k_{SO\text{-}ADS}$ represents the rate constant for sorbitol adsorption. K_{SO} is the equilibrium constant for sorbitol adsorption. Concentrations of liquid phase compounds are described with brackets. For example, glucose concentration is represented by [G]. Catalytic site concentrations are designated with C and a subscript, e.g. $C_{H\text{-}S2}$ describes the concentration of type 2 catalytic sites occupied by hydrogen. Table 6-2 lists the abbreviations for the compounds of interest.

Table 6-2: Abbreviations used in kinetic model

Abbreviation	Description
G	Glucose
M	Mannose
F	Fructose
SO	Sorbitol
MO	Mannitol
GA	Glyceraldehyde
PA	Pyruvaldehyde
GA2	Glycolaldehyde
EG	Ethylene glycol
PG	Propylene glycol
GO	Glycerol
LA	Lactic acid
FA	Formic acid
GLYA	Glyceric acid
GLYA2	Glycolic acid
CD	Condensation products
CZ	Cannizzaro reaction
H_2, H2	Hydrogen
S_1, S1	Catalytic site – type 1
S_2, S2	Catalytic site – type 2
R	Reaction rate
P	Pressure
t	Time
k	Rate constant
ADS	Adsorption
DES	Desorption
K	Equilibrium constant – k_{ADS} / k_{DES}

6.3.1- Hydrogenation

The addition of supported-metal catalyst and hydrogen add the element of hydrogenation to the alkaline degradation pathways. Sorbitol, mannitol, glycerol, propylene glycol, and ethylene glycol are the main products from hydrogenation.

Hydrogenation was modeled using a two-site Langmuir-Hinshelwood model[97]. On type 1 sites, reactants adsorb and react with hydrogen adsorbed on adjacent type 2 sites. Hydrogen dissociates to adsorb atomically to the type 2 site, consistent with work from Neurock[98] and sugar hydrogenation work from Wisniak et al.[23]. The derivation for the adsorption of hydrogen follows:

$$H_2 + 2\ S_2 \leftrightarrows 2\ H{\cdot}S_2 \tag{14}$$

This equation represents the reversible dissociative adsorption of hydrogen on to type 2 sites (S_2) from the model. Diatomic hydrogen adsorbs on to two separate sites and then desorbs to form the diatomic form again. In equation form:

$$r_{H2\text{-}ADS} = k_{H-DES} \cdot C_{H{\cdot}S2}^2 - k_{H-ADS} \cdot P_{H2} \cdot C_{V2}^2 \tag{15}$$

$$r_{H2\text{-}ADS} = k_{H-ADS}\left(\frac{C_{H{\cdot}S2}^2}{K_H} - P_{H2} \cdot C_{V2}^2\right) \tag{16}$$

Where:

$r_{H2\text{-}ADS}$ = rate of hydrogen adsorption

$k_{H\text{-}DES}$ = rate constant for hydrogen desorption

$C_{H{\cdot}S2}$ = concentration of type 2 sites occupied by monatomic hydrogen

$k_{H\text{-}ADS}$ = rate constant for hydrogen adsorption

P_{H2} = hydrogen pressure

C_{V2} = concentration of vacant type 2 sites

K_H = equilibrium constant for hydrogen ($k_{H\text{-}ADS}$ / $k_{H\text{-}DES}$)

---

[97] Fogler H.S., *Elements of Chemical Reaction Engineering*, 2nd Ed., p.256, Prentice-Hall, New York, 1992

[98] Pallasana, V., Neurock, M., *J. Catal.*, **2002**, *209*, 289-305

Assuming that hydrogen adsorption and desorption are rapid, $r_{H2\text{-}ADS} = 0$, yielding:

$$0 = k_{H-ADS}\left(\frac{C_{H\cdot S2}^2}{K_H} - P_{H2}\cdot C_{V2}^2\right) \tag{17}$$

$$C_{H\cdot S2}^2 = K_H \cdot P_{H2} \cdot C_{V2}^2 \tag{18}$$

$$C_{H\cdot S2} = C_{V2}\cdot\sqrt{K_H \cdot P_{H2}} \tag{19}$$

Using a total site balance for type 2 sites (C_{T2}):

$$C_{T2} = C_{V2} + C_{H\cdot S2} \tag{20}$$

$$C_{V2} = C_{T2} - C_{H\cdot S2} \tag{21}$$

$$C_{H\cdot S2} = \left(C_{T2} - C_{H\cdot S2}\right)\cdot\sqrt{K_H \cdot P_{H2}} \tag{22}$$

$$C_{H\cdot S2} = \frac{C_{T2}\cdot\sqrt{K_H \cdot P_{H2}}}{1+\sqrt{K_H \cdot P_{H2}}} \tag{23}$$

Or in terms of fractional coverage, Θ:

$$\Theta_{H\cdot S2} = \frac{\sqrt{K_H \cdot P_{H2}}}{1+\sqrt{K_H \cdot P_{H2}}} \tag{24}$$

Thus, the fraction of type 2 sites occupied by hydrogen was described by the hydrogen pressure and equilibrium constant for hydrogen in this system.

The hydrogenation products of sorbitol, mannitol, glycerol, propylene glycol, and ethylene glycol are formed from unsaturated intermediates of the reaction. Glucose forms sorbitol, mannose forms mannitol, and fructose forms a combination of sorbitol and mannitol when hydrogenated. Glycerol is formed from the reduction of the intermediate glyceraldehyde, propylene glycol from pyruvaldehyde, and ethylene glycol

from glycolaldehyde. Each of these aldehydes is formed via alkaline degradation pathways.

Several sugar hydrogenation papers[21-25] give experimental evidence that sugar hydrogenation proceeds via a simple mechanism: Unadsorbed sugar reacts with disassociately chemisorbed hydrogen (i.e. monatomic) to form an adsorbed molecule of sugar alcohol, which desorbs to complete the reaction.

To simplify the model, the aldehydic intermediates glyceraldehyde, pyruvaldehyde, and glycolaldehyde have been assumed to follow the same mechanism. Thus, once formed in solution, the aldehydes react with chemisorbed hydrogen to produce their corresponding polyol and desorb to their respective product. Further, each saturated product is taken to be an end product. Thus, no hydrogenolysis occurs to complicate the reaction model. This is a fair assumption, given the low temperature (40°C) considered for the work. Work by Peereboom[86] in our lab has shown dehydrogenation of saturated polyols occurring at temperatures at or below 40°C, but the rate of reaction was so low that it can be ignored in contrast to the conditions used in these reactions. Previous hydrogenolysis work required temperatures at approximately 200°C to cause significant polyol hydrogenolysis. With these assumptions in mind, the hydrogenation reactions are as follows:

$$G + 2\,H{\cdot}S_2 + S_1 \rightarrow SO{\cdot}S_1 + 2\,S_2 \quad (25)$$

$$M + 2\,H{\cdot}S_2 + S_1 \rightarrow MO{\cdot}S_1 + 2\,S_2 \quad (26)$$

$$F + 2\,H{\cdot}S_2 + S_1 \rightarrow SO{\cdot}S_1 + 2\,S_2 \quad (27)$$

$$F + 2\,H{\cdot}S_2 + S_1 \rightarrow MO{\cdot}S_1 + 2\,S_2 \quad (28)$$

$$GA + 2\,H{\cdot}S_2 + S_1 \rightarrow GO{\cdot}S_1 + 2\,S_2 \quad (29)$$

$$PA + 2\,H{\cdot}S_2 + S_1 \rightarrow PG{\cdot}S_1 + 2\,S_2 \quad (30)$$

$$GA2 + 2\,H{\cdot}S_2 + S_1 \rightarrow EG{\cdot}S_1 + 2\,S_2 \quad (31)$$

The products desorb reversibly to complete the description:

$$SO{\cdot}S_1 \leftrightarrows SO + S_1 \quad (32)$$

$$MO{\cdot}S_1 \leftrightarrows MO + S_1 \quad (33)$$

$$GO{\cdot}S_1 \leftrightarrows GO + S_1 \quad (34)$$

$$PG{\cdot}S_1 \leftrightarrows PG + S_1 \quad (35)$$

$$EG{\cdot}S_1 \leftrightarrows EG + S_1 \quad (36)$$

Rate equations for each of the adsorbed intermediates are as follows:

$$r_{SO{\cdot}S1} = k_{G-SO}[G]\cdot C_{H{\cdot}S2}^2 C_{V1} + k_{SO-ADS}\left([SO]\cdot C_{V1} - \frac{[SO\cdot S_1]}{K_{SO}}\right) + k_{F-SO}[F]\cdot C_{H{\cdot}S2}^2 C_{V1} \quad (37)$$

$$r_{MO{\cdot}S1} = k_{M-MO}[M]\cdot C_{H{\cdot}S2}^2 C_{V1} + k_{MO-ADS}\left([MO]\cdot C_{V1} - \frac{[MO\cdot S_1]}{K_{MO}}\right) + k_{F-MO}[F]\cdot C_{H{\cdot}S2}^2 C_{V1} \quad (38)$$

$$r_{GO{\cdot}S1} = k_{GA-GO}[GA]\cdot C_{H{\cdot}S2}^2 C_{V1} + k_{GO-ADS}[MO]\cdot C_{V1} - k_{GO-DES}\cdot[GO\cdot S_1] \quad (39)$$

$$r_{PG{\cdot}S1} = k_{PA-PG}[PA]\cdot C_{H{\cdot}S2}^2 C_{V1} + k_{PG-ADS}[PG]\cdot C_{V1} - k_{PG-DES}\cdot[PG\cdot S_1] \quad (40)$$

$$r_{EG{\cdot}S1} = k_{GA2-EG}[GA2]\cdot C_{H{\cdot}S2}^2 C_{V1} + k_{EG-ADS}[EG]\cdot C_{V1} - k_{EG-DES}\cdot[EG\cdot S_1] \quad (41)$$

Using the psuedo steady state hypothesis (PSSH)[99],each of these equations is set to zero. This assumed that the rates of adsorption intermediate formation and product desorption were fast relative the overall reaction rate. Thus, the concentration of each intermediate can be solved for in terms of measurable product concentrations.

[99] Fogler H.S., *Elements of Chemical Reaction Engineering*, 2nd Ed., p.341, Prentice-Hall, New York, 1992

$$[SO \cdot S_1] = (k_{G-SO}[G] + k_{F-SO}[F]) \cdot \frac{C_{H\cdot S2}^2 C_{V1}}{k_{SO-DES}} + K_{SO}[SO] \cdot C_{V1} \quad (42)$$

$$[MO \cdot S_1] = (k_{M-MO}[M] + k_{F-MO}[F]) \cdot \frac{C_{H\cdot S2}^2 C_{V1}}{k_{MO-DES}} + K_{MO}[MO] \cdot C_{V1} \quad (43)$$

$$[GO \cdot S_1] = k_{GA-GO}[GA] \cdot \frac{C_{H\cdot S2}^2 C_{V1}}{k_{GO-DES}} + K_{GO}[GO] \cdot C_{V1} \quad (44)$$

$$[PG \cdot S_1] = k_{PA-PG}[PA] \cdot \frac{C_{H\cdot S2}^2 C_{V1}}{k_{PG-DES}} + K_{PG}[PG] \cdot C_{V1} \quad (45)$$

$$[EG \cdot S_1] = k_{GA2-EG}[GA2] \cdot \frac{C_{H\cdot S2}^2 C_{V1}}{k_{EG-DES}} + K_{EG}[EG] \cdot C_{V1} \quad (46)$$

Using a total site balance for type 1 sites, fractional coverage was derived and the results are listed on Figure 6-2.

The rate equations for desorbed products are as follows:

$$r_{SO} = -k_{SO-ADS}[SO] \cdot C_{V1} + k_{SO-DES} \cdot [SO \cdot S_1] \quad (51)$$

$$r_{MO} = -k_{MO-ADS}[MO] \cdot C_{V1} + k_{MO-DES} \cdot [MO \cdot S_1] \quad (52)$$

$$r_{GO} = -k_{GO-ADS}[MO] \cdot C_{V1} + k_{GO-DES} \cdot [GO \cdot S_1] \quad (53)$$

$$r_{PG} = -k_{PG-ADS}[PG] \cdot C_{V1} + k_{PG-DES} \cdot [PG \cdot S_1] \quad (54)$$

$$r_{EG} = -k_{EG-ADS}[EG] \cdot C_{V1} + k_{EG-DES} \cdot [EG \cdot S_1] \quad (55)$$

$$C_{T1} = C_{V1} + C_{SO\cdot S1} + C_{MO\cdot S1} + C_{GO\cdot S1} + C_{PG\cdot S1} + C_{EG\cdot S1}$$

$$C_{T1} = C_{V1}\left[A + C_{H\cdot S2}^{2}\left(\frac{k_{G-SO}[G]+k_{F-SO}[F]}{k_{SO-DES}} + \frac{k_{M-MO}[M]+k_{F-MO}[F]}{k_{MO-DES}} + \frac{k_{GA-GO}[GA]}{k_{GO-DES}} + \frac{k_{PA-PG}[PA]}{k_{PG-DES}} + \frac{k_{GA2-EG}[GA2]}{k_{EG-DES}}\right)\right]$$

$$\Theta_{V1} = \frac{1}{\left[A + C_{H\cdot S2}^{2}\left(\frac{k_{G-SO}[G]+k_{F-SO}[F]}{k_{SO-DES}} + \frac{k_{M-MO}[M]+k_{F-MO}[F]}{k_{MO-DES}} + \frac{k_{GA-GO}[GA]}{k_{GO-DES}} + \frac{k_{PA-PG}[PA]}{k_{PG-DES}} + \frac{k_{GA2-EG}[GA2]}{k_{EG-DES}}\right)\right]}$$

Where :

$$A = 1 + K_{SO}[SO] + K_{MO}[MO] + K_{GO}[GO] + K_{PG}[PG] + K_{EG}[EG]$$

Figure 6-2: Derived result for fractional coverage of vacant sites of type 1 (Θ_{V1}) for adsorption of hydrogenation products (Equations 47-50)

Substituting in expressions for the adsorbed species, the final equations become:

$$r_{SO} = \left(k_{G-SO}[G] + k_{F-SO}[F]\right) \cdot \Theta_{H\cdot S2}^{2} \Theta_{V1} \tag{56}$$

$$r_{MO} = \left(k_{M-MO}[M] + k_{F-MO}[F]\right) \cdot \Theta_{H\cdot S2}^{2} \Theta_{V1} \tag{57}$$

$$r_{GO} = k_{GA-GO}[GA] \cdot \Theta_{H\cdot S2}^{2} \Theta_{V1} \tag{58}$$

$$r_{PG} = k_{PA-PG}[PA] \cdot \Theta_{H\cdot S2}^{2} \Theta_{V1} \tag{59}$$

$$r_{EG} = k_{GA2-EG}[GA2] \cdot \Theta_{H\cdot S2}^{2} \Theta_{V1} \tag{60}$$

No reversible reaction was included in the model (i.e. dehydrogenation) due to the low temperature of the reaction system. While dehydrogenation may occur at 40°C, hydrogenation is greatly favored.

Each rate equation is first order with respect to the reactant. Since the reaction is in a batch system, the change in concentration versus time is as such:

$$\frac{d[SO]}{dt} = \left(k_{G-SO}[G] + k_{F-SO}[F]\right) \cdot \Theta_{H\cdot S2}^{2} \Theta_{V1} \tag{61}$$

$$\frac{d[MO]}{dt} = \left(k_{M-MO}[M] + k_{F-MO}[F]\right) \cdot \Theta_{H\cdot S2}^{2} \Theta_{V1} \tag{62}$$

$$\frac{d[GO]}{dt} = k_{GA-GO}[GA] \cdot \Theta_{H\cdot S2}^{2} \Theta_{V1} \tag{63}$$

$$\frac{d[PG]}{dt} = k_{PA-PG}[PA] \cdot \Theta_{H\cdot S2}^{2} \Theta_{V1} \tag{64}$$

$$\frac{d[EG]}{dt} = k_{GA2-EG}[GA2] \cdot \Theta_{H\cdot S2}^{2} \Theta_{V1} \tag{65}$$

These equations were taken into account with the alkaline degradation equations and combined to form the overall model. The next section discusses the derivation of the alkaline degradation pathways.

6.3.2. - Alkaline degradation

To begin, the feedstock sugars (glucose, fructose, and mannose) isomerize to form the other sugars, via the Lobry de Bruyn – Alberda von Ekenstein pathways.[61,62] For simplicity and to remain consistent with similar papers, isomerization reactions are first order with respect to the sugars. Their equations take this form:

$$r_F = -(k_{F\text{-}G} + k_{F\text{-}M})[F] + k_{M\text{-}F}[M] + k_{G\text{-}F}[G] \quad (66)$$

$$r_G = -(k_{G\text{-}F} + k_{G\text{-}M})[G] + k_{M\text{-}G}[M] + k_{F\text{-}G}[F] \quad (67)$$

$$r_M = -(k_{M\text{-}F} + k_{M\text{-}G})[M] + k_{F\text{-}M}[F] + k_{G\text{-}M}[G] \quad (68)$$

In addition to isomerization, fructose undergoes alkaline degradation to two moles of glyceraldehyde, primarily, via base-catalyzed retro-aldol condensation. At superstoichiometric loadings of base with respect to the feedstock sugar, retro-aldol condensation is the preferred conversion pathway.

From kinetic modeling, de Bruijn et al.[73] show that fructose and psicose account for 80-90% of the acid products formed from the degradation reactions. Since psicose is formed from fructose, it was eliminated from the model and acids formed from psicose were assumed to come from fructose. Glucose and mannose accounted for the remaining 10-20% of acid products, of which glucose is responsible for nearly all of the acidic material. Thus, the model included only isomerization and hydrogenation reactions for mannose and included a degradation pathway for glucose to intermediates. Since glucose

is an aldose, it forms a C_2 and C_4 aldehyde during the retro-aldol reaction. The aldehydes formed have short lifetimes at the high pH of reaction and undergo further conversions. The potential reactions for each are discussed below.

6.3.2.1 – Aldehydic intermediates: Glycolaldehyde

Glycolaldehyde, the C_2 intermediate formed from glucose, can undergo a Cannizzaro reaction[100] to form one mole of glycolic acid and one mole of ethylene glycol. It can also be hydrogenated to form ethylene glycol. The C_4 intermediate can form threaldehyde or erythraldehyde since it has a chiral center. Again, these intermediates can undergo the Cannizzaro reaction to form the corresponding carboxylic acid and sugar alcohol (threonic acid and threitol or erythonic acid and erythritol) or simply hydrogenate to the sugar alcohol. In the overall model, only the C_2 compounds were included for consideration to simplify the model and because there is more interest in ethylene glycol than in threitol or erythritol. In addition, the reactions would have added parameters to the model without contributing very much to the overall picture. The reactions yielded the following equation for the kinetic model:

$$\frac{d[GA2]}{dt} = k_{G-GA2}[G] - k_{GA2-G}[GA2]^2 - k_{GA2-CZ}[GA2]^2 - k_{GA2-EG}[GA2]\cdot\Theta_{H\cdot S2}^2\Theta_{V1} \qquad (69)$$

Glucose to glycolaldehyde is reversible, but requires a mole each of glycolaldehyde and threaldehyde (a C_4 intermediate). However, since the C_4 compounds were not accounted for in the model, another equivalent of [GA2] was included to estimate the concentration of threaldehyde to produce the $[GA2]^2$ term to estimate the condensation of glycolaldehyde and threaldehyde to glucose. Glycerol, as noted in

[100] Cannizzaro, S., *Ann.*, **1853**, *88*, 129

section 6.2.1, was assumed to be an end-product and thus, not react further. Glyceric acid was considered an end product as well once it formed the salt potassium glycerate.

6.3.2.2 – Aldehydic intermediates: Glyceraldehyde

The other intermediate formed directly from feedstock sugar, glyceraldehyde, played an important role in the model. The C_3 intermediate could:

- Disproportionate to one mole of glyceric acid and glycerol, via the Cannizzaro reaction
- Undergo hydrogenation to form glycerol
- Undergo β-elimination of water to form pyruvaldehyde
- Condense to by-products

In equation form:

$$\frac{d[GA]}{dt} = k_{G\text{-}GA}[F] - (k_{GA\text{-}F} + k_{GA\text{-}CZ})[GA]^2 - (k_{GA\text{-}PA} + k_{GA\text{-}CD} + k_{GA\text{-}GO} \cdot \Theta_{H\text{-}S2}^2 \Theta_{V1})[GA] \quad (70)$$

Similar to glucose, fructose to glyceraldehyde was considered reversible. The second order term reflects two moles of glyceraldehyde necessary to form one mole of fructose. The other reactions, as listed above, were considered one-way with no backward reaction occurring, consistent with hydrogenation products remaining stable and salt formation being irreversible under alkaline conditions.

6.3.2.3 – Aldehydic intermediates: Pyruvaldehyde

Pyruvaldehyde was the other intermediate of interest in the kinetic model. Formed via the β-elimination of hydrogen from glyceraldehyde, the intermediate is the precursor for a number of pathways:

- Hydrogenates to form propylene glycol
- Undergoes benzylic acid rearrangement to form lactic acid

- Dicarbonyl cleavage to form formic acetic acids
- Condenses to by-products

With these reactions, the rate equation became:

$$\frac{d[PA]}{dt} = k_{GA-PA}[GA] - \left(k_{PA-LA} + k_{PA-FA} + k_{PA-CD} + k_{PA-PG} \cdot \Theta_{H\cdot S2}^{4} \Theta_{V1}\right)[PA] \quad (71)$$

Propylene glycol production required two moles of H2, which accounts for the 4th power term for $\Theta_{H\cdot S2}$. Formic and lactic acid (in salt form), condensation by-products, and propylene glycol were assumed to all form irreversibly.

6.3.3 – Combining the equations

With the isomerization and hydrogenation reactions accounted for, the derived equations must be combined to completely describe the system. The sugar isomerization, degradation, and hydrogenation equations occur simultaneously and must be modeled appropriately. Figure 6-3 gives an illustration of the modeled pathways.

In all, 16 differential equations with 40 parameters describe the reaction environment. These equations (Appendix A) were solved simultaneously using a 4th order Runge-Kutta numerical method as described by Carnahan et al.[101] in Microsoft Excel using Visual Basic[102] (see Appendix B for program code). Initial conditions were set by the makeup of the feedstock and conditions of the reaction.

[101] Carnahan, B.; Luther, H. ; Wilkes, J., *Applied Numerical Methods*, Wiley, New York, 1969
[102] Modified version of program in Jere, F.T., Ph.D. Dissertation, Michigan State University, 2003

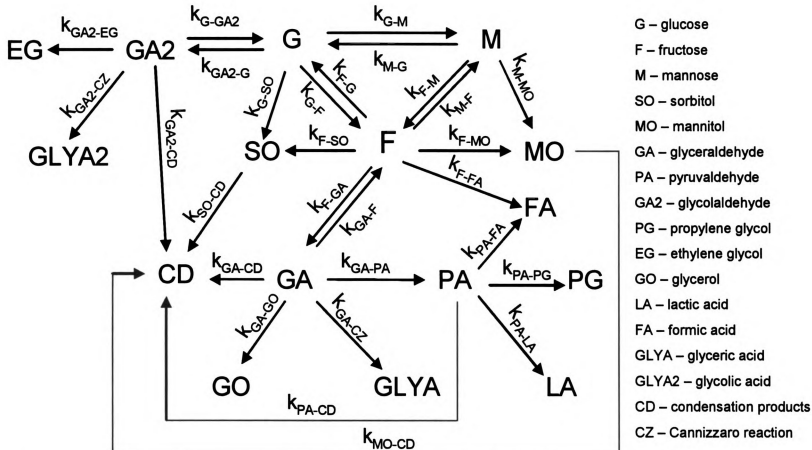

Figure 6-3: Reaction pathways of proposed alkaline degradation with hydrogenation model

k_{A-B}: Rate constant for reactant (A) to product (B)

6.3.4 – Assumptions of the model

A number of assumptions for this kinetic model have already been discussed. They are summarized here:

- Reactions are first order with respect to the reactant
- Organic acids formed are in salt form and do not react further
- The drop in hydroxide concentration from the formation of acid products does not affect the rates of alkaline degradation pathways
- Glycerol, propylene glycol, and ethylene glycol are stable under reaction conditions and do not react further
- Sorbitol and mannitol do not dehydrogenate. This was based on the reaction rates at the process temperature of 40°C. A degradation term was added to account for apparent conversion of the sugar alcohols toward the end of experiments.
- The pathway of glyceraldehyde to pyruvaldehyde is not reversible. It was assumed that the conversion of pyruvaldehyde to PG would be rapid enough to not allow a reverse reaction.
- Ruthenium metal has two separate sites: one for hydrogen adsorption, another for the organic substrates
- All substrates that hydrogenate are in solution as reactants and complete the reaction adsorbed to the catalyst site

6.4 – Calculation of concentration versus time

In all, ten experiments were considered in the fitting of the kinetic model. These experiments represent the standard conditions of 40°C, 100 psig H_2 pressure, 0.1 grams of catalyst loading, and 3.17 wt% fructose feedstock, and variations based on hydrogen pressure, sugar loading, feedstock sugar used and catalyst loading. Each reaction had the same loading of potassium hydroxide, 5.3 wt%, agitation rates (1000 rpm), and catalyst reduction conditions (see Table 6-2). Using a 4th order Runge-Kutta numerical method,[91] the derived equations previously discussed were solved simultaneously at discrete times

and then compared to the collected data. One hundred eighty-six time steps were used for the calculations to reduce the amount of rounding error between iterations and set time steps at two minutes exactly for comparison to concentration versus time data.

Table 6-3: Experimental conditions used for kinetic model - 40°C, 0.85 M KOH

Experiment	Feedstock sugar	Loading (wt%)	Catalyst Loading (g)	H_2 Pressure (psig)
115	Fructose	3.17	0.05	100
119	Fructose	1.00	0.10	100
140	Fructose	3.17	0.10	200
141	Glucose	3.17	0.10	100
142	Mannose	3.17	0.10	100
144	Fructose	2.01	0.10	100
146	Fructose	3.17	0.10	100
147	Fructose	3.17	0.10	25
149	Fructose	3.17	0.10	50
152	Fructose	3.17	0.20	100

Concentration versus time data were collected for thirteen compounds in each experiment, giving a total of 1274 data points. These data were compared to the calculated value from the model at the nearest time point over ten experiments. The difference was then squared and combined with the other residuals to form a total error used to compare how well the model fit the data.

To reduce the total error and improve the model, parameters were varied in random walk fashion by a set percentage (e.g. 10%). The new value for the parameter was then used to calculate new concentrations for the kinetic model. Once complete, the total error from the 10 experiments was calculated and compared to the best result. If the error was reduced, the new value for the parameter was kept and the program proceeded

to the next step using the refined parametric set. If not, the previous set of parameters was restored and then the next random walk was performed.

When no improvement was found, the random number generated, and thus the walk taken, was recorded into an array. For each new walk, the random number was compared to those used since the last improvement. Any matches in the array led to the generation of another number since the random walk had already been taken. If all of the steps were used without further improvement, the program notified the user and halted computation. Any reduction in the total error wiped out the values in the array and allowed any step to occur after that point. For 40 parameters, this bit of coding reduced the amount of random walks needed by over 80% and ensured that each permutation had been exhausted.

6.5 – Results

Table 6-3 lists the values of the 40 parameters that yielded the lowest total sum of squares error from the 10 experiments. The exact values have been truncated for easier presentation. Confidence intervals were not determined due to the large number of parameters in the set of equations. As described by Belohlav et al.[103], models with a large number of parameters tend to have interdependence between each rate constant creating large confidence intervals that serve no useful purpose and, thus, were not included.

The kinetic model shows good agreement with the data collected from the ten experiments included. Trends in sugar isomerization, hydrogenation, and degradation were matched very well as seen in Figures 6-4, 6-5, and 6-6 for Experiment 146.

---

[103] Belohlav, Z.; Zamostny, P.; Kluson, P.; Volf, J., *Can. J. of Chem. Eng*, **1997**, *75*, 735-742

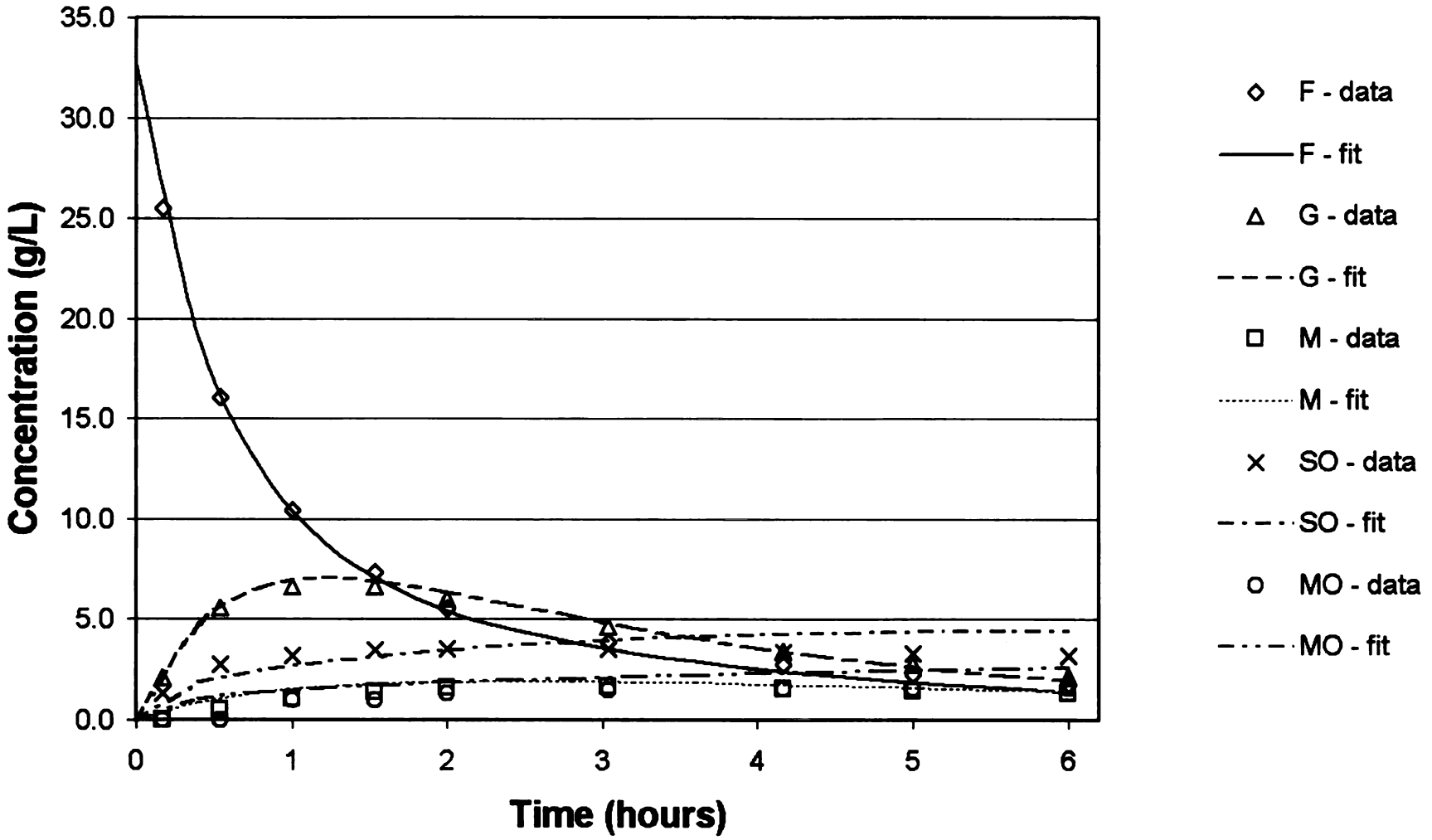

Figure 6-4: Comparison of experimental data and kinetic model - Experiment 146
3.17% fructose, 5.3% KOH, 40°C, 100 psig H_2, 0.10 grams 5 wt% Ru/C
Fructose, glucose, mannose, sorbitol, and mannitol vs. Time

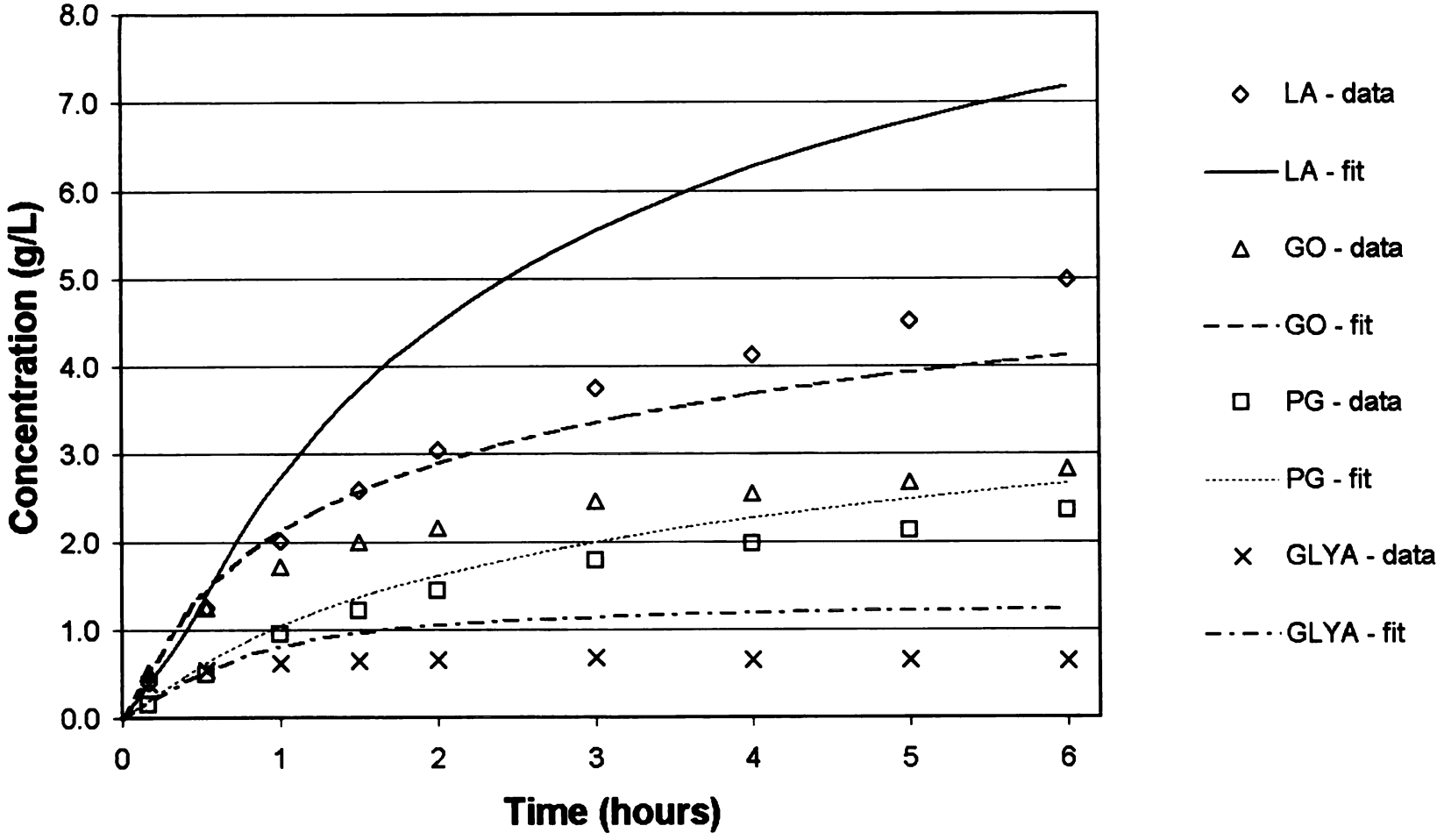

Figure 6-5: Comparison of experimental data and kinetic model - Experiment 146
3.17% fructose, 5.3% KOH, 40°C, 100 psig H_2, 0.10 grams 5 wt% Ru/C
Lactic acid, glycerol, propylene glycol, and glyceric acid vs. Time

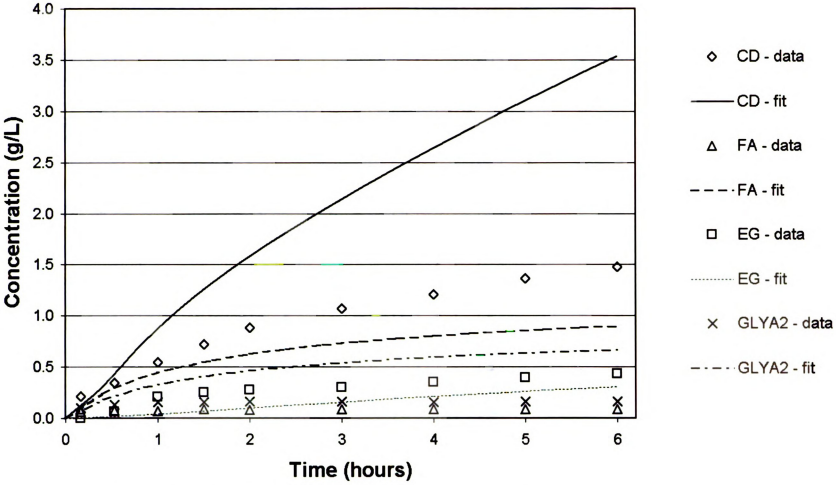

Figure 6-6: Comparison of experimental data and kinetic model - Experiment 146
3.17% fructose, 5.3% KOH, 40°C, 100 psig H_2, 0.10 grams 5 wt% Ru/C
Condensation products, formic acid, EG, and glycolic acid vs. Time

Appendix C contains the graphs that compare the experimental data to the fitted model. Some difficulties did arise in fitting sorbitol and mannitol data from experiments with varying hydrogen pressure and catalyst loading. Pressures from 25-100 psig (Experiments 147, 149, and 146) showed very similar amounts of sugar alcohol production. An increase to 200 psig showed a much larger response, which caused significant errors early on in the calculations. Further details of the specific portions of the model, namely the sugar isomerization reactions, hydrogenation, and alkaline degradation reactions, are continued in the sections below.

Table 6-4: Best fit parametric values

Constant	Value	Units		Constant	Value	Units
$k_{F\text{-}G}$	0.598	hr^{-1}		$k_{PA\text{-}PG}$	1.2×10^{14}	$hr^{-1}\ g_{metal}^{-5}$
$k_{G\text{-}F}$	0.668	hr^{-1}		$k_{PA\text{-}LA}$	6.6	hr^{-1}
$k_{F\text{-}M}$	0.089	hr^{-1}		$k_{PA\text{-}CD}$	1.8	hr^{-1}
$k_{M\text{-}F}$	0.197	hr^{-1}		$k_{GA2\text{-}EG}$	1.2×10^{8}	$hr^{-1}\ g_{metal}^{-3}$
$k_{G\text{-}M}$	0.022	hr^{-1}		$k_{GA2\text{-}CZ}$	0.0006	$L\ mol^{-1}\ hr^{-1}$
$k_{M\text{-}G}$	0.059	hr^{-1}		$k_{GA2\text{-}CD}$	0.00008	hr^{-1}
$k_{F\text{-}SO}$	8.9×10^{7}	$hr^{-1}\ g_{metal}^{-3}$		$k_{SO\text{-}ADS}$	21.8	—
$k_{F\text{-}MO}$	5.2×10^{7}	$hr^{-1}\ g_{metal}^{-3}$		$k_{SO\text{-}DES}$	2.5×10^{6}	$mol\ L^{-1}\ hr^{-1}$
$k_{G\text{-}SO}$	6.1×10^{7}	$hr^{-1}\ g_{metal}^{-3}$		$k_{MO\text{-}ADS}$	116	—
$k_{M\text{-}MO}$	7.8×10^{6}	$hr^{-1}\ g_{metal}^{-3}$		$k_{MO\text{-}DES}$	2430	$mol\ L^{-1}\ hr^{-1}$
$k_{F\text{-}GA}$	0.52	hr^{-1}		$k_{GO\text{-}ADS}$	4.5	—
$k_{GA\text{-}F}$	3.9	$L\ mol^{-1}\ hr^{-1}$		$k_{GO\text{-}DES}$	799	$mol\ L^{-1}\ hr^{-1}$
$k_{G\text{-}GA2}$	0.486	hr^{-1}		$k_{PG\text{-}ADS}$	154	—
$k_{GA2\text{-}G}$	12.5	$L\ mol^{-1}\ hr^{-1}$		$k_{PG\text{-}DES}$	1.3×10^{10}	$mol\ L^{-1}\ hr^{-1}$
$k_{F\text{-}FA}$	0.024	hr^{-1}		$k_{EG\text{-}ADS}$	1483	—
$k_{GA\text{-}CZ}$	4.5	$L\ mol^{-1}\ hr^{-1}$		$k_{EG\text{-}DES}$	15.5	$mol\ L^{-1}\ hr^{-1}$
$k_{GA\text{-}GO}$	1.8×10^{9}	$hr^{-1}\ g_{metal}^{-3}$		K_H	8.4	psi^{-1}
$k_{GA\text{-}PA}$	8.4	hr^{-1}		$k_{SO\text{-}CD}$	0.073	hr^{-1}
$k_{GA\text{-}CD}$	0.007	hr^{-1}		$k_{MO\text{-}CD}$	0.0005	hr^{-1}
$k_{PA\text{-}FA}$	0.0001	hr^{-1}		$k_{F\text{-}GLY2}$	0.018	hr^{-1}

6.5.1 – Isomerization equilibria

Isomerization equilibrium terms were compared to literature values to verify the validity of the determined rate constants, or at least demonstrate consistency with previous research. Sugar isomerization reactions have been previously characterized[69,71,104,105,106], which allowed for reasonable benchmarks. Table 6-4 summarizes the equilibrium constants from the kinetic model and literature values.

Table 6-5: Sugar isomerization equilibria values ($k_{forward}$ / $k_{reverse}$)

K_{G-M}	K_{G-F}	K_{M-F}	Temp (°C)	pH	Ref.
0.39	1.12	2.21	40	13.8	from Table 6-8
0.52 – 1.94	0.91 – 0.99	1.67 – 2.04	22	14	MacLaurin[69]
0.42	1.09	2.67	78	13	de Bruijn et al.[79]
0.29	0.85 – 0.89	3.00	25	7.4	Tewari[94]

Ranges for the equilibrium results are based on uncertainty ranges provided by the appropriate references. For the results of MacLaurin and Green[69], 1000 equilibrium constants were calculated based on a Gaussian distribution of the error for each parameter. The confidence interval was then found to be the range of the 2.5th percentile to the 97.5th percentile for ~95% confidence. Equilibrium constants for Tewari[94] were calculated using the standard Gibbs energy change of reaction, or $\Delta G°$. With this value for each reaction (glucose to mannose, etc.), the equilibrium constant for the reaction was calculated by relating K and $\Delta G°$[107]:

---

[104] Tewari, Y.B.; Goldberg, R.N., *Biophys. Chem.*, **1986**, *24*, 291-294
[105] Camacho-Rubio, F. et al., *Can. J. of Chem. Eng.*, **1995**, *73*, 935-940
[106] Franks, F., *Pure and Appl. Chem.*, **1987**, *59 (9)*, 1189-1202
[107] Smith, J.M.; Van Ness, H.C.; Abbott, M.M., *Introduction to Chemical Engineering Thermodynamics*, 5th Ed., p. 567, The McGraw-Hill Companies, New York, 1996

$$-RT \ln K = \Delta G^{\circ} \tag{72}$$

$$K = \exp\left(\frac{-\Delta G^{\circ}}{RT}\right) \tag{73}$$

Equations 59 and 60 also verified the validity of the isomerization equilibrium constants determined from the kinetic model fitting. Each isomerization reaction has a value for ΔG°. When placed in series, i.e. glucose to fructose to mannose to glucose, the total ΔG° equals zero because the initial and end states are identical. Table 6-5 the equilibrium constants, calculated ΔG° for each isomerization, and the total ΔG°.

Table 6-6: Equilibrium constants, reaction ΔG° (kJ/mol), and total ΔG° (kJ/mol)

	K_{G-M}	K_{M-F}	K_{F-G}	ΔG° G-F	ΔG° F-M	ΔG° M-G	Total ΔG°
This research	0.39	2.21	0.89	2.3	-1.9	0.3	0.7
MacLaurin[69]	1.0	1.83	1.05	0.0	-1.5	-0.1	-1.6
de Bruijn et al.[79]	0.42	2.67	0.92	2.1	-2.4	0.2	-0.1
Tewari[94]	0.29	3.00	1.15	3.0	-2.7	-0.3	0.0

The kinetic model showed a total ΔG° of reaction of 0.7 kJ/mol based on calculations from the fitted rate constants. This was a significant discrepancy from the expected value of 0.0 kJ/mol. To improve this aspect of the model, an additional equation is needed to calculate total ΔG° for the system and adjust rate constants in such a way that ΔG° = 0.

High pH levels also affect K values, as illustrated by de Bruijn.[77] Table 6-6 shows equilibrium constants for the isomerization reactions over a range of hydroxide concentrations as calculated in the paper.

Table 6-7: Comparing equilibrium values with hydroxide concentrations at 78°C

	OH^- concentration (M)				
	0.001	**0.0035**	**0.010**	**0.035**	**0.100**
K_{G-M}	0.39	0.38	0.39	0.38	0.42
K_{G-F}	1.3	1.2	1.3	1.2	1.1
K_{M-F}	3.3	3.3	3.3	3.3	2.7

The pH effect was more pronounced at the higher base concentrations, which was of interest with the reactions used for the kinetic model. It was assumed that reductions in base concentration due to acid formation/neutralization would not affect the rate of reaction. The relatively large change in all three equilibrium constants between 0.035 M and 0.100 M suggested that this hypothesis was incorrect.

6.5.2 – Hydrogenation rate constants

Parameters that described the rate of hydrogenation of various aldehydes were numerically large, which reflected the inclusion of catalyst weight, in grams of metal, in the rate equations. These amounts were typically 0.005 grams and were cubed to include the fractional coverage terms, $\Theta_{H\cdot S2}^2$ and Θ_{V1}, from each hydrogenation term. The relative rates of hydrogenation either reflect trends observed in literature or those implicitly included with the model, as is described below.

The rate constants for hydrogenation to glycerol, propylene glycol, and ethylene glycol were all an order of magnitude larger than the hydrogenation rates for the sugars. This reflects the high reactivity of glyceraldehyde, pyruvaldehyde, and glycolaldehyde and the assumption that these aldehydic intermediates had minimal concentrations over the course of the experiment. The maximum concentrations for glyceraldehyde,

glycolaldehyde and pyruvaldehyde over the course of all ten experiments were 0.77, 0.95, and 0.69 g/L, respectively. After six hours of reaction, these concentrations were typically less than 0.1 g/L.

Relative rates of sorbitol and mannitol production were fairly different from published results. From Table 6-3, fructose shows a 9:5 preference toward sorbitol production over mannitol during hydrogenation. Wisniak and Simon[21] reported a slight preference to mannitol during experiments. However, their results did not include temperatures below 85°C. In addition, the experiments for the Wisniak paper were run at neutral pH instead of alkaline conditions, which makes comparison difficult.

6.5.3 – Adsorption equilibrium constants

The model also determined rates of adsorption and desorption for the hydrogenation products. In each case, desorption was preferred by many orders of magnitude, which was apparent from the amounts of these products in the liquid phase and indicated little product affinity for the catalytic surface. Relative adsorption rates between the five hydrogenation products show little difference in binding ability of each substrate. Further, the large values for each equilibrium constant suggested little or no product inhibition. Table 6-8 has the values for adsorption, desorption, and equilibrium for each hydrogenation product.

Table 6-8: Parameters for adsorption/desorption pathways

Product	k_{ADS}	k_{DES}	K
SO	21.8	2.5×10^{6}	8.7×10^{-6}
MO	116	2430	0.048
GO	4.5	799	0.006
PG	153	1.3×10^{10}	1.1×10^{-8}
EG	1483	15.5	95.4
H_2			8.4

The small value of K for four of the compounds (sorbitol, mannitol, glycerol, and propylene glycol) suggests that these terms can be removed from the kinetic modeling. This would further simplify calculations without losing accuracy in the model.

6.5.4 – Alkaline degradation reactions

Unfortunately, not much comparison was available for rates of reaction for the degradation portion of the model. Previous work merely described sugars going to acidic products[69, 73] as opposed to specific products as done in this work. Overall, the acidic products observed in the experiments were included in the kinetic model and accounted for sufficiently.

Chapter 7 – Continued development of alkaline degradation with hydrogenation and related work

This chapter outlines efforts to further improve C_3 yields of the alkaline degradation hydrogenation reaction and describes other projects related to this work that were conducted to enrich the overall effort.

7.1 – Modified catalyst for selective C_3 hydrogenation

The alkaline degradation with hydrogenation reaction involves a competition between carbon-carbon cleavage of the sugar feedstock to C_3 intermediates and hydrogenation of the sugar to the corresponding sugar alcohol. With the typical ruthenium catalysts, unsaturated compounds are hydrogenated indiscriminately, which lowers potential C_3 yields of the reaction significantly. If a catalyst could hydrogenate the intermediates glyceraldehyde and pyruvaldehyde without reacting with the sugar feedstock, C_3 yields would rise significantly.

7.1.1 – Selective C_3 hydrogenation in the presence of glucose

Two modified platinum catalysts, a bimetallic platinum-germanium catalyst and a sulfided platinum catalyst, were obtained from Pacific Northwest National Laboratories (PNNL). Both catalysts demonstrated selective hydrogenation of aldehydes in the presence of sugars and were candidates for the desired selective hydrogenation of glyceraldehyde and pyruvaldehyde.

Reactions used 0.1 grams of catalyst (dry basis) to hydrogenate a solution of 0.4 wt% (0.044 M) glyceraldehyde dimer with 0.8 wt% glucose (0.044 M) added to the feedstock. Hydrogenations were carried out at 40 to 60°C and under 100 to 200 psig of hydrogen at neutral pH. Figures 7-1 and 7-2 show the selective hydrogenation of

glyceraldehyde from the feedstock (Figure 7-1) to a sample after four hours of reaction (Figure 7-2). Sixty percent of the glyceraldehyde converted to glycerol while less than 2% of the feedstock glucose hydrogenated, which demonstrated the desired effect of selective hydrogenation. Control experiments with glucose with Pt(S)/C (Exp 161) and fructose with Pt(S)/C (Exp 164) under hydrogen showed a similar low amount of hydrogenation after four hours of reaction (< 2% conversion for both experiments).

Ideally, this catalyst can be used in the alkaline degradation with hydrogenation reaction to capture aldehydic intermediates (i.e. glyceraldehyde and pyruvaldehyde) to form the saturated polyols glycerol and propylene glycol. This would benefit the reaction by reducing the amount of organic acid formation, which would maintain a high pH level to promote selectivity to C_3 products via retro-aldol condensation. More importantly, sorbitol and mannitol production would be avoided, thus allowing more of the feedstock sugar to undergo carbon-carbon cleavage to C_3 intermediates and further enhance C_3 yield.

7.1.2 – Alkaline degradation with hydrogenation using Pt catalysts

Using the sulfided platinum catalyst, alkaline degradation with hydrogenation reactions were carried out for comparison to ruthenium on carbon. The reaction was carried out at 40°C with a hydrogen pressure of 100 psig and a catalyst loading of 0.2 grams (dry basis). Experiments used fructose and base concentrations of 0.18 M and 0.85 M, respectively. Table 7-1 compares the product distribution of the two runs.

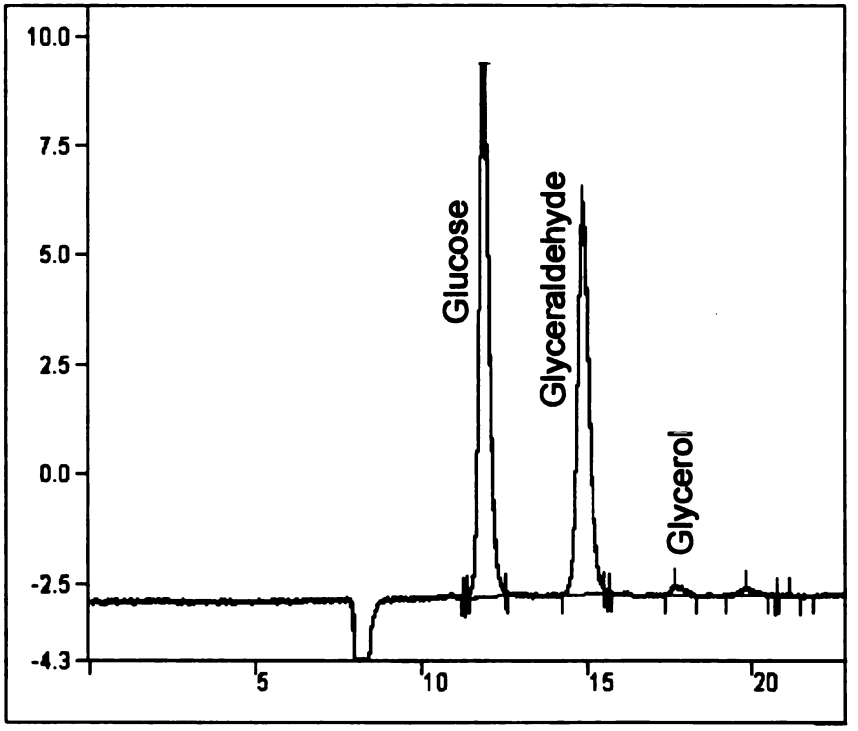

Figure 7-1: Selective hydrogenation of glyceraldehyde with glucose
Feedstock: 0.2 wt% glyceraldehyde, 0.2 wt% glucose
Conditions: 40°C, 200 psig H_2, 0.1g - 3% Pt(S)/C

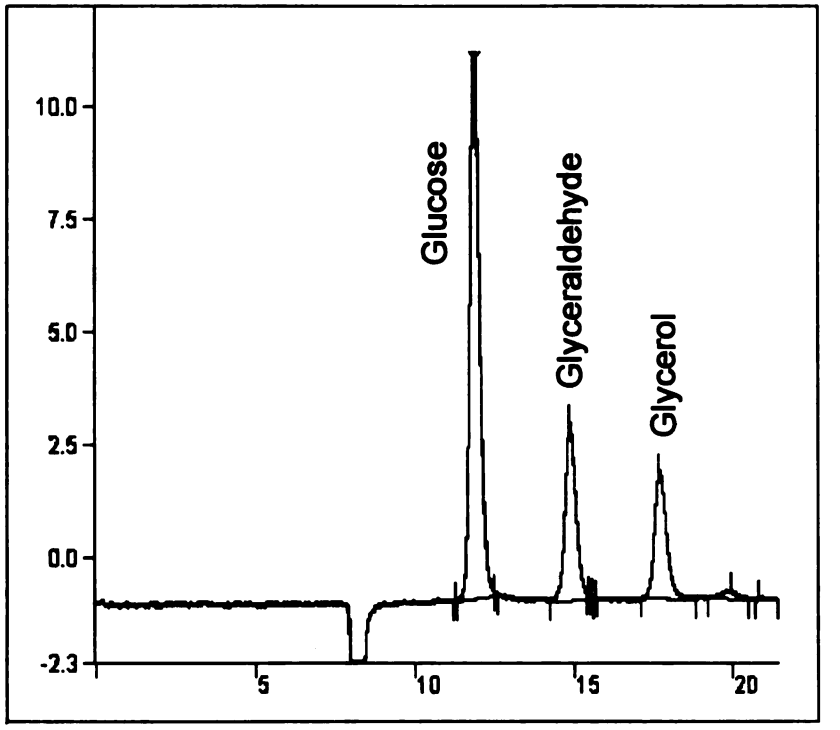

Figure 7-2: Selective hydrogenation of glyceraldehyde with glucose
After four hours of reaction
Conditions: 40°C, 200 psig H_2, 0.1g - 3% Pt(S)/C

Table 7-1: Comparison of Ru/C and Pt(S)/C catalysts

Conditions - 40°C, 100 psig, 0.18 M fructose, 0.85 M KOH, 0.1g catalyst (dry basis)

Exp	Catalyst	Conv.	Hyd.	Iso.	Deg.	C_3 Sel.	Max C_3	% of max	C_3 yield
146	5% Ru/C	95%	0.15	0.11	0.69	1.00	1.38	72	0.94
167	3% Pt(S)/C	96%	0.21	0.08	0.67	0.82	1.34	62	0.79
168	5% Pt(Ge)/C	97%	0.37	0.07	0.53	0.70	1.06	66	0.68

The sulfided platinum showed no apparent improved selectivity for C_3 hydrogenation. Mannitol and sorbitol formed readily and the fraction of degraded material that formed C_3 products was the same as the ruthenium on carbon catalyst. The change in reactivity of the sugars from neutral conditions to basic conditions was an effect of ionizing the sugar. At neutral conditions, all but a negligible amount of sugar is in cyclic form[108] while glyceraldehyde is linear in nature and is able to adsorb to the metal. Glucose and fructose hydrogenate in the liquid phase, as opposed to an adsorbed state[19-22], which does not allow the sugar to compete with glyceraldehyde for the open sites.

When ionized under high pH conditions, sugars assume an open form to isomerize and enolize.[109] In this open form, the sugar can adsorb to active sites and is no longer strongly affected by other adsorbed species. Thus, sorbitol and mannitol formed readily, which decreased the C_3 yield due to the loss of feedstock to hydrogenation products in a similar fashion as Ru/C catalyst.

[108] Ellis, A.V.; Wilson, M.A., *J. Org. Chem.*, **2002**, *67*, 8469-8474

[109] deWit, G. ; Kieboom, A.P.G.; van Bekkum, H., *Carbohyd. Res.*, **1979**, *74*, 157-175

7.2 – Methane production from carbohydrate feedstock

Catalyst screening by Chopade et al.[4] for sorbitol hydrogenolysis revealed that certain catalysts converted sorbitol into methane with high selectivity. Initially, the reaction was not of interest due to the loss of potential yield to desired products. However, in light of increased interest in hydrogen production, the reaction was revisited.

Hydrogen is produced mainly by steam reformation. Natural gas and steam are passed over a nickel-based catalyst at temperatures of 800-870°C and pressures of 300-400 psig to form three moles of hydrogen from one mole of water and methane.[110] Thus, methane to hydrogen is a well-developed process, albeit energy intensive. With a bio-based source of methane, hydrogen could be produced directly from renewable resources in lieu of petroleum feedstocks.

With the previous results of methane production, we investigated the use of sorbitol and glucose as feedstock, relating it directly to previous work. We also included glycerol due to its increasing growth as a side product from bio-diesel production.

7.2.1 – Sorbitol to methane

For these reactions, 10 wt% sorbitol (0.55 M) solution was reacted at 200-210°C under 1000 psi of hydrogen pressure. Five weight percent (5 wt%) ruthenium on carbon and 3 wt% ruthenium on titania were the two catalysts used in this study to compare the effect of support. The catalyst loading was 1.0 grams (dry basis) for each. Reaction times were typically four to six hours, or until liquid phase products were no longer detectable by HPLC. Table 7-2 shows the reaction conditions along with selectivity and yield to product gases.

---

[110] Kroschwitz, J.; Howe-Grant, M., editors, *Kirk-Othmer Encyclopedia of chemical technology*, 4th Edition, 13, p. 852, Wiley, New York, 1992

Table 7-2: Yield of methane and ethane from hydrogenolysis of sorbitol
Conditions – 1200 psig total pressure, 1.0g catalyst, 0.55 M sorbitol

Exp	Catalyst	Temp. °C	H_2 pressure (psi)	CH_4 Yield	C_2H_6 Yield	Carbon balance
L7	Ru/ TiO_2	210	1000	5.7	0.5	112%
L13	Ru/C	200	1000	7.1	0.3	136%

Yields of methane and ethane have units of moles of product per mole of reactant converted. For these experiments, the maximum value for yield is 6.0, corresponding the six carbons in sorbitol and one carbon in methane. Carbon balances were above 100% closure due to errors associated with dilution of the reactor during repressurization after sampling and quantitative analysis of gas chromatography.

Both carbon and titania supports show high yield to methane and readily convert sorbitol. Analysis with gas chromatography showed only methane and ethane produced in the reaction. No appreciable difference between the titania and carbon support was noted with respect to methane selectivity. Thus, carbon support would be preferable to titania due to lower costs per gram of material.

7.2.2 – Glucose to methane

Given the success of sorbitol to methane, glucose to methane was the logical progression for the reaction. Ideally, glucose would hydrogenate to sorbitol and then form methane with similar yields while reducing the feedstock cost from $0.40 to $0.07 per pound. Table 7-3 outlines the results of these runs. For this reaction, glucose was hydrogenated to sorbitol at 120°C and 600 psig of hydrogen and then heated to 200°C and pressurized to 1200 psig to begin hydrogenolysis.

Table 7-3: Yield of methane and ethane from hydrogenolysis of glucose
Conditions – 1200 psig total pressure, 1.0g catalyst, 0.55 M glucose

Exp	Catalyst	Temp °C	H_2 pressure (psi)	CH_4 Yield	C_2H_6 Yield	Carbon balance
L11	Ru/TiO_2	120/200	600/1000	5.1	0.4	99%

Glucose shows the same selectivity to methane as sorbitol, although the reaction rate was slower. After six hours of reaction, about 2% of the original carbon from the feedstock remained in the liquid phase compared to none with the sorbitol cracking experiment. Cracking of the liquid phase products continued beyond six hours as after 24 hours, the liquid phase products were completely reacted. High methane yield and complete conversion of the feedstock makes glucose a viable option as a feedstock for this process.

7.2.3 – Glycerol to methane

Another set of cracking reactions was conducted to convert glycerol to methane. Ruthenium supported on titania was used as catalyst for these reactions. Table 7-4 outlines the results of these runs.

Table 7-4: Yield of methane and ethane from hydrogenolysis of glycerol
Conditions - 1200 psig total pressure, 1.0g catalyst, 1.1 M glycerol

Exp	Catalyst	Temp °C	H_2 pressure (psi)	CH_4 Yield	C_2H_6 Yield	Carbon balance
L10	Ru/TiO_2	200	1000	3.2	0.3	118%
L12	Ru/TiO_2	190	1000	2.8	0.2	103%
L14	Ru/TiO_2	200	1000	3.2	0.3	117%

Glycerol showed high methane yields in the same manner as sorbitol and glucose. An interested observation was also made while analyzing the liquid phase products over time. As glycerol cracks to form methane and ethane, ethylene glycol, propylene glycol, ethanol, and 1-propanol form as the only intermediates of the reaction. This simple product set could make this system especially interesting for study of the mechanisms of polyol cracking. Such an analysis, however, was beyond the scope of this particular study.

7.3 – Summary

Two modified platinum catalysts, Pt(Ge)/C and Pt(S)/C, demonstrated selective hydrogenation of the C_3 intermediate glyceraldehyde while in the presence of glucose at neutral pH. This reaction showed potential for improving C_3 yields of alkaline degradation with hydrogenation of fructose and glucose by reducing the amount of sorbitol and mannitol produced from hydrogenation of the feedstock. However, these catalysts had higher activity for sugar alcohol production than Ru/C. The addition of base to the reaction enabled the platinum catalysts to hydrogenate the sugars, presumably, due to unsaturated, acyclic intermediates that formed during isomerization (e.g. enediols).

Selective hydrogenation of C_3 intermediates still holds promise, however. Size exclusion catalysts have yet to be explored as a method for hydrogenating the C_3 intermediates while ignoring the C_6 feedstock sugars. With a proper pore size distribution, glyceraldehyde and pyruvaldehyde could diffuse readily into the catalyst to form glycerol and propylene glycol while glucose, fructose, and mannose remain in solution to undergo alkaline degradation. Catalysts with high hydrogenation activity would be ideal to maximize production of PG and GO while minimizing the residence

time of C_3 intermediates, which would reduce the amount of organic acid produced from rearrangement reactions of the intermediates.

While selective hydrogenation of C_3 intermediates was not very successful, experiments that converted carbohydrates to methane showed interesting results. Using sorbitol, glucose, and glycerol as feedstock, between 80 and 90% of the feedstock carbon converted into methane while the rest converted to ethane when using a ruthenium catalyst. Complete conversion of the feedstock was usually observed within six hours at temperatures and pressures comparable to sorbitol hydrogenolysis (200°C, 1200 psi). With glycerol as feedstock, only four liquid phase intermediates appeared over the course of the reaction: ethylene glycol, propylene glycol, 1-propanol, and ethanol. Further study of this reaction may lead to insight on the hydrogenolysis pathways of glycerol to PG and EG.

Economically, the production of methane from sorbitol (SO), glucose (G), or glycerol (GO) feedstock is currently unfavorable. Table 7-5 outlines raw material costs for feedstock, hydrogen, and an estimate of overall price of methane production.

Table 7-5: Estimated price of methane production with bio-based feedstock

Feed	Equation	Feed cost*	H_2 cost*	RM cost*	Total cost**
SO	$C_6H_{14}O_6 + 11\ H_2 \rightarrow 6\ CH_4 + 6\ H_2O$	\$0.038 [10]	\$0.004	\$0.042	\$0.084
G	$C_6H_{12}O_6 + 12\ H_2 \rightarrow 6\ CH_4 + 6\ H_2O$	\$0.005 [11]	\$0.004	\$0.009	\$0.018
GO	$C_3H_8O_3 + 5\ H_2 \rightarrow 3\ CH_4 + 3\ H_2O$	\$0.053 [10]	\$0.004	\$0.057	\$0.114

* Cost basis is per mole of methane produced

** Total cost is calculated by estimating raw material (RM) costs to be 50% of the total process costs

Natural gas prices in August, 2004 were $6.25 per 1000 scf [111] (1 ft^3 at 1 atm pressure and 60°F) or roughly $0.005 per mole of methane. While glucose is the closest to being competitive with pricing, it is still three times as large as the current price of natural gas. Thus, only a sizable increase in methane/natural gas pricing would promote conversion of glucose to methane on a large scale.

[111] U.S. Natural Gas Prices, http://tonto.eia.doe.gov/dnav/ng/ng_pri_sum_dcu_nus_m.htm, viewed November 15, 2004, last updated October 29, 2004

Chapter 8 – Conclusions and Future Work

To conclude this dissertation, a summary of and conclusions drawn from the research is provided to give a roadmap of the work completed. In addition, a brief look at process economics is taken to compare current prices of propylene glycol and glycerol to the process costs involved with alkaline degradation with hydrogenation. Finally, a section on future work draws up directions this work provides for further process improvement and alternate directions the research may take.

8.1 – Summary

This research started as a continuation of prior group work to convert sorbitol into propylene glycol and glycerol via hydrogenolysis. While the conditions were optimized to maximize the amount of PG and GO produced, little was known about the mechanisms involved with sorbitol conversion and cleavage. To begin investigating the mechanisms, sorbitol adsorption experiments were used to observe the interaction between sorbitol and the metal catalyst. Analysis showed two surprising results: 1) Sorbitol dehydrogenates before cleaving into products and 2) The addition of soluble base to these adsorption experiments increases the rate of conversion and raises the yield to C_3 products with respect to runs with just sorbitol in the feedstock. Searching the literature searching led to the well-known pathways of base-catalyzed degradation of sugar. Alkaline degradation of sugar, however, leads to the production of organic acids, mainly lactic acid, instead of the desired polyols propylene glycol and glycerol. To address this problem, a hydrogenation catalyst was added to the reaction in order to hydrogenate intermediates as they form and capture them as desired C_3 products instead of organic

acid salts. Experiments that varied reaction parameters mapped out the product distribution and the effects of each variable on the product distribution. To further improve C_3 yield and selectivity, other catalysts were used as alternatives to ruthenium on carbon to preferentially hydrogenate C_3 intermediates over the sugar feedstock. In addition, a kinetic model was developed to mathematically describe the reaction and to determine the relative rates of the pathways that promote PG and GO production. The model also provides prognostic value by predicting product distributions given feedstock composition, catalyst loading, and hydrogen pressure. Other work presented was an extension of the main work for other potential applications such as conversion of carbohydrates to methane.

8.2 – Conclusions

8.2.1 – Adsorption studies

Adsorption work with sorbitol and ruthenium metal in combination with ^{13}C NMR analysis of sorbitol hydrogenolysis showed dehydrogenation of the sugar alcohol as the primary step of hydrogenolysis. Additionally, $< C_6$ acid products, such as lactic acid, formed when soluble base (e.g. potassium hydroxide) was added to the feedstock in the adsorption experiments. Through the combination of catalyzed dehydrogenation of sorbitol and the alkaline degradation of the subsequent sugar analog, C_3 products of interest formed. From this, we conclude that sorbitol hydrogenolysis proceeds through the same combination of dehydrogenation and alkaline degradation to products. The negligible amount of organic acids (< 2%) in the product distribution of sorbitol hydrogenolysis experiments is consistent with this conclusion given the hydrogenation activity of ruthenium catalyst and high hydrogen pressure present. Unsaturated

intermediates hydrogenate immediately upon formation to form propylene glycol and glycerol.

8.2.2 – Alkaline degradation with hydrogenation

The combination of alkaline degradation of monosaccharides with the simultaneous hydrogenation of the reaction intermediates presents a novel process for the production of propylene glycol and glycerol at reduced temperature and pressure with respect to sorbitol hydrogenolysis (40-50°C, 100 psig H_2 vs. 230°C, 1200 psig H_2). The highest C_3 yield observed was 1.09 moles C_3 product per mole of fructose fed (55% of theoretical) with process conditions 50°C, 100 psig H_2, 0.18 M fructose, 0.85 M KOH, and 0.1g of 5% Ru/C (Experiment 153). This is comparable to yields reported by Chopade et al.[4] Further, the reaction shows the potential for C_3 product yields as high as 85% of theoretical. At conditions of 40°C, 100 psig H_2, 0.12 M fructose, 0.85 M KOH, 0.1g of 5% Ru/C (Experiment 144), 85% of the feedstock sugar that converted to $< C_6$ products formed C_3 products of interest. This result is a significant improvement from current technologies. However, the overall C_3 yield of the experiment, 53% of theoretical, reflects the formation of sorbitol and mannitol from hydrogenation of the fructose feedstock. Thus, there is potential for high C_3 yield, but it has not yet to be realized.

Some process concerns require further attention in future work. The high feedstock concentration of soluble base would essentially double the raw material cost and present potential corrosion problems for process equipment. Dilute concentrations of the feedstock sugar with respect to sorbitol hydrogenolysis (3.2 wt% vs. 25 wt%) lessen the potential throughput of this process as well. Finally, a proper catalyst must be found

to reach the potential C_3 yield of 85%. Traditional ruthenium catalysts hydrogenate without regard for the nature of the unsaturated species. Without preferential C_3 hydrogenation over C_6 hydrogenation, sugar alcohols form readily, which lessens the C_3 yield of the process.

8.2.3 – C_3 selective hydrogenation

Work with modified platinum catalysts from PNNL demonstrated selective C_3 hydrogenation. At neutral conditions, glyceraldehyde hydrogenated to glycerol in the presence of glucose or fructose with little conversion of the sugars (< 2%). However, at the conditions of the experiments (pH > 14), sugars hydrogenated readily in addition to the aldehydic intermediates that formed during alkaline degradation. Thus, the hydrogenation of sugars was an effect of the base addition. Presumably, hydrogenation occurred during isomerization of the sugar with the formation of an acyclic, enediol intermediate and subsequent C=C bond, which reacted with the active metal and hydrogen to saturate the bond.

Modifying the active metal on the catalyst was not sufficient to selectively hydrogenate the C_3 intermediates in alkaline conditions. A catalyst that excludes reactants based on size would be very useful. The larger sugar molecules would remain in the bulk liquid phase to degrade into C_3 intermediates while the smaller intermediates would diffuse into the catalyst to hydrogenate and form propylene glycol and glycerol. In addition, high hydrogenation activity would be necessary to minimize the amount of organic acid formation.

8.2.4 – Kinetic model of alkaline degradation with hydrogenation

The kinetic model of the alkaline degradation with hydrogenation reaction presented in Chapter 6 provides a starting point for continued mathematical description of this reaction. Concentration versus time data and the calculated concentrations from the fitted model show general trends of sugar isomerization, conversion, and proper distribution of products. However, some of the quirks of the reactions are not accounted for from the model. For instance, in Experiment 140, sorbitol and mannitol formed rather quickly with respect to the other products and then leveled off for the remainder of the reaction. The model reaches the same concentration eventually, but not with the same profile.

From the fitted rate constants, the model can be simplified by removing the equilibrium constant terms for sorbitol, mannitol, propylene glycol, and glycerol (K_{SO}, K_{MO}, K_{PG}, K_{GO}) from the rate equations. These constants were essentially zero and did not contribute significantly to the overall model. Physically, this means that as the products form, they desorb readily and do not readsorb to the catalyst surface. This is consistent with kinetic analyses with sugar hydrogenation.[21, 22, 23]

To further improve the model, it may be necessary to include hydroxide concentration when calculating sugar isomerization and conversion rates. From de Bruijn et al.[73] the rate of isomerization changes at different pH levels. Unfortunately, this may be true for nearly all rate constants as alkaline degradation chemistry is dependent on base concentration. Adding base dependent terms to each rate constant associated with alkaline degradation would nearly double the number of parameters used, making the

model unwieldy. However, limiting the base dependent terms to just the isomerization terms may be sufficient for a better fit to the data.

For a more robust model, higher concentrations of initial feedstock will need to be included. Ideally, the sugar reactants will reach concentrations in excess of 250 grams per liter to increase production of C_3 products. Neutralization of the reaction media will certainly play a larger role with potentially more organic acid that can form from alkaline degradation. The higher sugar loading will also affect hydrogenation rates, which must be taken into account. Further, determining intermediate concentrations (i.e. glyceraldehyde, pyruvaldehyde) over the course of the reaction will be important as well. If large amounts of intermediate form at the higher sugar loadings relative to the current feedstock concentrations, the rate constants will need to be adjusted accordingly.

8.2.5 – Conversion of carbohydrates to methane

Hydrogenolysis of carbohydrate feedstock (sorbitol, glucose, and glycerol) at neutral conditions produced methane with yields in excess of 85% of quantitative with ethane as the lone by-product. The only raw materials of the reaction were hydrogen and the carbohydrate, which made the reaction very simple. Quantitative analysis of the gas products was complicated by dilution of the reactor headspace to maintain hydrogen pressure and continue the reaction. Combined with quantitative uncertainties involved with gas chromatography, carbon balances in some cases were in excess of 130%. With only two gas phase products, however, the proportions of each could be easily determined.

Of the three feedstocks, glucose was the most economically favorable at $0.07 per pound versus $0.40 and $0.80 per pound for sorbitol and glycerol respectively. Despite

the lower price of glucose, production of methane from the sugar would still cost roughly three times more than market price of methane. In a biorefinery setting, however, the process may become more viable due to a reduction in cost for glucose feedstock. Instead of purchasing the sugar, it could be produced directly at the facility and used in the hydrogenolysis process. This could conceivably reduce the price to $0.03 a pound or less and cut the methane production cost by one-third. This option may be particularly attractive in areas where natural gas and methane are not readily available or relatively expensive. Methane production for fuel cells may be another option worth consideration.

8.3 – Process economics of alkaline degradation with hydrogenation

Ideally, with the right process conditions and catalyst, alkaline degradation and hydrogenation of sugar will be an economically viable way to produce propylene glycol and glycerol. This section outlines raw material costs for the process and shows estimates of total production cost for PG and glycerol. For comparison, these values were calculated for both current yields realized and potential yields from experimental work.

Raw material costs of the process include the feedstock sugar, soluble base, and hydrogen. For the majority of experiments presented, fructose served as feedstock and potassium hydroxide as the soluble base. Prices for these and hydrogen are listed in Table 8-1. Experiment 152 showed the best yield for propylene glycol and glycerol with feedstock of 3.2 wt% fructose and 5.3 wt% potassium hydroxide. KOH was added in flake form at ~85%, which brought the actual amount of base added to 4.5 wt%. Thus, for every pound of fructose added, 1.4 pounds of KOH was added to the reaction.

Hydrogenation products accounted for 0.013 pounds of H_2 per pound fructose fed. Table 8-1 outlines the raw material costs for the experiment.

Table 8-1: Raw material cost for Experiment 152 (Basis: 1 lb of fructose)

Raw Material	Amount of raw material (lb)	Cost of RM ($/lb)	Feedstock price ($/lb fructose)
Fructose	1.0	0.11	0.11
Potassium hydroxide	1.4	0.33	0.46
Hydrogen	0.013	0.50	0.0065
Total Cost per lb fructose			0.58

From this feedstock, propylene glycol and glycerol were produced with yields of 0.28 and 0.32 moles product per mole fructose fed, respectively. This corresponded to yields of 0.12 lbs PG and 0.16 lbs glycerol per pound of fructose fed. Raw material costs for the two products separately were $4.80 per lb PG and $3.60 per lb glycerol produced. With PG and glycerol combined, the raw material cost was $2.10 per pound. Overall process costs would be roughly twice the raw material cost leading to a total of $4.00 per pound of product. Market prices for PG and glycerol are $0.65 and $0.80 per pound, respectively. Clearly, yields were not sufficient for a reasonable selling price.

With different feedstock and significantly higher yields to PG and glycerol, the economics change considerably. In Experiment 144, 85% of the degraded material formed C_3 products. Assuming a proper catalyst (i.e. selectively hydrogenated C_3 intermediates) was found and all of the C_3 products were propylene glycol and glycerol, hydrogenation products would account for 2.4 moles of H_2 per mole of glucose fed, or

0.027 lb H_2 per lb glucose. Table 8-2 shows the raw material costs associated with the alternate feedstock.

Table 8-2: Raw material cost for alternate feedstock (Basis: 1 lb of glucose)

Raw Material	Amount of raw material (lb)	Cost of RM ($/lb)	Feedstock price ($/lb fructose)
Glucose	1.0	0.07	0.07
Sodium hydroxide	1.0	0.065	0.065
Hydrogen	0.027	0.50	0.014
Total Cost per lb fructose			0.15

With the two substitutions of fructose to glucose and KOH to NaOH, the raw material cost was cut by nearly 75%. Further, with 80% of theoretical yield to propylene glycol and glycerol, production costs drop significantly as well. With an assumed distribution of 0.8 moles of product per mole of glucose fed for both PG and GO (1:1), 0.34 pounds of PG and 0.41 pounds of GO would be produced per pound of glucose fed. Separately, the cost of each would be $0.44 per pound PG and $0.37 per pound of glycerol. Combined, the production cost would be only $0.20 per pound. Even with raw material costs at a conservative 50% of the total process expense, PG and GO could be manufactured for $0.40 per pound. Thus, the potential exists for this process to be competitive with current methods of PG and glycerol manufacturing.

8.4 – Future Work

8.4.1 – Catalyst screening for alkaline degradation with hydrogenation

In order for the alkaline degradation with hydrogenation reaction to be successful, a catalyst needs to be found to selectively hydrogenate C_3 intermediates as they form to produce the desired products of propylene glycol. Presumably, a catalyst with particular pore sizes would allow the smaller C_3 molecules to enter the freely while excluding the C_6 feedstock molecules. Said catalyst would also have metal dispersed within the pores to hydrogenate the intermediates as they enter the catalyst and allow the products to diffuse to the bulk liquid phase. While molecular sieves have been already used in similar size-selective reactions,[32] the catalysts used in that work are unstable at high pH. Other supports, such as carbon, are stable at high pH but are difficult to produce with precise pore size distributions necessary for the reaction. As catalyst technologies improve, this option will be more viable and worth further study.

8.4.2 – Hydrogenolysis of carbohydrates to methane

Conversion of sorbitol, glucose, and glycerol showed high yields to methane (>85% of theoretical) with only the carbohydrates and hydrogen as raw materials, standard catalyst (5 wt% Ru/C), and typical hydrogenolysis conditions (200°C, 1200 psig). Continued work should focus on further improving the methane yield to at or near 100% by changing reaction temperature and pressure and observing the effects on the gas phase products.

Further economic analysis of glucose to methane is warranted as well. While converting purchased glucose to methane does not show economic potential, sugars

produced on-site would provide a suitable feedstock at a more favorable raw material cost. The offset in price may be sufficient for process considerations.

Conversion of glycerol to methane is also of further interest due to the small number of intermediates (propylene glycol, ethylene glycol, ethanol, and 1-propanol) produced during the reaction. This would simplify mechanistic work of glycerol cracking to methane and, more importantly, to propylene glycol. With the increased production of biodiesel, glycerol as a by-product becomes a potential feedstock for further processing.

8.4.3 – Catalyst characterization

Ruthenium on carbon catalyst was used as the primary catalyst for most of the reactions presented in this work and in prior group work with sorbitol hydrogenolysis.[4] Prior to experiments, the catalyst was pre-reduced to activate the metal and promote catalytic activity. While the pre-reduction conditions remained consistent for each set of studies, the effect of different pre-reduction conditions, however, was not examined. Different oxidation states of the dispersed ruthenium metal may have an effect on the overall product distribution or the rate of reaction. In addition, pretreatment of the catalyst with alkaline solution may have an effect due to interaction with the cations present. Surface techniques, such as x-ray photoelectron spectroscopy (XPS), may provide insight on changes to the catalyst due to different pre-reduction conditions and the effects of alkali metals. Temperature programmed desorption (TPD) would also provide information on what temperatures and lengths of time would be suitable for pre-reduction to yield consistent catalytic activity.

APPENDIX A

Rate equations for the kinetic model

Sixteen equations describe the kinetic model derived for the alkaline degradation – hydrogenation system. Abbreviations and descriptions of rate constants are provided in Tables A-1 and A-2.

Table A-1: Abbreviations used for rate constants and kinetic model

Abbreviation	Description
G	Glucose
M	Mannose
F	Fructose
SO	Sorbitol
MO	Mannitol
GA	Glyceraldehyde
PA	Pyruvaldehyde
GA2	Glycolaldehyde
EG	Ethylene glycol
PG	Propylene glycol
GO	Glycerol
LA	Lactic acid
FA	Formic acid
GLYA	Glyceric acid
GLYA2	Glycolic acid
CD	Condensation products
CZ	Cannizzaro reaction
H_2	Hydrogen
S_1	Catalytic site – type 1
S_2	Catalytic site – type 2
$\Theta_{H\cdot S2}$	Fractional coverage of hydrogen on type 2 sites
Θ_{V1}	Fraction of vacant type 1 sites
r	Reaction rate
t	Time
[ ]	Concentration

Table A-2: Description of rate constants and abbreviations used in the kinetic model

Rate Constant	Description
$k_{F\text{-}G}$	Isomerization of fructose to glucose
$k_{G\text{-}F}$	Isomerization of glucose to fructose
$k_{F\text{-}M}$	Isomerization of fructose to mannose
$k_{M\text{-}F}$	Isomerization of mannose to fructose
$k_{G\text{-}M}$	Isomerization of glucose to mannose
$k_{M\text{-}G}$	Isomerization of mannose to glucose
$k_{F\text{-}SO}$	Hydrogenation of fructose to sorbitol
$k_{F\text{-}MO}$	Hydrogenation of fructose to mannitol
$k_{G\text{-}SO}$	Hydrogenation of glucose to sorbitol
$k_{M\text{-}MO}$	Hydrogenation of mannose to mannitol
$k_{F\text{-}GA}$	Retro-aldol condensation of fructose to glyceraldehyde
$k_{GA\text{-}F}$	Aldol condensation of glyceraldehyde to fructose
$k_{G\text{-}GA2}$	Retro-aldol condensation of glucose to glycolaldehyde
$k_{GA2\text{-}G}$	Aldol condensation of glycolaldehyde to glucose
$k_{F\text{-}FA}$	Degradation of fructose to formic acid
$k_{F\text{-}GLYA2}$	Degradation of fructose to glycolic acid
$k_{GA\text{-}CZ}$	Cannizzaro reaction of glyceraldehyde to glyceric acid and glycerol
$k_{GA\text{-}GO}$	Hydrogenation of glyceraldehyde to glycerol
$k_{GA\text{-}PA}$	β-elimination of glyceraldehyde to pyruvaldehyde
$k_{GA\text{-}CD}$	Condensation of glyceraldehyde to by-products
$k_{PA\text{-}FA}$	α-dicarbonyl cleavage of pyruvaldehyde to formic acid
$k_{PA\text{-}PG}$	Hydrogenation of pyruvaldehyde to propylene glycol
$k_{PA\text{-}LA}$	Benzylic acid rearrangement of pyruvaldehyde to lactic acid
$k_{PA\text{-}CD}$	Condensation of pyruvaldehyde to by-products
$k_{GA2\text{-}EG}$	Hydrogenation of glycolaldehyde to ethylene glycol
$k_{GA2\text{-}CZ}$	Cannizzaro reaction of glycolaldehyde to glycolic acid and ethylene glycol
$k_{GA2\text{-}CD}$	Condensation of glycolaldehyde to by-products
K_{SO}	Adsorption equilibrium constant of sorbitol
K_{MO}	Adsorption equilibrium constant of mannitol
K_{GO}	Adsorption equilibrium constant of glycerol
K_{PG}	Adsorption equilibrium constant of propylene glycol
K_{EG}	Adsorption equilibrium constant of ethylene glycol
K_{H}	Adsorption equilibrium constant of hydrogen

$$\frac{d[SO]}{dt} = \left(k_{G-SO}[G] + k_{F-SO}[F]\right)\cdot\Theta_{H\cdot S2}^{2}\Theta_{V1} - k_{SO-CD}[SO]$$

$$\frac{d[MO]}{dt} = \left(k_{M-MO}[M] + k_{F-MO}[F]\right)\cdot\Theta_{H\cdot S2}^{2}\Theta_{V1} - k_{MO-CD}[MO]$$

$$\frac{d[GO]}{dt} = k_{GA-GO}[GA]\cdot\Theta_{H\cdot S2}^{2}\Theta_{V1} + \frac{k_{GA-CZ}}{2}[GA]^{2}$$

$$\frac{d[PG]}{dt} = k_{PA-PG}[PA]\cdot\Theta_{H\cdot S2}^{2}\Theta_{V1}$$

$$\frac{d[EG]}{dt} = k_{GA2-EG}[GA2]\cdot\Theta_{H\cdot S2}^{2}\Theta_{V1} + \frac{k_{GA2-CZ}}{2}[GA2]^{2}$$

$$\frac{d[G]}{dt} = -\left(k_{G-F} + k_{G-M} + k_{G-GA2}\right)[G] + k_{F-G}[F] + k_{M-G}[M] - k_{G-SO}[G]\cdot\Theta_{H\cdot S2}^{2}\Theta_{V1} + k_{GA2-G}[GA2]^{2}$$

$$\frac{d[F]}{dt} = -\left(k_{F-G} + k_{F-M} + k_{F-GA}\right)[F] + k_{G-F}[G] + k_{M-F}[M] - \left(k_{F-SO} + k_{F-MO}\right)[F]\cdot\Theta_{H\cdot S2}^{2}\Theta_{V1} + k_{GA-F}[GA]^{2}$$

$$\frac{d[M]}{dt} = -\left(k_{M-G} + k_{M-F}\right)[M] + k_{G-M}[G] + k_{F-M}[F] - k_{M-MO}[M]\cdot\Theta_{H\cdot S2}^{2}\Theta_{V1}$$

$$\frac{d[GA]}{dt} = -(k_{GA-PA} + k_{GA-CD})[GA] - (k_{GA-CZ} + k_{GA-F})[GA]^2 + k_{F-GA}[F] - k_{GA-GO}[GA] \cdot \Theta_{H \cdot S2}^2 \Theta_{V1}$$

$$\frac{d[GA2]}{dt} = -k_{GA2-CD}[GA2] + k_{G-GA2}[G] - k_{GA2}[GA2] \cdot \Theta_{H \cdot S2}^2 \Theta_{V1} - k_{GA2-CZ}[GA2]^2$$

$$\frac{d[PA]}{dt} = -(k_{PA-LA} + k_{PA-FA} + k_{PA-CD})[PA] + k_{GA-PA}[GA] - k_{PA-PG}[PA] \cdot \Theta_{H \cdot S2}^2 \Theta_{V1}$$

$$\frac{d[LA]}{dt} = k_{PA-LA}[PA]$$

$$\frac{d[FA]}{dt} = k_{PA-FA}[PA] + k_{F-FA}[F]$$

$$\frac{d[GLYA]}{dt} = \frac{k_{GA-CZ}}{2}[GA]^2$$

$$\frac{d[GLYA2]}{dt} = \frac{k_{GA2-CZ}}{2}[GA2]^2 + k_{F-GA2}[F]$$

$$\frac{d[CD]}{dt} = k_{GA-CD}[GA] + k_{PA-CD}[PA] + k_{GA2-CD}[GA2] + k_{SO-CD}[SO] + k_{MO-CD}[MO]$$

APPENDIX B

Visual Basic coding used for kinetic model calculations

The numerical method coded was adapted from Applied Numerical Methods by B. Carnahan, H. Luther, and J. Wilkes, published in 1969 by Wiley. Mathematical notation is consistent with Carnahan et al.

```
Sub RungeKutta4()

Dim rowvar(1 To 100)              'Row location of dependent variable
Dim y(1 To 100) As Double         'Array for dependent variable values
Dim k1(30) As Double              'k1, k2, k3, and k4 are the
Dim k2(30) As Double              'coefficients for the 4th order Runge-
Dim k3(30) As Double              'Kutta method
Dim k4(30) As Double
Dim tempy(100) As Double          'Holds temporary values of y( )
Dim expnames(1 To 30) As Variant   'Used for labeling Excel worksheets
Dim cao(19) As Double             'cao-cso hold initial values of
Dim cbo(19) As Double             'dependent variables
Dim cco(19) As Double
Dim cdo(19) As Double
Dim ceo(19) As Double
Dim cfo(19) As Double
Dim cgo(19) As Double
Dim cho(19) As Double
Dim cio(19) As Double
Dim cjo(19) As Double
Dim cko(19) As Double
Dim clo(19) As Double
Dim cmo(19) As Double
Dim cno(19) As Double
Dim coo(19) As Double
Dim cpo(19) As Double
Dim cqo(19) As Double
Dim cro(19) As Double
Dim cso(19) As Double
Dim repchk(100) As Double         'Array to keep track of random walks
Dim parameters(50) As Double      'Constants used in differential eqns
Dim rowform(1 To 100) As Single 'Array to note rows with dependent vars

walks = Worksheets("Set Up").Cells(19, 10).Value
  'Number of random walks to take before stopping the program

runs = Worksheets("Set Up").Cells(13, 10).Value
  'Number of experiments to solve differential equations for

summary_col = 1
summary_row = 0
  'Position to start recording parameters on the 'Summary' sheet

jump = 0
  'Used to move from row to row when storing experiment data
```

```
For i = 1 To runs
expnames(i) = Worksheets("Experiments").Cells(1 + jump, 1).Value
cao(i) = Worksheets("Experiments").Cells(3 + jump, 2).Value
cbo(i) = Worksheets("Experiments").Cells(4 + jump, 2).Value
cco(i) = Worksheets("Experiments").Cells(5 + jump, 2).Value
cdo(i) = Worksheets("Experiments").Cells(6 + jump, 2).Value
ceo(i) = Worksheets("Experiments").Cells(7 + jump, 2).Value
cfo(i) = Worksheets("Experiments").Cells(8 + jump, 2).Value
cgo(i) = Worksheets("Experiments").Cells(9 + jump, 2).Value
cho(i) = Worksheets("Experiments").Cells(10 + jump, 2).Value
cio(i) = Worksheets("Experiments").Cells(11 + jump, 2).Value
cjo(i) = Worksheets("Experiments").Cells(12 + jump, 2).Value
cko(i) = Worksheets("Experiments").Cells(13 + jump, 2).Value
clo(i) = Worksheets("Experiments").Cells(14 + jump, 2).Value
cmo(i) = Worksheets("Experiments").Cells(15 + jump, 2).Value
cno(i) = Worksheets("Experiments").Cells(16 + jump, 2).Value
coo(i) = Worksheets("Experiments").Cells(17 + jump, 2).Value
cpo(i) = Worksheets("Experiments").Cells(18 + jump, 2).Value
cqo(i) = Worksheets("Experiments").Cells(19 + jump, 2).Value
cro(i) = Worksheets("Experiments").Cells(20 + jump, 2).Value

jump = jump + 39
Next i
  'The for-next loop collects the initial boundary conditions, i.e. the
  'feedstock concentrations of the reactions, and stores them in the
  'corresponding arrays of cao( ) to cro( ).  More initial conditions
  'are possible, but separate arrays must be included for the program
  'to run properly

'START OF COMPUTATION LOOP

For current_step = 0 To walks
Worksheets("Set Up").Range("j17").Value = current_step
  'Displays current step on worksheet

For pmer = 1 To 50
  parameters(pmer) = Worksheets("Set Up").Cells(26 + pmer, 8).Value
Next pmer
  'Stores current parameters into array 'parameters'

check = 0
  'flag to make sure a random step has not been taken yet.  If check=1,
  'then the program continues.  Otherwise, the loop repeats

Do While check = 0

Randomize
random1 = Int(40 * Rnd + 27)
random2 = Int(2 * Rnd)
repchk(no_imp) = random1 * 10 + random2
  'Generates a random number representing a random walk and stores the
  'result in the array 'repchk'
```

```
If no_imp = 0 Then
  GoTo 10
End If
  'If the random walk is the first since an improvement, then there is
  'no need to check for a repeat

For i = 0 To no_imp - 1
  If repchk(no_imp) = repchk(i) Then
    check = 0
    i = 10000
  End If
  If i = no_imp - 1 Then
    check = 1
  End If
Next i
  'The for-next loop compares the current walk to the recorded walks.
  'If there is a match, then another random number is generated.  With
  'no match, check=1 and the program continues

Loop

10 Worksheets("Set Up").Range("j24").Value = no_imp
  'Displays number of steps taken since an improvement was observed

If random2 = 1 Then
  Worksheets("Set Up").Cells(random1, 8).Value = _
  Worksheets("Set Up").Cells(random1, 8).Value * 1.1
Else
  Worksheets("Set Up").Cells(random1, 8).Value = _
  Worksheets("Set Up").Cells(random1, 8).Value * 0.9
End If
  'Changes the chosen parameter up or down a set percentage (10% in
  'this case)

Worksheets("Set Up").Cells(random1, 2).Value = _
Worksheets("Set Up").Cells(random1, 8).Value
  'Replaces the altered parameter to be used for calculations
```

```
For reaction = 1 To runs
Worksheets("Set Up").Range("j16").Value = reaction
  'Displays the number of the experiment being calculated

j = 0         '# of dependent variables that match the differential eqn
jj = 0        '# of differential equations

Worksheets("Set Up").Range("b9").Value = cao(reaction)
Worksheets("Set Up").Range("b10").Value = cbo(reaction)
Worksheets("Set Up").Range("b11").Value = cco(reaction)
Worksheets("Set Up").Range("b12").Value = cdo(reaction)
Worksheets("Set Up").Range("b13").Value = ceo(reaction)
Worksheets("Set Up").Range("b14").Value = cfo(reaction)
Worksheets("Set Up").Range("b15").Value = cgo(reaction)
Worksheets("Set Up").Range("b16").Value = cho(reaction)
Worksheets("Set Up").Range("b17").Value = cio(reaction)
Worksheets("Set Up").Range("b18").Value = cjo(reaction)
Worksheets("Set Up").Range("b19").Value = cko(reaction)
Worksheets("Set Up").Range("b20").Value = clo(reaction)
Worksheets("Set Up").Range("b21").Value = cmo(reaction)
Worksheets("Set Up").Range("b22").Value = cno(reaction)
Worksheets("Set Up").Range("b23").Value = coo(reaction)
Worksheets("Set Up").Range("b24").Value = cpo(reaction)
Worksheets("Set Up").Range("b25").Value = cqo(reaction)
Worksheets("Set Up").Range("b26").Value = cro(reaction)
  'Displays initial boundary conditions of differential equation


Worksheets(expnames(reaction) & " Output").Cells(2, 1) =
Worksheets("Set Up").Range("indepvar").Value
  'Displays the independent variable on the Output Sheet

Worksheets(expnames(reaction) & " Output").Cells(3, 1) =
Worksheets("Set Up").Range("initialindep").Value
  'Places initial value of independent variable on the Output Sheet

row1 = ActiveWorkbook.Names("startingpt").RefersToRange.Row + 1
column1 = ActiveWorkbook.Names("startingpt").RefersToRange.Column
  'Used as reference point for locating variable names

columnvar = column1 + 1
  'Column number of all the variables (column B)
```

```
For i = 0 To 100

  If Worksheets("Set Up").Cells(row1 + i, column1)) Like "d(*" Then
    jj = jj + 1
    'Cells with d(*)/dt are counted as differential equations

    If (jj > 20) Then
      notice = MsgBox("You have more than 20 Diff Eqns. The program can
      only solve 20.", vbOKOnly, "Error")
      End
    End If
    'If there are more than 20 diff eqns, then end the program.  More
    'equations are possible, but this version is limited to 20.

  rowdeq(jj) = row1 + i
    'Stores the row number of the differential equation in 'rowdeq'

  temp = Worksheets("Set Up").Cells(row1 + i, column1).Value
  temp = Right(temp, Len(temp) - 2)
  temp = Left(temp, InStr(temp, ")"))
  temp = Left(temp, Len(temp) - 1)
    'Finds the dependent variable of the differential equation

    For k = 0 To 100

      If (Not IsEmpty(Worksheets("Set Up").Cells(row1 + k, column1))) _
      And (Worksheets("Set Up").Cells(row1 + k, column1)) _
      Like temp Then
        j = j + 1
        'If the dependent variable of the differential equation matches
        'a variable listed on the set up page, # of dependent variables
        'increments by 1

        rowvar(j) = row1 + k
        'Stores row number of dependent variable in 'rowvar'

        z(j) = Worksheets("Set Up").Cells(row1 + k, column1 + 1)
        'Stores initial value of jth dependent variable

        Worksheets(expnames(reaction) & " Output").Cells(3, 1 + j) = _
        Worksheets("Set Up").Cells(row1 + k, column1 + 1)
          'Displays initial value of dependent variable on the output
          'sheet of the corresponding experiment

        Worksheets(expnames(reaction) & " Output").Cells(2, 1 + j) = _
        Worksheets("Set Up").Cells(row1 + k, column1).Value
          'Displays name of dependent variable on the output sheet of
          'the corresponding experiment
      End If

    Next k

  End If

Next i
```

```
If (jj <> j) Then
  notice = MsgBox("The program cannot continue because differential
  equations were not found for every dependent variable.", vbOKOnly,
  "Error")
  End
End If
  'If the # of differential equations does not match the number of
  'dependent variables, then the program ends with an error

Worksheets(expnames(reaction) & " Output").Range("A1") =
expnames(reaction) & " Output"
Worksheets(expnames(reaction) & "
Output").Range("A1").HorizontalAlignment = xlLeft
Worksheets(expnames(reaction) & " Output").Range("A1").Font.Bold = True
Worksheets(expnames(reaction) & " Output").Range("A1").Font.Italic =
True
Worksheets(expnames(reaction) & " Output").Range("A1").Font.Size = 12
Worksheets(expnames(reaction) & "
Output").Range("2:2").HorizontalAlignment = xlCenter
Worksheets(expnames(reaction) & " Output").Range("2:2").Font.Bold =
True
  'Formats experiment output sheet for results of calculations

Stoprow = 3 + Worksheets("Set Up").Range("numsteps")
  'Stops iteration desired amount of time steps have been taken

h = Worksheets("Set Up").Range("stepsize")
  'Step size of time.  Consistent with Carnahan

CurrentRow = 3
  'Starting point on Output sheet

initial = Worksheets("Set Up").Range("initialindep").Value
  'First time point of the calculation
```

```
'MAIN CALCULATION LOOP

Do While CurrentRow < Stoprow
t = Worksheets(expnames(reaction) & " Output").Cells(CurrentRow,
column1).Value
Worksheets("Set Up").Range("initialindep").Value = t

For i = 1 To j
  y(i) = Worksheets(expnames(reaction) & " Output").Cells(CurrentRow,
  column1 + i).Value
  Worksheets("Set Up").Cells(rowvar(i), columnvar) = y(i)
  tempy(i) = y(i)
Next i
  'For-next loop takes values of dependent variables at time t and
  'stores them in y(). Then, copies those values to the 'Set Up' sheet
  'so that derivatives can be calculated from formulas entered by the
  'user. Then, tempy() stores initial y values to be used in Runge-
  'Kutta coefficient determination

  For k = 1 To j
    k1(k) = Worksheets("Set Up").Cells(rowdeq(k), columnvar).Value
    tempy(k) = y(k) + h / 2 * k1(k)
    Worksheets("Set Up").Cells(rowvar(k), columnvar) = tempy(k)
    k2(k) = Worksheets("Set Up").Cells(rowdeq(k), columnvar).Value
  Next k
    'Calculates the coefficients k1 and k2

  For k = 1 To j
    tempy(k) = y(k) + h / 2 * k2(k)
    Worksheets("Set Up").Cells(rowvar(k), columnvar) = tempy(k)
    k3(k) = Worksheets("Set Up").Cells(rowdeq(k), columnvar).Value
  Next k
    'Calculates the coefficient k3

  For k = 1 To j
    tempy(k) = y(k) + h * k3(k)
    Worksheets("Set Up").Cells(rowvar(k), columnvar) = tempy(k)
    k4(k) = Worksheets("Set Up").Cells(rowdeq(k), columnvar).Value
  Next k
    'Calculates the coefficient k4

'For each coefficient calculation, concentration and derivative
'values must be refreshed to ensure proper calculation
```

```
  For k = 1 To j
    If (Not IsNumeric(Worksheets("Set Up").Cells(rowdeq(k),
    columnvar).Value)) Then
      msg = "There was a problem with the calculation. "
      msg = msg & "At least one derivative"
      msg = msg & " has become non-numeric due to an error."
      msg = msg & " You will need to reinitialize all dependent
                  variables after"
      msg = msg & " you find the error. Be sure to reinitialize the"
      msg = msg & " independent variable also."
      notice = MsgBox(msg, vbOKOnly, "Runtime Error")
      End
    End If
  Next k
    'If any of the differential equations becomes non-numeric, the
    'program is stopped

CurrentRow = CurrentRow + 1
  'Increment the row number to allow proper placement of calculated
  'value of dependent variable

Worksheets(expnames(reaction) & " Output").Cells(CurrentRow,
column1).Value = t + h
Worksheets("Set Up").Range("initialindep").Value = t + h
  'Prints out next time step on Output sheet and updates the time on
  'the Set Up sheet

For i = 1 To j
  Worksheets(expnames(reaction) & " Output").Cells(CurrentRow, column1
  + i) = y(i) + h / 6 * (k1(i) + 2 * k2(i) + 2 * k3(i) + k4(i))
Next i
  'Predicts next value of dependent variable using the Runge-Kutta
  'algorithm from the calculated coefficients and displays the result
  'on the Output sheet

Loop
  'Repeats the loop until the last time step has been taken for the
  'experiment


'Adds final values of dependent variables to Runge Kutta Sheet
For i = 1 To j
  y(i) = Worksheets(expnames(reaction) & " Output").Cells(Stoprow,
  column1 + i).Value
  Worksheets("Set Up").Cells(rowvar(i), columnvar) = y(i)
Next i
  'Adds the final values of the dependent variables to the Output sheet
  'and the Set Up sheet

Worksheets("Set Up").Range("initialindep") = initial
Worksheets("Set Up").Activate
  'Resets the independent variable to its initial value

Next reaction
  'Continues on to the next reaction for calculation
```

```
'SECTION TO COMPARE CALCULATED RESULTS WITH EXPERIMENTAL DATA AND TO
'DETERMINE IF RANDOM WALK IMPROVED MODEL OR NOT

jump3 = 1
  'Place holder for finding variables on Experiments worksheet

For reaction3 = 1 To runs

p = 1
  '# of the data point from the experimental data

For q = 0 To 1000
  'Larger qmax would be necessary for more than 1000 steps in the
  'process.  For the work done with the model, 1000 was more than
  'sufficient.

  If IsEmpty(Worksheets("Experiments").Cells(21 + p + jump3, 1).Value)
  Then
    Exit For
  End If
    'If there are no more experimental points, exit the for-next loop

  If Worksheets(expnames(reaction3) & " Output").Cells(3 + q, 1).Value
  >= Worksheets("Experiments").Cells(21 + p + jump3, 1).Value Then

    For i = 1 To j
      Worksheets("Experiments").Cells(21 + p + jump3, 20 + i).Value = _
      Worksheets(expnames(reaction3) & " Output").Cells(3 + q, i +
      1).Value
    Next i

    p = p + 1

  End If
    'If the independent variable on the output sheet is >= the
    'independent variable from the Experiments sheet, then print the
    'dependent variable results from Output on to the Experiments
    'sheets for comparison.  Increment p to look for the p+1th data
    'point.

Next q

jump3 = jump3 + 39
  'Moves place holder from one experiment to the next

Next reaction3
  'Repeat for all reactions to be calculated

Worksheets("Set Up").Activate

If parameters(41) < (Worksheets("Experiments").Cells(9, 16).Value +
0.01) Then
  For pmer = 1 To 40
    Worksheets("Set Up").Cells(26 + pmer, 8).Value = parameters(pmer)
  Next pmer

  no_imp = no_imp + 1
```

```
  If no_imp = 80 Then
    notice = MsgBox("All random walks have been taken without
    improvement.", vbOKOnly, "Error")
    End
  End If

End If
  'If the total error from the latest iteration is greater than the
  'best case, then reset the parameters to the best case and try
  'another random walk.  However, if all of the walks have been taken,
  'then the program ends.

If parameters(41) > (Worksheets("Experiments").Cells(9, 16).Value +
0.01) Then

  no_imp = 0
  Worksheets("Set Up").Cells(67, 8).Value =
  Worksheets("Experiments").Cells(9, 16).Value

  For k = 0 To 39
    Worksheets("Summary").Cells(2 + k + summary_row, summary_col).Value
    = Worksheets("Set Up").Cells(27 + k, 1).Value
    Worksheets("Summary").Cells(2 + k + summary_row, summary_col +
    1).Value = Worksheets("Set Up").Cells(27 + k, 2).Value
  Next k

  Worksheets("Summary").Cells(43 + summary_row, summary_col).Value =
  "Grand Average"
  Worksheets("Summary").Cells(43 + summary_row, summary_col + 1).Value
  = Worksheets("Experiments").Cells(9, 16).Value

  summary_row = summary_row + 50
    If summary_row > 65000 Then
      summary_row = 0
      summary_col = summary_col + 3
    End If
End If
  'If the total error from the current iteration is less than the best
  'case by more than 0.01 then the new set of parameters is copied to
  'the Set Up sheet as the next starting point for random walks.  The
  'new, lowest total error replaces the old result on the Set Up sheet.
  'Further, the new parameters are recorded on the Summary sheet with
  'the total error associated with it.  If there are over 1300
  'improvements, then the parameters will be reported on the Summary
  'sheet 3 columns over to avoid an error.

Worksheets("Set Up").Activate
Next current_step
  'Repeat the procedure until the number of desired random walks are
  'taken or until all random walks have been taken without improvement

End Sub
```

APPENDIX C

Comparison of kinetic model to experimental data for alkaline degradation with hydrogenation

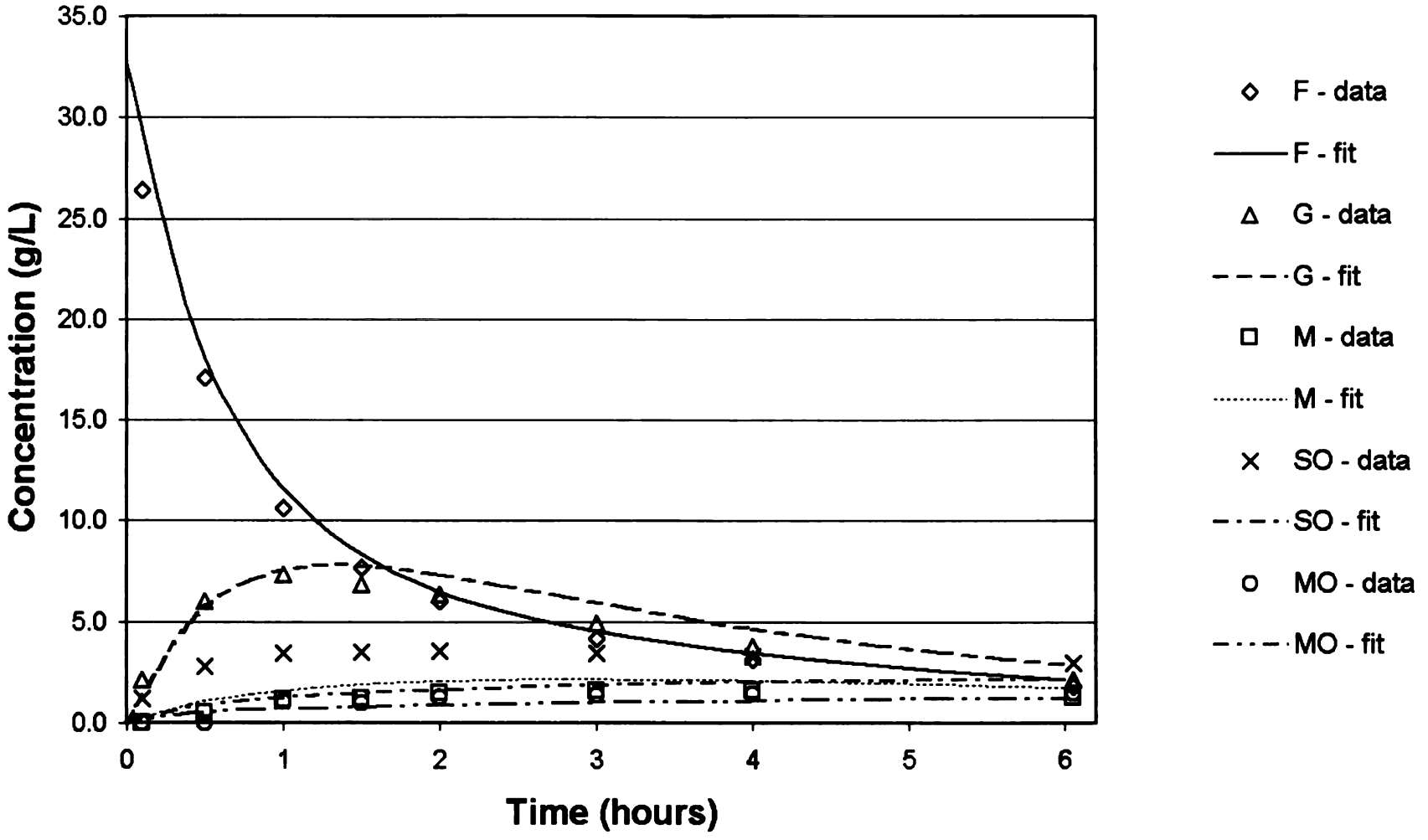

Figure C-1: Comparison of experimental data and kinetic model - Exp 115
3.16% fructose, 5.3% KOH, 40°C, 100 psig H_2, 0.05 grams 5 wt% Ru/C
Fructose, glucose, mannose, sorbitol, and mannitol vs. Time

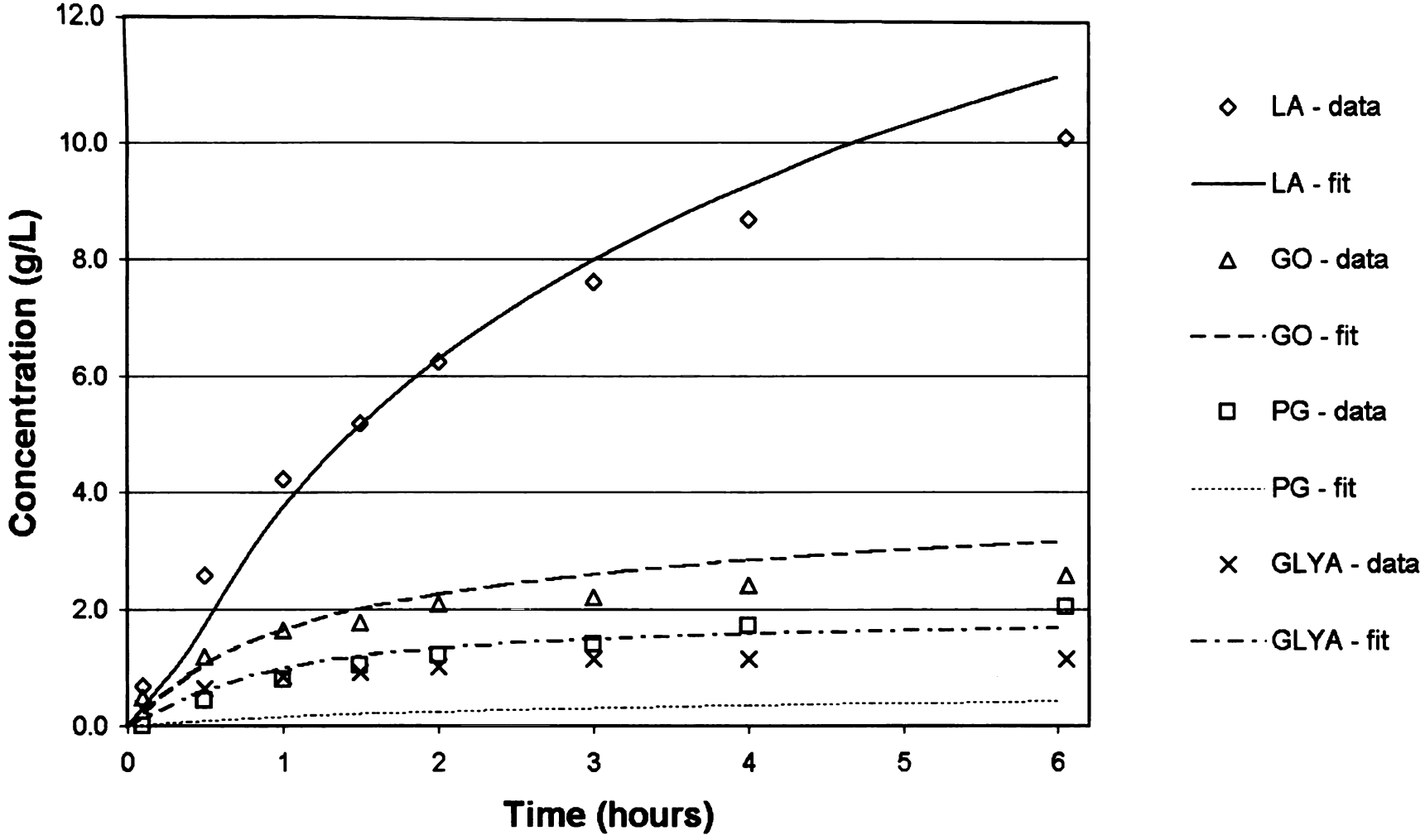

Figure C-2: Comparison of experimental data and kinetic model - Exp 115
3.16% fructose, 5.3% KOH, 40°C, 100 psig H_2, 0.05 grams 5 wt% Ru/C
Lactic acid, glycerol, propylene glycol, and glyceric acid vs. Time

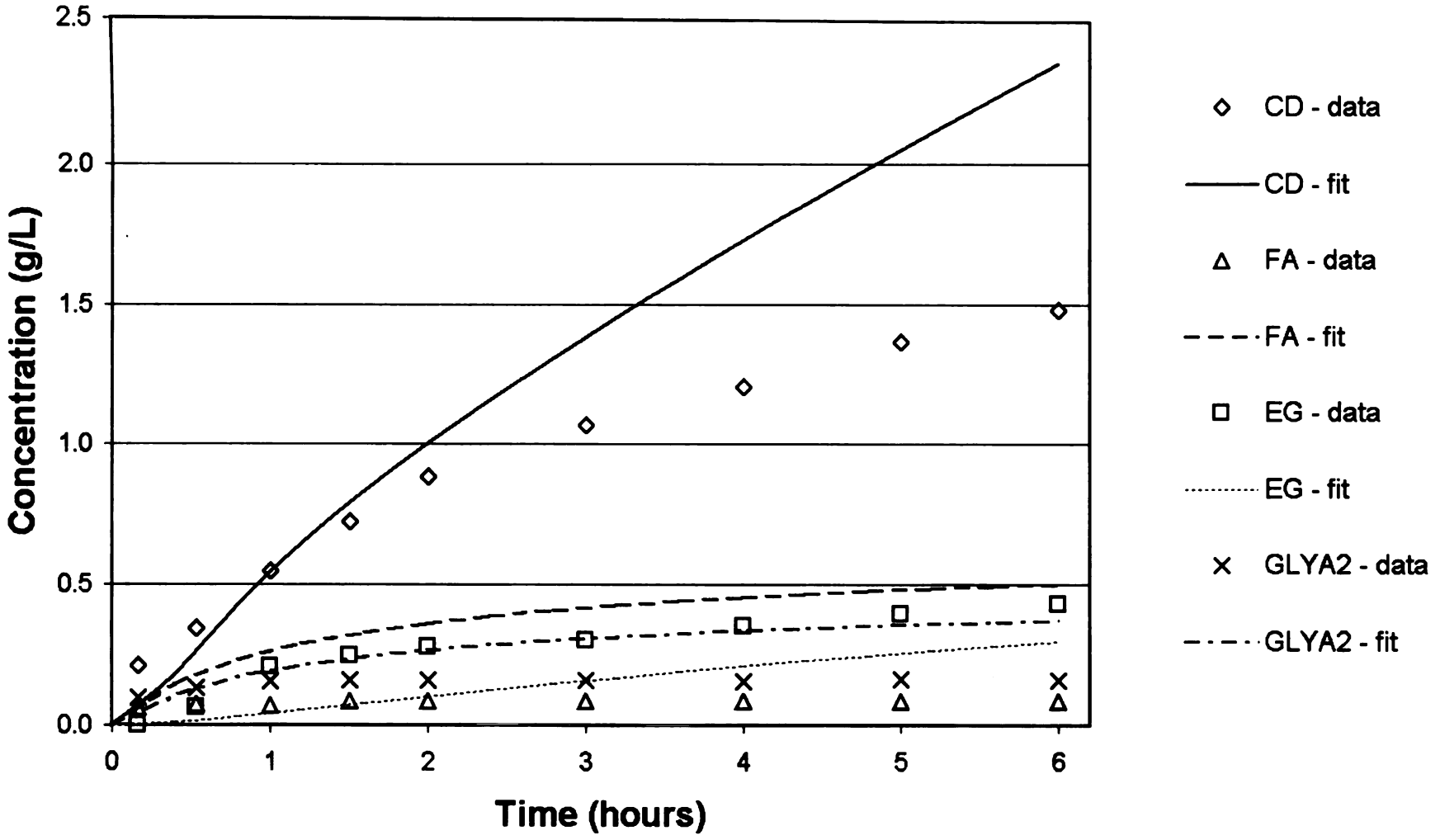

Figure C-3: Comparison of experimental data and kinetic model - Exp 115
2.0% fructose, 5.3% KOH, 40°C, 100 psig H_2, 0.1 grams 5 wt% Ru/C
Condensation products, formic acid, EG, and glycolic acid vs. Time

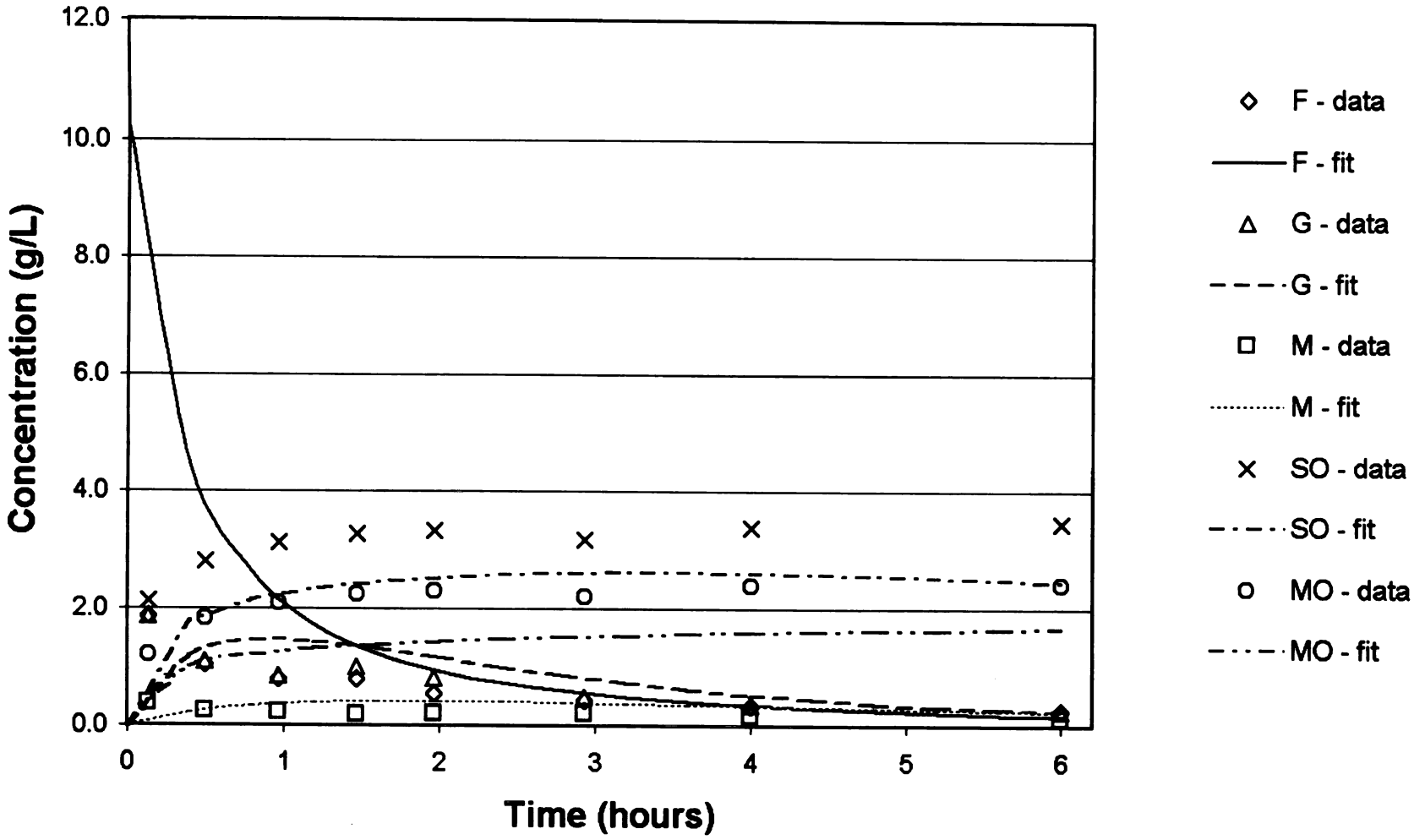

Figure C-4: Comparison of experimental data and kinetic model - Exp 119
1.00% fructose, 5.3% KOH, 40°C, 100 psig H_2, 0.10 grams 5 wt% Ru/C
Fructose, glucose, mannose, sorbitol, and mannitol vs. Time

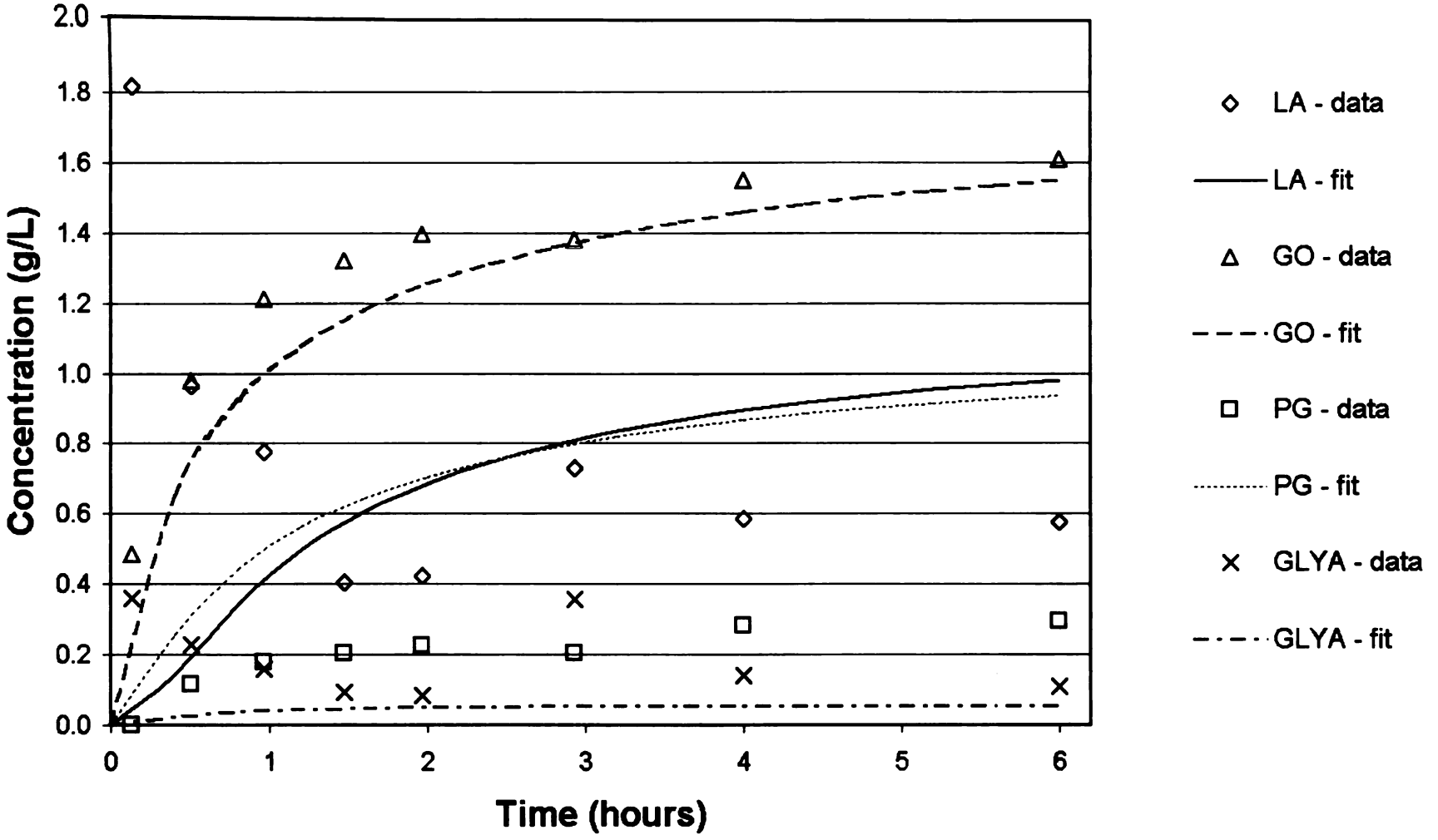

Figure C-5: Comparison of experimental data and kinetic model - Exp 119
1.00% fructose, 5.3% KOH, 40°C, 100 psig H2, 0.10 grams 5 wt% Ru/C
Lactic acid, glycerol, propylene glycol, and glyceric acid vs. Time

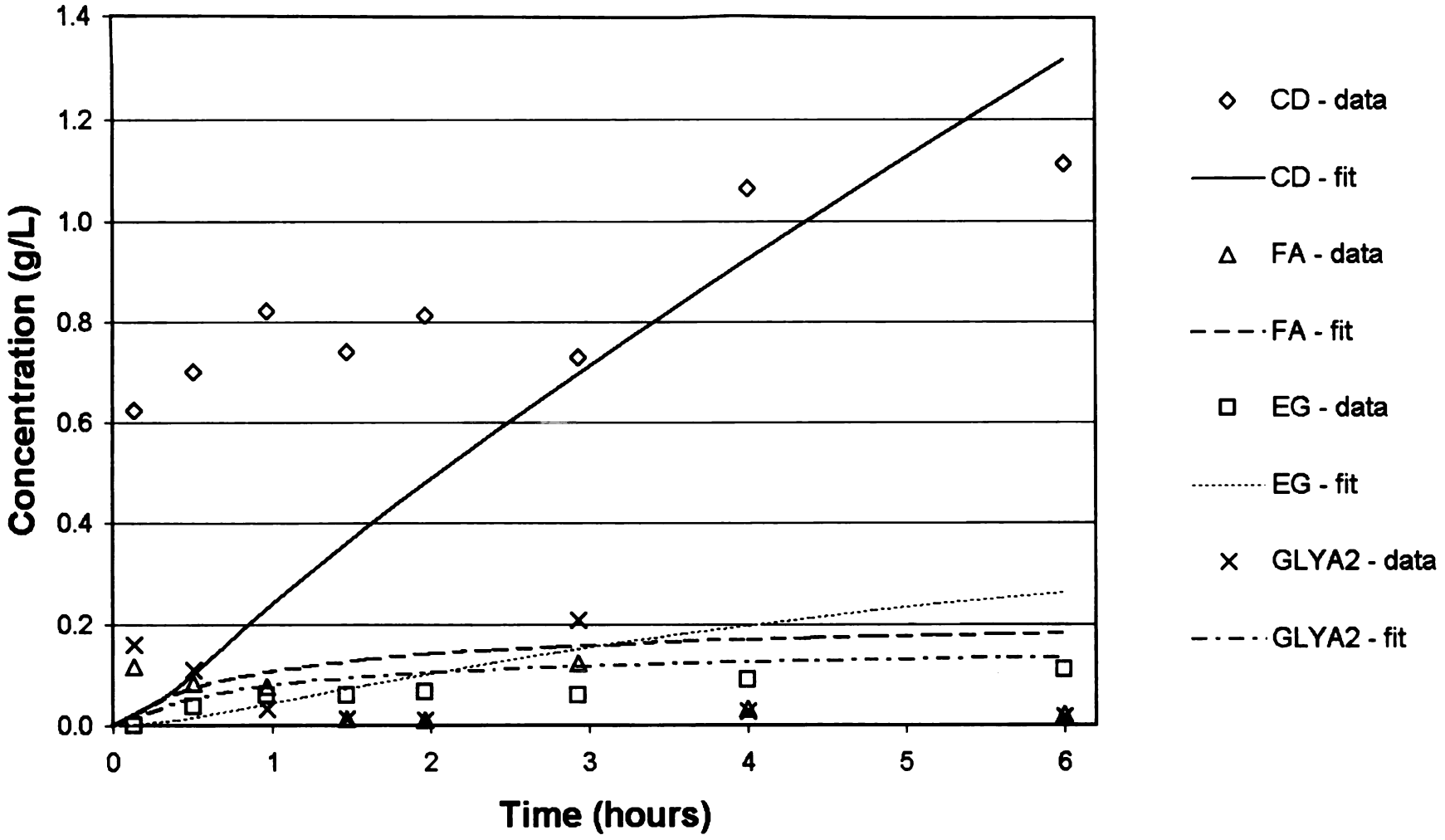

Figure C-6: Comparison of experimental data and kinetic model - Exp 119
1.00% fructose, 5.3% KOH, 40°C, 100 psig H2, 0.10 grams 5 wt% Ru/C
Condensation products, formic acid, EG, and glycolic acid vs. Time

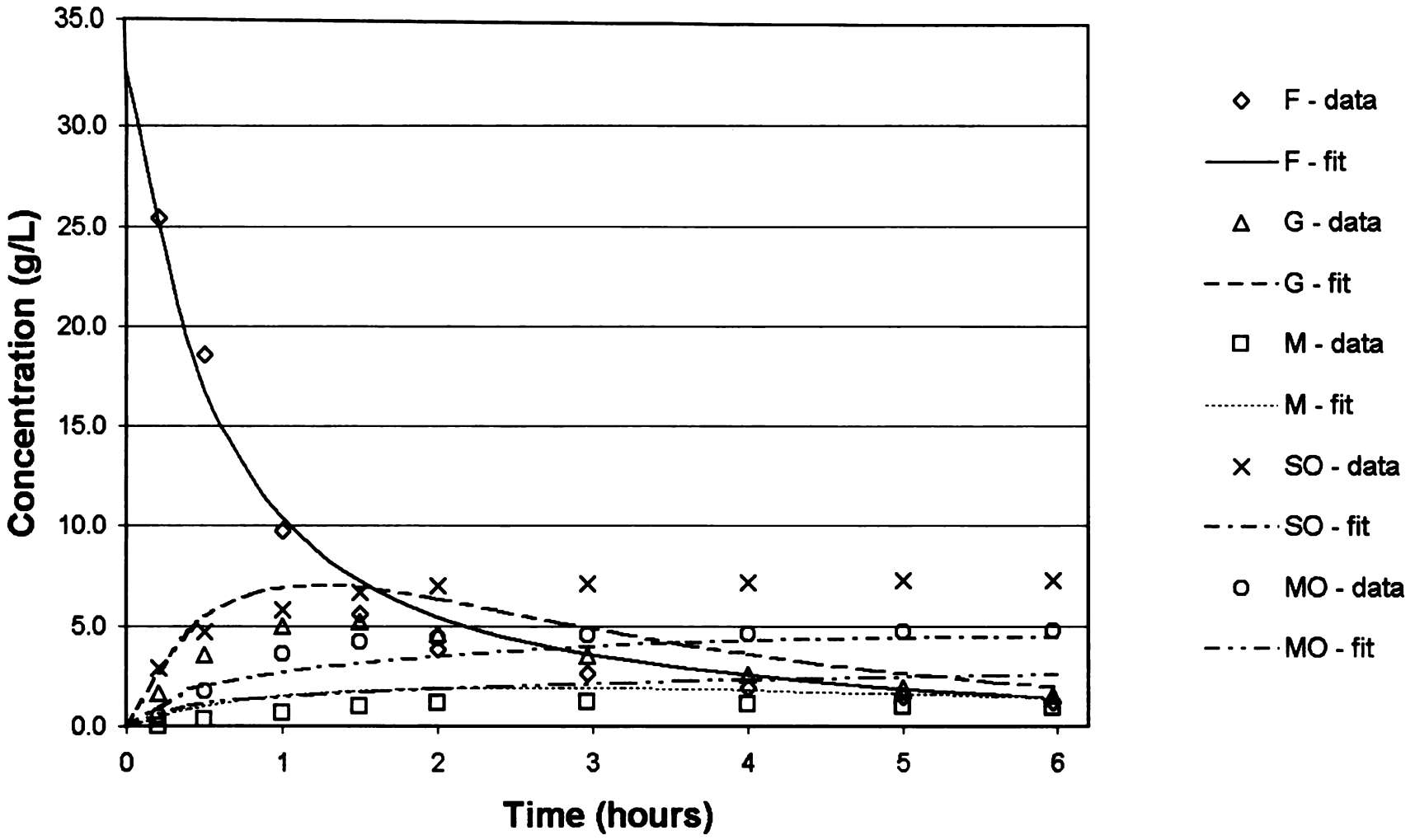

Figure C-7: Comparison of experimental data and kinetic model - Exp 140
3.17% fructose, 5.3% KOH, 40°C, 200 psig H_2, 0.10 grams 5 wt% Ru/C
Fructose, glucose, mannose, sorbitol, and mannitol vs. Time

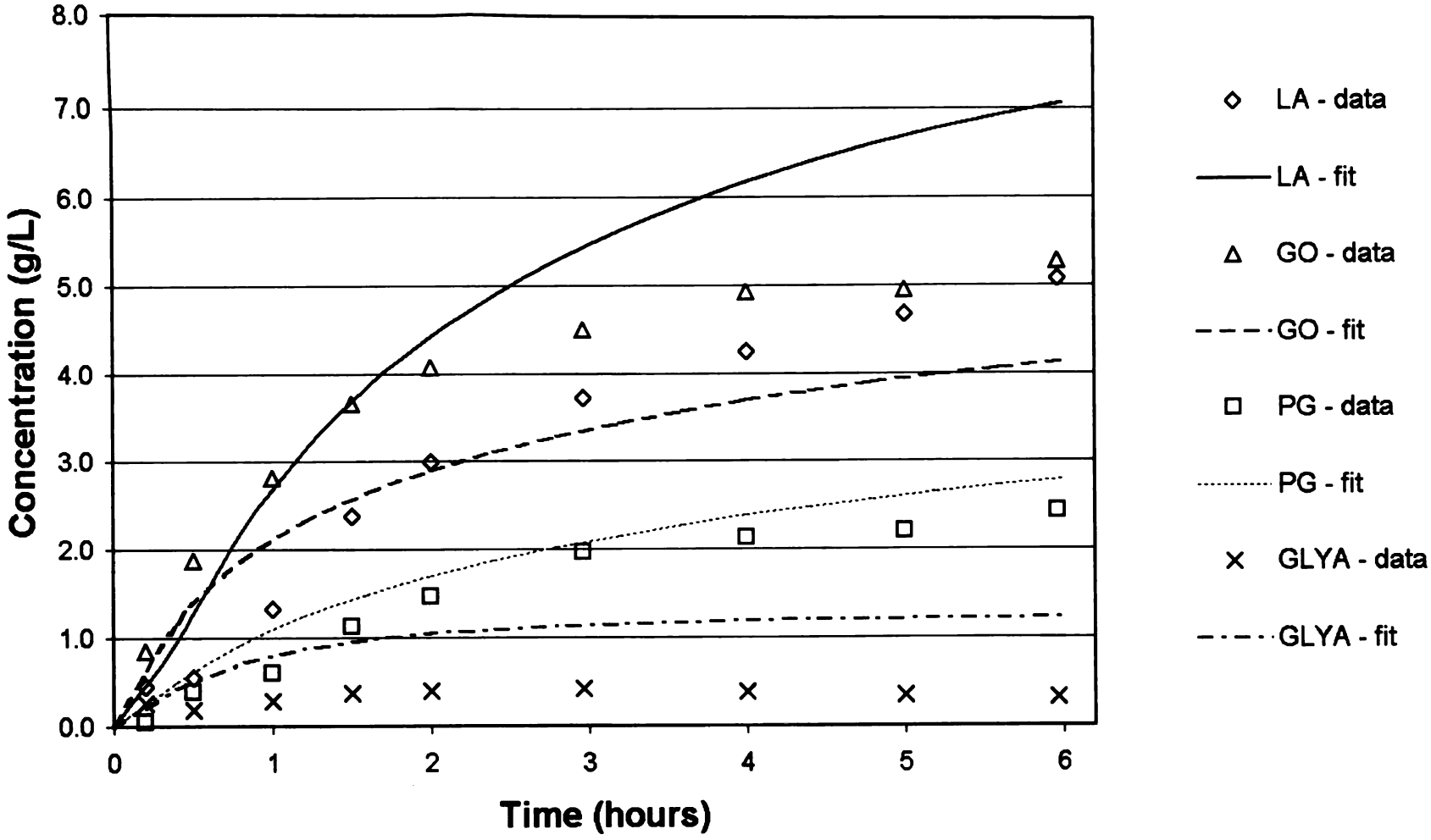

Figure C-8: Comparison of experimental data and kinetic model - Exp 140
3.17% fructose, 5.3% KOH, 40°C, 200 psig H_2, 0.10 grams 5 wt% Ru/C
Lactic acid, glycerol, propylene glycol, and glyceric acid vs. Time

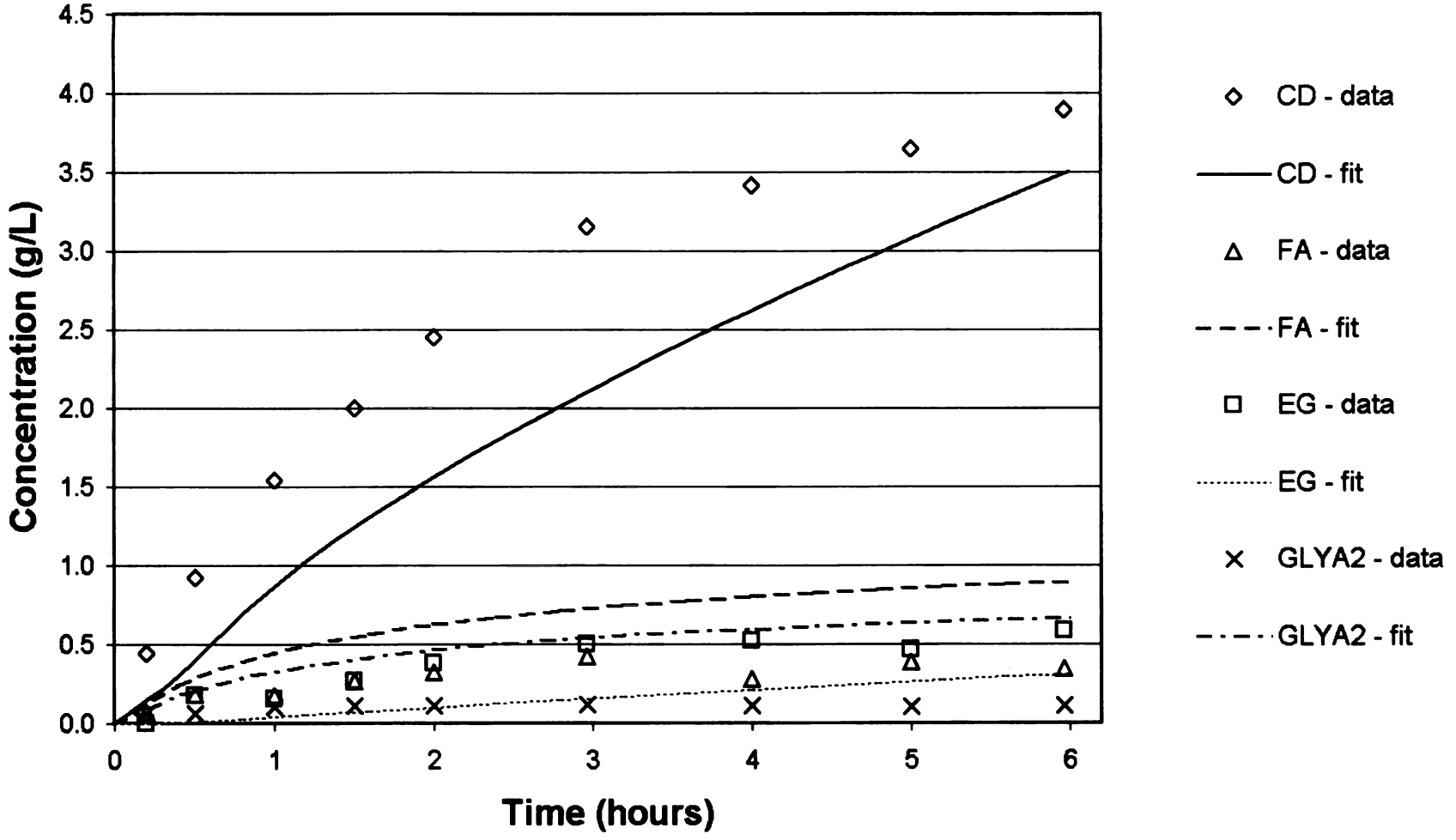

Figure C-9: Comparison of experimental data and kinetic model - Exp 140
3.17% fructose, 5.3% KOH, 40°C, 200 psig H_2, 0.10 grams 5 wt% Ru/C
Condensation products, formic acid, EG, and glycolic acid vs. Time

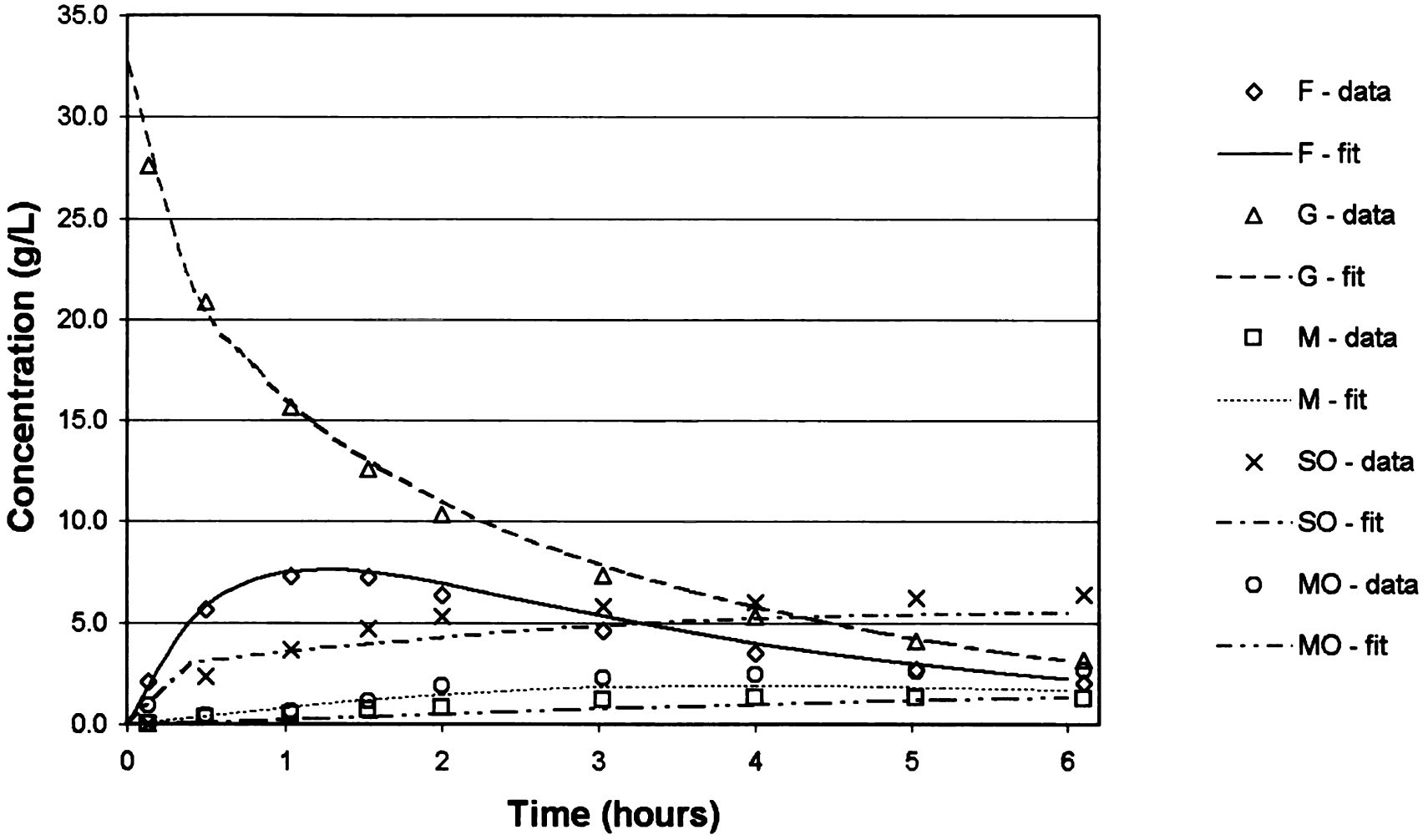

Figure C-10: Comparison of experimental data and kinetic model - Exp 141
3.17% glucose, 5.3% KOH, 40°C, 100 psig H_2, 0.10 grams 5 wt% Ru/C
Fructose, glucose, mannose, sorbitol, and mannitol vs. Time

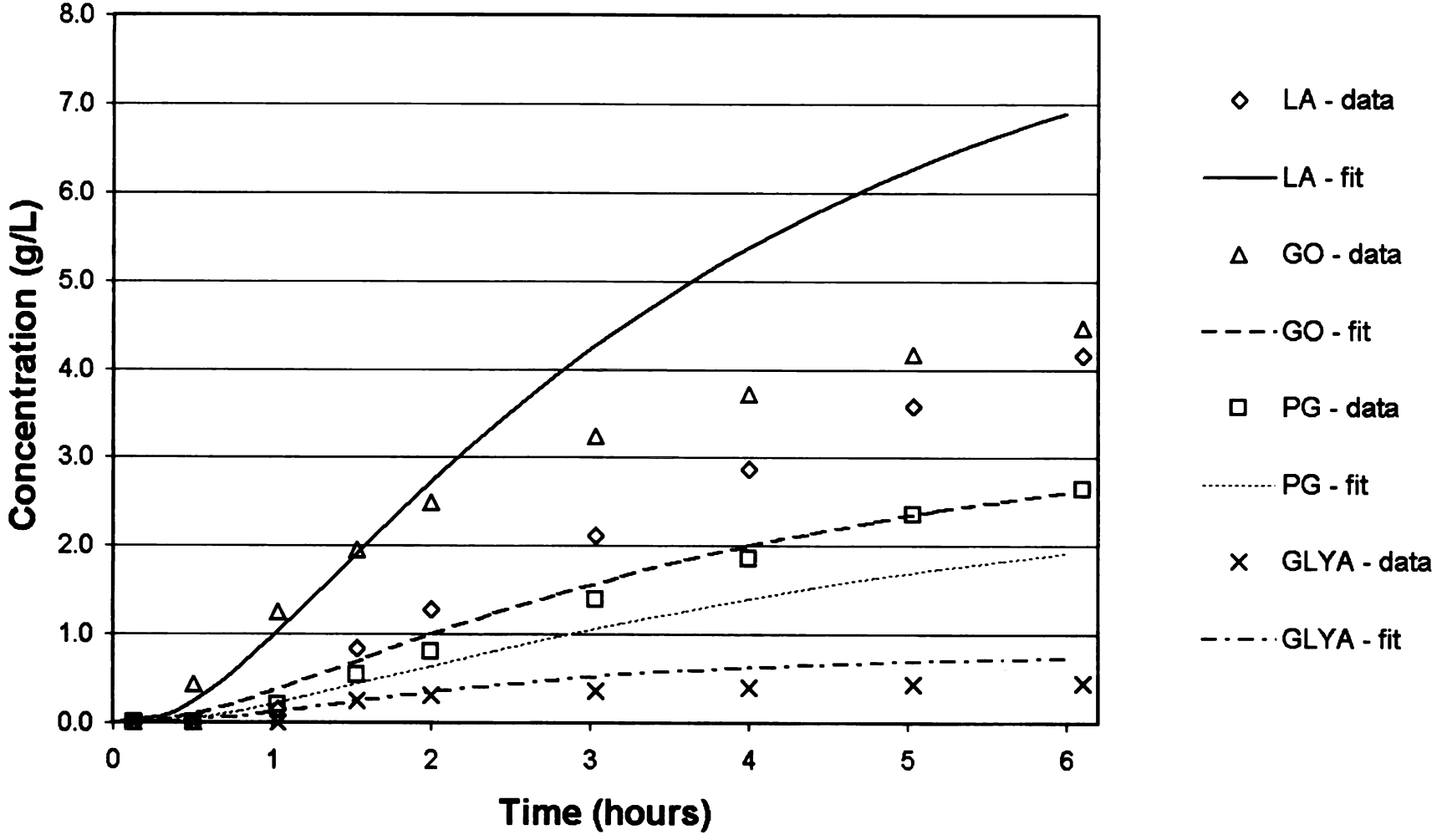

Figure C-11: Comparison of experimental data and kinetic model - Exp 141
3.17% glucose, 5.3% KOH, 40°C, 100 psig H_2, 0.10 grams 5 wt% Ru/C
Lactic acid, glycerol, propylene glycol, and glyceric acid vs. Time

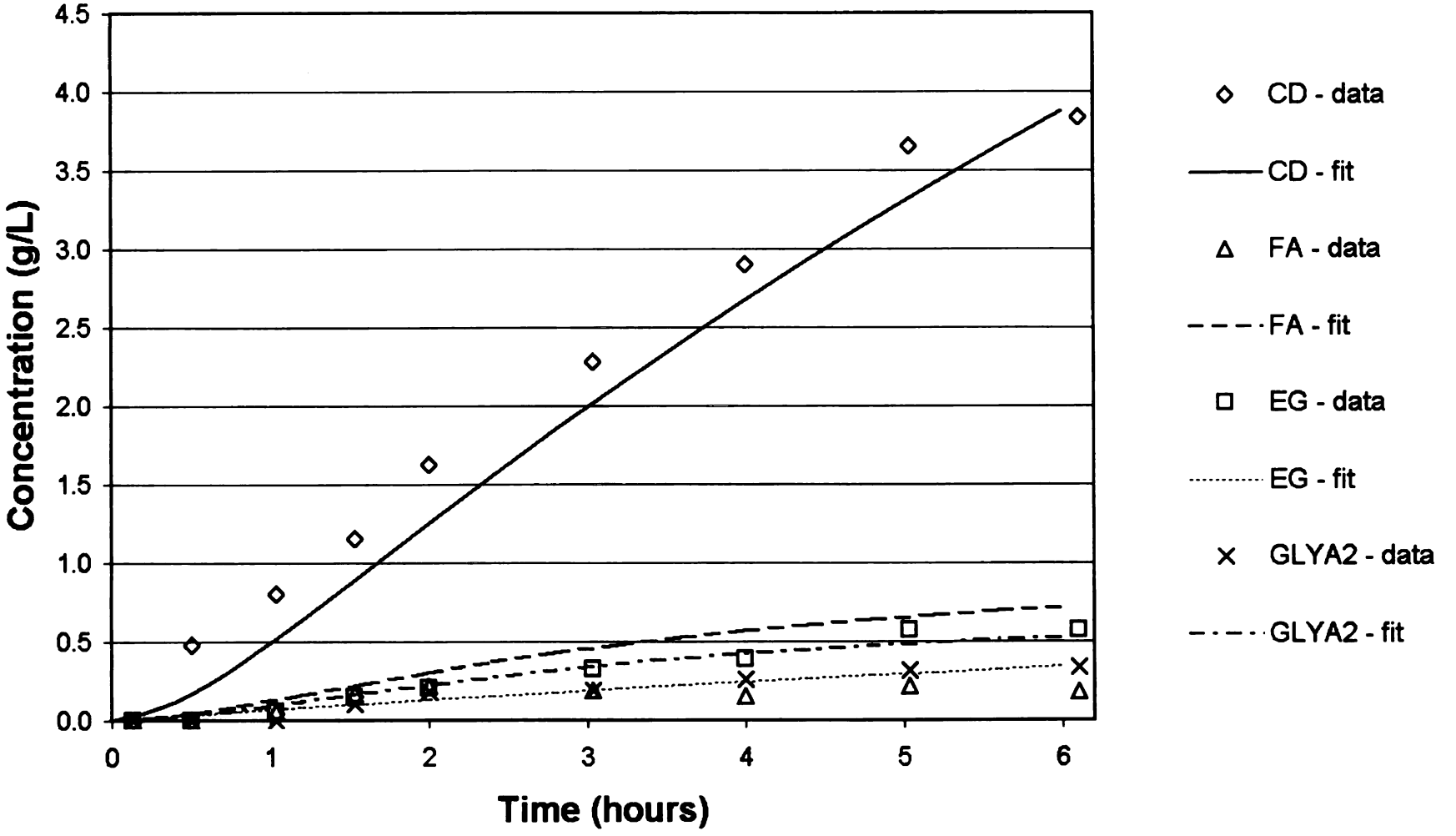

Figure C-12: Comparison of experimental data and kinetic model - Exp 141
3.17% glucose, 5.3% KOH, 40°C, 100 psig H_2, 0.10 grams 5 wt% Ru/C
Condensation products, formic acid, EG, and glycolic acid vs. Time

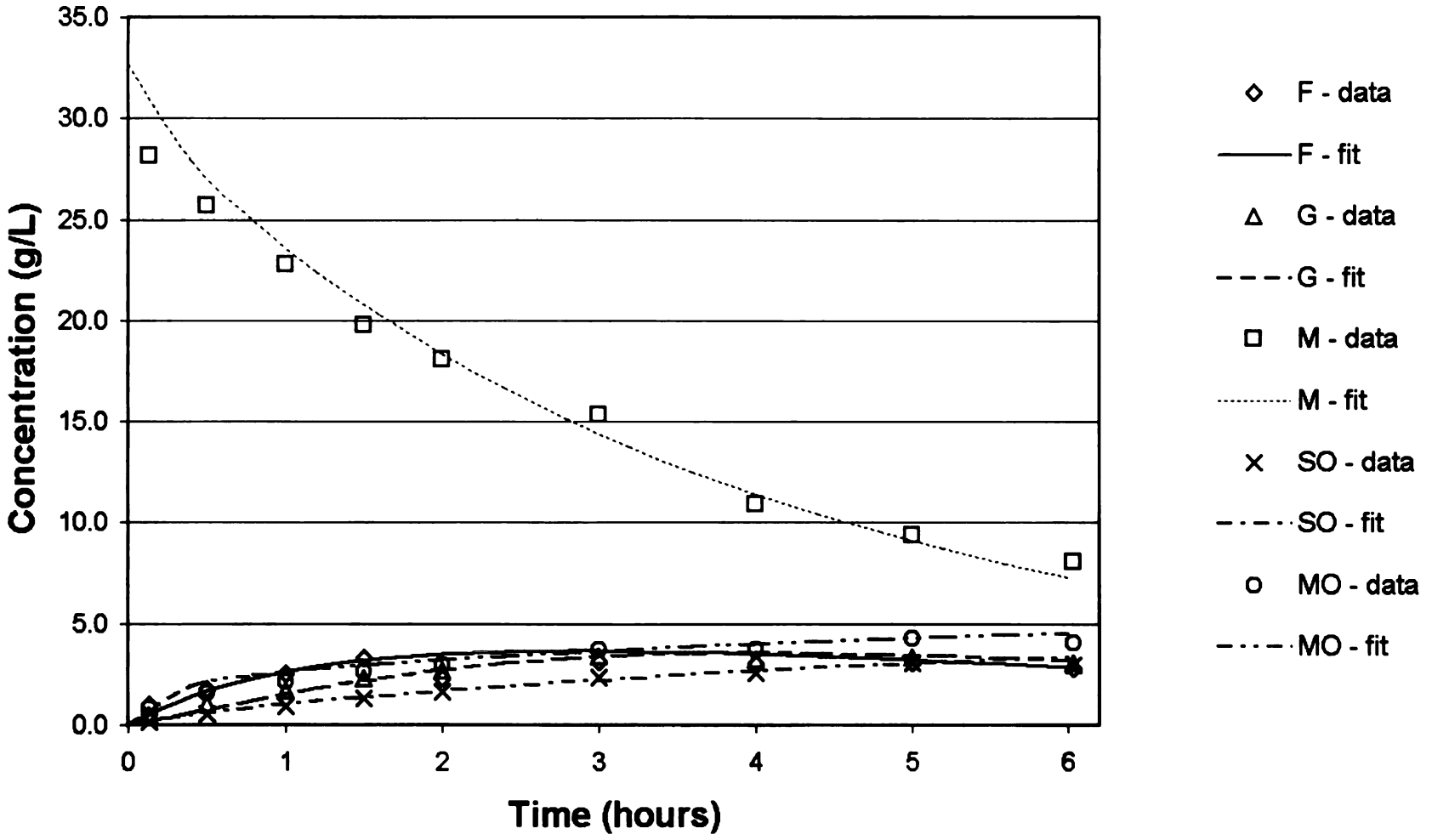

Figure C-13: Comparison of experimental data and kinetic model - Exp 142
3.17% mannose, 5.3% KOH, 40°C, 100 psig H_2, 0.10 grams 5 wt% Ru/C
Fructose, glucose, mannose, sorbitol, and mannitol vs. Time

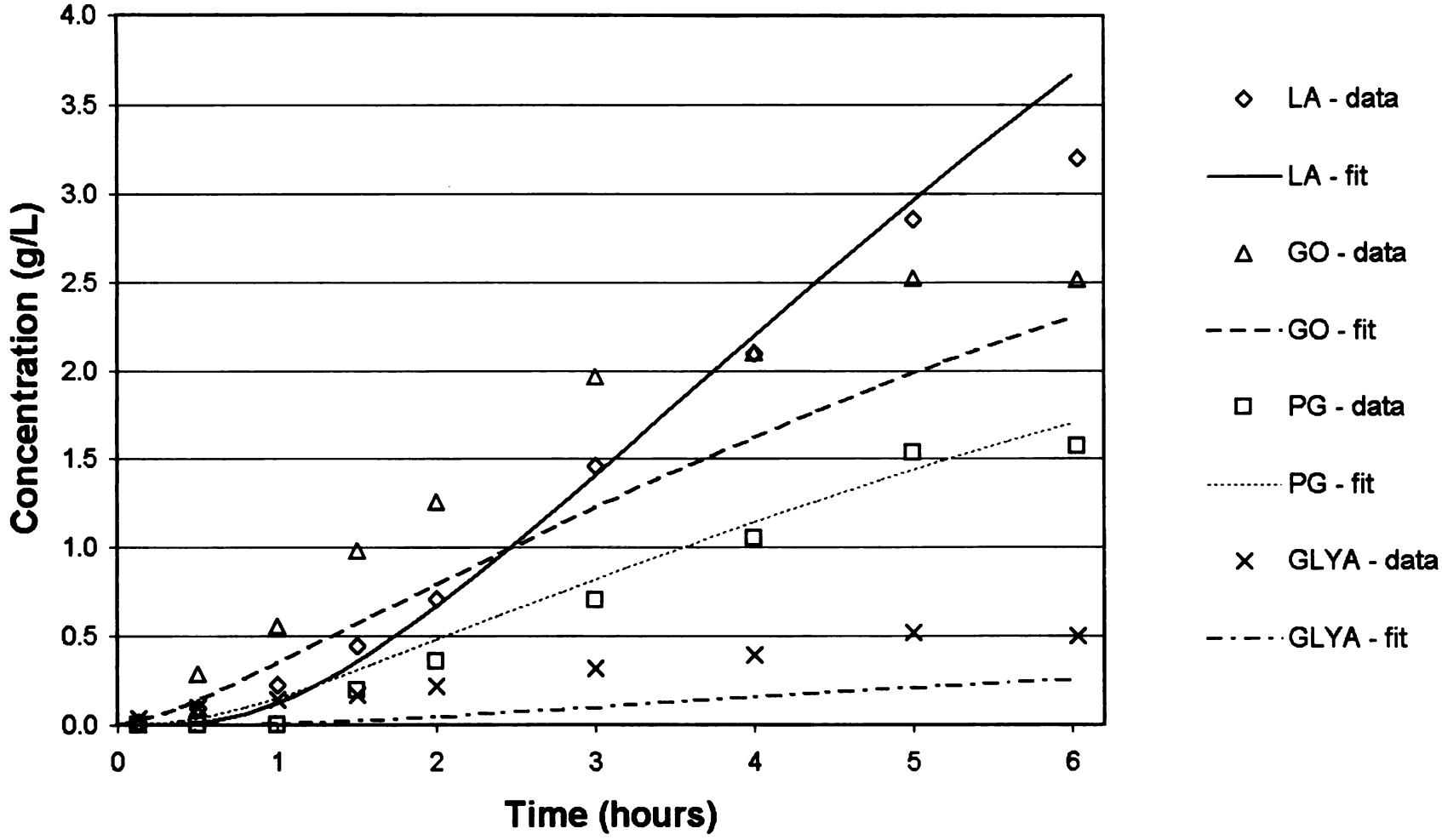

Figure C-14: Comparison of experimental data and kinetic model - Exp 142
3.17% mannose, 5.3% KOH, 40°C, 100 psig H_2, 0.10 grams 5 wt% Ru/C
Lactic acid, glycerol, propylene glycol, and glyceric acid vs. Time

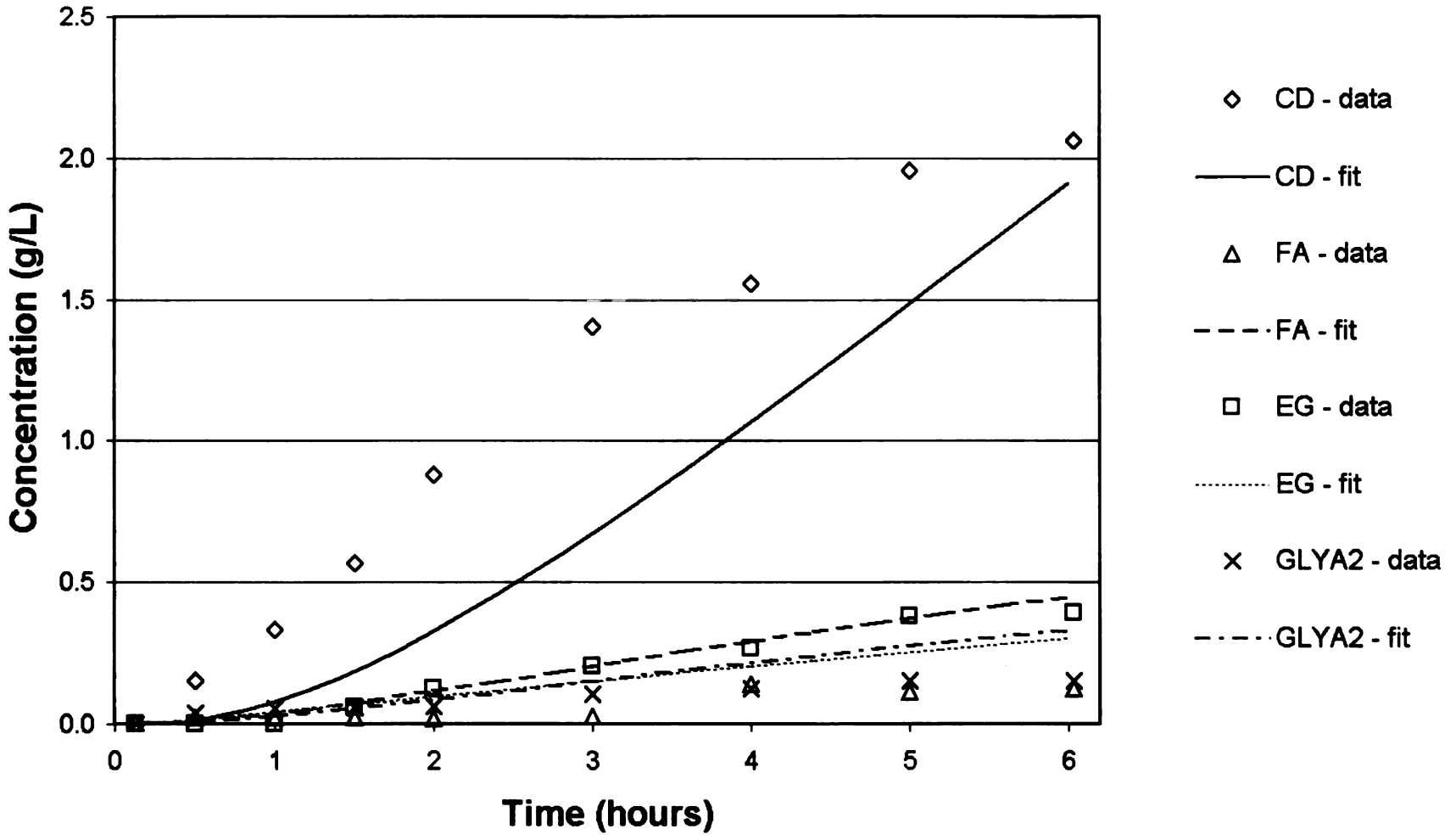

Figure C-15: Comparison of experimental data and kinetic model - Exp 142
3.17% mannose, 5.3% KOH, 40°C, 100 psig H_2, 0.10 grams 5 wt% Ru/C
Condensation products, formic acid, EG, and glycolic acid vs. Time

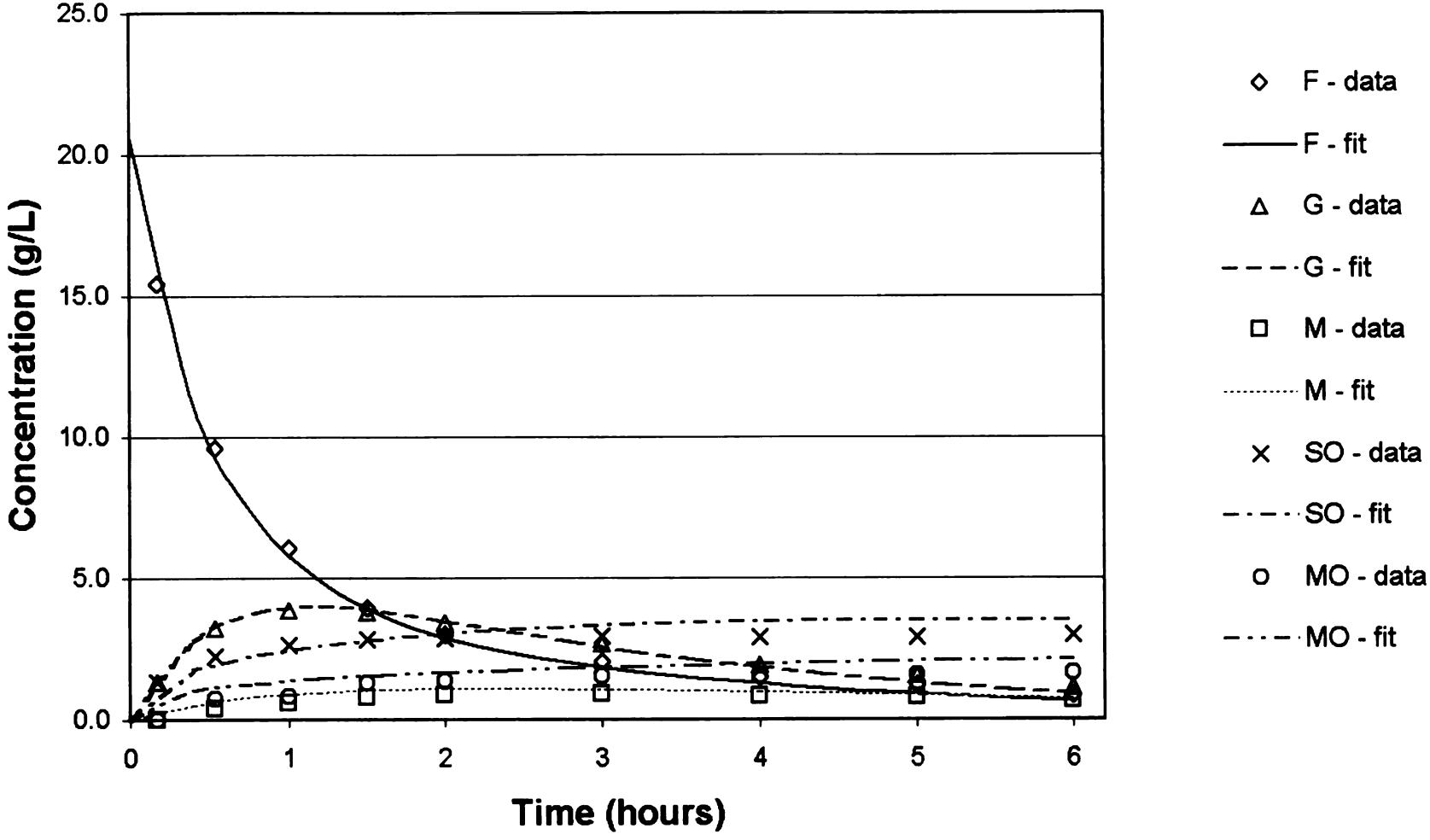

Figure C-16: Comparison of experimental data and kinetic model - Exp 144
2.0% fructose, 5.3% KOH, 40°C, 100 psig H_2, 0.10 grams 5 wt% Ru/C
Fructose, glucose, mannose, sorbitol, and mannitol vs. Time

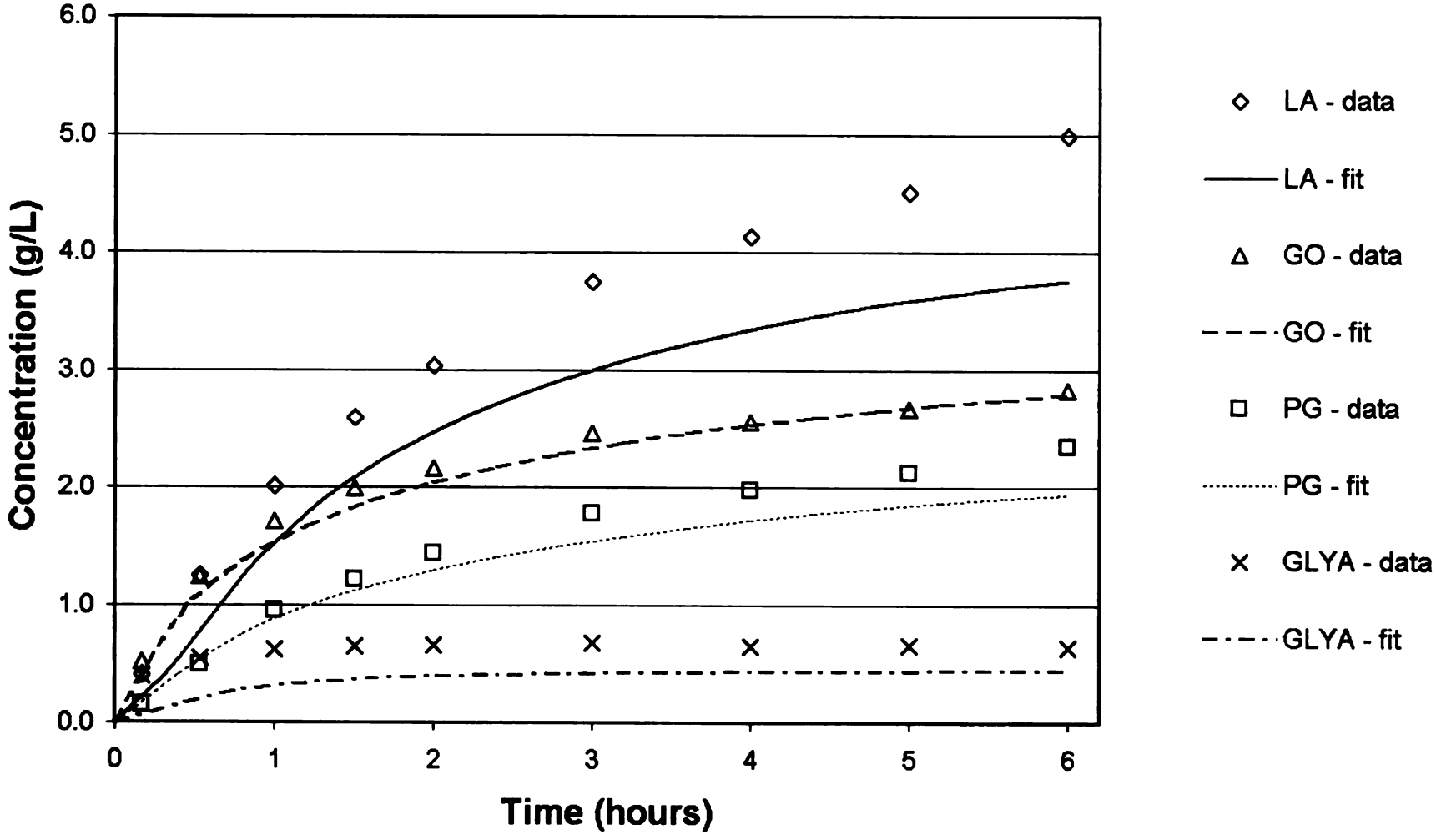

Figure C-17: Comparison of experimental data and kinetic model - Exp 144
2.0% fructose, 5.3% KOH, 40°C, 100 psig H_2, 0.10 grams 5 wt% Ru/C
Lactic acid, glycerol, propylene glycol, and glyceric acid vs. Time

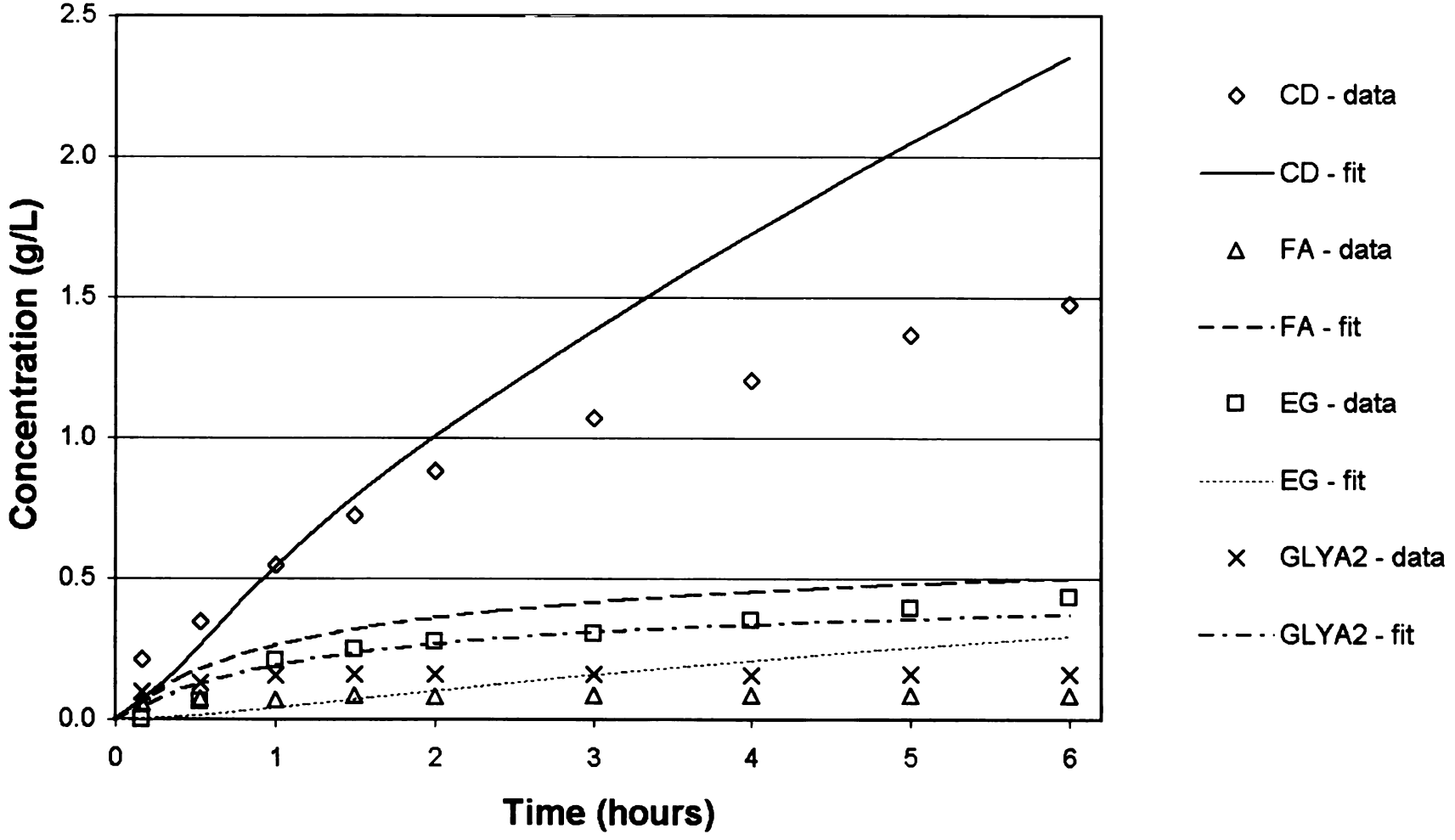

Figure C-18: Comparison of experimental data and kinetic model - Exp 144
2.0% fructose, 5.3% KOH, 40°C, 100 psig H_2, 0.10 grams 5 wt% Ru/C
Condensation products, formic acid, EG, and glycolic acid vs. Time

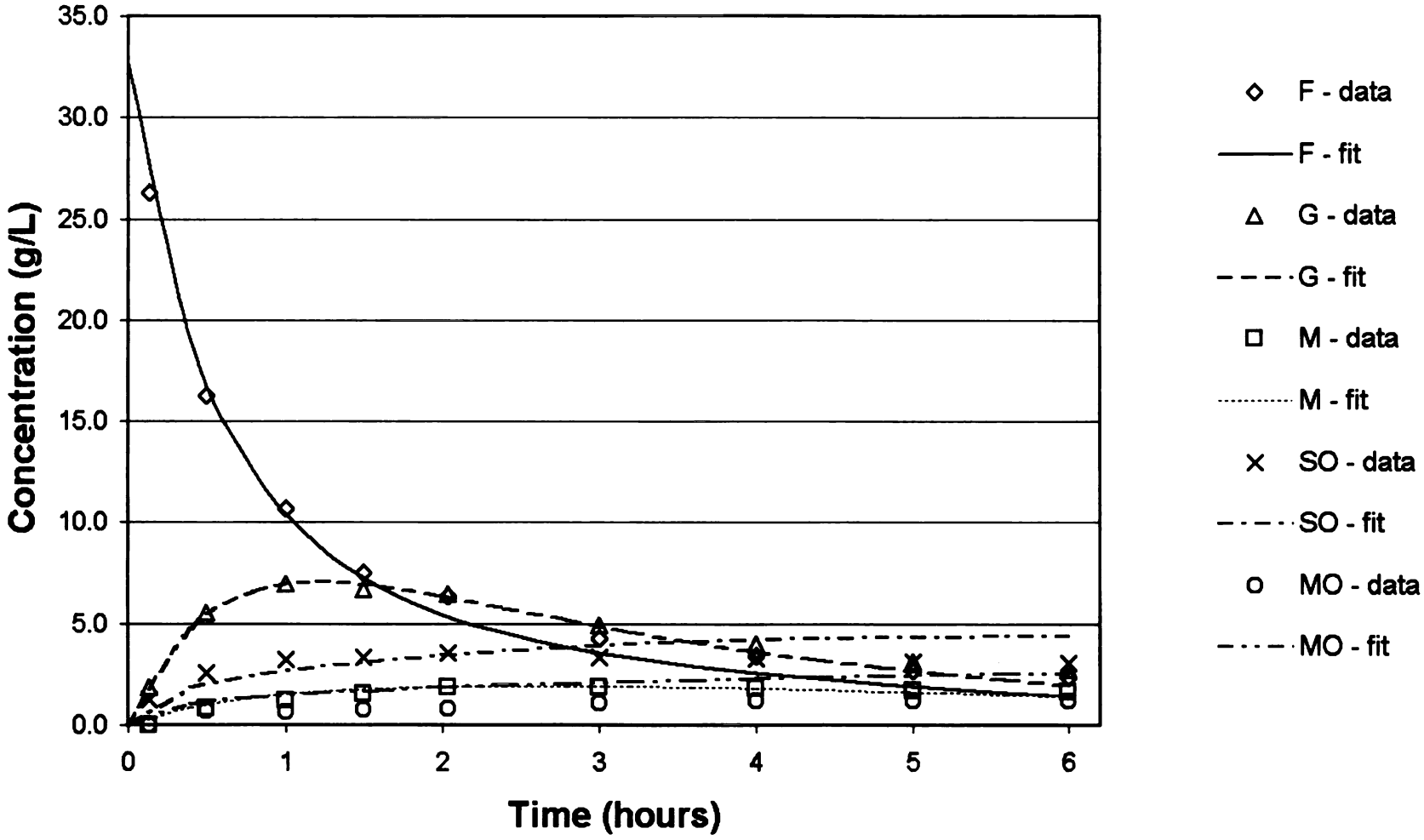

Figure C-19: Comparison of experimental data and kinetic model - Exp 147
3.17% fructose, 5.3% KOH, 40°C, 25 psig H_2, 0.10 grams 5 wt% Ru/C
Fructose, glucose, mannose, sorbitol, and mannitol vs. Time

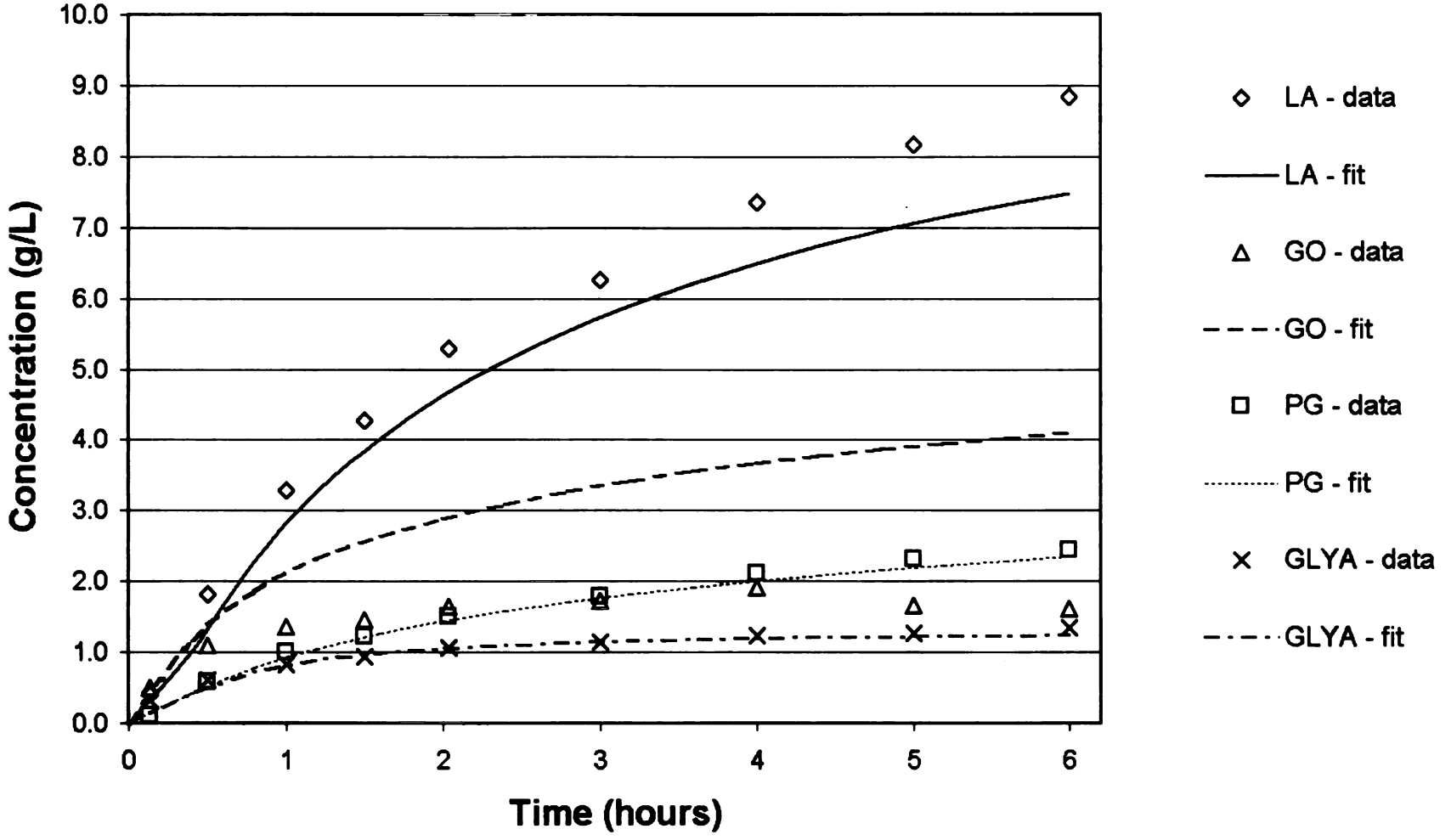

Figure C-20: Comparison of experimental data and kinetic model - Exp 147
3.17% fructose, 5.3% KOH, 40°C, 25 psig H_2, 0.10 grams 5 wt% Ru/C
Lactic acid, glycerol, propylene glycol, and glyceric acid vs. Time

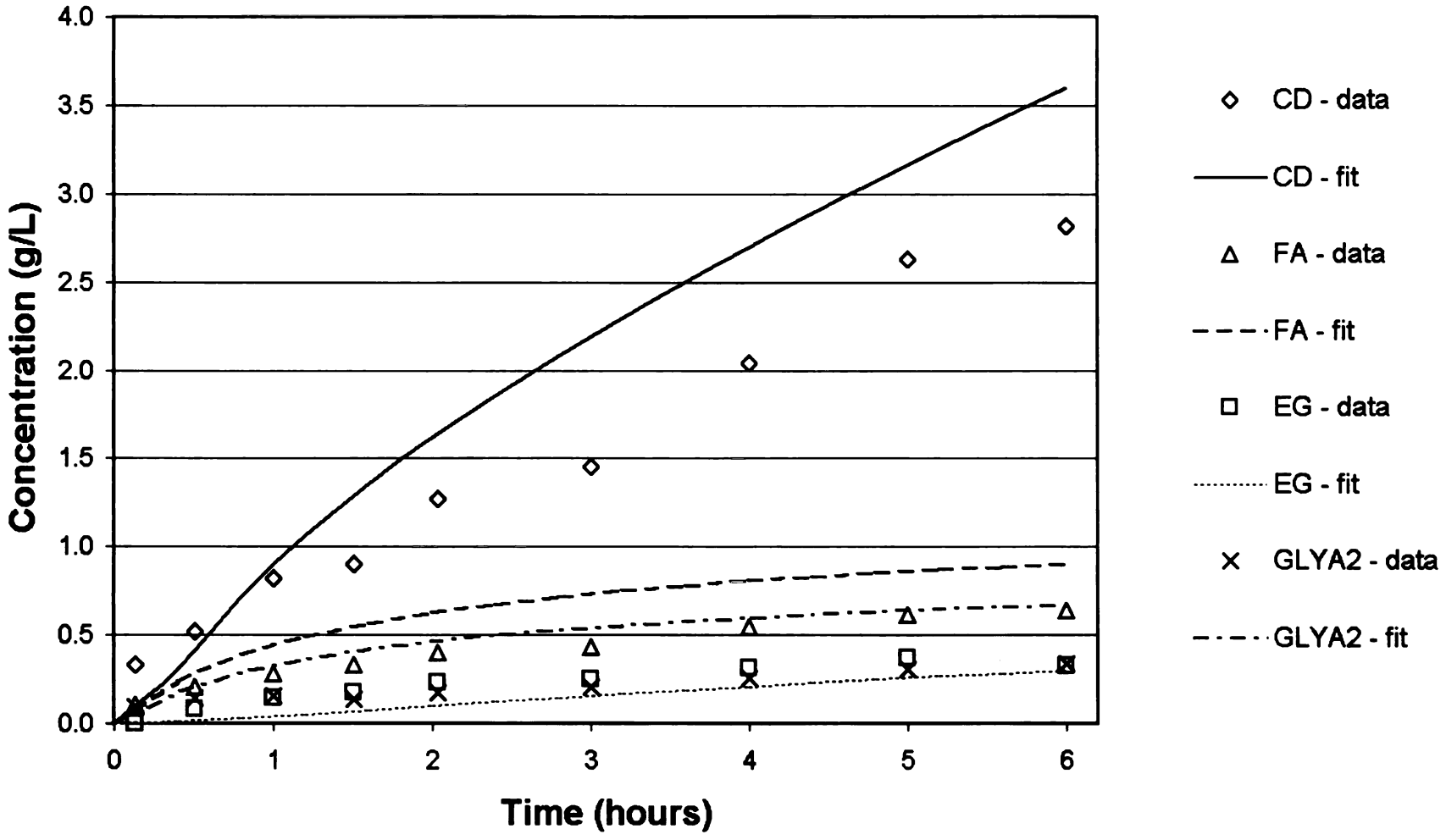

Figure C-21: Comparison of experimental data and kinetic model - Exp 147
3.17% fructose, 5.3% KOH, 40°C, 25 psig H_2, 0.10 grams 5 wt% Ru/C
Condensation products, formic acid, EG, and glycolic acid vs. Time

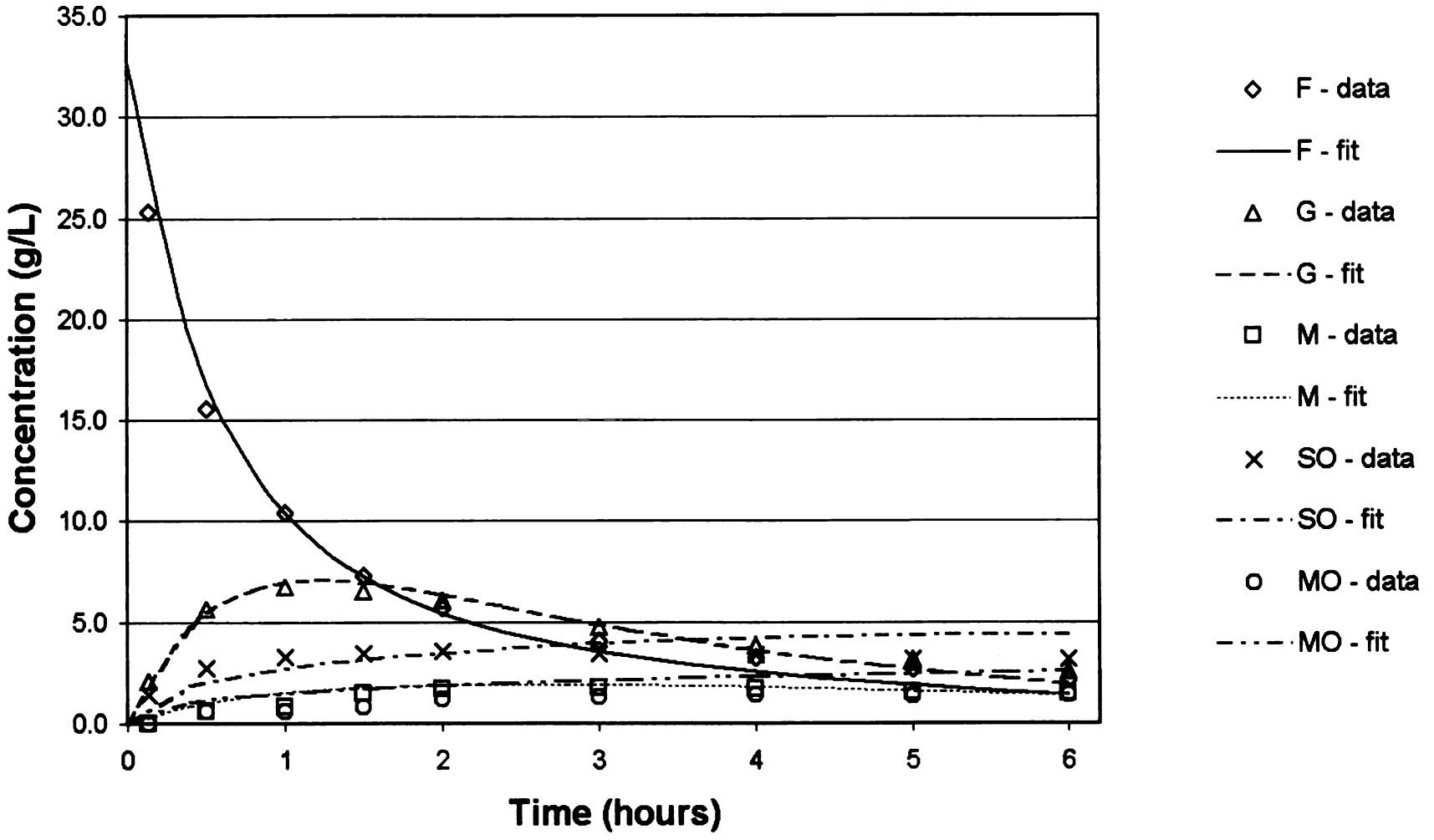

Figure C-22: Comparison of experimental data and kinetic model - Exp 149
3.17% fructose, 5.3% KOH, 40°C, 50 psig H_2, 0.10 grams 5 wt% Ru/C
Fructose, glucose, mannose, sorbitol, and mannitol vs. Time

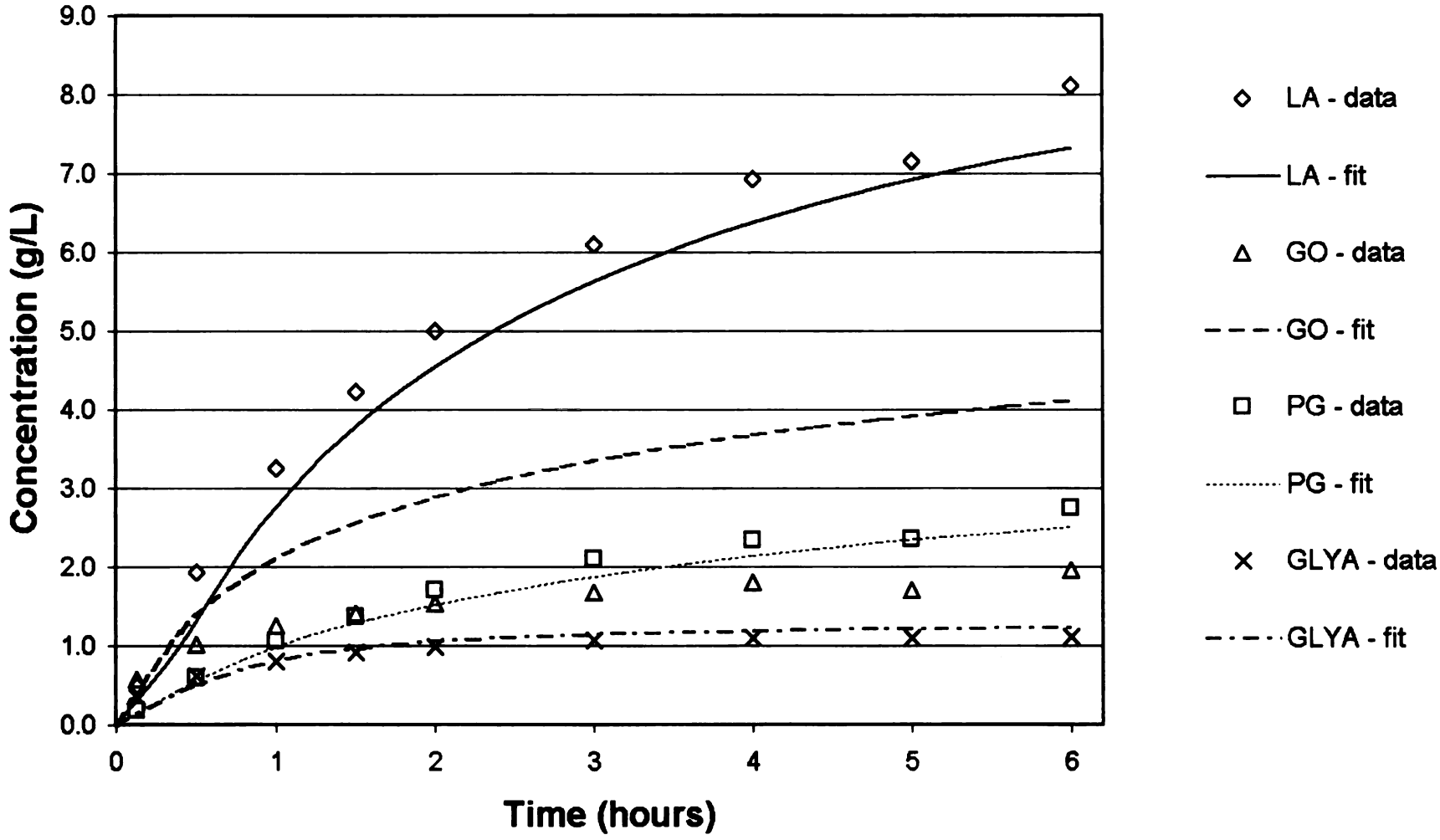

Figure C-23: Comparison of experimental data and kinetic model - Exp 149
3.17% fructose, 5.3% KOH, 40°C, 50 psig H_2, 0.10 grams 5 wt% Ru/C
Lactic acid, glycerol, propylene glycol, and glyceric acid vs. Time

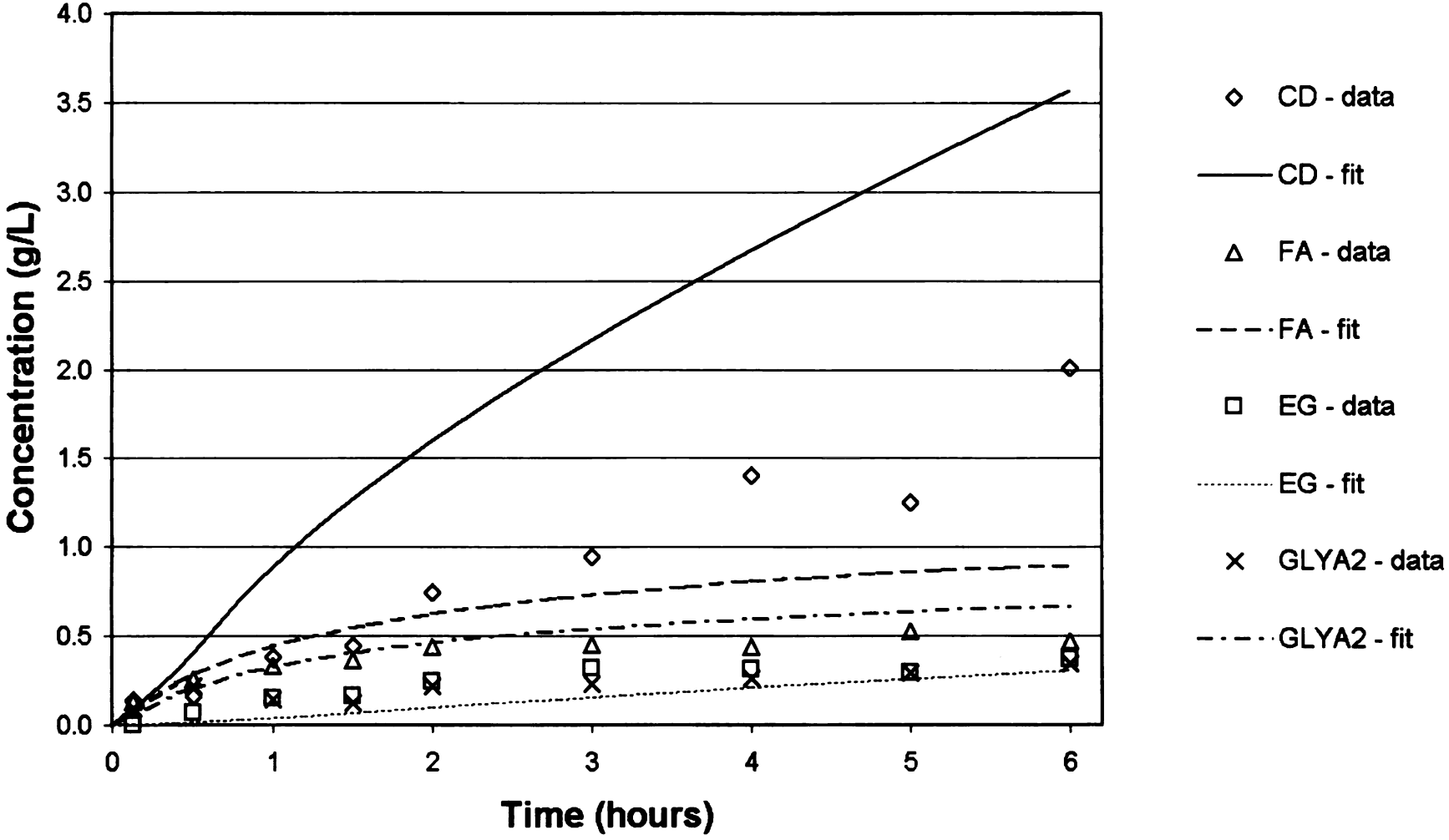

Figure C-24: Comparison of experimental data and kinetic model - Exp 149
3.17% fructose, 5.3% KOH, 40°C, 50 psig H_2, 0.10 grams 5 wt% Ru/C
Condensation products, formic acid, EG, and glycolic acid vs. Time

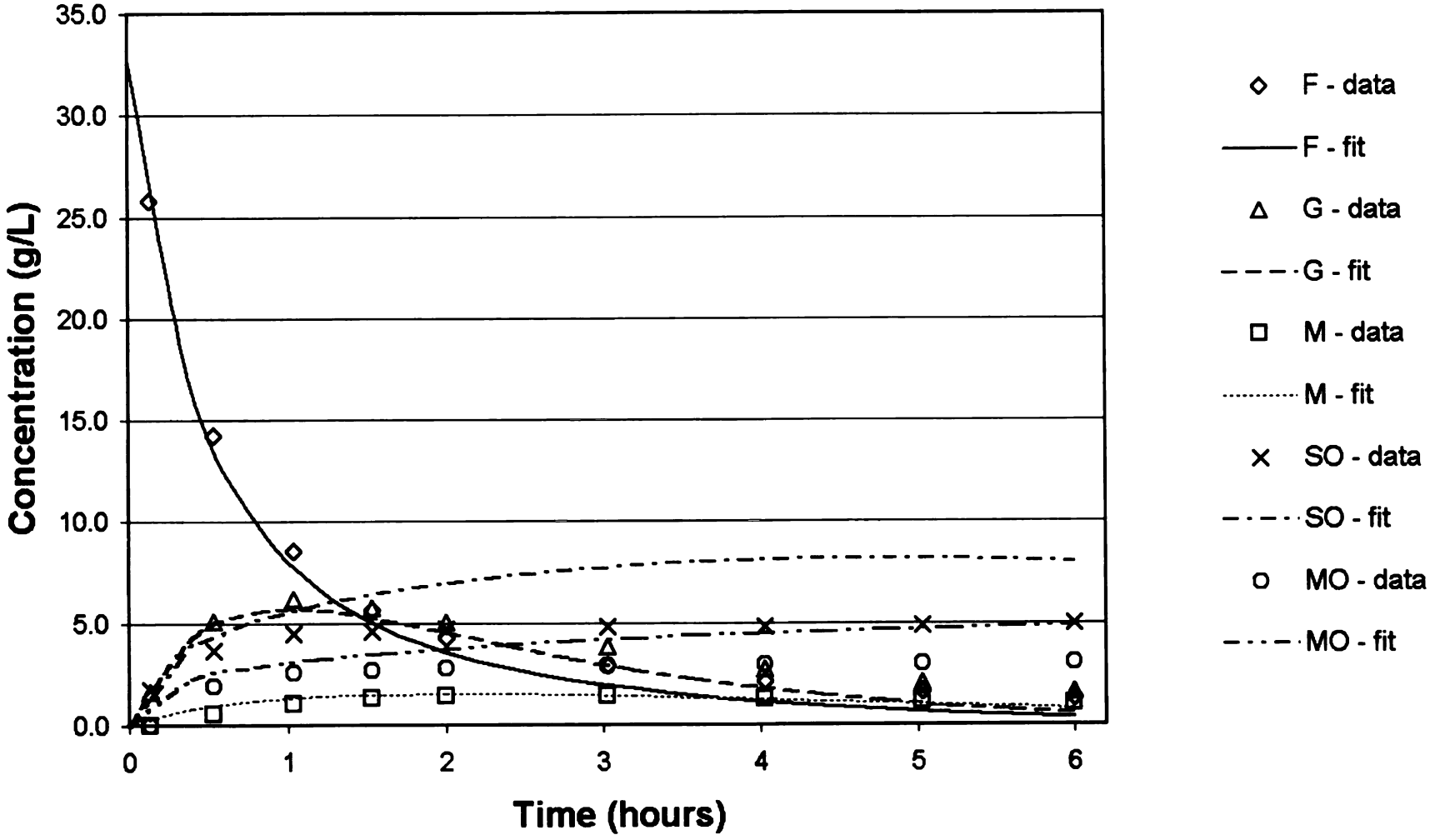

Figure C-25: Comparison of experimental data and kinetic model - Exp 152
3.17% fructose, 5.3% KOH, 40°C, 100 psig H_2, 0.20 grams 5 wt% Ru/C
Fructose, glucose, mannose, sorbitol, and mannitol vs. Time

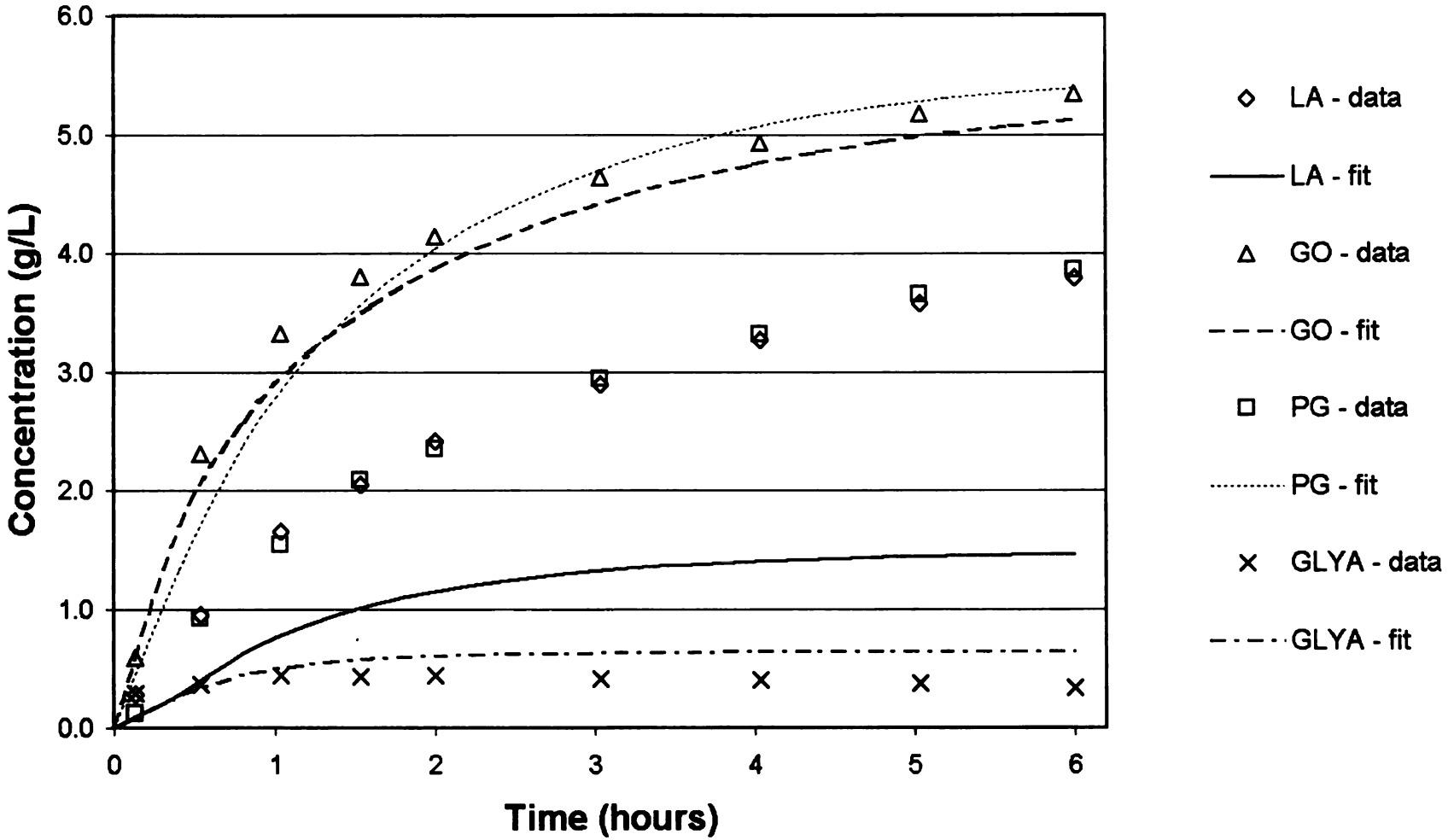

Figure C-26: Comparison of experimental data and kinetic model - Exp 152
3.17% fructose, 5.3% KOH, 40°C, 100 psig H_2, 0.20 grams 5 wt% Ru/C
Lactic acid, glycerol, propylene glycol, and glyceric acid vs. Time

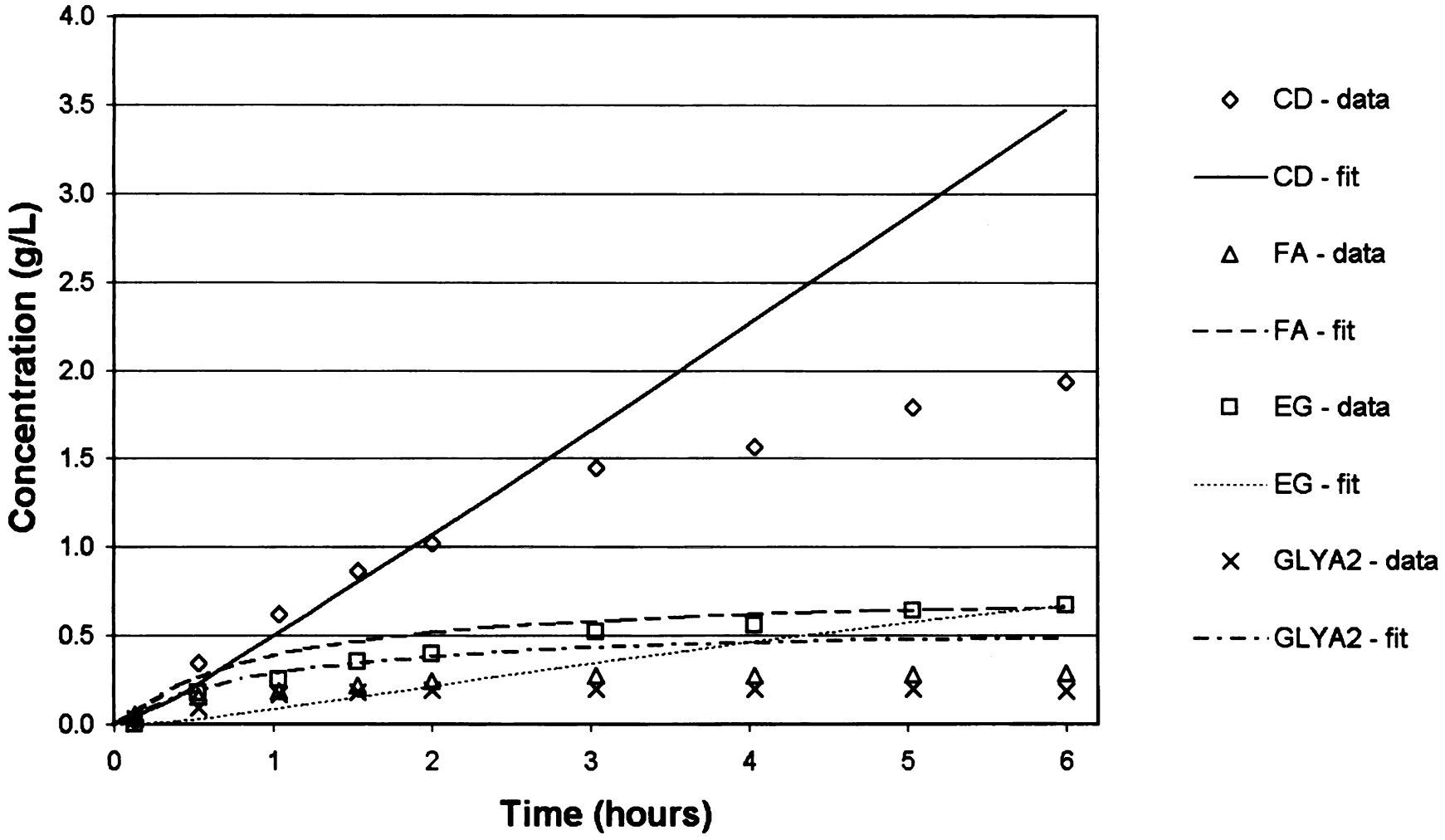

Figure C-27: Comparison of experimental data and kinetic model - Exp 152
3.17% fructose, 5.3% KOH, 40°C, 100 psig H_2, 0.20 grams 5 wt% Ru/C
Condensation products, formic acid, EG, and glycolic acid vs. Time

APPENDIX D

Master list of experiments

Date	Exp	Reactants	Catalyst	Description
10/19/00	20	0.025 g sorb, no KOH, 100g solution.	1.0g carbon support.	Adsorption with temperature ramping. T=25, 100, 150, 200°C. 2 hrs at each temperature
10/31/00	22	0.025 g sorb, no KOH, 100g solution.	1.0g carbon support.	Adsorption with temperature ramping. T=25, 100, 150, 200°C. 2 hrs at each temperature
11/15/00	24	0.025 g sorb, no KOH, 100g solution.	1.0g carbon support.	Adsorption with temperature ramping. T=25, 100, 150, 200°C. 2 hrs at each temperature
11/28/00	25	2.00 g sorb, no KOH, 100g solution.	1.0g carbon support.	Adsorption with temperature ramping. T=25, 100, 150, 200°C. 90 min at each temperature
11/30/00	26	5.00 g sorb, no KOH, 100g solution.	1.0g carbon support.	Adsorption with temperature ramping. T=25, 100, 150, 200°C. 90 min at each temperature
12/05/00	28	10.0 g sorb, no KOH, 100g solution	1.0g carbon support.	Adsorption with temperature ramping. T=25, 100, 150, 200°C. 90 min at each temperature
12/12/00	29	2.50 g sorb, no KOH, 25g solution	1.0g carbon support.	Adsorption with temperature ramping. T=25, 100, 150, 200°C. 90 min at each temperature
12/15/00	30	2.00 g sorb, no KOH, 100g solution.	1.0g carbon support.	Adsorption with temperature ramping. T=25, 50, 75, 100°C. 90 minutes at each temperature
12/19/00	31	2.00 g sorb, no KOH, 40g solution.	1.0g carbon support.	Adsorption with temperature ramping. T=25, 50, 75, 100°C. 90 minutes at each temperature
12/20/01	32	3.00 g sorb, no KOH, 30g solution	1.0g carbon support.	Adsorption with temperature ramping. T=25, 50, 75, 100°C. 90 minutes at each temperature
01/05/01	33	2.00 g sorb, no KOH, 100g solution.	1.0g carbon support.	Adsorption with temperature ramping. T=25, 50, 75, 100°C. 90 minutes at each temperature
04/05/01	35	0.025 g sorb, no KOH, 100g solution.	10.0g Ru sponge	Adsorption with temperature ramping. T=25, 100, 200°C. 60 minutes at each temperature

04/12/01	36	0.052 g sorb, no KOH, 100g solution	10.0g Ru sponge	Adsorption with temperature ramping. T=25, 100,150°C. 60 minutes at each temperature
05/03/01	38	0.050 g sorb, no KOH, 100g solution	No catalyst	Observe stability of sorbitol in higher temps. T=25, 50, 100, 150, 200, 250°C
05/08/01	39	0.050 g sorb, 0.010g KOH, 100g sol'n	10.0g Ru sponge	Adsorption experiment with base and temperature ramping. T = 50, 100, 150, 200, 250°C. 60 minutes at each temperature
05/15/01	40	0.050 g sorb, 0.012g KOH, 100g sol'n	10.0g Ru sponge	Ad. study with temp ramping T = 50, 100, 150, 200, 250°C. 60 min at each temp. Sponge reduced at 400°C to remove possible H_2
06/08/01	43	0.608 g sorb, no KOH, 100g sol'n	10.0g Ru sponge	Adsorption Study. T = 150°C, t = 160 minutes.
06/22/01	44	0.200 g sorb, no KOH, 100g sol'n	10.0g Ru sponge	Adsorption Study. T = 150°C, t = 120 minutes.
07/02/01	45	0.101 g sorb, no KOH, 100g sol'n	10.0g Ru sponge	Adsorption Study. T = 150°C, t = 150 minutes.
08/01/01	54	0.601 g sorb, no KOH, 100g sol'n	10.0g Ru sponge	Adsorption study with temperature ramping. T = 150, 200°C, 120 min at 150°C. 145 minutes at 200°C
08/13/01	55	0.600 g sorb, no KOH, 100g sol'n	10.0g Ru sponge	Adsorption study with temperature ramping. T = 150, 200°C, 120 min at 150°C. 140 minutes at 200°C
08/20/01	56	0.600 g sorb, 1.0g KOH, 100g sol'n	10.0g Ru sponge	Adsorption study with temperature ramping and base. T = 150, 200°C, 120 min at 150°C. 240 minutes at 200°C
08/29/01	58	0.601 g sorb, 1.0g KOH, 100g sol'n	10.0g Ru sponge	Alkaline degradation of sorbitol. T=150°C. Samp @ 15, 30, 45, 60, 75, 90, 105, 120, 150 min

09/06/01	59	0.600 g sorb, 1.0g KOH, 100g sol'n	10.0g Ru sponge	Alkaline degradation of sorbitol. T=150°C. Samp @ 15, 30, 45, 60, 75, 90, 105, 120, 150 min
10/02/01	60	5.0g sorb, 1.0g KOH, 100g sol'n	10.0g Ru sponge	Alkaline degradation of sorbitol. T=150°C. Samp @ 60, 133 min
10/09/01	61	0.600g sorb, 1.0g KOH, 100g sol'n	10.0g Ru sponge	Alkaline degradation of sorbitol. T=150°C. Samp @ 60, 120 min. Sponge reduced at 400°C.
10/15/01	62	3.2g sorb, 1.0g KOH, 100g sol'n	10.0g Ru sponge	Alkaline degradation of sorbitol. T=150°C. Samp @ 136, 240, 480 min
10/17/01	63	15.0g sorb, 1.0g KOH, 100g sol'n	10.0g Ru sponge	Alkaline degradation of sorbitol. T=150°C. Samp @ 155, 240, 360, 507 min.
11/06/01	64	0.6g sorb, 1.0g KOH, 100g sol'n	10.0g Ru sponge	Alkaline degradation of sorbitol. T=150°C. Samp @ 60, 120, 180 min.
11/08/01	65	0.6g sorb, 1.0g KOH, 100g sol'n	No catalyst	Alkaline degradation of sorbitol. T=150°C. Samp @ 60, 120 min.
11/13/01	66	0.6g glycerol, 1.0g KOH, 100g sol'n	10.0g Ru sponge	Alkaline degradation of glycerol. T=150°C. Samp @ 30, 60, 120, 180 min.
11/15/01	67	3.2g sorb, 5.33g KOH, 100g sol'n	10.0g Ru sponge	Alkaline degradation of sorbitol. T=150°C. Samp @ 1, 2, 3, 4, 6, 7 hrs
11/29/01	68	15.0g sorb, 9.25g KOH, 100g sol'n	10.0g Ru sponge	Alkaline degradation of sorbitol. T=150°C. Samp @ 120, 240, 360, 500 min
12/19/01	69	3.2g sorb, 5.32g KOH, 100g sol'n	1.0g - 2.5 wt% Ru/C	Alkaline degradation of sorbitol. T=150°C. Samp @ 30, 60, 90, 120, 194, 244, rxr remains
12/20/01	70	3.2g sorb, 5.33g KOH, 100g sol'n	1.0g - 2.5 wt% Ru/C	One pot synthesis. Alk. deg. of sorbitol 150°C: 6 hrs. Add 1200 psig H_2, 200°C: 4 hrs. Neutralize with H_2SO_4, 150°C

01/21/02	71	3.2g sorb, 5.33g KOH, 100g sol'n	10.0g Ru sponge	Sorbitol hydrogenolysis. 1200 psig H_2, T=150°C. Samp @ 1, 2, 3, 4, 6 hrs.
01/30/02	72	0.6g glycerol, 1.0g KOH, 100g sol'n	10.0g Ru sponge	Alkaline degradation of glycerol. T=150°C. Samp @ 3, 6, 8 hrs.
02/08/02	73	3.2g xylitol, 5.32g KOH, 100g sol'n	10.0g Ru sponge	Alkaline degradation of xylitol. T=150°C. Samp @ 1, 3, 6 hrs.
03/06/02	74	3.2g sorb, 5.32g KOH, 100g sol'n	10.0g Ru sponge	Low pressure hydrogenolysis of sorbitol. T=150°C. Samp @ 7 hrs.
03/08/02	75	3.2g sorb, 3.53g $Ca(OH)_2$, 100g sol'n	10.0g Ru sponge	Alkaline degradation of sorbitol with addition of $Ca(OH)_2$ as base promoter.
03/21/02	76	3.2g sorb, 5.35g KOH, 100g sol'n	10.0g Ru sponge	Alkaline degradation of sorbitol. T=170°C. Samp @ 1, 2, 3, 4, 5 hrs.
03/28/02	77	3.2g sorb, 5.33g KOH, 100g sol'n	10.0g Ru sponge	Alkaline degradation of sorbitol. T=190°C. Samp @ 1, 2, 3, 5 hrs. Also, acid addition and subsequent hydrogenation.
04/15/02	78	1.71g glycerol, 5.32g KOH, 100g sol'n	10.0g Ru sponge	Alkaline degradation of glycerol. T=150°C. Samp @ 3, 6, 9 hrs.
04/16/02	79	2.67g xylitol, 5.34g KOH, 100g sol'n	10.0g Ru sponge	Alkaline degradation of xylitol. T=150°C. Samp @ 2, 4, 6 hrs.
04/17/02	80	3.2g sorb, 5.34g KOH, 100g sol'n	10.0g Ru sponge	Alkaline degradation of sorbitol. T=150°C. Samp @ 3, 6, 8 hrs.
04/25/02	81	3.17g glucose, 5.34g KOH, 100g sol'n	No catalyst	Alkaline degradation of glucose. T=150°C. Samp @ 2, 4, 6 hrs.
04/26/02	82	0.16g glucose, 5.32g KOH, 100g sol'n	No catalyst	Alkaline degradation of glucose. T=150°C. Samp @ 30, 60, 160 min.
05/06/02	83	3.2g sorbitol, 5.33g KOH, 100g sol'n	1.0g - 5 wt% Pd/C	Alkaline degradation of sorbitol. T=150°C. Samp @ 2, 4, 6, 8 hrs.
05/14/02	84	2.63g xylose, 5.32g KOH, 100g sol'n	No catalyst	Alkaline degradation of xylose. T=150°C. Samp @ 30, 60, 90, 120 min.

05/16/02	85	0.13g xylose, 5.32g KOH, 100g sol'n	No catalyst	Alkaline degradation of xylose. T=150°C. Samp @ 30, 60 min
06/14/02	86	3.2g sorb, 5.33g KOH, 3.9g $CaCl_2$,100g sol'n	10.0g Ru sponge	Alkaline degradation of sorbitol using $CaCl_2$ and KOH. T=150°C
07/01/02	87	3.17g fructose, 5.35g KOH, 100g sol'n	No catalyst	Alkaline degradation of fructose. T=150°C. Samp @ 90 min
07/02/02	88	3.17g glucose, 5.34g KOH, 100g sol'n	No catalyst	Alkaline degradation of glucose. T=150°C. Samp @ 90 min.
07/16/02	89	3.17g glucose, 5.34g KOH, 100g sol'n	No catalyst	Alkaline degradation of glucose. T=70°C. Samp @ 30, 60, 120 min.
07/18/02	90	3.17g glucose, 5.34g KOH, 100g sol'n	No catalyst	Alkaline degradation of glucose. T=40°C. Samp @ 30, 60, 90, 120, 240, 360 min.
07/23/02	91	3.17g glucose, 5.34g KOH, 100g sol'n	1.0g - 5 wt% Pt/C	Hydrogenation of glucose. T=40°C, 1200 psig H2. Samp @ 30, 60, 90, 120, 180, 240, 360 min.
08/01/02	92	3.17g glucose, 5.33g KOH, 100g sol'n	1.0g - 5 wt% Pt/C	T=40°C, 100 psig H2. Hydrogenation and alkaline degradation.
08/08/02	93	3.17g glucose, 5.33g KOH, 100g sol'n	1.0g - 5 wt% Pt/C	T=40°C, 15 psig H2. Hydrogenation and alkaline degradation.
09/10/02	94	3.16g gluc, 4.73g KOH, 0.31g Ca(OH)2, 100g sol'n	1.0g - 5 wt% Pt/C	T=40°C, 100 psig H2. Hydrogenation and alkaline degradation.
09/24/02	95	3.16g gluc, 4.73g KOH, 0.31g Ca(OH)2, 100g sol'n	1.0g 2.5 wt% Ru/C	T=40°C, 100 psig H2. Hydrogenation and alkaline degradation.
09/26/02	96	3.16g gluc, 4.73g KOH, 0.31g Ca(OH)2, 100g sol'n	1.0g 5 wt% Pd/C	T=40°C, 100 psig H2. Hydrogenation and alkaline degradation.
10/01/02	97	3.16g gluc, 4.73g KOH, 0.31g Ca(OH)2, 100g sol'n	1.0g 2.5 wt% Ru/C	T=40°C, 100 psig H2. Hydrogenation and alkaline degradation.
10/15/02	98	3.17g glucose, 2.67g KOH, 100g sol'n	1.0g - 5 wt% Pt/C	T=40°C, 100 psig H2. Hydrogenation and alkaline degradation.

10/17/02	99	2.64g xylose, 5.34g KOH, 100g sol'n	1.0g - 5 wt% Pt/C	T=40°C, 100 psig H2. Hydrogenation and alkaline degradation.
10/24/02	100	49.8 mg sorbitol, 100g sol'n	10.0g Ru sponge	T=150°C, 100 psig He, 1500 rpm agit.
10/31/02	101	50.0 mg sorbitol, 100g sol'n	10.0g Ru sponge	T=40°C, 100 psig He, 1500 rpm agitation
11/04/02	102	49.7 mg sorbitol, 100g sol'n	10.0g Ru sponge	T=120°C, 100 psig He, 1500 rpm agit
11/13/02	103	50.2 mg sorbitol, 100g sol'n	10.0g Ru sponge	T=110°C, 100 psig He, 1500 rpm agit
12/19/02	104	3.16g fructose, 5.34g KOH, 100g sol'n	1.0g 5 wt% Ru/C (PMC)	T=40°C, 100 psig H2. Hydrogenation and alkaline degradation.
01/17/03	105	3.17g fructose, 100g sol'n	1.0g 5 wt% Ru/C (PMC)	T=40°C, 100 psig H2. Hydrogenation
01/24/03	106	3.16g fructose, 5.3g KOH, 100g sol'n	0.22g 5 wt% Ru/C (PMC)	T=40°C, 100 psig H2. Hydrogenation and alk. deg.
02/27/03	107	3.16g fructose, 5.3g KOH, 100g sol'n	0.1g 5 wt% Pt/C (Aldrich)	T=40°C, 100 psig H2. Hydrogenation and alk. deg.
03/03/03	108	3.16g fructose, 5.3g KOH, 100g sol'n	0.1g 5 wt% Pd/C (Aldrich)	T=40°C, 100 psig H2. Hydrogenation and alk. deg.
03/04/03	109	50.0 mg sorbitol, 100g sol'n	10.0g Ru sponge	T=100°C, 100 psig He, 1500 rpm agit
03/21/03	110	50.0 mg sorbitol, 100g sol'n	10.0g Ru sponge	T=80°C, 100 psig He, 1500 rpm agit
03/25/03	111	50.0 mg sorbitol, 100g sol'n	10.0g Ru sponge	T=135°C, 100 psig He, 1500 rpm agit
03/28/03	112	3.16g fructose, 5.3g KOH, 100g sol'n	1.0g 5 wt% Ru/C (Aldrich)	T=40°C, 100 psig H2. Hydrogenation and alk. deg.
04/01/03	113	3.16g fructose, 5.3g KOH, 100g sol'n	0.5g 5 wt% Ru/C (Aldrich)	T=40°C, 100 psig H2. Hydrogenation and alk. deg.
04/02/03	114	3.16g fructose, 5.3g KOH, 100g sol'n	0.1g 5 wt% Ru/C (Aldrich)	T=40°C, 100 psig H2. Hydrogenation and alk. deg. 150°C reduction temp
04/09/03	115	3.16g fructose, 5.3g KOH, 100g sol'n	0.05g 5 wt% Ru/C (Aldrich)	T=40°C, 100 psig H2. Hydrogenation and alk. deg. 230°C reduction temp

04/22/03	116	3.16g fructose, 2.0g KOH, 100g sol'n	0.1g 5 wt% Ru/C (Aldrich)	T=40°C, 100 psig H2. Hydrogenation and alk. deg.
04/23/03	117	3.16g fructose, 1.0g KOH, 100g sol'n	0.1g 5 wt% Ru/C (Aldrich)	T=40°C, 100 psig H2. Hydrogenation and alk. deg.
05/08/03	118	3.16g fructose, 5.3g KOH, 100g sol'n	0.1g 5 wt% Ru/C (Aldrich)	T=55°C, 100 psig H2. Hydrogenation and alk. deg.
05/15/03	119	1.0g fructose, 5.3g KOH, 100g sol'n	0.1g 5 wt% Ru/C (Aldrich)	T=40°C, 100 psig H2. Hydrogenation and alk. deg.
05/19/03	120	3.16g fructose, 5.3g KOH, 100g sol'n	0.1g 5 wt% Ru/C (Aldrich)	T=40°C, 100 psig H2. Hydrogenation and alk. deg. Extended run
06/18/03	121	3.16g fructose, no base, 100g sol'n	0.1g 5 wt% Ru/C (Aldrich)	T=40°C, 100 psig H2. Hydrogenation
06/19/03	122	3.16g fructose, 1.6g sorbitol, 100g sol'n	0.1g 5 wt% Ru/C (Aldrich)	T=40°C, 100 psig H2. Hydrogenation (competitve ads)
06/23/03	123	3.16g fructose, 1.6 g mannitol, 100g sol'n	0.1g 5 wt% Ru/C (Aldrich)	T=40°C, 100 psig H2. Hydrogenation (competitve ads)
06/25/03	124	9.5g fructose, no base, 100g sol'n	0.1g 5 wt% Ru/C (Aldrich)	T=40°C, 100 psig H2. Hydrogenation
10/28/03	125	3.17g glucose, 5.33g KOH, 100g sol'n	0.22g 3% Pt(S)/C (Engelhard)	T=40°C, 100 psig H2. No hydrogenation of products. Due to prereduction of the catalyst deactivating it.
10/30/03	126	3.17g glucose, 5.33g KOH, 100g sol'n	0.23g 5% Pt(Ge)/C (Engelhard)	T=40°C, 100 psig H2. Only degradation products. Catalyst shut off because of pre-reduction
11/06/03	127	3.17g glucose, no base, 100g sol'n	0.23g 5% Pt(Ge)/C (Engelhard)	T=40°C, 100 psig H2. Again, no hydrogenation due to pre-reduction. Pt does not need it while Ru does.
11/11/03	128	3.17g glucose, no base, 100g sol'n	0.23g 5% Pt(Ge)/C (Engelhard)	T=40°C, 100 psig H2. Tiny amount of sorb produced after 2 hours. No pre-reduction.

11/13/03	129	1.03g 40 wt% pyruvaldehyde, no base, 100g	0.23g 5% Pt(Ge)/C (Engelhard)	T=40°C, 100 psig H2. Production of PG and GO, but prod dist of feedstock not pure. Not sure what is in feed.
11/18/03	130	0.20g glyceraldehyde, no base, 100g	0.24 3% Pt(S)/C (Engelhard)	T=40°C, 100 psig H2. Clean reduction to GO, but slow. 3.5 hrs, ~35% conversion
11/25/03	131	0.20g glyc, 0.20 glucose, no base, 100g	0.22g 3% Pt(S)/C (Engelhard)	T=40°C, 200 psig H2. GO is primary product. No appearance of SO after 4 hrs. 58% conv.
12/02/03	132	3.17g glucose, 5.32g KOH, 100g sol'n	0.22g 3% Pt(S)/C (Engelhard)	T=40°C, 200 psig H2. Active hydrog. Forms SO and MO w/ EG, PG, GO.
12/09/03	133	3.17g glucose, 5.32g KOH, 100g sol'n	0.22g 3% Pt(S)/C (Engelhard)	T=40°C, 100 psig H2. Active hydrog. Compare w/ 132 @ lower H2 pressure
12/11/03	134	1.0g glucose, 5.33g KOH, 100g sol'n	0.22g 3% Pt(S)/C (Engelhard)	40°C, 200 psig H2. Analysis complete on 1/13/04. Samples degraded (form LA) but hydrog prods should be accurate
12/16/03	135	0.2g glyceraldehyde (1% solution)	0.22g 3% Pt(S)/C (Engelhard)	40°C, 200 psig H2. Accidentally too dilute to analyze (0.002 wt% instead of 0.2 wt%)
01/15/04	136	3.17g fructose, 5.35g KOH, 100g sol'n	0.1g 5 wt% Ru/C (Aldrich)	40°C, 25 psig H2. 230°C reduction.
01/16/04	137	3.17g fructose, 5.35g KOH, 100g sol'n	0.1g 5 wt% Ru/C (Aldrich)	40°C, 50 psig H2. 230°C reduction.
01/19/04	138	3.17g fructose, 5.35g KOH, 100g sol'n	0.1g 5 wt% Pt/C (Aldrich)	40°C, 100 psig H2, no pre-reduction
01/20/04	139	3.17g fructose, 5.35g KOH, 100g sol'n	0.1g 5 wt% Pd/C (Aldrich)	40°C, 100 psig H2, no pre-reduction
01/22/04	140	3.17g fructose, 5.35g KOH, 100g sol'n	0.1g 5 wt% Ru/C (Aldrich)	40°C, 200 psig H2, 230°C reduction

01/26/04	141	3.17g glucose, 5.32g KOH, 100g sol'n	0.1g 5 wt% Ru/C (Aldrich)	40°C, 100 psig H2. Better C3 for degraded material (~75%)
01/27/04	142	3.17g mannose, 5.33g KOH, 100g sol'n	0.1g 5 wt% Ru/C (Aldrich)	40°C, 100 psig H2, 230°C reduction.
01/29/04	143	3.17g fructose, 5.35g KOH, 100g sol'n	0.1g 5 wt% Ru/C (Aldrich)	30°C, 100 psig H2, 230°C reduction
02/17/04	144	2.0g fructose, 5.33g KOH, 100g sol'n	0.1g 5 wt% Ru/C (Aldrich)	40°C, 100 psig H2, 230°C reduction. Highest % of max observed (85%)
02/19/04	145	0.4g glyceraldehyde, 100g sol'n	0.22g 5% Pt(S)/C (Engelhard)	60°C, 100 psig H2, no pre-reduction
02/25/04	146	3.17g fructose, 5.33g KOH, 100g sol'n	0.1g 5 wt% Ru/C (Aldrich)	40°C, 100 psig H2, 230°C reduction.
02/26/04	147	3.17g fructose, 5.33g KOH, 100g sol'n	0.1g 5 wt% Ru/C (Aldrich)	40°C, 25 psig H2, 230°C reduction.
03/01/04	148	0.4g glyceraldehyde, 200g sol'n	0.23g Pt(S)/C (Engelhard)	60°C, 100 psig H2, no pre-reduction
03/02/04	149	3.17g fructose, 5.34g KOH, 100g sol'n	0.1g 5 wt% Ru/C (Aldrich)	40°C, 50 psig H2. 230°C reduction.
03/04/04	150	0.4g glyceraldehyde, 0.4g glycerol, 200g sol'n	0.23g Pt(S)/C (Engelhard)	60°C, 200 psig H2, no pre-reduction
03/08/04	151	0.4g glyceraldehyde, 0.34g PG, 200g sol'n	0.23g Pt(S)/C (Engelhard)	60°C, 200 psig H2, no pre-reduction
03/09/04	152	3.17g fructose, 5.33g KOH, 100g sol'n	0.2g Ru/C (Aldrich)	40°C, 100 psig H2, 230°C reduction.
03/12/04	153	3.17g fructose, 5.35g KOH, 100g sol'n	0.1g Ru/C (Aldrich)	50°C, 100 psig H2, 230°C reduction
03/16/04	154	0.4g glyceraldehyde, 0.8g sorbitol, 200g sol'n	0.23g Pt(S)/C (Engelhard)	60°C, 200 psig H2, no pre-reduction

03/23/04	155	0.4g glyceraldehyde, 200g sol'n	0.23g Pt(S)/C (Engelhard)	60°C, 200 psig H2, no pre-reduction
03/25/04	156	0.4g glyceraldehyde, 0.8g sorbitol, 200g sol'n	0.23g Pt(S)/C (Engelhard)	60°C, 200 psig H2, no pre-reduction
03/30/04	157	3.17g fructose, 5.33g KOH, 200g sol'n	0.1g Ru/C (Aldrich)	50°C, 200 psig H2, 230°C reduction
04/08/04	158	0.4g glyceraldehyde, 100g sol'n	0.1g Pt(S)/C - dry (Englehard)	60°C, 200 psig H2, no pre-reduction
04/13/04	159	0.4g glyceraldehyde, 100g sol'n	0.1g Pt(S)/C - dry (Englehard)	60°C, 200 psig H2, no pre-reduction
04/15/04	160	0.4g glyceraldehyde, 100g sol'n	0.1g Pt(S)/C - dry (Englehard)	60°C, 200 psig H2, no pre-reduction
04/20/04	161	0.8g glucose, 100g sol'n	0.1g Pt(S)/C - dry (Englehard)	60°C, 200 psig H2, no reduction. <0.3% conversion to sorbitol
04/26/04	162	3.17g fructose, 5.31g KOH, 200g sol'n	0.2g Pt(S)/C - dry (Englehard)	40°C, 100 psig H2, no pre-reduction
05/03/04	163	50mg sorbitol, 100g sol'n	10.0g Ru sponge	120°C, 100 psig He, pre-reduced at 200°C
08/23/04	164	0.8g fructose, 100g sol'n	0.22g Pt(S)/C (Englehard)	60°C, 200 psig H2, no pre-reduction
08/25/04	165	0.8g glucose, 100g sol'n	0.23g Pt(S)/C (Englehard)	60°C, 200 psig H2, no pre-reduction
08/26/04	166	0.4g glyceraldehyde, 0.8g glucose, 200g sol'n	0.23g Pt(Ge)/C (Englehard)	60°C, 200 psig H2, no pre-reduction
08/31/04	167	3.17g fructose, 5.32g KOH, 100g sol'n	0.23g Pt(Ge)/C (Englehard)	40°C, 100 psig H2, no pre-reduction
09/02/04	168	3.17g fructose, 5.37g KOH, 100g sol'n	0.23g 5% Pt(Ge)/C (Engelhard)	40°C, 100 psig H2, no pre-reduction

06/08/04	L7	10.0g sorbitol, 100g sol'n	1.0g 3% Ru/TiO_2 (Degussa)	210°C, 1200 psig H2
06/18/04	L10	10.0g glycerol, 100g sol'n	1.0g 3% Ru/TiO_2 (Degussa)	200°C, 1200 psig H2
06/22/04	L11	10.0g glucose, 100g sol'n	1.0g 3% Ru/TiO_2 (Degussa)	120°C / 200°C, 600/1200 psig H2 - Glucose to sorbitol to methane
06/24/04	L12	10.0g glycerol, 100g sol'n	1.0g 3% Ru/TiO_2 (Degussa)	210°C, 1200 psig H2
06/25/04	L13	10.0g sorbitol, 100g sol'n	1.0g 5% Ru/C (PMC)	210°C, 1200 psig H2
06/29/04	L14	10.0g glycerol, 100g sol'n	1.0g 3% Ru/TiO_2 (Degussa)	210°C, 1200 psig H2

REFERENCES

1. Hogle B. et al., *Ind. Eng. Chem. Res.*, **2001**, *41*, 2069-2073

2. Zhang, Z. et al., *Appl. Cat. A: Gen.*, **2001**, *219*, 89-98

3. Jere, F.T., *Org. Lett.*, **2003**, *5*, 527-530

4. Chopade, S. et al., U.S. Patent 6,291,725, 2001

5. The American Chemical Society, Technology Vision 2020: The U.S. Chemical Industry, July 2001

6. British Petroleum, BP Statistical Review of World Energy, June 2003

7. British Petroleum, BP Statistical Review of World Energy, June 2002

8. British Petroleum, BP Statistical Review of World Energy, June 2001

9. Biomass Technical Advisory Committee, Vision for Bioenergy and Biobased Products in the United States, October 2002

10. *Chemical Market Reporter*, **March 15, 2004**, *265*

11. http://ers.usda.gov/briefing/sugar/Data/data.htm, viewed on August 27, 2004, last update July 13, 2004

12. *Chemical Market Reporter*, **September 24, 2001**, *260*

13. *Chemical Market Reporter*, **December 17, 2001**, *260*

14. Vollhardt, K. Peter C. and Schore, N.E., *Organic Chemistry*, 2nd Ed., p. 250, W.H. Freeman and Company, New York, 1995

15. Kroschwitz, J.; Howe-Grant, M., editors, *Kirk-Othmer Encyclopedia of chemical technology*, 4th Ed., **18**, pp. 446-447, Wiley, New York, 1992

16. Bowden, E.; Adkins, H., *J. Am. Chem. Soc.*, **1934**, *56*, 689-691

17. Adkins, H.; Pavlic, A.A., *J. Am. Chem. Soc.*, **1947**, *69*, 3039-3041

18. Adkins, H.; Billica, H.R., *J. Am. Chem. Soc.*, **1948**, *70*, 3121-3125

19. Carnahan, J.E. et al., *J. Am. Chem. Soc.*, **1955**, *77*, 3766-3768

20. Kroschwitz, J.; Howe-Grant, M., editors, *Kirk-Othmer Encyclopedia of chemical technology*, 4th Ed., **23**, pp. 105-106, Wiley, New York, 1992

21. Wisniak, J.et al., *Ind. Eng. Chem. Prod. Res. Develop.*, **1974**, *13 (1)*, 75-79

22. Wisniak, J.; Hershkowitz, M.; Stein, S., *Ind. Eng. Chem. Prod. Res Develop.*, **1974**, *13 (4)*, 232-236

23. Wisniak, J.; Simon, R.; *Ind. Eng. Chem. Prod. Res. Dev.*, **1979**, *18 (1)*, 50-57

24. Brahme, P.H.; Doraiswamy, L.K.; *Ind. Eng. Chem., Process Des. Dev.*, **1976**, *15 (1)*, 130-137

25. Verma, R.; Gehlawat, J.K.; *J. Chem. Tech. Biotechnol.*, **1989**, *46*, 295-301

26. van Gorp, K. et al., *Cat. Today*, **1999**, *52*, 349-361

27. Cerino, P.J.; Fleche, G.; Gallezot, P.; Salome, J.P., *Heterogeneous Catalysis and Fine Chemicals II: proceedings of the 2nd international symposium, Poitiers, October 2-5, 1990*, pp. 231-236, Guisnet M. et al. (editors), Elsevier, Amsterdam; New York, 1991

28. Guo, H.; Li, H.; Xu, Y.; Wang, M., *Mater. Lett.*, **2002**, *57*, 392-398

29. Hegedüs, M.; Göbölös, S.; Margitfalvi, J.L., *Heterogenous Catalysis and Fine Chemicals III: proceedings of the 3rd international symposium, Poitiers, April 5-8, 1993*, pp. 187-194, Guisnet, M. et al. (editors), Elsevier, Amsterdam; New York, 1993

30. Heinen, A.W.; Peters, J.A.; van Bekkum, H., *Carbohyd. Res.*, **2000**, *328*, 449-457

31. Mikkola, J.-P. et al., *J. Chem. Tech. and Biotech.*, **2001**, *76*, 90-100

32. Kusserow, B.; Schimpf, S.; Claus, P., *Adv. Synth. Catal.*, **2003**, *345*, 289-299

33. Ellis, C., *Hydrogenation of Organic Substances*, 3rd Ed., D. Van Nostrand Company, New York, 1930

34. Connor, R.; Adkins, H., *J. Am. Chem. Soc.*, **1932**, *54*, 4678-4690

35. Natta, G.; Rigamonti, R.; Beati, E., *Berichte D. Chem. Gesellschaft*, **1943**, *76B*, 641-656

36. Clark, I., *Ind. Eng. Chem.*, **1958**, *50 (8)*, 1125-1126

37. van Ling, G.; Vlugter, J., *J. of App. Chem.*, **1969**, *19*, 43-45

38. Sohounloue, D. et al., *React. Kin. Catal. Lett.*, **1983**, *22 (3-4)*, 391-397

39. Montassier, C. et al., *Bull. Soc. Chim.*, **1989**, *126 (2)*, 148-155

40. Müller, P.; Rimmelin, P.; Hindermann, J.; Kieffer, R.; Kiennemann, A.; Carré, J., *Heterogeneous Catalysis and Fine Chemicals II*, Guisnet M. et al. (Editors), Elsevier Science Publishers B.V., Amsterdam, 1991

41. Montassier, C. et al., *J. of Mol. Catal.*, **1991**, *70 (1)*, 99-110

42. Larchar, A., U.S. Patent 1,963,997, 1934

43. Rothrock, H., U.S. Patent 2,004,135, 1935

44. Conradin, F. et al, U.S. Patent 2,852,570, 1958

45. Conradin, F. et al, U.S. Patent 2,965,679, 1960

46. Conradin, F. et al, U.S. Patent 3,030,429, 1962

47. Kasehagen, L., U.S. Patent 3,396,199, 1968

48. Sirkar, U.S. Patent 4,338,472, 1982

49. Sirkar, A., U.S. Patent 4,380,678, 1983

50. Chao, J.; Hulbers, D., U.S. Patent 4,366,332, 1982

51. Arena, B., U.S. Patent 4,401,823, 1983

52. Tanikella, M., U.S. Patent 4,404,411, 1983

53. Dubeck, M.; Knapp, G., U.S. Patent 4,430,253, 1984

54. Dubeck, M.; Knapp, G., U.S. Patent 4,476,331, 1984

55. Andrews, M.; Klaeren, S., U.S. Patent 5,026,927, 1991

56. Gubitosa, G.; Casale, C., U.S. Patent 5,326,912, 1994

57. Gubitosa, G.; Casale, C., U.S. Patent 5,354,914, 1994

58. Gubitosa, G.; Casale, C., U.S. Patent 5,403,805, 1995

59. Gubitosa, G.; Casale, C., U.S. Patent 5,543,379, 1996

60. Gubitosa, G.; Casale, C., U.S. Patent 5,600,028, 1997

61. de Bruyn, C. A. L., *Recl. Trav. Chem. Pays-Bas*, **1895**, *14*, 156-165

62. de Bruyn C. A. L.; van Ekenstein, W. A., *Recl. Trav. Chem. Pays-Bas*, **1895**, *14*, 203-216

63. Nef, J., *Ann.*, **1907**, *357*, 294-312

64. Evans, W. L.; Edgar, R. H.; Hoff, G. P., *J. Am. Chem. Soc.*, **1926**, *48*, 2665-2677

65. Denis, W. *Am. Chem. J.*, **1907**, *38*, 561-594

66. Shaffer, P. A.; Friedemann, T. E., *J. of Biol. Chem.*, **1930**, *86*, 345-375

67. Braun, G., U.S. Patent 2,024,565, 1935

68. Lock, R. H., U.S. Patent 2,382,889, 1945

69. Tronconi, E. et al., *Chem. Eng. Sci.*, **1992**, *47 (9-11)*, 2451-2456

70. Montgomery R.; Ranca, R. A., *Ind. Eng. Chem.*, **1953**, *45 (5)*, 1136-1147

71. MacLaurin, D. J.; Green, J. W., *Can. J. Chem.*, **1969**, *47*, 3947-3955

72. de Wit, G.; Kieboom, A. P. G.; van Bekkum, H., *Carbohyd. Res.*, **1979**, *74*, 157-175

73. de Bruijn, J. M.; Kieboom, A. P. G.; van Bekkum, H., *Recl. Trav. Chim. Pays-Bas*, **1986**, *105*, 176-183

74. de Bruijn, J. M., et al., *Int. Sugar Journal*, **1987**, 89 *(1066)*, 194-210

75. de Bruijn, J. M.; Kieboom, A. P. G.; van Bekkum, H., *Recl. Trav. Chim. Pays-Bas*, **1987**, *106*, 35-43

76. de Bruijn, J. M.; Kieboom, A. P. G.; van Bekkum, *J. Carbohyd. Chem.*, **1986**, *5 (4)*, 561-569

77. de Bruijn, J. M.; Kieboom, A. P. G.; van Bekkum, *Starch*, **1987**, *39 (1)*, 23-28

78. de Bruijn, J. M.; Touwslager, F.; Kieboom, A. P. G.; van Bekkum, H., *Starch*, **1987**, *39 (2)*, 49-52

79. de Bruijn, J. M.; Kieboom, A. P. G.; van Bekkum, *Sug. Tech. Rev.*, **1986**, *13*, 21-52

80. Gregg, S.J.; Sing, K.S.W., *Adsorption, Surface Area and Porosity*, 2nd Ed., pp. 173-190, New York, 1982

81. Brunauer, S.; Emmett, P.H.; Teller, E., *J. Am. Chem. Soc*, **1938**, *60 (2)*, 309-319

82. Micromeritics, *ASAP 2010 Chemi: Accelerated Surface Area and Porosimetry System Operator's Manual*, Appendix C, September 1996

83. Al-Dahhan, M.H.; Duduković, M.P., *AIChE Journal*, **1996**, *42 (9)*, 2594-2604

84. Al-Dahhan, M.H.; Duduković, M.P., *Chem. Eng. Sci.*, **1995**, *50 (15)*, 2377-2389

85. McCabe, W.L. et al., *Unit Operations of Chemical Engineering*, 5th Ed., p. 153, McGraw Hill Inc., New York, 1993

86. McCabe, W.L. et al., *Unit Operations of Chemical Engineering*, 5th Ed., p. 155, McGraw Hill Inc., New York, 1993

87. McCabe, W.L. et al., *Unit Operations of Chemical Engineering*, 5th Ed., p. 928 McGraw Hill Inc., New York, 1993

88. Levenspiel, O., *Chemical Reaction Engineering*, 3rd Edition, p. 27, Wiley, New York, 1999

89. Unpublished data from Miller group produced by L. Peereboom

90. Zwietering, T. H., *Chem. Eng. Sci.*, **1958**, *8*, 244

91. Felder, R.M.; Rousseau, R.W., *Elementary Principles of Chemical Processes*, 2nd Ed., p. 248, Wiley, New York, 1986

92. Perry, R.H.; Green, D.W., *Perry's Chemical Engineers' Handbook*, 7th Ed., p. 2-126, McGraw-Hill, New York, 1997

93. Yagi, H.; Yoshida, F., *Ind. Eng. Chem. Proc. Des. Dev.*, **1975**, *14*, 488

94. Bern, L.; Lidefelt, J.O.; Schoon, N.H., *J. Am. Chem. Soc.*, **1976**, *53*, 463

95. Boon-Long, S.; Laguerie, C.; Couderc, J.P., *Chem. Eng. Sci.*, **1978**, *33*, 813

96. Weiss, P.B.; Prater, C.D., *Adv. Catal.*, **1954**, *6*, 143

97. Fogler H.S., *Elements of Chemical Reaction Engineering*, 2nd Ed., p.256, Prentice-Hall, New York, 1992

98. Pallasana, V., Neurock, M., *J. Catal.*, **2002**, *209*, 289-305

99. Fogler H.S., *Elements of Chemical Reaction Engineering*, 2nd Ed., p.341, Prentice-Hall, New York, 1992

100. Cannizzaro, S., *Ann.*, **1853**, *88*, 129

101. Carnahan, B.; Luther, H. ; Wilkes, J., *Applied Numerical Methods*, Wiley, New York, 1969

102. Jere, F.T., Ph.D. Dissertation, Michigan State University, 2003

103. Belohlav, Z.; Zamostny, P.; Kluson, P.; Volf, J., *Can. J. of Chem. Eng*, **1997**, *75*, 735-742

104. Tewari, Y.B.; Goldberg, R.N., *Biophys. Chem.*, **1986**, *24*, 291-294

105. Camacho-Rubio, F. et al., *Can. J. of Chem. Eng.*, **1995**, *73*, 935-940

106. Franks, F., *Pure and Appl. Chem.*, **1987**, *59 (9)*, 1189-1202

107. Smith, J.M.; Van Ness, H.C.; Abbott, M.M., *Introduction to Chemical Engineering Thermodynamics*, 5th Ed., p. 567, The McGraw-Hill Companies, New York, 1996

108. Ellis, A.V.; Wilson, M.A., *J. Org. Chem.*, **2002**, *67*, 8469-8474

109. deWit, G. ; Kieboom, A.P.G.; van Bekkum, H., *Carbohyd. Res.*, **1979**, *74*, 157-175

110. Kroschwitz, J.; Howe-Grant, M., editors, *Kirk-Othmer Encyclopedia of chemical technology*, 4th Edition, **13**, p. 852, Wiley, New York, 1992

111. U.S. Natural Gas Prices, http://tonto.eia.doe.gov/dnav/ng/ng_pri_sum_dcu_nus_m.htm, viewed November 15, 2004, last updated October 29, 2004